

THE SPACE-TIME CONTINUUM OF RAS SIGNAL TRANSDUCTION PATHWAY

Dissertation

Zur Erlangung des Grades eines
Doktors der Naturwissenschaften
der Fakultät für Chemie der
Technischen Universität Dortmund

vorgelegt von

Anchal Chandra

Aus Hardwar, Indien

Dortmund 2011

The work described in this thesis was performed under the supervision of Prof. Dr. Philippe Bastiaens from January 2007 to June 2011 at the Max Planck Institute for Molecular Physiology, Dortmund and funding of International Max Planck research school-Chemical Biology.

1st Examiner:

Prof. Dr. Philippe Bastiaens

Department of Systemic Cell Biology
Max-Planck Institute for Molecular
Physiology
Department of Chemistry
Technical University, Dortmund

2nd Examiner:

Prof. Dr. Alfred Wittinghofer

Department of Structural Biology
Max-Planck Institute for Molecular
Physiology
Professor of Biochemistry
Ruhr-University, Bochum

Tag der Abgabe: 02.11.2011

Tag der Disputation: 29.07.2011

Zusammenfassung

Die räumliche Aufteilung peripherer Membran-Proteine, wie GNBPs (Ras) moduliert deren Spezifität der Signalverarbeitung innerhalb der Zelle. Reversible Palmitoylierung durch Palmitoylacyltransferasen (PATs der DHHC der DHHC Familie) erzeugt die Verteilung von Ras hin zu der Plasma-Membran (PM) über den sekretorischen Weg, indem der entropie-getriebenen Gleichverteilung palmitoylierter Proteine auf alle Zellmembrane entgegenwirkt wird (Rocks et al., 2010). In dieser Arbeit wird beschrieben, dass DHHC-PATs sich nicht durch Substratspezifität auszeichnen und es wird postuliert, dass DHHC Proteine die Palmitoylierungsreaktion nicht katalysieren. Stattdessen verstärken sie die Konzentration des Palmitat-Thioester-Zwischenproduktes und erzeugen auf diese Weise ein zytosolisches Reservoir um Palmitoylierung zu vereinfachen.

In dieser Arbeit soll ebenfalls beschrieben werden, wie GEF PDE δ den zügigen Transfer von Ras Protein zwischen PM, Golgi Apparat, endoplasmatischem Retikulum (ER) und Zytoplasma unterstützt. Weiterhin wird aufgezeigt werden, dass dies allein solche farnesylierten Ras Proteine betrifft, welche depalmitoyliert oder, im Fall von Ras mit polykationischem Motiv, PM-desorbiert sind. In Verbindung mit dem Palmitoylierungskreislauf wirkt PDE δ , indem es die Diffusion von depalmitoyliertem Ras vereinfacht und erlaubt so dessen kinetisches Eingefangenwerden am Golgi Apparat ermöglicht. Andererseits erhöht die Solubilisierung von Kras, welches ein polybasisches Segment auszeichnet, weg von Endomembranen die Geschwindigkeit, mit der Kras von der PM wieder eingefangen werden kann, wodurch dessen Equilibriumsverteilung aufrecht erhalten wird. Dies ist wichtig, da PDE δ auf diese Art die durch Ras vermittelte Signaltransduktion verstärkt, indem es die Ras-Konzentration an der PM erhöht, und im Gegenzug bewirkt das Herunterregeln von PDE δ ein Unterdrücken von regulierten und onkogenischen Ras Signalen. Zusätzlich wird die Regulierung von farnesyliertem Ras*PDE δ Einheiten via G-Protein Arl2/Arl3 auf eine GTP-abhängige Art beschrieben. Diese Erkenntnis deckt einen von PDE δ -abhängigen Mechanismus auf, der für die räumliche Organisation von Ras Proteinen in Zellmembranen verantwortlich ist und dessen Einfluss auf das Signalverhalten von Ras Wildtyp- bzw. mutierter Form.

Abstract

Spatial partitioning of peripheral membrane proteins such as GNBPs (Ras) modulates its intracellular signaling specificity. Reversible palmitoylation by Palmitoylacyltransferases (DHHC family PATs) creates cellular partitioning of Ras to the plasma membrane (PM) via the secretory pathway by counteracting entropy-driven equipartitioning of palmitoylated proteins to all cellular membranes (Rocks et al., 2010). This work describes that DHHC-PATs lack substrate specificity and postulates that DHHC proteins do not catalyze the palmitoylation reaction. Rather, they enhance the concentration of palmitate-thioester intermediate to generate a cytosolic reservoir in order to facilitate palmitoylation.

This study also describes how the GSF PDE δ mediates rapid shuttling of Ras protein pools between PM, Golgi apparatus, endoplasmic reticulum (ER), cytoplasm and demonstrate that this is specific only to farnesylated Ras proteins that are either depalmitoylated or PM-desorbed in case of polycationic Ras. PDE δ functions in conjunction with the palmitoylation cycle by facilitating depalmitoylated Ras diffusion thus permitting its kinetic trapping at the Golgi apparatus. On the other hand, solubilization of polybasic stretch-containing Kras from endomembranes by PDE δ enhances the speed of re-trapping at the PM and thereby reinstates equilibrium. Importantly, PDE δ activity augments Ras mediated signal transduction by maintaining Ras at the PM and that down-modulation of PDE δ suppresses both regulated and oncogenic Ras signaling. In addition to this, allosteric regulation of farnesylated Ras*PDE δ cargo via G-proteins Arl2/Arl3 in a GTP-dependent manner is described. These findings reveal PDE δ -dependent mechanisms responsible for the spatial organization of Ras proteins in cellular membranes, and their importance in signaling via wild type and mutant Ras.

Table of Contents

1	Introduction.....	10
1.1	Guanine nucleotide binding proteins.....	10
1.2	Structural outlines of the G domain	11
1.3	Ras/mitogen-activated protein (MAP or ERK) kinase cascade.....	12
1.4	Ras lipidation	14
1.5	Cellular palmitoylation machinery	17
1.5.1	Significance of Palmitoylation.....	17
1.5.2	Function of Palmitoylation.....	18
1.5.3	Ras Acylation cycle.....	19
1.5.4	Enzymology of palmitoylation	20
1.5.5	DHHC family of Palmitoyl acyl transferases	21
1.5.6	Sequence conservation and phylogeny of DHHC domain	22
1.5.7	Yeast, mammalian PATs and their substrate specificity.....	23
1.6	Targeting of peripheral membrane proteins	25
1.6.1	Lipid composition of plasma membrane:.....	25
1.6.2	Surface charge of the plasma membrane:	27
1.6.3	Polycationic Ras subfamily proteins.....	29
1.6.4	Regulation of polybasic Ras proteins at the PM.....	30
1.7	Cyclic nucleotide Phosphodiesterases.....	32
1.7.1	cGMP PDEs	32
1.7.2	cGMP specific phosphodiesterase-6 (PDE6).....	32
1.7.3	PDE6 enzymes	34
1.7.4	PDE6 regulatory binding protein (PDE δ).....	34
1.7.5	PDE δ homologues.....	35
1.7.6	Similarities between PDE δ and RhoGDI.....	35
1.7.7	PDE δ interaction with Arl2 and Arl3: Structural insight.....	37
1.7.8	PDE δ and Arl2 role in maintaining photoreceptor physiology.....	38
2	Experimental Procedures	42
2.1	Materials	42
2.1.1	<i>Antibodies and Dyes</i>	42
2.1.2	<i>Buffers and solutions</i>	43
2.1.3	<i>Consumables and kits</i>	43
2.1.4	<i>Reagents</i>	44
2.1.5	<i>Plasmids</i>	44
	(A) Dictyostelium constructs:	44
	(B) Mammalian expression constructs:.....	44
2.1.6	<i>Cell culture medium & antibiotics</i>	45
2.1.7	<i>siRNA</i>	46
2.1.8	<i>Cell lines</i>	46
2.2	Molecular biology techniques.....	48
2.2.1	<i>Transformation of E. coli</i>	48
2.2.2	<i>Transformation in Dictyostelium cells</i>	48
2.2.3	<i>RNA preparation and RT-PCR</i>	48
2.3	Cell biology techniques	49
2.3.1	<i>Mammalian cell culture</i>	49
2.3.2	<i>Dictyostelium cell culture</i>	49
2.3.3	<i>Preparation of mammalian cell lysates</i>	50

2.3.4	<i>GST Pulldown Assay</i>	50
2.3.5	<i>RNA Interference</i>	51
2.3.6	<i>Western blots</i>	51
2.3.7	<i>Biotin acyl exchange assay</i>	52
2.3.8	<i>Triple (3X)-RBD staining</i>	53
2.3.9	<i>In vitro Clonogenic assay of cells</i>	53
2.4	Microscopy and imaging techniques	54
2.4.1	<i>Microscopes</i>	54
2.4.2	<i>FRAP and FLAP</i>	55
2.4.3	<i>FRET-FLIM</i>	55
2.5	Data analysis	56
2.5.1	<i>Fluorescence loss after photoactivation (FLAP)</i>	56
2.5.2	<i>Fluorescence recovery after photobleaching (FRAP)</i>	56
2.5.3	<i>FRET-FLIM</i>	56
2.5.4	<i>Western blots quantification</i>	57
2.5.5	<i>RT-PCR</i>	57
3	Investigating palmitoylation machinery specificity in DHHC motif containing Dictyostelium PATs	59
3.1	Abstract	60
3.2	Rationale and hypothesis	61
3.3	Results	64
3.3.1	<i>Dictyostelium discoideus as a model organism</i>	64
3.3.2	<i>Subcellular localization of human Hras in Dictyostelium discoideus</i>	65
3.3.3	<i>Effect of 2-Bromopalmitate on subcellular localization of human Ras in Dictyostelium</i>	66
3.3.4	<i>Depalmitoylated Hras displays faster diffusion kinetics over wildtype</i> ...	67
3.4	Discussion and future perspectives	69
	<i>Substrate tolerance of palmitoylation machinery</i>	69
4	The GDI-like solubilizing factor PDEδ sustains the spatial organization and signaling of Ras family proteins	72
4.1	Abstract	73
4.2	Rationale and Hypothesis	74
4.3	Results	75
4.3.1	<i>PDEδ affects spatial distribution of Ras family proteins</i>	75
4.3.2	<i>Prenylation/farnesylation is essential for PDEδ-Ras interaction</i>	81
4.3.3	<i>PDEδ-Ras interaction is independent of Ras nucleotide bound state</i>	82
4.3.4	<i>PDEδ downregulation alters Ras spatial localization</i>	84
4.3.5	<i>PM desorbed Kras interacts with PDEδ</i>	90
4.3.6	<i>Pharmacological intervention of Ras acylation cycle</i>	92
4.3.7	<i>PDEδ acts as a shuttling factor for palmitoylatable Ras</i>	94
4.3.8	<i>PDEδ rescues Ras localization in HepG2 cells</i>	98
4.3.9	<i>PDEδ modulates Ras signaling response in normal and transformed cells</i>	102
4.3.10	<i>PDEδ ablation inhibits cell proliferation and viability in oncogenic Ras transformed cells</i>	106
4.4	Discussion and future perspectives	109
4.4.1	<i>Polycationic Ras protein trafficking and membrane targeting</i>	109
4.4.2	<i>Inter-compartmental exchange of palmitoylated and polycationic Ras</i>	110
4.4.3	<i>Prenylation specificity of PDEδ and its homologues</i>	110

4.4.4	<i>Modulating Ras signaling at the PM</i>	113
4.4.5	<i>PDEδ gene targeting studies</i>	114
5	Regulation of a GDI-like transport system for farnesylated cargo by Arl2/3-GTP	116
5.1	Abstract	117
5.2	Rationale and hypothesis	118
5.3	Results	121
5.3.1	<i>Conformational differences between far-Rheb•PDEδ and Arl2•GTP•PDEδ complexes</i>	121
5.3.2	<i>Rationale design of PDEδ mutants: Structural insights</i>	123
5.3.3	<i>Spatial distribution of Ras*PDEδ in presence of constitutive active Arl2</i>	125
5.3.4	<i>Disruption of Rheb*PDEδ complex by Arl2Q70L</i>	129
5.3.5	<i>Influence of PDEδ mutants on Golgi apparatus</i>	131
5.4	Discussion and future perspectives	135
5.4.1	<i>Arl2 acts as a displacement factor for PDEδ in cells</i>	135
5.4.2	<i>Functional significance of regulated Ras release mechanism</i>	136
5.4.3	<i>GDI (-like) regulation via GNBPs cross-talk</i>	137
5.4.4	<i>Arl2*PDEδ mediated Golgi structure and function maintenance</i>	138
6	References	141
7	Acknowledgements	160
8	Publications and presentations	161
9	Curriculum Vitae	162

List of Figures

Chapter 1

Figure 1.1	Schematic representation of GTPase cycle	11
Figure 1.2	Structure of Ras G domains	12
Figure 1.3	Overview of the Ras-MAPK pathway and the associated disorders	14
Figure 1.4	Major Lipid Modifications of Proteins	15
Figure 1.5	S-palmitoylation versus N-palmitoylation	16
Figure 1.6	Schematic representation of Ras acylation cycle	20
Figure 1.7	Domain organization and topology of DHHC family PATs	21
Figure 1.8	Homology and phylogeny of DHHC proteins	22
Figure 1.9	Schematic representation of the intracellular sites of protein palmitoylation	23
Figure 1.10	DHHC-CRD palmitoyl acyl transferases (PATs) and their substrates	25
Figure 1.11	Lipid composition of membranes in different cell compartments	26
Figure 1.12	Surface potential attracts cationic molecules to the inner leaflet of the plasma membrane	28
Figure 1.13	Polybasic C-terminal containing Ras superfamily proteins	29
Figure 1.14	Changes in the net charge of the protein modulate the effect of surface charge on protein localization	30
Figure 1.15	PIP2 cleavage to IP3 and DAG initiates intracellular calcium release and PKC activation	31
Figure 1.16	Schematic subunit composition and structure of rod and cone	33
Figure 1.17	Alignments of PDE δ , RhoGDI and UNC119/RG4 proteins	36
Figure 1.18	Structural homology of PrBP/PDE δ , unc119, and RhoGDI	37
Figure 1.19	Crystal structure	38
Figure 1.20	The hydrophobic pocket in PDE δ	38
Figure 1.21	Localization of rod and cone PDE6 in WT and Pde6d $^{-/-}$ retina	39
Figure 1.22	Putative model of post-biosynthesis transport of membrane proteins in rods and cones	41

Chapter 2

Figure 2.1	Schematic of the proteomic acyl-biotinyl exchange methodology	53
------------	---	----

Chapter 3

Figure 3.1	Equivalent distribution of the tH versus full-length Hras protein	61
Figure 3.2	shRNA mediated DHHC9 downregulation	62
Figure 3.3	Consensus sequence alignment of mammalian and yeast genome	63
Figure 3.4	Sequence alignment of <i>Dictyostelium</i> Ras proteins	64
Figure 3.5	Human Hras spatial localization in <i>Dictyostelium discoideus</i>	66
Figure 3.6	2-Bromopalmitate inhibits human Hras palmitoylation	66
Figure 3.7	FRAP kinetics of human Hras in <i>Dictyostelium</i>	68

Chapter 4

Figure 4.1	PDE δ affects the spatial distribution of palmitoylated Ras proteins	76
Figure 4.2	FRET-FLIM based PDE δ -Ras interaction studies	78
Figure 4.3	PDE δ solubilizes polybasic stretch containing Ras proteins	80
Figure 4.4	PDE δ does not interact with geranylgeranylated Ras proteins	81
Figure 4.5	GST pulldown assay	82
Figure 4.6	Structural overlay of PDE δ with Rho-RhoGDI complex	83
Figure 4.7	PDE δ shows no preference to GDP or GTP bound Ras	84

Figure 4.8	Endogenous PDE δ , Ras protein concentration determination	85
Figure 4.9	Validation of siRNA specificity towards canine PDE δ	87
Figure 4.10	siRNA mediated downregulation of PDE δ causes redistribution of Ras	88
Figure 4.11	PDE δ downregulation does not alter surface charge distribution on the PM	89
Figure 4.12	Farnesylation is the only pre-requisite for PDE δ -Ras interaction	89
Figure 4.13	PDE δ solubilizes Kras mostly from endomembranes	91
Figure 4.14	Pharmacological intervention with the Ras acylation cycle affects PDE δ activity	93
Figure 4.15	Palmitoylated Ras levels after thioesterase inhibition (BAE assay)	94
Figure 4.16	PDE δ enhances the effective diffusion of farnesylated Ras proteins	96
Figure 4.17	PDE δ enhances the effective diffusion of Ras	98
Figure 4.18	PDE δ expression reinstates PM Ras localization in HepG2 cells	100
Figure 4.19	Confocal imaging of HepG2 cells	101
Figure 4.20	PDE δ modulates wild type Ras signaling	104
Figure 4.21	Effect of siRNA mediated PDE δ down-regulation on pErk1/phosphorylation levels in oncogenic Ras transformed cells	105
Figure 4.22	PDE δ downregulation disturbs oncogenic KasG12D spatial partitioning	106
Figure 4.23	Effect of PDE δ ablation on Ras induced proliferative growth and viability	107
Figure 4.24	Long-term PDE δ shRNA treatment	108

Chapter 5

Figure 5.1	Proposed role of Arl in photoreceptor physiology	118
Figure 5.2	Structural analysis of farnesylated Rheb*PDE δ complex	121
Figure 5.3	Electrostatic surface charge distribution	122
Figure 5.4	Diagrammatic representation of hydrophobic pocket of PDE δ in complex with Arl2	123
Figure 5.5	The interface of Arl2 and PDE δ -Schematic representation	124
Figure 5.6	Mutations influencing Arl2*PDE δ interaction	125
Figure 5.7	Restoration of Rheb and NRas cellular steady state localization upon Arl2Q70L expression	128
Figure 5.8	PDE δ double mutant and wild type interaction with Arl2 Q70L	130
Figure 5.9	Effect of PDE δ mutants on Golgi apparatus	133
Figure 5.10	Substitution of mutated valine to glycine	133
Figure 5.11	PDE δ sequence alignment in different species	134

I

Introduction

1.1 Guanine nucleotide binding proteins

The Guanine nucleotide-binding proteins (GNBPs), together with their associated regulators and effectors, participate as central control elements in signal transduction pathways. Many fundamental cellular processes such as cell growth, differentiation, vesicular and nuclear transport, are regulated by GNBPs. Ras serves as a prototype for the super-family of GNBPs: which cycles between the active GTP-bound state (the “on” state) and the inactive GDP-bound state (the “off” state). The exchange of GDP to GTP turns the switch on and the hydrolysis of GTP turns it off. In the GTP bound form, the GNBPs display a binding surface with high affinity for downstream effector proteins [for instance, Hras-GTP has a K_d (dissociation constant) of 18nM for a protein kinase Raf1 (Herrmann et al., 1996)]. The structural changes are confined to two loop regions called switch I and II (Milburn et al., 1990). However, the intrinsic GTPase activity of Ras-related proteins is typically low [$4.2 \times 10^{-4} \text{ s}^{-1}$ for Hras (Neal et al., 1988)], which would tend to prolong signal transduction. Thus the high affinity effector-binding conformation of Ras proteins is transient; GTP hydrolysis and release of γ -phosphate leads to reorientation of effector binding residues, the release of effector proteins (due to reduced affinity), and attenuation of downstream signaling. The hydrolysis of GTP to GDP is greatly enhanced by the action of GTPase activating proteins (GAPs) (Figure 1.1). There are often multiple GAPs that function on a given Ras protein, allowing for a variety of input sources at this stage of regulation.

The rate-limiting step in Ras protein activation is the exchange of bound GDP for GTP [$3.4 \times 10^{-4} \text{ s}^{-1}$ for Hras (Neal et al., 1988)]. This favors an inactive steady-state conformation of Ras even in the presence of a high cellular GTP/GDP ratio [~ 10 fold (Van Dyke et al., 1977)]. This kinetic limitation is the basis for stimulus-induced mechanisms of Ras protein regulation. Activation of GNBPs thus requires guanine nucleotide exchange factors (GEFs) that catalyze the release of GDP (Figure 1.1), thus promoting GTP loading and activation of Ras [~ 6 fold stimulation of Hras by exchange factor SOS1 (Chardin et al., 1993)]. Several GEFs may act on a particular

Ras protein, with each GEF responding to distinct upstream stimuli thus generating different biological outputs.

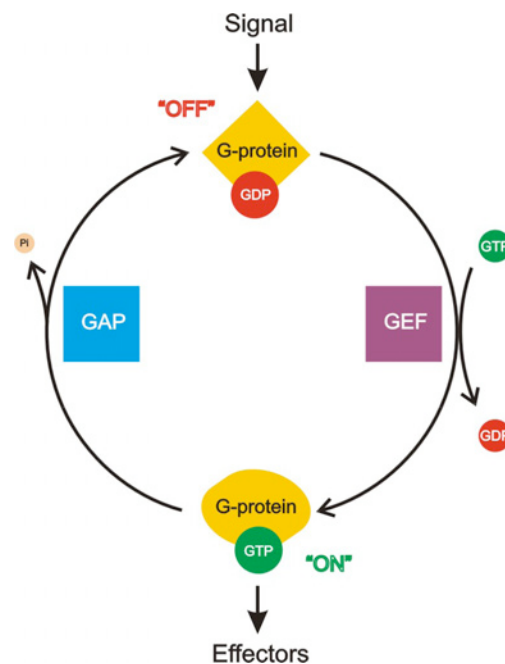


Figure 1.1 Schematic representation of GTPase cycle
Reproduced from Dissertation Sirajuddin M. 2007.

1.2 Structural outlines of the G domain

The G domain is highly conserved in all GNBPs. The conserved G domain has an approximate molecular mass of 21 kDa and has a typical fold consisting of a mixed six-stranded β sheet and five α helices (Figure 1.2). Crystal structures of all available GNBPs show that Ras shares a common structural core – the G domain fold (Vetter and Wittinghofer, 2001). Therefore, Ras is considered a paradigm for most of the GNBPs of the TRAFAC class.

The G domain contains five conserved sequence elements around the guanine nucleotide binding site, called G1 to G5 (Bourne et al., 1991; Saraste et al., 1990). The G1 motif (GxxxxGKS), also known as P-loop (phosphate binding loop) interacts with the α - and β -phosphates of the nucleotide. The G2 motif contains an invariant threonine (Thr35 in Ras), which is involved in Mg^{2+} coordination and direct binding to the γ -phosphate. The conserved aspartate (Asp57 in Ras) of G3 motif (DxxG) binds to the magnesium ion via a water molecule and the glycine (Gly60 in Ras) makes a main chain contact to the γ -phosphate. Together these two motifs G2 and G3 trigger

conformational changes when the γ -phosphate is hydrolyzed. Therefore the regions that include these motifs are termed switch regions. Switch I includes the G2 motif and switch II includes the G3 motif. The switches are the main determinants for binding of effector molecules. The G4 motif (NKxD) is important for guanine nucleotide specificity. The aspartate (Asp119 in Ras) makes a bi-furcated contact to the guanine base ensuring the specificity. The alanine (Ala146 in Ras) of G5 motif (SAL/K) makes a main chain interaction with the guanine base (Vetter and Wittinghofer, 2001).

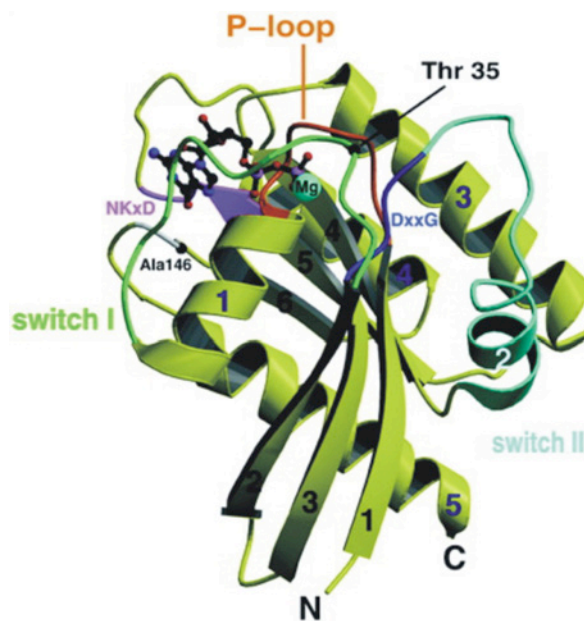


Figure 1.2 Structure of Ras G domains
Ribbon plot of the minimal G domain, with the conserved sequence elements and the switch regions in different colors as indicated. The nucleotide and Mg^{2+} ion are shown in ball-and-stick representation. Reproduced from Vetter and Wittinghofer, 2001.

1.3 Ras/mitogen-activated protein (MAP or ERK) kinase cascade

The signal transduction via the Ras-MAPK cascade is mediated by sequential phosphorylation and activation of protein kinases along the different tiers of the cascade. Although the main core phosphorylation chain of the cascade includes Raf kinases, MEK1/2, ERK1/2 (ERKs) and RSKs, other alternatively spliced forms and distinct components exist in the different tiers, and participate in Ras signaling under specific conditions. These components enhance the complexity of the Ras cascade

and thereby, enable the wide variety of functions that are regulated by the pathway itself. Another factor that is important for the dissemination of Ras signals is the multiplicity of the cascade's substrates, which include transcription factors, protein kinases and phosphatases, cytoskeletal elements, regulators of apoptosis, and a variety of other signaling-related molecules. Growth factor context determines the topology of the MAPK signaling network and that the resulting dynamics govern cell fate.

Ras can be activated when a growth factor binds to a receptor tyrosine kinase such as the epidermal growth factor receptor (EGFR) resulting in dimerization and autophosphorylation of the receptor. This autophosphorylated receptor then binds to the SH2 domain of the adaptor protein GRB2. Through its SH3 domains, GRB2 is bound to SOS (Son of Sevenless), which is thus recruited to the plasma membrane. SOS proteins (SOS1 and SOS2) are important RAS-GEFs (guanosine nucleotide exchange factors), which catalyze exchange of GDP to GTP in Ras. The increased proximity of SOS to membrane bound RAS results in increased nucleotide exchange on Ras. Many other receptor types, including the G protein-coupled receptors, can activate Ras through stimulation of the exchange factors. Ras-GTP has wide range effector molecules of which the serine-threonine kinase RAF (MAPKKK = MAP kinase kinase kinase) is the most important effector. Activated RAF-kinases phosphorylate the MEK (MAPKK = MAP kinase kinase), which in turn phosphorylates and activates ERK (MAP Kinase) (Figure 1.3). ERK/MAPK has many nuclear as well as cytosolic substrates, such as transcription factors and signaling proteins. This mitogen stimulated Ras signaling results in a change in the pattern of gene expression, which may stimulate cell proliferation, promote cell survival or control cell differentiation.

Over the past few years, a number of Ras related genetic disorder known as RASopathies have been described (Shaw et al., 2007; Roberts et al., 2007; Schubbert et al., 2006; Tartaglia et al., 2007; Pandit et al., 2007; Razzaque et al., 2007; Digilio et al., 2002; Hart et al., 2002; Wallace et al., 1990; Aoki et al., 2005; Niihori et al., 2006). These disorders are mainly caused by germline mutations in genes encoding components of Ras/MAPK/pathway. All the mutations result in dysregulation of the RAS/MAPK pathway, share a predisposition to develop malignancies and with functional studies confirming a constitutively active Ras pathway. This underscores

the essential role the Ras pathway in normal embryonic and postnatal development.

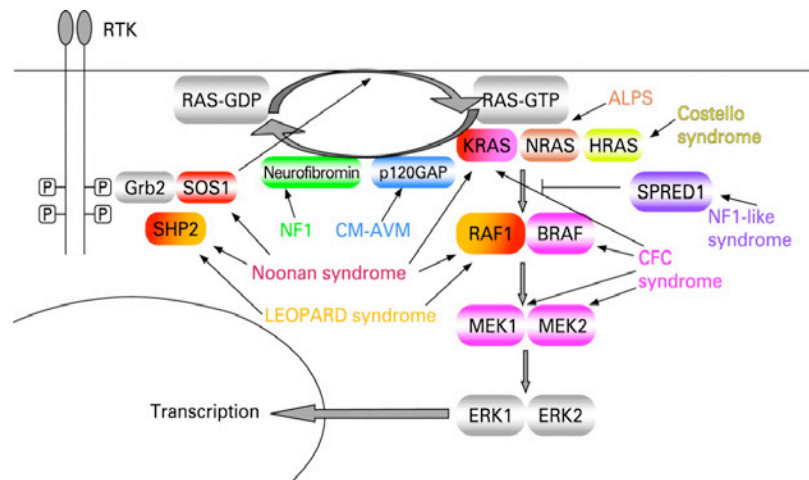


Figure 1.3 Overview of the Ras-MAPK pathway and the associated disorders
Reproduced from Denayer et al., 2008.

1.4 Ras lipidation

Cellular proteins undergo a vast array of dynamic and static modifications in their amino acid backbone, which can dramatically extend and regulate their functional output. After protein synthesis, post-translational modifications (PTMs) impart proteins with additional function and regulatory control beyond genomic information. This allows cells to maintain homeostasis of proteins and respond to extracellular signals. Proteins are often subjected to the different co- and post-translational modifications, such as phosphorylation, glycosylation and lipidation (lipid modifications). The covalent attachment of the lipid moieties represents an essential modification found in many Ras family proteins. Three types of lipid modifications are known so far: GPI-anchoring, prenylation and acylation (Figure 1.4). Prenylation includes attaching farnesyl and geranylgeranyl groups and acylation includes N-myristoylation, N-palmitoylation and S-palmitoylation (Bhatnagar and Gordon, 1997; Casey and Seabra, 1996; Resh, 1999).

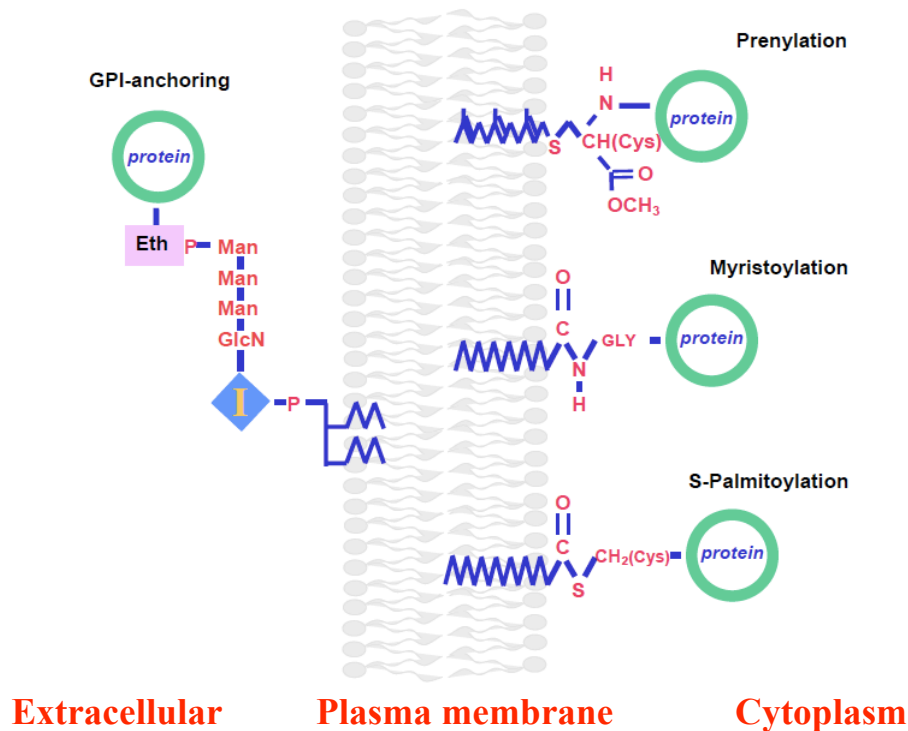


Figure 1.4 Major Lipid Modifications of Proteins

Prenylation is an irreversible post-translational modification of the protein by unsaturated fatty acids via the stable thioester bond. Myristoylation is a stable co-translational modification of the N-terminal glycine by the saturated myristic acid. Reversible S-palmitoylation occurs at the cysteine residues via the thioester-type bond. Gly-glycine, Cys-cysteine, Eth-ethanolamine, P-phosphate, Man-mannose, GlcN-glucosamine, I-inositol. Reproduced from Yeung Tony., 2008).

Prenylation is an irreversible lipid modification involving covalent attachment to the cysteine residues located near to the C terminus of the target proteins. Two types of prenyl groups are known to form thioester linkage with the cysteines, farnesyl (15-carbon) and geranylgeranyl (20-carbon) isoprenoids. Specific prenyltransferases catalyze the prenylation reaction: the CAAX prenyltransferases and the protein geranylgeranyltransferase type I. The prenylation is often required for the proper functioning of the modified proteins, either as a mediator of the membrane association, as a transport signal, or as a determinant for the specific protein-protein interactions (Casey and Seabra, 1996).

N-myristoylation occurs co-translationally by addition of the 14-carbon saturated myristic fatty acid to the N-terminal glycine residue localized within the consensus sequence. The myristoylation occurs via the amide bound catalyzed by the specific enzyme N-myristoyl-transferase (Raju and Sharma, 1999). Functionally,

myristoylation is involved in the membrane anchoring of the target proteins (Resh, 1999).

Palmitoylation occurs either through labile thioester linkage (**S-palmitoylation**) at cysteine residue or stable amide linkage (**N-palmitoylation**) at glycine/cysteine residue (Figure 1.5). In contrast to other static lipid modifications, the versatility of palmitoylation as a membrane interaction and the protein-sorting module is greatly enhanced by its reversibility. S-palmitoylation is unique in that it allows reversible attachment of palmitate or other saturated long chain fatty acids to the target proteins and is dynamically regulated by extracellular cues. The reversible nature of protein palmitoylation enables proteins to shuttle between intracellular compartments. Irreversible N-palmitoylation is observed with limited proteins, such as secreted morphogen Sonic hedgehog (Pepinsky et al., 1998). Among the cellular palmitoylated proteins, polypeptides involved in the signal transduction (e.g. GPCRs, α -subunits of G-proteins, Ras-protein, endothelial nitric oxide synthase, adenylate cyclase, phospholipase C and non-receptor tyrosine kinases) are often targets for this dynamic modification (Bijlmakers and Marsh, 2003; Dunphy and Linder, 1998). When discussing the possible functions of palmitoylation, a distinction must be made between “constitutive” and “dynamic” palmitoylation. “Constitutive” palmitoylation will refer to the original palmitoylation that takes place before the substrate protein reaches its final destination, in this case plasma membrane while “Dynamic” palmitoylation will refer to the regulation of the acylated state of the substrate protein once its began functioning within the signaling network.

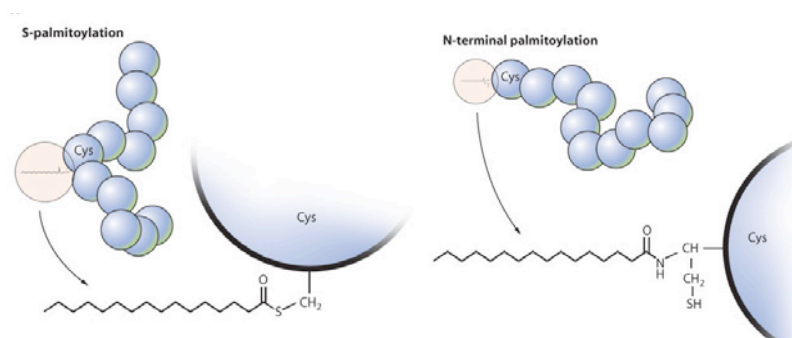


Figure 1.5 S-palmitoylation versus N-palmitoylation
Chemical structures of thioester-linked S-palmitoylation (**Left**) and amide-linked N-palmitoylation (**right**) palmitate attached to a protein. Reproduced from Resh, 2006.

1.5 Cellular palmitoylation machinery

1.5.1 Significance of Palmitoylation

Palmitoylation is versatile in modifying a protein function beyond membrane binding and targeting. The visual transduction cycle relies on signaling via a G-protein coupled receptor (GPCR)- Rhodopsin and G-proteins. Palmitoylation of G-protein coupled receptor Rhodopsin slows the shutoff of photoexcited rhodopsin, thereby extending the activity of this G-protein coupled receptor *in vitro* (Wang et al., 2005). Light absorption triggers isomerization of the rhodopsin- bound chromophore 11-cis-retinal to all-trans-retinal and thereby initiates visual signaling. Resynthesis of 11-cis-retinal begins with the conversion of all-trans-retinal to all-trans-retinol (vitamin A). The next step is esterification of all-trans-retinol with palmitate to generate an all-trans-retinyl ester. In this reaction, the retinal protein LRAT (lecithin retinol acyltransferase) functions as a palmitoyl acyl transferase. In addition, the reaction requires RPE65 (retinal pigment epithelium 65), a protein that exists in a membrane-bound, palmitoylated form (mRPE65) and a soluble form. mRPE65 functions as the palmitate donor (Xue et al., 2004). Moreover, palmitoylation generates a switch that alters ligand-binding specificity. The membrane-bound, palmitoylated RPE65 binds all-trans-retinyl esters, whereas the soluble form binds all-trans-retinol. Thus, ligand-binding selectivity is regulated during cycles of light and dark by protein palmitoylation. Protein palmitoylation also plays an important role in BMP-induced MAPK activation, osterix expression, and osteoblast differentiation (Leong et al., 2009). A study of Huntington protein, Htt illustrates altering dynamics of protein-protein interaction by palmitoylation (Yanai et al., 2006; Huang et al., 2004).

Myristoylated, palmitoylated protein Vac8 mediates vacuole fusion, vacuolar inheritance in yeast and cytosol to vacuole transport. Specificity of palmitoylation at the three-cysteine residues determines the functional relevance of Vac8. Palmitoylation of either Cys⁴ or Cys⁵ confers membrane binding and vacuole fusion whereas; palmitoylation at of Cys⁷ does not (Subramanian et al., 2006).

Furthermore, as palmitoylation is reversible, it allows dynamic regulation of membrane localization and trafficking. This has been best demonstrated in case of Ras proteins where the acylation state of Ras proteins regulates its dynamic localization (Rocks et al., 2005) and in case of synapses where palmitoylation

regulate membrane localization and activity of AMPA (Hayashi et al., 2005) and GABA_A receptor (Keller et al., 2004). Palmitoylation of the post-synaptic density protein PSD95 permits clustering of the protein at synapses and regulates synaptic strength (El-Husseini et al., 2002). A recent global study of the neural palmitoyl-proteome highlights the breadth of targets that are rapidly modulated by palmitoylation (Kang et al., 2008), further emphasizing the importance of this modification in dynamic biological processes.

1.5.2 Function of Palmitoylation

Palmitoylation regulate diverse functions of the modified proteins to bind to lipid bilayers (membrane binding), to cycle around in the cell (membrane trafficking), and to associate with specific membranes (membrane targeting) (Plowman and Hancock, 2005; Wright and Philips, 2006). Membrane binding of a protein is enhanced by hydrophobic insertion of the acyl chain into the lipid bilayer thus altering its localisation and function. Although in the case of Ras proteins, a single lipid modification such as prenylation is usually enough to transiently associate soluble protein with endomembranes (Choy et al., 1999; Shahinian and Silvius, 1995), kinetic trapping owing to its palmitoylation aids is stable anchoring of Ras proteins to the PM (Shahinian and Silvius, 1995). Membrane targeting may occur by kinetic trapping. Addition of a palmitate by a Palmitoyl acyltransferase (PAT) yields a dually lipidated protein that has a long lived association with the membranes. The subcellular localisation of a PAT then determines topological distribution of a dually lipidated Ras protein. Upon encountering the membrane harboring its cognate PAT, the farnesylated Ras protein is palmitoylated and is stably associated with that compartment. Targeting of palmitoylated proteins into membrane rafts can be accounted for by the saturated nature of the fatty acyl chain. Saturated fatty acids prefer to insert into liquid ordered raft domains rather than the bulk plasma membrane (Webb et al., 2000; Liang et al., 2001, 2004).

Interestingly, regulation of palmitate exposure has been suggested, similar to several N-terminal myristoylated proteins that undergo a “myristoyl switch”. Myristate is sequestered within a hydrophobic pocket of the protein in one state and then flipped out when the stimulus is applied such as ligand binding (Resh, 2004). Such a function has also been suggested for BET3, a protein involved in tethering transport vesicles to the Golgi. The crystal structure reveals a molecule of palmitate completely buried

within a hydrophobic channel of the protein (Turnbull et al., 2005).

A newly defined role of palmitoylation is as a checkpoint of protein quality control as described in case of yeast chitin synthase Chs3 (Lam et al., 2006) and yeast SNARE protein Tlg1 (Valdez-Taubas and Pelham, 2005). Palmitoylation of Chs3 serves as an indicator of proper protein folding and loss of palmitoylation leads to protein aggregation and retention in ER thus regulating ER export of this multi membrane spanning protein (Lam K.K et al., 2006).

1.5.3 Ras Acylation cycle

Cycles of de-/reacylation (Figure 1.6) contribute to the specific localization and rapid inter-compartmental exchange of peripheral, palmitoylated proteins like Ras. Typically all Ras proteins undergo three steps of post-translational modifications, which include prenylation at the cysteine of C-terminal CaaX region, proteolysis of terminal AAX and carboxymethylation at the ER. H and Nras undergo an irreversible farnesylation as well as secondary modification- palmitoylation imparting reversibility and dynamic behavior. These modifications render Ras molecules extremely hydrophobic hence increasing their affinity towards cellular membranes. Ras acylation cycle is mainly regulated by two sets of enzymes- Palmitoyl acyl transferases (PATs) and thioesterases. Subcellular specificity of PATs and ubiquitous expression of thioesterases regulates the Ras acylation status. Thus ensuring Ras enrichment in cellular compartments essential for its functioning. H/Nras is trapped at Golgi apparatus since Golgi serves as primary site of palmitoylation (Rocks et al., 2010), catalyzed by Golgi resident palmitoylating enzymes (PATs) (Hancock et al., 1989, 1990). After palmitoylation at the Golgi, palmitoylated Ras is enriched at the PM via vesicular transport (Choy et al., 1999). On the other hand, a depalmitoylation step catalyzed by an Acyl-Protein Thioesterase (APT) releases the protein by cleaving the palmitoyl anchor hence reducing Ras affinity for PM. This results in retrograde trafficking back to Golgi membranes by a non-vesicular pathway (Goodwin et al., 2005). However, the mechanism detailing transport of depalmitoylated Hras and Nras (together with several other palmitoylated Ras proteins) to Golgi apparatus for another round of palmitoylation has not been described so far and is a matter of further investigation. Chapter 4 of this thesis provides details regarding the PDE δ mediated regulatory mechanism for depalmitoylated Ras proteins and how it shields the lipid moiety of depalmitoylated, farnesylated Ras and prevents its binding to other

subcellular membranes such as ER in the vicinity and aqueous cytosolic environment. PDE δ thus enhances the encounter rate of depalmitoylated Ras for Golgi. Ras acylation cycle thus maintains the PM and Golgi localization of Ras by countering entropic homogenization of Ras and hence ensuring its compartment related activity.

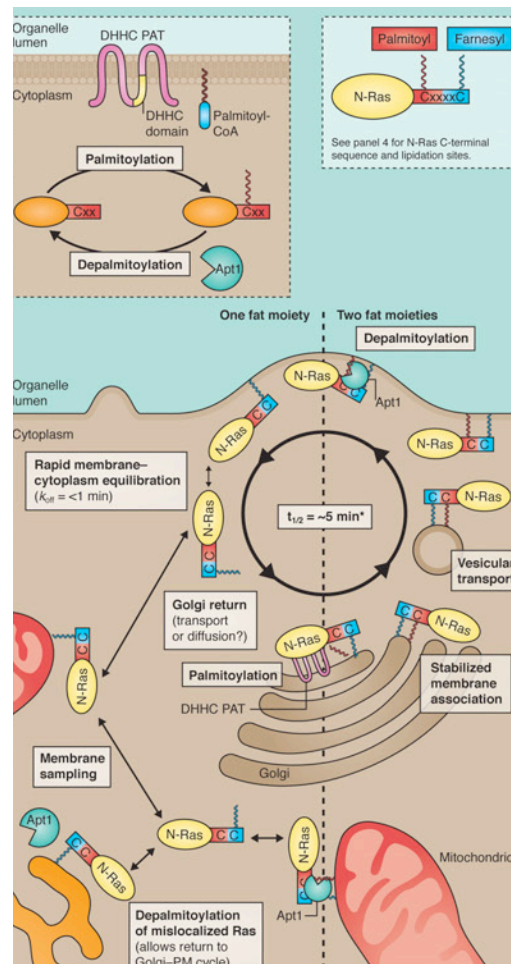


Figure 1.6 Schematic representation of Ras acylation cycle
Reproduced from Conibear and Davis, 2010.

1.5.4 Enzymology of palmitoylation

New insights into mechanism of protein palmitoylation have been provided with the identification of palmitoyl acyl transferases (PATs). PATs catalyze the attachment of palmitate to protein substrates. Much of the difficulty in working with these proteins arose from the fact that many PATs are integral membrane proteins, and thus largely insoluble in water. Palmitoylation has been shown to occur spontaneously *in vitro* in number of cases. The presence of palmitoyl-CoA alone can be enough to induce transfer of the palmitate moiety to an exposed cysteine residue. A basic environment

is required to de-protonate the cysteine residue to create a thiolate ion. This thiolate ion can then undergo nucleophilic attack of the partially positive carbonyl on the palmitoyl moiety. After resolution of the tetrahedral intermediate formed between the target protein and the palmitoyl-CoA, the palmitate is transferred to the target protein. Since the cytoplasm of a cell is a reducing environment, the prospect that this occurs *in vivo* has credibility. Most of the cytosolic acyl-CoA in the cell is bound to acyl-CoA binding proteins (ACBPs). This sequesters acyl-CoAs and provides a mechanism for minimizing otherwise uncontrolled effects of acyl-CoAs on cellular processes. Since it is highly dubious that *in vivo* palmitoylation reflects acyl-transfer under physiologically relevant conditions, a protein/enzyme mediated transfer mechanism has been proposed.

1.5.5 DHHC family of Palmitoyl acyl transferases

The enzymes that mediate palmitoylation- thiol directed Palmitoyl acyltransferases (PATs) are polytopic membrane proteins implying that cellular palmitoylation reaction occur at cytosol-membrane interface. There are 23 putative S-palmitoyl transferases in mammals and 7 in yeast characterized by presence of DHHC (aspartate-histidine-histidine-cysteine) motif within a 50 amino acid cysteine- rich domain denoted as $CX_2CX_9HCX_2CX_2CX_4DHHCX_5CX_4NX_3FX_4$ (Mesilaty-Gross et al., 1999; Putilina et al., 1999). In addition to the central DHHC domain three further sequence motifs have been identified in members of the DHHC family (Figure 1.7). A DPG (aspartate-proline-glycine) motif has been identified just to the C-terminus of the second transmembrane region. A TTxE (threonine-threonine-any-glutamate) motif has also been identified after the fourth transmembrane helix (Mitchell et al., 2006). A third motif towards the C-terminus of many proteins has been identified that contains a conserved glycine and asparagine (González Montoro et al., 2009). The large numbers of these DHHC proteins are coupled with their localization to distinct membrane compartments (Ohno et al., 2006) implying that the cellular palmitoylation machinery is a highly regulated and coordinated system.

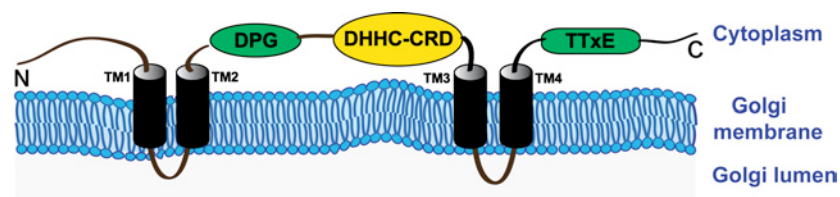


Figure 1.7 Domain organization and topology of DHHC family PATs

1.5.6 Sequence conservation and phylogeny of DHHC domain

Searching translated genomic databases with a 51 amino acid region that encompasses the DHHC-CRD region revealed a large number of eukaryotic DHHC proteins, but no examples of prokaryotes or archaea sequences have been found. This appears to coincide with the widespread occurrence of protein palmitoylation in eukaryotes and its apparent absence in prokaryotes. The sequence and predicted domain organization of a large number of eukaryotic DHHC proteins were compared (Figure 1.8). The sequences include 8 DHHC proteins from *S. cerevisiae*, 9 in *Trypanosoma brucei*, 23 in *D. melanogaster*, 16 in *C. elegans*, 18 in *Takifugo rubripes*, 31 in *Arabidopsis thaliana*, and 23 in *Homo sapiens* (GenBank). All DHHC proteins, with the exception of yeast Ynl155W, are polytopic integral membrane proteins with four or more transmembrane domains (Figure 1.8). The DHHC-CRD is generally located between TM2 and TM3, which is predicted to put it on the cytosolic face of the membrane along with the N terminus that precedes TM1 and the C terminus that lies after TM4.

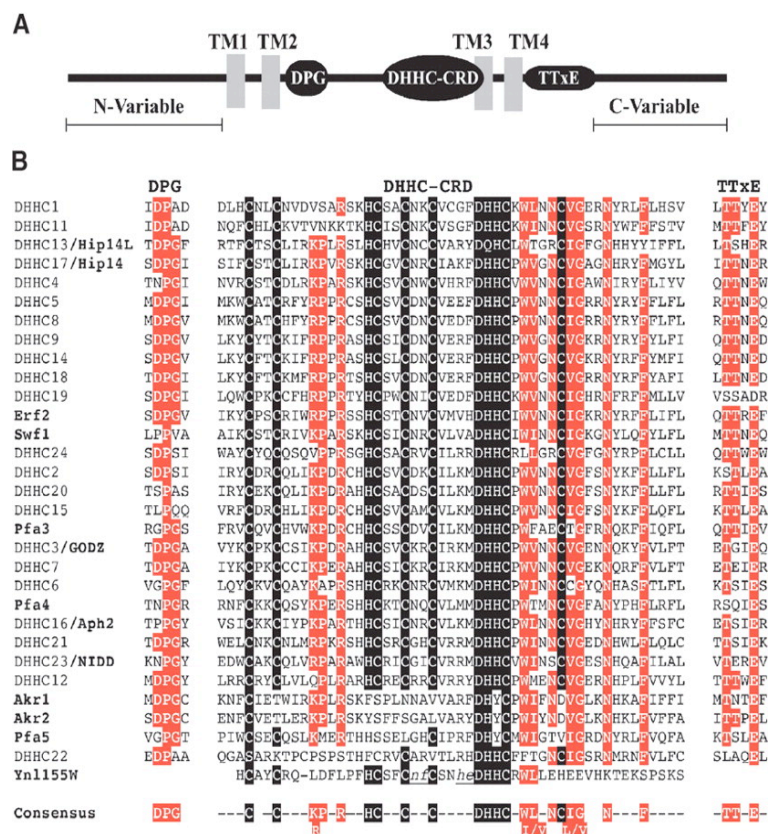


Figure 1.8 Homology and phylogeny of DHHC (aspartate-histidine-histidine-cysteine) proteins

(A) Schematic diagram of a DHHC domain protein. The N-terminal region, transmembrane domains (gray boxes; TM), DPG (aspartate-proline-glycine) motif, DHHC, TTxE (threonine-threonine-asparagine-glutamate) motif, and

C-terminal regions are indicated. **(B)** The 51 amino acid core sequence derived from the DHHC of human and yeast Erf2 homologs was aligned using ClustalX. Two classes of conserved residues are highlighted. The cysteine, histidine, and aspartate residues that make up the DHHC domain are shaded black. Additional conserved residues found in the DPG, DHHC, and TTxE motifs are shaded red. The letters nf represent the sequence NEDF (asparagine-glutamate-aspartate-phenylalanine), and the letters he represent the sequence HRLKE (histidine-arginine-leucine-lysine-glutamate). Reproduced from Mitchell D.A et al., 2006.

1.5.7 Yeast, mammalian PATs and their substrate specificity

Yeast DHHC Family of Proteins

DHHC-CRD domain has been identified in various known as well as putative PATs in both yeast and higher eukaryotes. In addition to Akr1 and Erf2, there are 5 yeast DHHC proteins identified (Mitchell et al., 2006) so far. Protein palmitoylation can clearly contribute to membrane binding, membrane targeting, and membrane trafficking. These effects can be explained by multiple molecular mechanisms (Figure 1.9). Membrane binding is enhanced by hydrophobic insertion of the acyl chain into the lipid bilayer. Membrane targeting may occur by kinetic trapping: For some proteins, once the protein is modified by a membrane-bound PAT, the palmitoylated protein remains trapped in that particular membrane because of the strength of the hydrophobic interaction between the palmitate moiety and the bilayer (Shahinian and Silvius, 1995; Schroeder et al., 1996). Thus, in some cases, the localization of the PAT determines the initial site of localization of the modified protein (**Figure 1.9**).

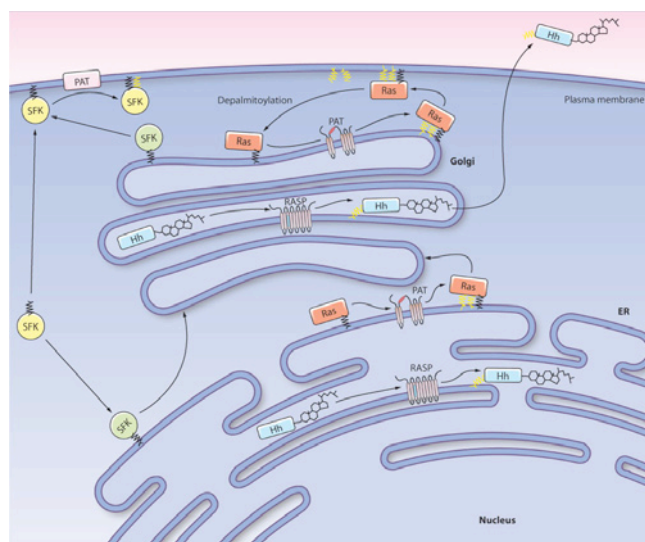


Figure 1.9 Schematic representation of the intracellular sites of protein palmitoylation

Ras proteins (red) are palmitoylated at the cytoplasmic surface of the ER and then traffic through the secretory pathway to the inner leaflet of the plasma membrane, where they can be depalmitoylated. Depalmitoylated Ras becomes repalmitoylated at the Golgi surface. Hh (Hedgehog) also traffics

through the secretory pathway. N-palmitoylation of Hh may occur within the lumen of the ER, the Golgi, or both. The dually lipidated (cholesterol + palmitate) Hh protein is then secreted from the cell. SFKs are cotranslationally N-myristoylated on soluble polysomes in the cytosol. SFKs such as Fyn appear to traffic directly to the plasma membrane, where palmitoylation occurs. Other SFKs such as Lck traffic through the secretory pathway. Palmitoylation could occur during biosynthetic transit or at the plasma membrane. Reproduced from Marilyn D. Resh, 2006.

Consistent with this model, the yeast DHHC proteins are widely distributed on cellular membranes. Erf2 (Bartels et al., 1999), Swfl (Valdez-Taubas and Pelham, 2005) and Pfa4 (Ohno et al., 2006) reside on the ER. Akrl and Akr2 are localized at the Golgi (Roth et al., 2002; Ohno et al., 2006), Pfa5 is found at the plasma membrane (Ohno et al., 2006) and Pfa3 is localized on the vacuole (Smotryst et al., 2005). Recent evidence also suggests that Swfl localizes to actin patches, however the majority of Swfl's function here appears to be independent of its PAT activity (Dighe and Kozminski, 2008). Over the years various DHHC proteins: substrate pairs have been identified using yeast genetics and /or biochemical analysis (**Figure 1.10**).

A global analysis of protein palmitoylation performed in yeast has considerably expanded the palmitoyl-proteome (Roth et al., 2006). The analysis identified thirty-five new palmitoyl-proteins, increasing the yeast palmitoylproteome to fifty-four proteins. Among the proteins identified was a family of amino acid permeases, which fall into the subclass of palmitoylated proteins with multiple transmembrane domains. The site of palmitoylation in these permeases is a cysteine located at the extreme C-terminus within a 'FWC' sequence (Roth et al., 2006). Whether this palmitoylation consensus sequence extends outside of this family of proteins has yet to be determined. Similar studies involving deletion of genes encoding DHHC proteins either singly or in combination in yeast strains revealed putative enzyme: substrate pairs and demonstrated that DHHC proteins account for most cellular palmitoylation events (Roth et al., 2006). Of note, the family of amino acid permeases was discovered to be palmitoylated by Pfa4 (Roth et al., 2006), the same DHHC protein that palmitoylates another multiple transmembrane domain protein Chs3 (Lam et al., 2006). Also, Pfa3 for instance, was reported to be a general palmitoyltransferase with minimal specificity towards the protein substrate (Nadolski and Linder, 2009).

DHHC PAT*	Selected substrates	Localization	Phenotype when the gene for the DHHC PAT is deleted	Biochemical reconstitution of PAT activity for substrate	Reduced or absent palmitoylation of substrate when the gene for the DHHC PAT is deleted
Erf2–Erf4 ¹	Ras2	ER	Ras2 mislocalization	Yes	Yes
Akr1	Yck2, Sphingoid Lcb4	Golgi	Yck2 mislocalization; Lcb4 mislocalization, reduced phosphorylation, loss of downregulation during stationary phase	Yes	Yes
Pfa3	Vac8	Vacuole	Vac8 mislocalization; altered vacuole morphology under stress	Yes	Yes
Pfa4	Amino-acid permeases, Chs3	ER	ER retention of Chs3	No	Yes
Swf1	SNARE proteins, including Tlg1	ER	Missorting of Tlg1 to the vacuole, ubiquitylation	No	Yes
Pfa5	Unknown	Plasma membrane	NA	NA	NA
Akr2	Unknown	Golgi	NA	NA	NA

Figure 1.10 DHHC-CRD palmitoyl acyl transferases (PATs) and their substrates

(Adapted from Marilyn D. Resh, 2006)

Mammalian DHHC Family of Proteins

The mammalian family of DHHC proteins is significantly larger than the yeast family however very little sequence similarity has been described apart from DHHC domain. There are 23 human DHHC genes denoted DHHC1-DHHC24 (DHHC10 is not annotated as a gene). Significant progress has been made in characterizing this large family of enzymes with respect to substrate identification, localization, and expression patterns (Mitchell DA et al., 2006). Like in yeast, the mammalian DHHC proteins have a diverse distribution and a majority localize to the ER/Golgi (Ohno et al., 2006). One of the most fruitful approaches to identify enzyme: substrate pairs was pioneered by (Fukata et al., 2004). Unfortunately, numerous studies on DHHC proteins have led to only partial agreement regarding the substrate specificity of DHHC proteins (Hou et al., 2009).

1.6 Targeting of peripheral membrane proteins

1.6.1 Lipid composition of plasma membrane:

The plasma membrane is rich in anionic phospholipids (15-20%), the majority of which are preferentially distributed to the inner leaflet (Quinn, 2002; Leventis and Silviu, 1998). This distinctive composition confers a uniquely negative surface charge to the cytosolic aspect of the cell membrane. The lipid composition of the plasma membrane largely comprises of the zwitterionic, electrically neutral lipids of phosphatidylcholine (PC) and phosphatidylethanolamine (PE) constituting ~ 60%,

with the charged monovalent acidic lipid phosphatidylserine (PS) constituting ~ 25% of the inner leaflet of the plasma membrane (Figure 1.11). Compared to other phospholipids, phosphoinositides are present in very low levels (1-2%) and have a strong negative valency of 4 (McLaughlin et al., 2002). Yet, the polyvalent anionic phosphoinositides, PI(4)P, PI(4,5)P₂ and PI(3,4,5)P₃, play an important role in nearly all aspects of cell physiology, as much as they may be laterally sequestered into microdomains by polycationic peptides (McLaughlin and Murray, 2005; Di Paolo and De Camilli, 2006; Lemmon, 2003; Heo et al., 2006; Golebiewska et al., 2006).

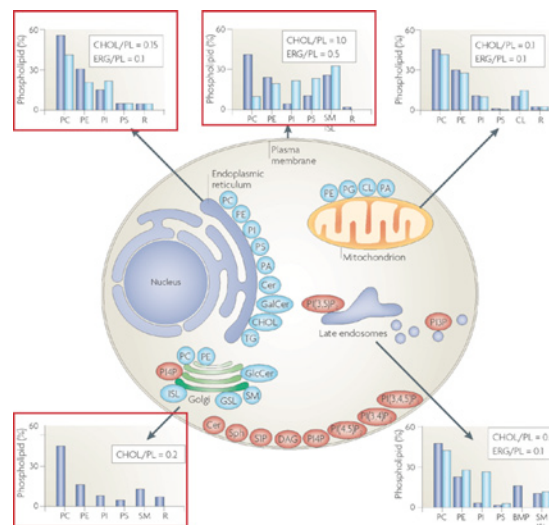


Figure 1.11 Lipid composition of membranes in different cell compartments

The lipid compositional data (shown in graphs) are expressed as a percentage of the total phospholipid (PL) in mammals (blue) and yeast (light blue). As a measure of sterol content, the molar ratio of cholesterol (CHOL; in mammals) and ergosterol (ERG; in yeast) to phospholipid is also included. The figure shows the site of synthesis of the major phospholipids (blue) and lipids that are involved in signaling and organelle recognition pathways (red). It should be appreciated that the levels of signaling and recognition lipids are significantly below 1% of the total phospholipid, except for ceramide (Cer). The major glycerophospholipids assembled in the endoplasmic reticulum (ER) are phosphatidylcholine (PtdCho; PC), phosphatidylethanolamine (PtdEtn; PE), phosphatidylinositol (PtdIns; PI), phosphatidylserine (PtdSer; PS) and phosphatidic acid (PA). In addition, the ER synthesizes Cer, galactosylceramide (GalCer), cholesterol and ergosterol. Both the ER and lipid droplets participate in steryl ester and triacylglycerol (TG) synthesis. The Golgi lumen is the site of synthesis of sphingomyelin (SM), complex glycosphingolipids (GSLs) and yeast inositol sphingolipid (ISL) synthesis. PtdCho is also synthesized in the Golgi, and may be coupled to protein secretion at the level of its diacylglycerol (DAG) precursor. Approximately 45% of the phospholipid in mitochondria (mostly PtdEtn, PA and cardiolipin (CL)) is autonomously synthesized by the organelle. BMP (bis (monoacylglycerol) phosphate) is a major phospholipid in the inner membrane of late endosomes (not shown). PG, phosphatidylglycerol; PI(3,5)P₂, phosphatidylinositol-(3,5)-bisphosphate; PI(4,5)P₂, phosphatidylinositol-(4,5)-bisphosphate; PI(3,4,5)P₃, phosphatidylinositol-

(3,4,5)-trisphosphate; PI4P, phosphatidylinositol-4-phosphate; R, remaining lipids; SIP, sphingosine-1-phosphate; Sph, sphingosine. Adapted from Won Do Heo et al., 2006.

1.6.2 Surface charge of the plasma membrane:

The accumulation of negative charges on the inner leaflet creates an electric field equivalent to 10^5 V/cm that strongly attracts cationic molecules, including inorganic ions and peptides or proteins with clusters of cationic residues (Figure 1.12) (McLaughlin, 1989; Olivotto et al., 1996). This electrostatic attraction is effective within the Debye length (estimated to approximate 1 nm) and, as described by the Gouy-Chapman theory, is directly proportional to the surface charge density and inversely proportional to the ionic strength (McLaughlin S. 1989). It is important to note that the surface potential is different from the transmembrane potential, which is largely an electrodiffusional (Nernst) voltage generated by the differential permeability of the membrane to inorganic ions. Transmembrane proteins, such as ion channels, are sensitive to the combined surface and Nernst potentials, while peripheral proteins are only subjected to the surface potential on their side of the bilayer.

The negative surface charge on the inner leaflet of the plasma membrane is crucial for the targeting of many intracellular signaling proteins. Most of the peripheral proteins including the myristoylated alanine-rich C-kinase substrate (MARCKS), c-Src, K-Ras4B and Rac1 contain a cationic motif that is necessary for their electrostatic attachment to the inner leaflet of the plasmalemma (McLaughlin and Aderem, 1995; Hancock et al., 1990; Choy et al., 1999; Michaelson et al., 2001; Murray et al., 1998).

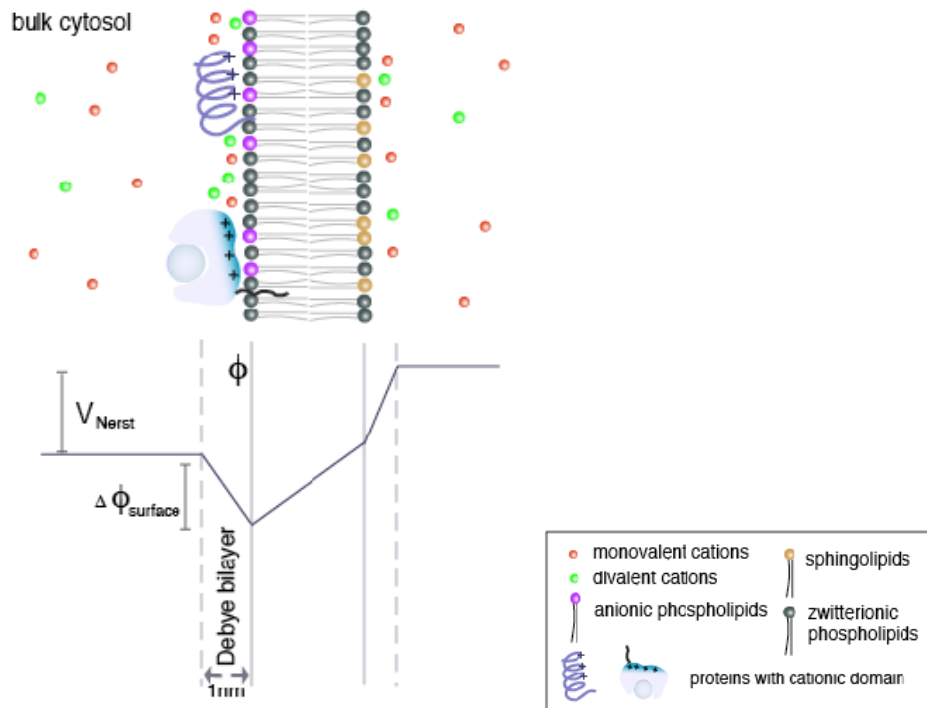


Figure 1.12 Surface potential attracts cationic molecules to the inner leaflet of the plasma membrane

Accumulation of anionic phospholipids on the inner leaflet of the plasma membrane leads to generation of a negative surface potential (ϕ_{surface}) within the Debye layer (~ 1 nm). The surface potential is directly proportional to the surface charge density and inversely proportional to the ionic strength of the cytosol. This potential attracts cations and macromolecules with polybasic motifs. A smaller surface potential is also thought to exist on the outer surface, due to the accumulation of negatively charged glycolipids and proteins. Superimposed on these surface potentials is an electrodiffusional (Nernst) potential caused by an imbalance in the transmembrane ionic composition and the differential ionic conductance of the membrane. While peripheral proteins are affected by the surface potential on the inner leaflet, they are not affected by the transmembrane (Nernst) potential. Transmembrane proteins are sensitive to the combined effects of surface and transmembrane potential. Reproduced from Yeung Tony, 2008.

It has become apparent that the electrostatic affinity of these polycationic proteins with the plasmalemma is not depended on the structure of the cationic motif but is regulated by equilibrium binding of positively charged amino acid clusters to negatively charged PI(4,5)P₂ and PI(3,4,5)P₃ lipids in the PM (Heo et al., 2006). Thus, mutations that alter the original sequence yet preserve the net cationic charge of the region have no effect on the localization of the protein (Hancock et al., 1990; Choy et al., 1999; Michaelson et al., 2001; Roy et al., 2000; Okeley and Gelb, 2004). Another important feature of such kind of equilibrium binding is proximity to an acylated or prenylated moiety (eg. a myristoyl or a farnesyl tail) that is important in membrane targeting.

1.6.3 Polycationic Ras subfamily proteins

Most of the polybasic cluster containing Ras superfamily proteins are distributed into 3 categories (Figure 1.13A): Polybasic proteins with N-terminal myristoylation sites, *polybasic-myristoyl* (such as Arl), with C-terminal prenylation sequence, *polybasic-prenyl* (Kras4B, Diras1/2, Rheb, RhebL1 etc) or without primary lipid modifications (Rit), *polybasic nonlipid PM targeting motifs*. Unstructured clusters of basic residues consisting of four or more Lys or Arg residues at positions 5 to 20 from the C-terminus (Heo et al., 2006), target a wide variety of peripheral Ras proteins to the plasma membrane (Figure 1.13B). In case of Ras subfamily proteins, polybasic proteins are basically categorized as polybasic-prenylated, polybasic-nonprenylated or polybasic-palmitoylated (Figure 1.13). A keen observation of these PM targeting proteins indicates presence of more lysine or arginine residues in proximity to the C-terminus thus ensuring strong affinity towards more anionic PM as compared to other endomembranes.

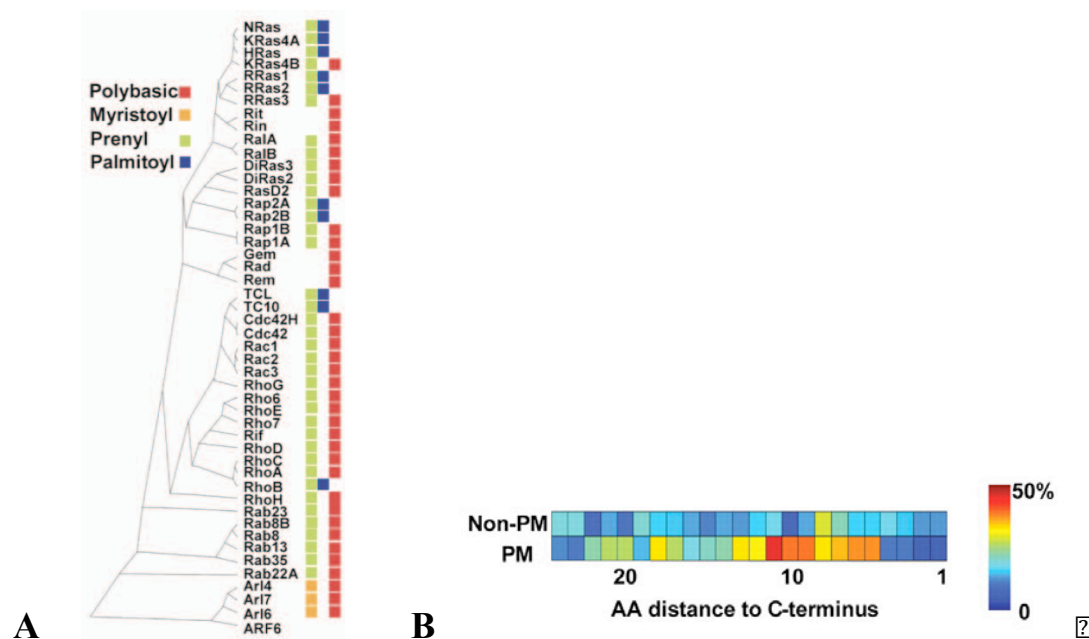


Figure 1.13 Polybasic C-terminal containing Ras superfamily proteins

(A) Phylogenetic tree of 48 small GTPases that were identified to be partially or fully localized to the PM. Individual membrane targeting elements are color coded: red for polybasic clusters and blue, green, and orange for palmitoyl, prenyl, and myristoyl consensus sequences, respectively. (B) Correlation between PM localization and the presence of lysine residues in region 5 to 20 amino acids from the C terminus. Reproduced from Heo et al., 2006.

1.6.4 Regulation of polybasic Ras proteins at the PM

To ensure that proteins that are intended to bind the inner aspect of the plasma membrane are not mistargeted to other (non-membranous) polyanionic structures, two independent components are required: an electrostatic interaction and partitioning of a hydrophobic tail into the lipid bilayer. Hence, altering the electrostatic interaction can affect membrane specific localization of these peripheral proteins. As originally proposed by (McLaughlin and Aderem, 1995), modulating net charges of either protein or surface charges of the membrane could release bound polypeptides, thereby operating as binary electrostatic switches. In this manner, electrostatics could provide a new dimension to the regulation of a large number of GTPases and of transmembrane proteins with juxtamembrane cationic domains (Strickfaden et al., 2007; Bivona et al., 2006; Kim et al., 1994). There are several ways to toggle the electrostatic switch (Figure 1.14). One is to alter the net charge of the bound protein through phosphorylation of residues in the immediate vicinity of the cationic motif. It has been demonstrated that phosphorylation of serine and/or threonine residues within the cationic domain of K-Ras, MARCKs, and the MAPK cascade scaffold protein Ste5 cause their dissociation from the membrane (Bivona et al., 2006; Allen and Aderem, 1995; McLaughlin and Aderem, 1995). Phosphorylation of amino acids in a positively charged protein domain decreases its net charge thereby dissociating it from the membrane.

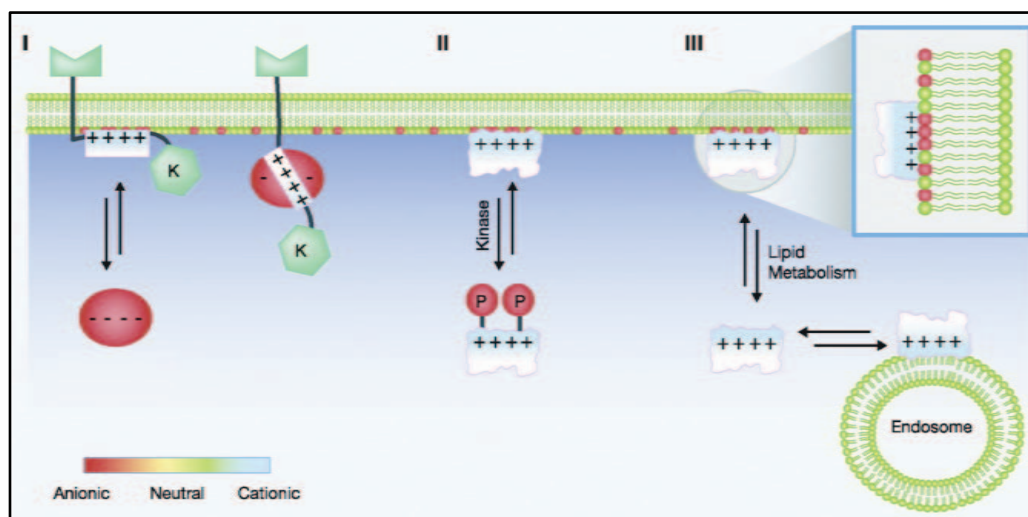


Figure 1.14 Changes in the net charge of the protein modulate the effect of surface charge on protein localization

(I) Basic residues can be electrostatically shielded by binding anionic proteins. (II) Similarly protein phosphorylation (red P) dissociates cationic residues from the membrane. (III) Lipid metabolism alters the membrane

charge leading to dissociation of cationic clusters from the plasma membrane. The membrane surface charge of the endocytic and secretory pathways may equally affect protein localization to intracellular signaling platforms. Anionic, neutral, and cationic clusters or species are respectively shown in red, green, and blue as indicated by the electric charge gradient scale. (Reproduced from Goldenberg and Steinberg, 2010).

Alternatively, instead of modifying the protein charges, changes in the electric field at the inner surface of the PM may take place. Treatment of intact cells with calcium ionophore leads to activation of phospholipase C (PLC) thus elevating cytosolic calcium levels which shields the anionic surface charges of the PM (Figure 1.15). On the other hand, PLC activation induces hydrolysis of +4 valency anionic phospholipids such as $\text{PI}(4,5)\text{P}_2$ thus reducing the anionic charges on the PM. Thirdly, calcium released from ER as a result of DAG production via $\text{PI}(4,5)\text{P}_2$ hydrolysis also aids in activating lipid scramblase, resulting in translocation of PS to the outer leaflet thus further altering the charges on the inner leaflet of the PM (Yeung et al., 2006). This ultimately leads to reduce affinity of polycationic proteins and hence causes their dissociation from the PM.

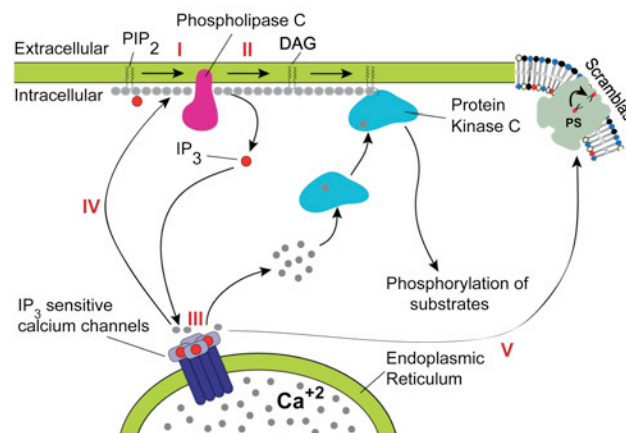


Figure 1.15 PIP_2 cleavage to IP_3 and DAG initiates intracellular calcium release and PKC activation

Diacylglycerol functions as a second messenger signaling lipid, and is a product of the hydrolysis of the phospholipid PIP_2 (phosphatidyl inositol-bisphosphate) by the enzyme phospholipase C (PLC) (a membrane-bound enzyme) that, through the same reaction, produces inositol triphosphate (IP_3). Although inositol triphosphate (IP_3) diffuses into the cytosol, diacylglycerol (DAG) remains within the plasma membrane, due to its hydrophobic properties. IP_3 stimulates the release of calcium ions from the smooth endoplasmic reticulum, whereas DAG is a physiological activator of protein kinase C (PKC). The production of DAG in the membrane facilitates translocation of PKC from the cytosol to plasma membrane. (Modified from Wikipedia, Erik Korte "PIP2 cleavage by PLC to release IP_3 and DAG").

1.7 Cyclic nucleotide Phosphodiesterases

Cyclic nucleotide second messengers (cAMP and cGMP) play a central role in signal transduction and regulation of physiologic responses. Cyclic nucleotide phosphodiesterases (PDEs) form a large superfamily of enzymes that regulate the cellular levels of second messengers, cAMP and cGMP, by controlling their rates of degradation. They regulate the compartmentalization, duration and amplitude of cyclic nucleotide signaling which is attributed to their unique tissue, cellular, and sometimes-subcellular distribution. 21 genes, 11 families encoding PDE with varying selectivities for cGMP and cAMP have been identified in human genome, and the corresponding proteins have been characterized in terms of their physiological and regulatory properties (Conti and Jin, 1999; Francis et al., 2001; Soderling and Beavo, 2000).

Of the 11 PDE families, 3 families specifically hydrolyze cGMP (PDE5, PDE6 and PDE9), 3 families hydrolyze cAMP (PDE4, PDE7 and PDE8) and 5 families hydrolyze both cyclic nucleotides with varying efficiency (PDE1, PDE2, PDE3, PDE10 and PDE11). The substrate specificity of the PDE enzymes is defined by the intricate network of hydrogen bonds formed by the conserved glutamine with the purine ring.

1.7.1 cGMP PDEs

cGMP controls a diverse array of physiological processes, including platelet function, neutrophil adhesion, sperm motility, neuronal signaling, and vascular, smooth muscle relaxation. cGMP PDEs are categorized in three major subgroups: cGMP-stimulated cyclic nucleotide PDEs, photoreceptor cGMP-specific PDEs, and cGMP-binding cGMP-specific PDEs.

cGMP PDEs play a key role in controlling epithelial cell functions such as ciliary motility and cytokine production. Moreover, cGMP specific PDE6 thermodynamics is of great importance for the photo-transduction responses in mammalian eye.

1.7.2 cGMP specific phosphodiesterase-6 (PDE6)

PDE6 is a key component exclusively expressed in photoreceptors, where it exists in a rod and cone specific form. Retinal rod *cGMP* phosphodiesterase (PDE6 family) is

an effector enzyme in the vertebrate visual transduction cascade. Unlike other known PDEs that form homodimers, the rod PDE6 catalytic core is a heterodimer composed of two catalytic subunits PDE6 α and PDE6 β , encoded by PDE6A and PDE6B genes respectively, two identical inhibitory subunits PDE6 γ , encoded by PDE6G (Baehr et al., 1979; Deterre et al., 1988) and one regulatory subunit PDE6 δ , encoded by the PDE6D gene (Norton, 2004). The cone PDE6 enzyme represents two identical catalytic subunits PDE6 α' , encoded by PDE6C gene and two identical cone-specific inhibitory subunits PDE6 γ' , encoded by PDE6H gene (Gillespie and Beavo, 1988) (Figure 1.16).

The catalytic subunits of PDE6, α and β , undergo posttranslational prenylation that is farnesyl- and geranylgeranyl side chains respectively at the C-terminus CAAX (C=cysteine, A=aliphatic, X=any amino acid) motif. The prenylated, carboxymethylated C-termini are responsible for anchoring PDE6 to the outer segment of disk membrane and thereby facilitating two-dimensional collisions with transducin during visual excitation (Anant et al., 1992; Qin et al., 1992). The inhibitory γ -subunits binding, is regulated allosterically by cGMP binding to a protein domain of the catalytic subunits, the so-called GAF domain (Norton et al., 2000). A putative fourth 17kDa subunit was co-purified with bovine retinal phosphodiesterase (Hurwitz et al., 1985) and was later referred to as delta subunit-PDE δ . The structure of the membrane bound rod PDE6 holoenzyme is $\alpha\beta\gamma_2$, whereas it is $\alpha'\gamma'_2$ for cone PDE6 (Artemyev et al., 1996).

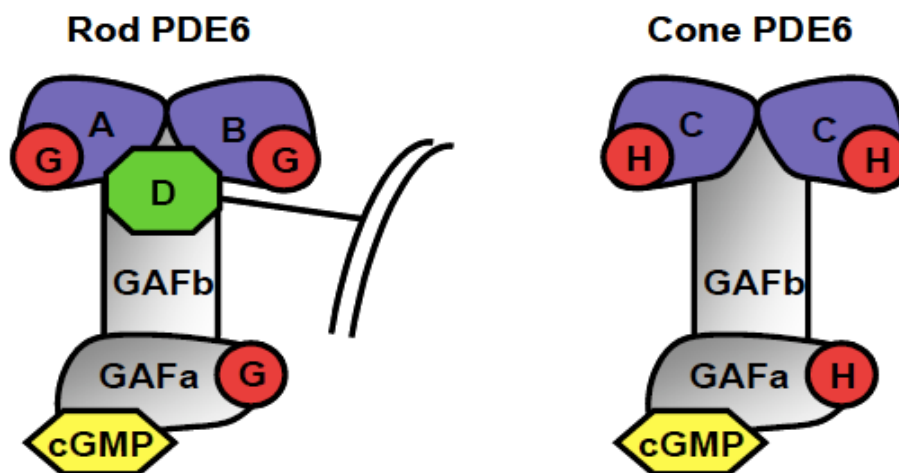


Figure 1.16 Schematic subunit composition and structure of rod and cone

The catalytic core of rod PDE6 enzyme is represented by PDE6A and PDE6B subunits. The catalytic core of cone PDE6 is represented by two identical PDE6C subunits. The regulatory domains of both rod and cone

PDE6 are represented by tandem GAF domains (GAFa and GAFb). Both enzymes contain regions at their catalytic and GAF domains that interact with the respective inhibitory subunit PDE6G and PDE6H. The PDE6D subunit, which is unique to the rod PDE6 enzyme, is also shown in the picture. PDE6D interacts with the catalytic core (PDE6A and PDE6B) of the rod PDE6 enzyme and defines enzyme solubilization from the plasma membrane. Reproduced from Ridge et al., 2003.

1.7.3 PDE6 enzymes

A number of hereditary eye diseases are caused by mutation in PDE6 genes. A form of dysplasia (RDC, rod-cone dysplasia) in Irish Setter Terrier is caused by a point mutation in codon 807 of PDE6 β , leading to C-terminal truncation of PDE β and to a total loss of catalytic activity in rods (Suber et al., 1993). The homozygous nonsense-mutation in *PDE α* and *PDE β* leads in humans to a form of autosomal-recessive retinitis pigmentosa and a missense mutation in *PDE β* causes an autosomal-dominant form of inherited congenital stationary night blindness (Lorenz et al., 1998).

1.7.4 PDE6 regulatory binding protein (PDE δ)

17kDa delta subunit (PDE δ) of Phosphodiesterase6 (PDE6) was originally reported to act in a negative feedback mechanism during light activation to impair transducin-mediated activation of PDE6. In photoreceptor rod cells binding of the PDE6 catalytic subunits results in the release of the complex from disk membranes and hence the termination of transducin-induced activation of PDE6 (Zhang et al., 2007). However, the role of PDE δ extends beyond retinal tissue and the photo-transduction cascade. This highly conserved protein sequence has been detected in a variety of non-retinal tissues, including, heart, placenta, lung, brain, skeletal muscles and liver (Ahumada et al., 2002; Ma and Wang, 2007). PDE δ has also been proposed to play a role in recycling and internalization of human prostacyclin receptor (Wilson and Smyth, 2006) and vesicular transport as an effector for, or via forming a complex with Arl2 and Arl3 (Hanzal-Bayer et al., 2002) and Rab13 (Marzesco et al., 1998).

Cytoplasmic prenyl binding factor PDE δ have been proposed to assist in H/N/Kras signaling in a similar way to Rho- and Rab-GDIs (Guanine-nucleotide Dissociation Inhibitors) that bind to prenylated GDP-bound small G-proteins and thus constitute a cytoplasmic pool of inactive G-proteins (Hanzal-Bayer et al., 2002). PDE δ has been reported as a binding partner for various prenylated small G proteins like K/Hras and non-prenylated small G proteins like Arl2 and Arl3 (Hanzal-Bayer et al., 2002; Nancy et al., 2002; Bhagatji et al., 2010; Chen et al., 2010). However, details about

function of PDE δ subunit in modulating Ras signaling and its consequences on Ras function are still elusive.

1.7.5 PDE δ homologues

The sequence of PDE δ is highly conserved among mammals, since the bovine, canine, and murine proteins only differ from the human protein by one non-conservative (T68A) and 0-3 conservative changes. In *Drosophila melanogaster* and the eyeless nematode *Caenorhabditis elegans*, orthologues exist sharing 61% and 69% identity with human PDE δ , respectively. Subsequent research for proteins closely related to PDE δ revealed significant similarities with the UNC-119/RG4 group of proteins from mammals, zebrafish, *C. elegans*, and *D. melanogaster*. These proteins were identified on the basis of their high expression in the *C. elegans* nervous system as well as in mammalian photoreceptor cells (Ershova et al., 1997). But to date, still very little is known about their function. The ubiquitous expression of PDE δ in tissues other than retina and expression of PDE δ orthologs in eyeless *C. elegans*, which do not express other prenylated PDE6 subunits (Li et al., 1998), supports additional functions, distinct from its role in photoreceptor physiology and stability in rod and cone cells (Florio et al., 1996; Marzesco et al., 1998; Zhang et al., 2007).

1.7.6 Similarities between PDE δ and RhoGDI

Besides an unrelated N-terminal region of 50-90 residues, the alignment of human PDE δ with human RG4 and RhoGDI proteins demonstrated that they exhibit 47% similarity and 22% identity for the human proteins, extending through to their C-termini. Alignment of UNC119/RG4, PDE δ and RhoGDI of human origin also revealed that the structural features, conserved between PDE δ and RhoGDI, are also conserved in UNC119/RG4 (Figure 1.17). These structural features contain the elements responsible for their immunoglobulin-like fold as well as hydrophobic residues at conserved positions, which could line the surface of a prenyl-binding pocket. The prenyl-binding domain of RhoGDI is similar in size to, PDE δ , and there is 18% amino acid identity between the PDE δ and the prenyl-binding domain of RhoGDI (Cook et al., 2000). The structure-based sequence alignment shows that the residues lining the inner surface of this hydrophobic pocket are in identical or very similar positions in both proteins, suggesting that not only the fold but also the lipid-binding pockets are common features of both PDE δ and RhoGDI. After

superimposition of the protein backbones of RhoGDI and PDE δ , the geranylgeranyl moiety of Cdc42 fits surprisingly well over almost its complete length into the hydrophobic pocket of PDE δ (Figure 1.17) (Linari et al., 1999).

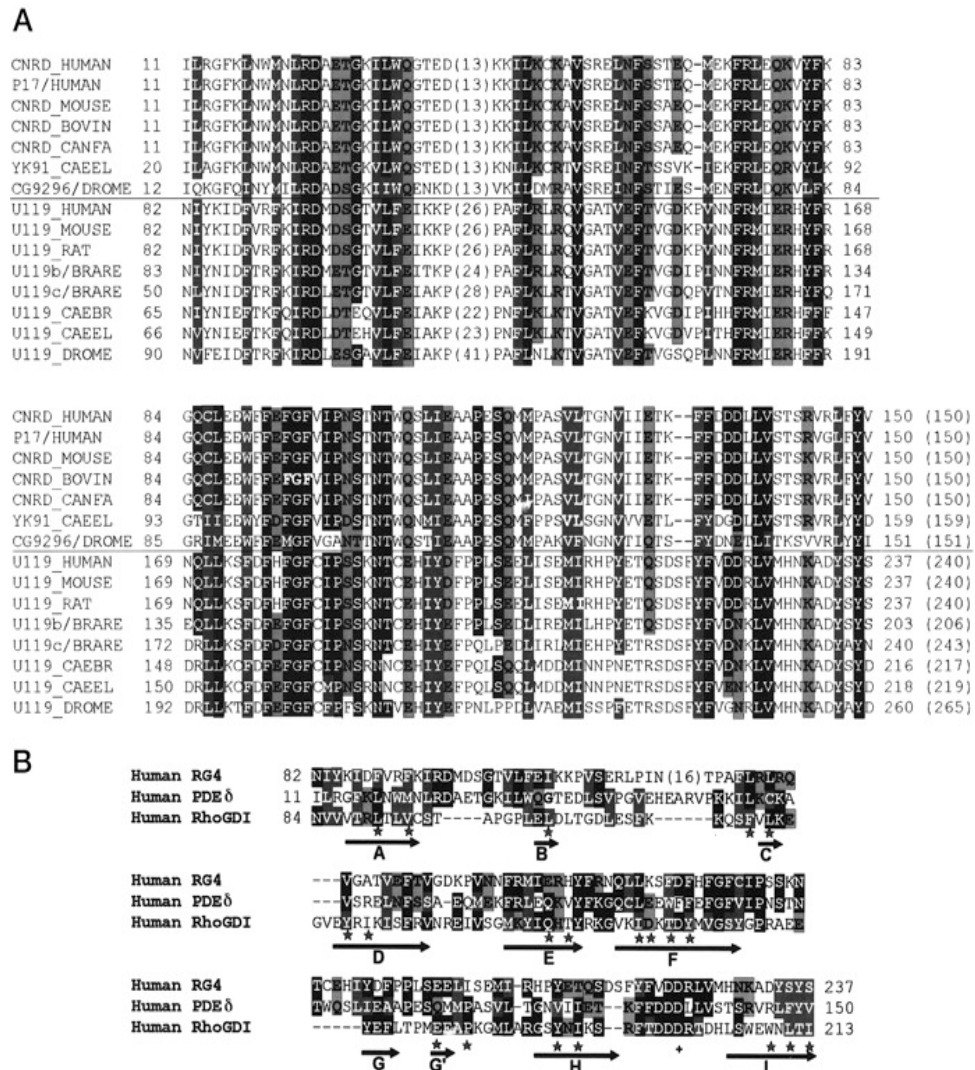


Figure 1.17 Alignments of PDE δ , RhoGDI and UNC119/RG4 proteins
 (A) Alignment of PDE δ (upper part) and UNC119/RG4 proteins (lower part) from various species. Identities are shown as white on a black background; similarities are shaded gray (white and black letters for hydrophobic and non hydrophobic amino acids, respectively). Sequences that could not be aligned are indicated by number of residues; Total length of each sequence is indicated within brackets. BRARE, *Danio rerio* (zebrafish); CAEEL, *Caenorhabditis elegans*; CAEBR, *Caenorhabditis briggsae*; CANFA, *Canis familiaris*; DROME, *Drosophila melanogster*. (B) Alignment of human RG4, PDE δ and RhoGDI proteins. Annotations are the same as in A. Reproduced from Nancy et al., 2002.



Figure 1.18 Structural homology of PrBP/PDE δ , unc119, and RhoGDI

Multiple sequence alignment of PrBP (PDE δ) (8 vertebrate, 5 invertebrate sequences), unc119 (7 vertebrate, 5 invertebrate sequences), and RhoGDI (15 vertebrate, 4 invertebrate sequences) identified amino acids that are invariant within each protein family (vertical lines within boxes). Sites that are identical in all sequences of PrBP (PDE δ) and unc119 are shown as lines connecting PrBP (PDE δ) and unc119 boxes. Structural homology of the prenyl-binding pocket shown at the top as α -helix and β -sheet is based on comparison of the three-dimensional structures for PrBP (PDE δ) (PDB 1KSH; (Hanzal-Bayer et al., 2002) and RhoGDI (PDB 1DOA; Hoffman et al., 2000). Reproduced from Zhang H. et al., 2006.

Hanzal-Bayer et al., 2002 and Nancy V et al., 2002 therefore proposed that UNC119/RG4, PDE δ and RhoGDI define a new family of proteins, conserved through evolution, that interact with prenylated proteins (Figure 1.18). Such a high evolutionary conservation suggests that the function of PDE δ has been conserved as well. In addition, the C-terminus of PDE δ contains putative SRV and FYV sequence motifs described as necessary and sufficient for the interaction with PDZ domains present in many proteins of synaptic, septate and tight junctions (PSD95, Dlg, ZO-1) (Marzesco et al., 1998). PDZ domains are involved in sub membranous protein networks and in the recruitment of proteins to specific plasma membrane microdomains (Fanning and Anderson, 1998; Kornau et al., 1995).

1.7.7 PDE δ interaction with Arl2 and Arl3: Structural insight

Other than the isoprenylated proteins identified from yeast-two-hybrid, PDE δ also interacts with certain proteins in a prenylation independent manner, such as Arl2 and Arl3 (Linari et al., 1999). Arl2/3 are small GTPases belonging to Arf family of Ras superfamily. Arf family members play important roles in intracellular vesicular trafficking processes. Crystal structure of PDE δ co-crystallized with Arl2/GTP verified the presence of a hydrophobic domain packed by two opposite β –sheets (Figure 1.19). A similar, anti-parallel, β -strand interaction has been observed in the complexes of Ras proteins with the Ras-binding domain of Raf (Nassar et al., 1995) or RalGDS (Huang et al., 1998; Vetter et al., 1999) and PI3-Kinase (Pacold et al., 2000).

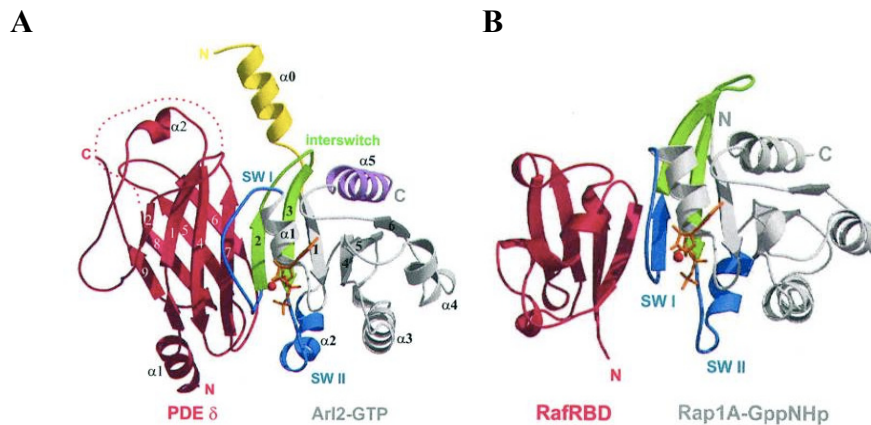


Figure 1.19 Crystal structure

Ribbon diagram: Arl2-GTP: PDE δ (A) & Rap1A-GppNHp: RafRBD (B).
Reproduced from Hanzal-Bayer et al., 2002.

The binding of Arl2 to PDE δ was found independent of lipids, suggesting that PDE δ can interact with proteins in two ways: (1) through a lipid binding pocket (Figure 1.20) and, (2) b-sheet/b-sheet interactions (Hanzal-Bayer et al., 2002). The interaction between PDE δ and Arl2 or Arl3 is GTP-specific, indicating that PDE δ is a bona fide effector protein of these two GNBPs. In addition to this, PDE δ exhibits a strong inhibitory effect on dissociation of GTP from Arl2 and Arl3 (Linari et al., 1999), which is not unusual for an effector (Herrmann et al., 1995).

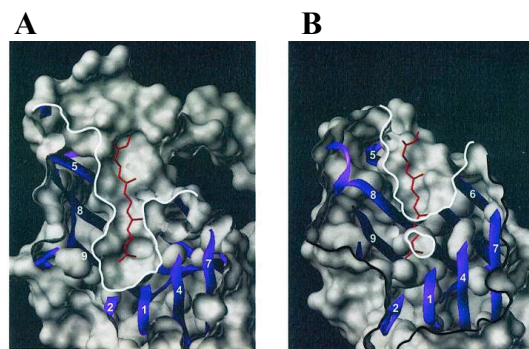


Figure 1.20 The hydrophobic pocket in PDE δ

(A) Cut through a surface representation of RhoGDI showing the deep hydrophobic pocket with the geranylgeranyl moiety (red) from Cdc42-GDP (violet ribbon). (B) PDE δ has a similar but less deep hydrophobic pocket. The geranylgeranyl moiety of Cdc42 has been positioned by superimposition of the protein backbone of RhoGDI to PDE δ , followed by a small manual adjustment within the pocket. (Hanzal-Bayer et al, 2002).

1.7.8 PDE δ and Arl2 role in maintaining photoreceptor physiology

In photoreceptor cells biochemically identified binding partners of PDE δ include rhodopsin kinase (GRK1), cone pigment kinase (GRK7) and the PDE catalytic subunits (PDE α , β), all of which are prenylated at their C-termini. It has been

demonstrated that absence of PDE δ in retina impairs transport of prenylated proteins, particularly GRK1 and cone PDE, to rod and cone outer segments, resulting in altered photoreceptor physiology and a phenotype of a slowly progressing rod/cone dystrophy (Zhang et al., 2007) (Figure 1.21).

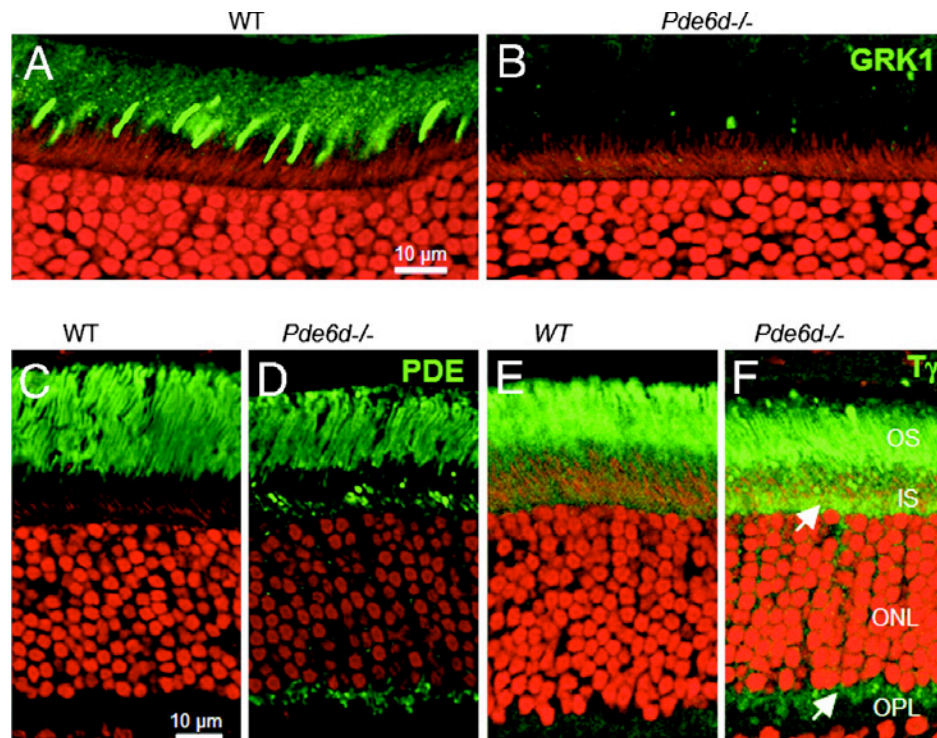


Figure 1.21 Localization of rod and cone PDE6 in WT and Pde6d^{-/-} retina
 Confocal immunolocalizations of GRK1, rod PDE6, and T γ in WT (A, C, and E) and PDE δ ^{-/-} (B, D, and F) retina cryosections. (A and B) Immunoreactivity for GRK1 is prominent over rod and cone outer segments (OS) in WT retina although nearly undetectable in PDE δ ^{-/-} rod and cone OS. (C and D) Localizations of rod PDE6 in WT and PDE δ ^{-/-} retinas, respectively (MOE antibody; Cytosignal). Rod PDE6 labeling is typically restricted to rod OS in WT retina. Aberrant distribution of rod PDE6 was observed in inner segments and synaptic terminals of PDE δ ^{-/-} rods. (E and F) Distributions of rod T γ in WT and PDE δ ^{-/-} retinas, respectively. T γ mislocalizes, in part, to the inner segment, perinuclear, and synaptic regions (white arrows) of PDE δ ^{-/-} photoreceptors. In each image, propidium iodide (red) demonstrates the extent of the ONL by binding nucleic acids (both DNA and RNA). IS, inner segments; OPL, outer plexiform layer. Reproduced from Zhang et al., 2007.

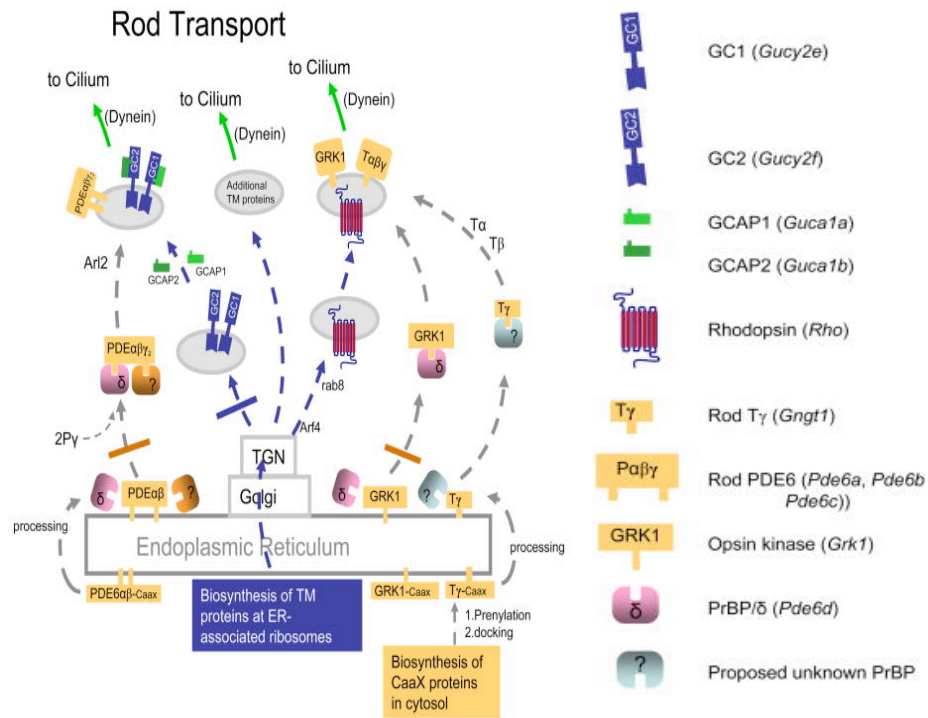
1.7.8.1 Hypothetical model for PDE δ function in photoreceptors

Based on observations from Zhang et al., 2007, it has been hypothesized that PDE δ may be involved in the intracellular trafficking of isoprenylated phototransduction proteins (GRK1, PDE6 $\langle\alpha, \beta\rangle$) from the inner segment to the outer segment. It is presumed that in WT photoreceptors, prenylated cone PDE6 α' , farnesylated GRK1 and farnesylated rod and cone T γ depend on a prenyl binding protein (PrBP) such as

PDE δ for extraction from the ER and delivery to a transport carrier. Subsequently, prenylated proteins may co-transport to the outer segments using vesicles with a transmembrane protein as guide, either rhodopsin or GC1/GC2, or another integral membrane protein (Figure 1.22A). In the absence of PDE δ , selected prenylated proteins fail to be delivered to a carrier and do not transport (Zhang et al., 2007). In rods, GRK1 is largely absent in *PDE δ -/-* ROS. In cones (Figure 1.22B), PDE δ deletion affects both GRK1 and cone PDE6 equally although the former is farnesylated and the latter geranylgeranylated. Hence in the absence of PDE δ , solubilization of these proteins is inhibited and transport to the COS impeded.

However details regarding several of these claims are still elusive, such as whether PDE δ prefers farnesylated or geranylgeranylated substrates. Geranylgeranylated PDE β is expressed as a dimer with its farnesylated partner PDE α and hence it is not clear if PDE δ binds to only its farnesylated subunit and not directly to geranylgeranylated subunit. Also, mechanisms of delivery of prenylated proteins as cargo to a vesicular transport carrier in photoreceptors are also unknown. Since PDE δ co-crystallized with Arl2 (Hanzal-Bayer et al., 2002), an Arf-like small GTPase, it is conceivable that Arl2 or its close cousin Arl3 may play a role in either docking to vesicles or in mediating release of prenylated cargos from PDE δ . In this work, we have answered these queries and have demonstrated how PDE δ regulate prenylated substrates such as Ras family proteins spatial distribution, signaling and its function in tumor models. Also the mechanism and putative role of Arl2/3 in regulating PDE δ function has been described.

A



B

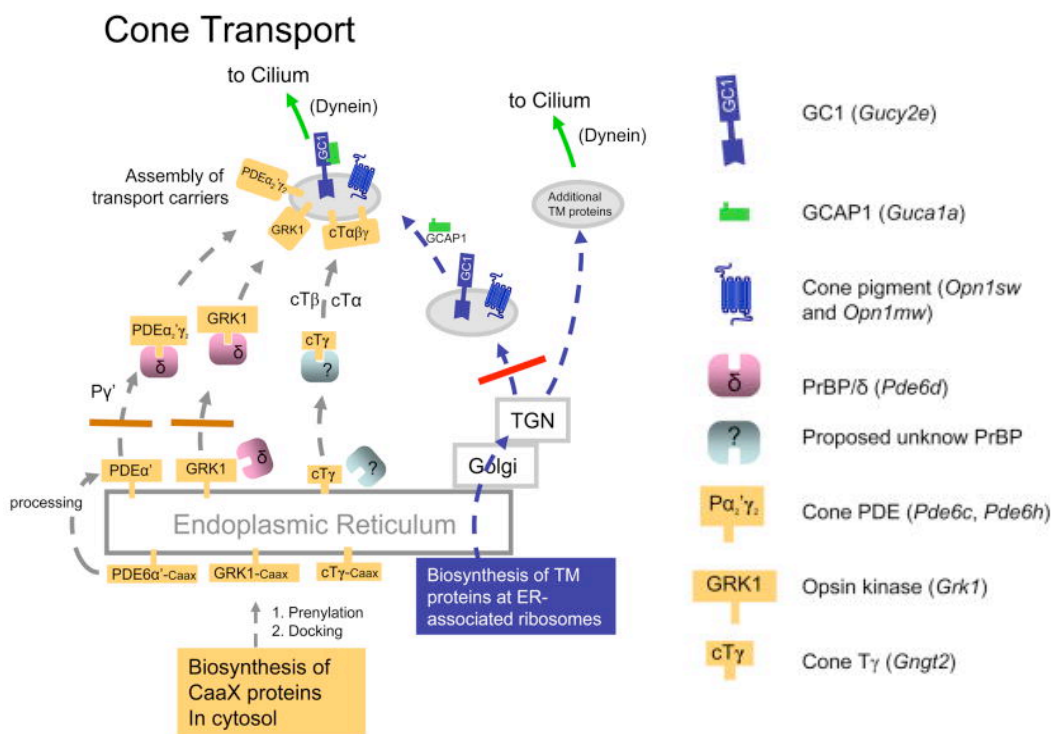


Figure 1.22 Putative model of post-biosynthesis transport of membrane proteins in rods and cones

Reproduced from Zhang et al., 2007.

II

Experimental Procedures

2.1 Materials

2.1.1 Antibodies and Dyes

Primary antibodies:

Anti GFP (JL-8)	Mouse	Clontech (632381)
Anti GST	Goat	Genescript (A01379)
Anti Rheb	Rabbit	Cell signaling (4935)
Anti Nras (F-155)	Mouse	SCBT (sc-31)
Anti Hras (C-20)	Rabbit	SCBT (sc-520)
Anti Kras-2B (C-19)	Rabbit	SCBT (sc-521)
Anti PDE δ (N-15)	Goat	SCBT (sc-50260)
pErk1/2	Mouse	Cell signaling (CS-9106)
Total Erk1/2	Mouse	Cell signaling (CS-4696)
pRaf	Rabbit	Cell signaling (CS-9427)
Total Raf	Mouse	BD-biosciences (610152)
Cyclophilin-B	Rabbit	Alexis (ALX-210-237)
Anti GAPDH (C65)	Mouse	Calbiochem (CB-1001)

Secondary antibodies:

Donkey anti Mouse IR-Dye 800CW	Licor
Donkey anti Mouse IR-Dye 680CW	Licor
Donkey anti Rabbit IR-Dye 680CW	Licor
Donkey anti Goat IR-Dye 800CW	Licor
Donkey anti Goat IR-Dye 680CW	Licor
IRDye 800CW Streptavidin	Licor

Dyes:

Cy3 and Cy5 mono-reactive dye	Amersham
-------------------------------	----------

2.1.2 Buffers and solutions

TBS (Tris buffered saline)	100 mM Tris·Cl pH 7.50 0.9% NaCl (w/v)
Sample loading buffer (5X)	250 mM Tris pH 6.8 10% SDS 50% glycerol 10% BME
SDS PAGE electrophoresis buffer (10X)	250 mM Tris 1.92 M glycine 1% SDS
Transfer buffer	25 mM Tris 192 mM glycine 20% Methanol
Imaging medium	1X Hanks with Ca ²⁺ and Mg ²⁺ 0.6% Glucose 10mM HEPES
Cell lysis buffer (1X)	20 mM Tris-HCl (pH 7.5) 150 mM NaCl 1 mM Na ₂ EDTA 1 mM EGTA 1% Triton 2.5 mM sodium pyrophosphate 1 mM beta-glycerophosphate 1 mM Na ₃ VO ₄ 1 µg/ml leupeptin

2.1.3 Consumables and kits

QIAprep Spin Miniprep Kit	Qiagen
HiSpeed Maxi Plasmid Kit	Qiagen
QIAquick Gel Extraction kit	Qiagen
QIAquick PCR purification kit	Qiagen
RNAeasy Spin Kit	Qiagen
OneStep RT-qPCR SYBR Green Kit	Qiagen
35 mm glass bottom culture dishes	MatTekCorp.

2.1.4 Reagents

Bryostatin	Enzo lifesciences
2-Bromopalmitate	Sigma
Cycloheximide	Sigma
Palmostatin-B	
Protease inhibitor cocktail	Roche's
Phosphatase inhibitor cocktail	Roche's
N-Ethylmaleimide (NEM)	Sigma
Hydroxylamine	Fluka
Biotin-BMCC	Pierce
Protein G-sepharose®	Sigma
Odyssey blocking buffer	Licor
Glutathione sepharose-4B	GE lifesciences
Effectene	Qiagen
GenJet™	Signagen
Lipofectamine 2000	Invitrogen

2.1.5 Plasmids

A) Dictyostelium constructs:

Human Hras wt, Hras C181S/C184S and Hras C181S/C184S CLLL were cloned C-terminal of GFP tag into an extra chromosomal expression vector pDm317 [act15] || GFP:gene || neoR || Extrachr (Ddp1-based) bearing neomycin resistance gene, using Bgl-II and Spe-I restriction sites. The open reading frame of the GFP gene is under the control of an endogenous actin-15 promoter and succeeded by an actin-8 terminator. Same inserts were cloned into pDM134, which contains a hygromycin-resistance cassette and the entire monomeric red fluorescent protein mRFP-mars.

B) Mammalian expression constructs:

Plasmid constructs for mCit-Nras wt, mCit-NrasG12D, GalT-ECFP, paGFP-Hras C181S/C184S have been described elsewhere (Rocks et al., 2010; Rocks et al., 2005). mCitrine fusion constructs for different Ras proteins including Rap1a, Rap1b, Rheb, Rheb-L1, Rap2c, Rap2b, Rap2a, Kras4B were generated by insertion of full length respective cDNAs into mCitrine-C1 or EYFP-C1 vector (Clontech). mCh-Hras C181S/C184S, paGFP-Hras C181S/C184S CLLL, paGFP-NrasG12D ΔCaaX, paGFP-Nras ΔCaaX, mCit-NrasG12D ΔCaaX, mCit-HrasC181S/C184S CLLL, mCit-

Kras $\Delta(2E)$, $\Delta(4E)$, $\Delta(6E)$ were generated by site directed mutagenesis. mCh-/dCh-PDE δ , mTFP-PDE δ were generated by inserting BspEI/EcoRI PCR amplified PDE δ fragment. GST fused 3X-RBD (52-132 amino acids) tandem fragments were cloned into pGEX-2T vector spaced with a 9 amino acids linker (-NLSSDSSNS). GST-PDE δ , GST-RafRBD recombinant proteins for pull down assays were kindly provided by Dr Lothar Gremer and Doro Vogt.

2.1.6 Cell culture medium & antibiotics

Dulbecco's Modified Eagle's medium (DMEM)	Sigma
Roswell Park Memorial Institute medium (RPMI-1640)	Invitrogen
HLC5 medium	Formedium
trypsin/EDTA	PAN
Fetal bovine serum (FBS)	PAN
Penicillin/streptomycin	Gibco
Amphotericin-B	PAN
Hygromycin-B	Sigma
G-418	Sigma
OptiMEM I + GlutaMax	Invitrogen
PBS (1X)	PAN
L-Glutamine	PAN
Imaging medium	Invitrogen

2.1.7 siRNA

Table 2.1: PDE δ specific siRNA sequences

Canine PDEδ specific siRNA sequences	
siRNA-1	Sense: r(GAA GGG CUU CAA ACU AAA U) dTdT Anti Sense: r(AUU UAG UUU GAA GCC CUU C) dAdG
siRNA-2	Sense: r(AAC UGG GAA UGU UAU CAU A)dTdT Anti Sense: r(UAU GAU AAC AUU CCC AGU U)dAdG
siRNA-3	Sense: r(CGC UUA CCA CGA GAG CCA A)dTdT Anti Sense: r(UUG GCU CUC GUG GUA AGC G)dTdT
Human PDEδ specific shRNA sequences	
sh- 1	FI363813 TACTCTGGCAAGGAACAGAAGACCTGTCT
sh- 3	FI363815 GGCTTCAAACCTAAATTGGATGAACCTTCG
Murine PDEδ specific shRNA sequences	
sh-1	FI567650 ATATCCTGAGAGGCTTCAAACCTAAATTGG
sh- 2	FI567652 TCCACAAACACCTGGCAGTCCTTGATAGA
sh- 3	FI567651 AATCCTCAAGTGCAAGGCAGTGTCTCGAG
sh- 4	FI567653 CTTCTTGTCAGCACATCCAAAGTGAGGCT

2.1.8 Cell lines

MDCK (ATCC No. CCL-34)

Madin-darby canine kidney cells- MDCK cells are immortalized, epithelial cells derived from a kidney of an adult female cocker spaniel. They grow in a monolayer, attached to each other by regular cell-to-cell contacts

MDCK-f3

Virally Hras oncogene transformed derivative of MDCK cell line. They display long, spindle-like morphology and grow in multiple layers without regular cell-to-cell contacts.

HepG2 (ATCC No. HB-8065)

Human hepatocellular carcinoma cells- Derived from the liver tissue of a 15-year-old Caucasian American male with a well differentiated hepatocellular carcinoma. These cells are epithelial in morphology.

mPDAC

Murine Pancreatic ductal adenocarcinomas cells lines from explanted murine tumors were established using previously published methods (Olive et al., 2009; Schreiber et al., 2004; Skoulidis et al., 2010).

mPDAC (79990) - Tissue-specific conditional *KrasG12D* allele (Hingorani et al., 2003; Hingorani et al., 2005; Skoulidis et al., 2010) has been ‘knocked in’ to a single endogenous locus, and is expressed under native regulatory control just as in the corresponding human cancers. *KrasG12D* activation is triggered via tissue-specific expression of Cre recombinase, driven by the regulatory elements of the pancreatic and duodenal homeobox 1 (Pdx1) promoter, without concurrent expression of the *Trp53R270H* trans-dominant mutant.

mPDAC (79751, 79217, 80000, 87038) - tissue-specific conditional *KrasG12D* allele has been ‘knocked in’ to a single endogenous locus, and is expressed under native regulatory control. *KrasG12D* activation is triggered via tissue-specific expression of Cre recombinase, driven by the regulatory elements of the pancreatic and duodenal homeobox 1 (Pdx1) promoter, with concurrent expression of the *Trp53R270H* trans-dominant mutant.

BJ cells (ATCC No. CRL-252)

Primary human foreskin fibroblasts derived cell lines

a) BJ/hTERT/SV40-Hraswt: derived from BJ cells by ectopic expression of telomerase catalytic subunit (hTERT), the simian virus 40 large-T oncoprotein & Hras wt allele.

b) BJ/hTERT/SV40-HRasG12V: derived by ectopic expression of telomerase catalytic subunit (hTERT) in combination with two oncogenes (the SV-40 virus large-T oncoprotein and an oncogenic allele of Hras).

These cell lines were kindly provided by Dr. Christian Schmees.

2.2 Molecular biology techniques

2.2.1 Transformation of *E. coli*

DNA (0.5 µg plasmid DNA) was mixed with 100 µl of thawed competent bacteria and incubated on ice for 15 min. After heat shock at 42°C for 90 sec and incubation on ice for 1 min, 1 ml of LB medium was added and the mixture was incubated for 45 min in a shaker at 37°C. The bacteria were carefully pelleted by short centrifugation and the supernatant was decanted. The resuspended bacteria were plated on antibiotic containing agar plates that were incubated over night at 37 °C.

2.2.2 Transformation in *Dictyostelium* cells

3 x 10⁷ log phase cells were washed and suspended in electroporation buffer. 2µg DNA was added to the cuvette containing cells and incubated on ice for 5 min. The used field strength was 1.2 kV/cm; capacitance was 3 µF and a 600-Ω resistance. Hygromycin (1:1000 final; stock = 20mg/ml) and G418 (1:1000 final; stock = 50mg/ml) was added 20 h after the electroporation. Positive clones were picked and cultured in fresh medium containing selection markers after 2 days.

2.2.3 RNA preparation and RT-PCR

For quantification of PDEδ mRNA content in MDCK cells, RNA was extracted using RNA-easy mini kit (Qiagen). RNA concentrations were measured and purity was verified spectroscopically. RT-PCR was performed using Quantifast-1 step RT-PCR kit (Qiagen) in an iQ5 thermocycler (Biorad). Gene specific amplification primers were ordered from Qiagen. Downregulation efficiency was estimated from samples treated with anti-PDEδ siRNA, non-targeting controls, mock controls and GAPDH siRNA as reference by applying Pfaffl's method (Livak and Schmittgen, 2001; Pfaffl, 2001).

2.3 Cell biology techniques

2.3.1 Mammalian cell culture

MDCK cells (Madine-Darby Canine Kidney, ATCC number: CCL-34) were routinely maintained in MEM Eagle's supplemented with 10 % fetal bovine serum, penicillin (1000U/ml) and streptomycin (1g/ml) at 37°C and 5% CO₂. For live cell microscopy, cells were cultured on 35-mm glass bottom MatTek dishes (Nalgene Nunc International, Naperville, IL) and transferred to low bicarbonate DMEM without phenol red supplemented with 25 mM HEPES pH 7.4 (imaging medium). Transfections were performed with Effectene transfection reagent (Qiagen) for plasmids and RNAiVect transfection reagent (Qiagen). Pancreatic cancer cell lines from explanted murine tumors were established using previously published methods (Olive et al., 2009; Schreiber et al., 2004; Skoulidis et al., 2010). All experiments using mPDAC lines reported in this study were conducted in early passage cell lines (\leq P10) grown in complete medium (DMEM+10%FBS+1% Penicillin/Streptomycin).

Stimulation with pharmacological reagents:

The cells were stimulated with 200 ng/mL recombinant human EGF, 100nM Bryostatin-1, 50 μ M Palmostatin-B, 50 μ M 2-bromopalmitate.

2.3.2 Dictyostelium cell culture

Wild type *D.discoideum* strain Ax2 cells were grown axenically in HL5 medium at 22°C. Transformation of *D.discoideum* amoebae was accomplished by electroporation using supercoiled DNA of pDm317 EGFP Hraswt, Hras C181S/C184S mutant. All transformants were maintained in G418 (20 μ g/ml).

Sample Preparation. For vegetative *D.discoideum* cells, 50-200ul of cell suspension from a confluent petridish was taken and added to 35mm dishes (MatTek Corp.). Cells were allowed to settle down and attach for 15-20 min and washed twice with 17mM phosphate buffer (pH 6.5). Measurements were performed on cells incubated in buffer.

For polarized cells and cell immobilization for FRAP experiments, cells from a confluent dish were washed in phosphate buffer and redissolved in 4.8ml phosphate

buffer and applied on top of 6 well non nutrient agar plate (800ul/well). Then allowed to dry for 20 min and incubated for 6 hours in an incubator at 22°C. For observation at higher magnification polarized cells growing on top of non-nutrient agar was carefully taken, inverted and placed in a 35mm dish (Mattek Corp.) with cells facing down and imaged.

2.3.3 Preparation of mammalian cell lysates

MDCK, HepG2 cells were grown in 35 mm cell culture dishes in DMEM with 10% FBS. Cells were starved for 20 hours in starving medium without serum. The starved cells were treated with EGF (200 ng/ml) and/or Palmostatin-B (50 µM). After washing cells twice with PBS, 200 µl of lysis buffer (containing protease inhibitors and phosphatase inhibitor cocktail I & II) was added to the cells and incubated for 10 min. Then the cells were scraped off the dish, transferred to a reaction tube and homogenized by passing several times through a 26-inch gauge needle. The resulting lysate was centrifuged for 30 minutes at 15,000 x g, 4°C and the pellet was discarded. The protein concentration of the supernatant was determined using the Bradford protein assay.

2.3.4 GST Pulldown Assay

50 µl GST, GST-RafRBD or GST-PDEδ fusion proteins were captured on 30 µl of pre-equilibrated GSH-sepharose beads for 30 min at 4 °C. Then 3 wash steps with an excess of assay buffer (30 mM Tris pH 7.5, 100 mM NaCl, 5 mM MgCl₂, 3 mM DTE and 0.1% Triton X-100) were performed. Whole cell lysates were isolated from mammalian MDCK cells expressing wild type Ras and their respective mutants. These lysates were incubated with GST/GST-RafRBD/GST-PDEδ loaded GSH-sepharose beads (as described above) for 30 min at 4 °C in a final volume of 500 µl assay buffer. After 4X washes, supernatant was removed and 25µl of 2X Laemmli buffer was added to the beads. Samples were then heated at 95°C for 5 min and SDS-PAGE was performed. For western blot analysis mouse anti-GFP (Clontech-632375) 1:5000, rabbit cyclophilin-B (Axxora-210237) 1:2000 and mouse anti-GST (Abcam-55129) 1:1000 were used. The primary antibody staining was visualized by using IR 680 Donkey anti-rabbit and IR 800 Donkey anti-mouse IgG (LICOR) on the Odyssey Infrared Imaging System.

2.3.5 RNA Interference

Alexa Fluor-647 labeled negative control siRNA and 4 canine-PDE δ specific siRNAs (Qiagen) (table 2.1) were designed from the transcript sequence retrieved from NCBI. siRNA transfections were performed using RNAifect (Qiagen) as prescribed by the company. Out of four sequences screened, three showed highest knockdown in MDCK cells with similar efficiency as deduced from both RT-PCR and western blotting whereas two sequences (si-1 and si-3) showed good knockdown efficiency against human and murine-PDE δ in BJ-(hTERT/SV40/HrasG12V) and mPDAC cells respectively. Dharmacon's ON-TARGET plus SMARTpool siRNA were also obtained to specifically target murine-PDE δ in different mPDAC clonal cell-lines.

siRNA transfection: 2×10^5 cells were seeded and cultured in full growth medium for 16h. After 16h, cells were transferred to Optimem + GlutaMax I (Invitrogen) and transfected with 200 nM siRNA-1, 100 nM siRNA-2, 100 nM siRNA-3 specific for PDE δ or non targeting control siRNA. After 10h of incubation, the transfection mix was aspirated and replaced with fresh Optimem + GlutaMax I. Cells were transfected the next day with paGFP HRasC181S/C184S (0.5 mg) or paGFP HRASC181S/184S CLLL (0.5 mg) or paGFP Nras-CaaX (0.5 mg) using Effectene transfection reagent. Approximately, 48h after siRNA transfections, live cell microscopy was performed.

2.3.6 Western blots

MDCK cells were plated at a density of 2×10^5 cells/ml in 35-mm MatTek dishes for 16h, then transfected with PDE δ specific siRNA and incubated for 48-72h. Cells were washed with ice cold PBS and 0.2 ml ice-cold lysis buffer containing protease inhibitors (Roche), phosphatase inhibitor I and II (Sigma) was added in each dish. After 10 min of incubation on ice, cells were scraped off the dish and centrifuged at 14,000 g for 20 min at 4°C. Supernatants were recovered and stored at -80 °C. 50 μ g of whole cell lysate from each sample was mixed with sample buffer and resolved onto 10% bis-tris SDS-PAGE gels by electrophoresis in MOPS buffer. The gel was blotted onto a 0.2 mm Nitrocellulose membrane and blocked in Licor blocking buffer for 1h at room temperature (RT). The blot was incubated with PDE δ , GAPDH, total Erk1/2, pErk1/2, pRaf, total Raf, cyclophilin-B, pAkt, total Akt, Hras, Nras, Kras antibodies overnight at 4 °C and then with IR secondary antibodies (Licor). The blots were scanned on a Licor odyssey imaging system. Antibodies used for western

blotting were PDE δ (N-15): (Santa Cruz Biotechnology-50260) 1:750, Nras (F-155): (Santa Cruz Biotechnology-31) 1:1000, Rheb: (Cell signaling-4935) 1:1000, total Raf: (BD biosciences-610152) 1:2000, pRaf: (Cell signaling-9427) 1:1000, total Erk: (Cell signaling-4696) 1:2000, pErk: (Cell signaling-9106) 1:2000, Cyclophilin-B: (Axxora-210237) 1:2000.

2.3.7 Biotin acyl exchange assay

BAE assay was performed as described (Drisdell and Green, 2004; Politis et al., 2005). MDCK cells were seeded in 35-mm dishes at a density of 2×10^5 cells/dish and incubated for 24h. The cells were then transfected with expression plasmids encoding for mCit-Hras wt, mCit-Hras C181S, mCit-Hras C184S, mCit-Nras, mCit-Rap2a/2b/2c (1 μ g) using the Effectene transfection reagent (Qiagen) and incubated for 20h. Separately, cells were treated with either Palmostatin-B or DMSO for 2h wherever required. Cells were then lysed with cell lysis buffer containing 5 mM EDTA, 1% Triton X-100, 50 mM N-ethylmaleimide, protease inhibitor cocktail (Roche) in PBS pH 7.4. After 5 min of incubation on ice the cells were scraped and the lysates were homogenized. The homogenized lysates were rotated for 1h at 4 °C and then centrifuged at 12,000 g for 20 min at 4°C. To prevent unspecific binding of protein to sepharose, the lysates were pre-incubated with Sepharose-G (Sigma). Samples were then centrifuged and the supernatants were rotated with Living Colors® Full-Length A.v. anti-GFP polyclonal antibody (Clontech) for 60 min at 4 °C. The protein-antibody complex was precipitated with Sepharose-G by rotation for 1 h at 4 °C. The purified protein was then additionally treated with 50 mM N-ethylmaleimide for 1 h at RT. After treatment and centrifugation, the pellets were washed twice with PBS and each sample was divided into two fractions. One fraction was treated with 1 M Hydroxylamine (pH = 7.4) by rotation for 1 h at RT to remove palmitate groups, and the other fraction was treated with PBS and served as control sample. All samples were then treated with 320 μ M (Btn)-BMCC™ and rotated for 2 h at RT or overnight at 4 °C. Samples were washed twice and resolved on SDS-PAGE and western blotting was performed with the mouse monoclonal anti-GFP N-terminal antibody (Clontech-632380) to detect total mCit-Ras. The primary antibody staining was visualized by using IR 800 Goat Anti-Mouse IgG Antibody (LICOR), while biotinylated protein (representing palmitoylated protein) was visualized with IR 680CW Streptavidin (LICOR) on the Odyssey® Infrared Imaging System (LICOR).

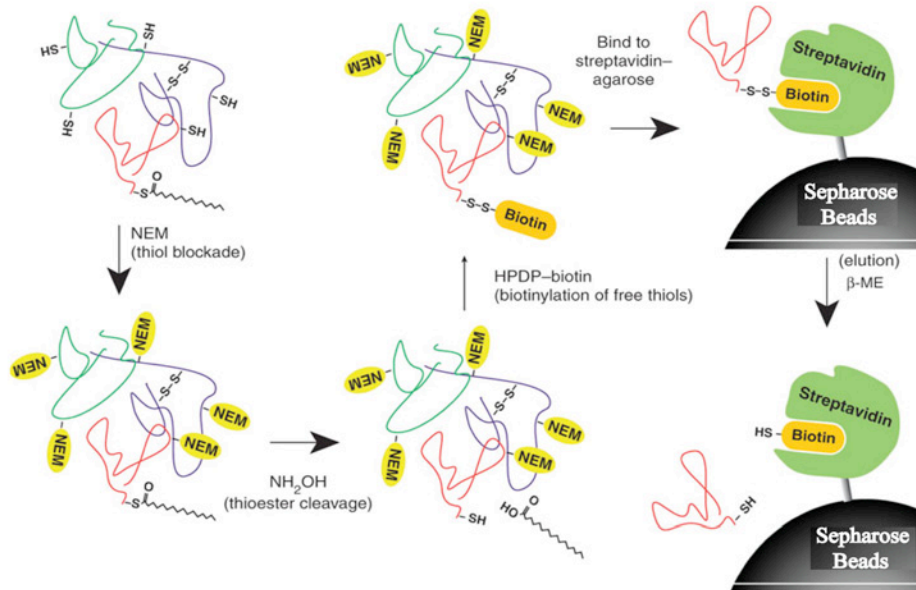


Figure 2.1 Schematic of the proteomic acyl-biotinyl exchange methodology
Reproduced from Wan et al., 2007.

2.3.8 Triple (3X)-RBD staining

(3X)-RBD, a construct containing three subsequent repeats of the Ras binding domain of Raf1, was labeled with Amersham Cy3.5 mono-reactive dye (GE healthcare) as per manufacturer's instruction. mPDAC cells were transfected with PDE δ -siRNA (50nM) and then incubated for 72h. Both, untreated as well as siRNA treated cells were fixed with 4% paraformaldehyde and permeabilized with 0.1% tween-20. Cy3.5 labeled (3X)-RBD was then added to these fixed cells on the microscope. Images were acquired immediately within 30-60 sec in order to avoid unspecific labeling observed after longer incubation times.

2.3.9 In vitro Clonogenic assay of cells

Murine PDAC cell lines were plated on 6-cm plates and transfected with 3 μ g of turboRFP-containing scrambled or PDE δ shRNA plasmids, using Lipofectamine 2000 according to manufacturer's instructions. 24h after transfection, RFP-positive cells were sorted using a Beckman Coulter MoFlo cell sorter and subsequently re-plated in DMEM plus 20% fetal calf serum. To measure cell viability, 5000 RFP-positive cells were plated in 6-well dishes and then fixed in 4% formaldehyde 5 days later (6 days post-transfection). Following one wash in water, cells were stained with 0.1% crystal violet for 20 minutes and then washed with several volumes of water. Plates were photographed, then bound dye was extracted with 10% acetic acid and the absorbance

at 595 nm was determined. Each point was determined in triplicate. A fraction of sorted cells was also plated for western blot analysis, using goat anti-PDE δ antibody: (Santa Cruz Biotechnology, sc-50260) diluted 1:500 in TBS + 0.1% Tween-20 + 5% non-fat dry milk, and rat anti-tubulin antibody: (Abcam, YOL1/34) diluted 1:5,000 as a loading control. Following incubation with HRP-conjugated secondary antibodies (Jackson ImmunoResearch) diluted 1:5000, blots were developed by chemiluminescence using ECL reagent (GE Healthcare).

2.4 Microscopy and imaging techniques

2.4.1 Microscopes

Laser scanning confocal microscopy:

FRAP and photoactivation experiments were performed on a Leica TCS SP5 AOBS equipped with HCX PL APO 60X/1.4 NA oil immersion lens and a temperature controlled incubation chamber maintained at 37°C and 5% CO₂. CFP, mCitrine and paGFP were excited by 458 nm, 514 nm and 488 nm Ar laser lines, respectively. mCherry was excited by using the 561nm DSSP laser line. Photoactivation of paGFP was achieved by using a 405 nm diode laser. Fluorophore emission bands were detected in the following range- CFP: 469-505 nm, Citrine: 524-551 nm, Cherry: 571-650 nm, paGFP (before excitation): 415-450 nm, paGFP (after excitation): 498-520 nm.

Time-domain FLIM:

Fluorescence lifetime images were acquired using a confocal laser-scanning microscope (FV1000, Olympus, Germany) equipped with a time correlated single photon counting module (LSM Upgrade Kit, Picoquant, Germany). For detection of mCitrine, the sample was excited using a 470 nm diode laser (LDH 470, Picoquant) at 40 MHz repetitions. Fluorescence was collected through an oil immersion objective (60X/1.35 UPlanSApo, Olympus) and spectrally filtered using a narrow band emission filter (HQ 525/15, Chroma, USA). Photons were detected using a single photon counting avalanche photodiode (PDM Series, MPD, Italy) and timed using a single photon counting module (PicoHarp 300, Picoquant). The instrument response

function of the system was measured to be below 200 ps (data not shown).

2.4.2 FRAP and FLAP

FRAP (Fluorescence recovery after photobleaching) is a useful method for measurement of the translational diffusion of fluorophores and fluorescently labeled macromolecules in cellular components. Fluorophores in a defined sample volume are irreversibly bleached using brief, intense laser pulse. The diffusion of unbleached molecules into bleached volume is then measured as a quantitative index of fluorophore translational diffusion. On the other hand FLAP (Fluorescence loss after photoactivation) allows fast switching of fluorescent protein properties with fewer photons by selective illumination with specific wavelength. The instrumentation for photobleaching/ photoactivation consists of a laser/light source to bleach, a fluorescence microscope, a defined sample volume and a detector. The beam intensity of an argon ion laser is modulated by an acousto-optic modulator and directed onto a fluorescent sample using an epifluorescence microscope with a dichroic mirror and objective lens. The emission path contains an interference filter, pinhole, and gated photomultiplier detector. For unrestricted diffusion of a single fluorescent species in a homogeneous environment, fluorescence recovers to the initial (prebleach) level and recovery curve contains a single component whose shape depends on geometry of bleached region. However, fluorescence recovery in cell systems is often incomplete (restricted diffusion) or multicomponent. Incomplete recovery often indicates that a fraction of the fluorescent molecules are immobile because of binding of slowly moving cellular components or trapping in noncontiguous compartments.

2.4.3 FRET-FLIM

FRET reduces the fluorescence lifetime of the donor fluorophore owing to the depopulation of its excited state; a phenomenon that fluorescence lifetime imaging microscopy (FLIM) makes use of. FRET can be detected purely via donor fluorescence because the fluorescence lifetime is an intrinsic fluorescence parameter, that is, only dependent on excited state processes. Specificity of the acceptor is not required because its fluorescence is not detected. Upon occurrence of FRET, the fluorescence lifetime is independent of the fluorophore concentrations as long as saturating amounts of acceptor are present.

The time domain FLIM- Here, a gated measurement of the fluorescence intensity is made following excitation of the sample with a short pulse of light (Sytsma et al., 1998; Squire and Bastiaens, 1999). The fluorescence intensity is therefore sampled at sequential time points along the exponential fluorescence decay. In cases where a sample contains a single fluorescence species, the fluorescence lifetime is given as the time over which the fluorescence intensity falls to 1/e of its initial value.

2.5 Data analysis

2.5.1 Fluorescence loss after photoactivation (FLAP)

In photoactivation experiments it was ensured that the duration of photoconversion did not exceed 5% of the fluorescent recovery half time. The radius of the illuminated area was kept small (< 25%) with respect to the radius of the diffusion area (Lopez et al., 1988). Images were background corrected, thresholded and the mean intensity in the ROI as well as in the whole cell was determined. To correct for bleaching the fluorescence intensity in the ROI was normalized by the whole cell fluorescence intensity at each time point. The initial peak intensities after photoconversion were normalized to one. The normalized data was fitted to the equation: $f(t) = 1 - (1 - \eta) \exp(-2t_D/t)[I_0(2t_D/t) + I_1(2t_D/t)] + \eta$ where η is the immobile fraction, I_0 and I_1 are modified Bessel functions as described in (Axelrod et al., 1976; Elson and Magde, 1974). Effective diffusion was calculated using the expression $D_{\text{eff}} = r^2/(4t_D)$ where t_D is the effective diffusion time (s), r is the radius of the photoconverted area (μm) and D_{eff} is the effective diffusion constant ($\mu\text{m}^2/\text{s}$).

2.5.2 Fluorescence recovery after photobleaching (FRAP)

Ratiometric analysis of Golgi FRAP data was performed as described in (Rocks et al., 2010). GalT-CFP images were thresholded, median filtered and binarised to get a Golgi mask. The mask was used to calculate the ratio of the sum of mCit-Nras intensity over the sum of CFP-GalT intensity at each time point at the Golgi. The plateau values were normalized to one.

2.5.3 FRET-FLIM

Briefly, images were first intensity thresholded to segment the cell from the background. The photon-counting histograms of the regions of interest were then

Fourier transformed from the time domain to the frequency domain. Using the information contained in the high harmonics, the functional form of the IRF was derived. “Phase” and “modulation” values were calculated for each pixel and corrected using the derived IRF properties. All pixels measured with the same FRET pair were pooled together and analyzed using global analysis. From this process the fluorescence lifetime of the donor in presence or absence of the acceptor was calculated. Finally, the fraction of donor in complex with the acceptor was calculated in each pixel from which the image was reconstructed (Grecco et al., 2009).

2.5.4 Western blots quantification

Densitometric analysis of western blots was performed using Image J software (<http://rsbweb.nih.gov/ij/index.html>). The area under the curve (AUC) of specific signals was corrected for the AUC of the loading control. Mean and integrated density was determined and was used to calculate the relative amount of pErk1/2, pRaf and pAkt proteins by dividing by the mean value of total Erk1/2, Raf and Akt.

To derive correlations between pErk1/2 and PDE δ levels for each concentration/timepoint, pErk1/2 and PDE δ levels were first normalized using the formulas (1) & (2). The normalized levels of pErk1/2 were plotted against the normalized levels of PDE δ in a scatter plot and correlation coefficients were determined.

$$pErk1/2 (siRNA/shRNA):tErk1/2 (siRNA/shRNA) / pErk1/2 (Scr):tErk1/2 (Scr) \quad (1)$$

$$PDE\delta (siRNA/shRNA): cyclophilin-B (siRNA/shRNA) / PDE\delta(Scr): cyclophilin-B(Scr) \quad (2)$$

2.5.5 RT-PCR

mRNA levels were estimated using a relative quantification method based on the cycle time (C_t) determination (Livak and Schmittgen, 2001). First, the ΔC_T value for each sample was determined by calculating the difference between the C_T value of the target gene and an endogenous reference gene. This was determined for each siRNA treated sample and calibrator sample (control or untreated sample) using the formula:

$$\Delta C_T (\text{sample}) = C_T \text{ target gene} - C_T \text{ reference gene}$$

$$\Delta C_T (\text{calibrator}) = C_T \text{ target gene} - C_T \text{ reference gene}$$

Next, the $\Delta\Delta C_T$ value for each sample was determined by subtracting the ΔC_T value of the sample from the ΔC_T value of the calibrator:

$$\Delta\Delta C_T = \Delta C_T (\text{sample}) - \Delta C_T (\text{calibrator})$$

PCR efficiencies of the target and endogenous reference gene were found to be comparable; the normalized level of target gene expression is calculated using the formula $2^{-\Delta\Delta C_T}$.

III

Investigating palmitoylation machinery specificity in DHHC motif containing Dictyostelium PATs

3.1 Abstract

Palmitoylation machinery, which includes the palmitoyl-acyl transferases (PATs) and the deacylation enzymes, are responsible for maintaining proper spatial organization of several signaling proteins. Although various palmitoylatable substrates are known, a consensus motif or region where palmitoylation occurs cannot be identified (Linder and Deschenes, 2007). Therefore, it was hypothesized that the DHHC PATs activity does not recognize a specific sequence in the substrate proteins. Ras proteins are well-characterized palmitoyl substrates, which were used in this study to delineate the specificity of DHHC PATs towards its substrates. Furthermore in an attempt to demonstrate the broad specificity of PATs, human Hras was ectopically expressed in *Dictyostelium*. The spatial organization and temporal kinetics of human Hras in *Dictyostelium* was reminiscent of mammalian cells, corroborating that there are no specific PATs for Ras proteins. From these studies it is clear that the DHHC PATs recognize and modify a broad spectrum of substrates, thereby regulating palmitoylated proteins at a global level.

3.2 Rationale and hypothesis

Acylation cycle controls the spatial organization of palmitoylated peripheral membrane proteins. Palmitoylation of farnesylated Ras proteins increases the affinity of these proteins towards specific membrane compartments and thus enhances kinetic trapping of Ras at the PM. Ras protein undergoes palmitoylation through a labile thioester linkage (S-palmitoylation) at the cysteine residues. This reaction is catalyzed by a set of enzymes called palmitoyl-acyl transferases (PATs), characteristic of DHHC family proteins (Roth et al., 2002). The main objective of this work is to investigate the following questions:

Do the PATs specifically recognize certain motif in the Ras proteins, either the G-domains or the hypervariable C-terminal region (HVR) of Ras?

Whether any specificity for the palmitoylation reaction resides in the DHHC domain containing PATs?

Preliminary data (from Rocks et al., 2010) using a genetically encoded YFP tagged tH (C-terminal fragment of Hras aa 175-190) as compared to that of mCherry tagged full length Hras (Figure 3.1) suggested that the palmitoylation machinery does not recognize structural motifs in the Ras G-domain. Involvement of Ras G-domains in imparting specificity to PATs is highly questionable since most of the Ras proteins share high sequence and structural homology in these regions (Dever et al., 1987; Bourne et al., 1991).

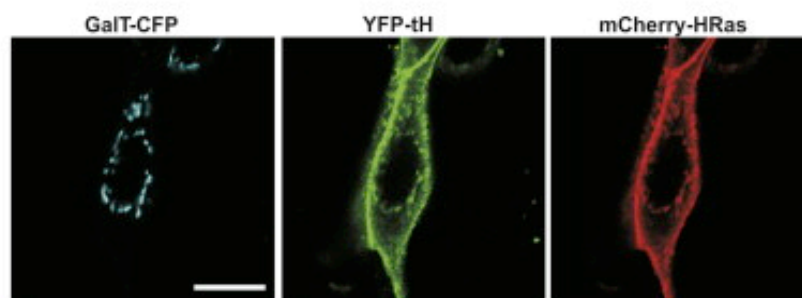


Figure 3.1 Equivalent distribution of the tH versus full-length Hras protein (Reproduced from Rocks et al., 2010).

Another finding highlighted the role of conserved acidic and basic residues in the HVR of Ras in stabilizing palmitoylation (Laude and Prior, 2008). Although it is not

clear whether the acidic patches in the HVR of these Ras isoforms serves as recognition site/motif for PATs and regulate the on/off rate of palmitoylation or they interfere with PAT binding at the cysteine residues hence modulating Ras palmitoylation.

On the other hand, previous studies suggest that DHHC9/17/18/ yeast Erf2p-Erf4p complex exhibit substrate selectivity by specifically palmitoylating Ras proteins (Fukata et al., 2004; Lobo et al., 2002; Swarthout et al., 2005; Huang et al., 2004). However, in cells lacking Erf2 or Erf4, palmitate labeling of Ras2 is reduced, but did not eliminate palmitoylation of Ras2 (Bartels et al., 1999). Similarly, palmitoylation of Vac8 was uninhibited in *S. cerevisiae* on deletion of gene encoding the vacuolar PAT Pfa3 (Smotryst et al., 2005). This is further supported by shRNA-mediated knockdown of DHHC 9 [Figure 3.2 (Rocks et al., 2010)] where the loss of DHHC9 neither affects the kinetics or spatial distribution of Hras. Hence the loss of function studies of DHHC family proteins in yeast and human cells suggested a discrete and partially overlapping PATs specificities for palmitoylated Ras proteins and argue against the specificity of palmitoylation reaction in DHHC motif containing PATs.

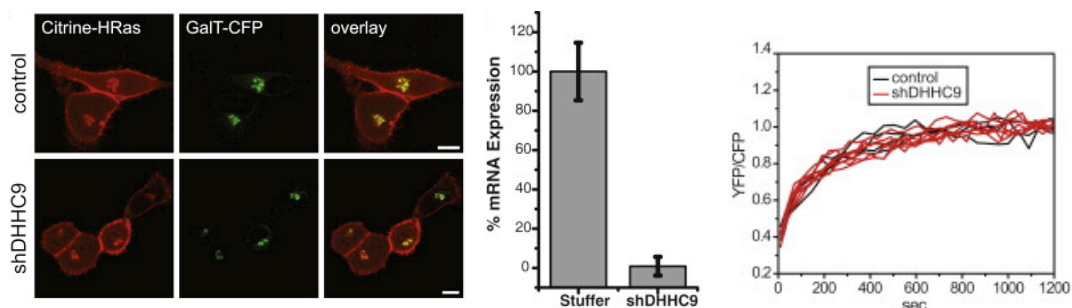


Figure 3.2 shRNA mediated DHHC9 downregulation

Left panel: Spatial distribution of mCitrine-Hras in Hela cells before/after DHHC9 downregulation. Middle panel: % mRNA expression in absence/presence of DHHC9 shRNA. Right panel: FRAP of Hras at Golgi in control shRNA (black) Vs DHHC9 shRNA (red) treated cells. (Reproduced from Rocks et al., 2010).

The lack of any apparent recognition signature sequence for the de-/reacylation cycle as revealed argues against the involvement of mammalian palmitoyltransferases with specific substrates. Classification of 25 human DHHC proteins using a Hidden Markov Model (HMM) based on the bioinformatics approach (Smyth, 1997) revealed a conserved consensus sequence ‘W-X(4)-L-X(12)-TTNE’ adjacent to DHHC-CRD domain (Figure 3.3). Database search of different genomes with the same consensus

sequence also identified various known Ras specific PATs although *Dictyostelium discoideum* showed no homologues of human Ras specific DHHC PATs such as DHHC 9, 17, 18. Therefore in order to demonstrate the lack of substrate specificity for Ras PATs, we used *Dictyostelium discoideum* as a model organism and analyzed the spatial distribution and kinetics of human Hras in these cells.

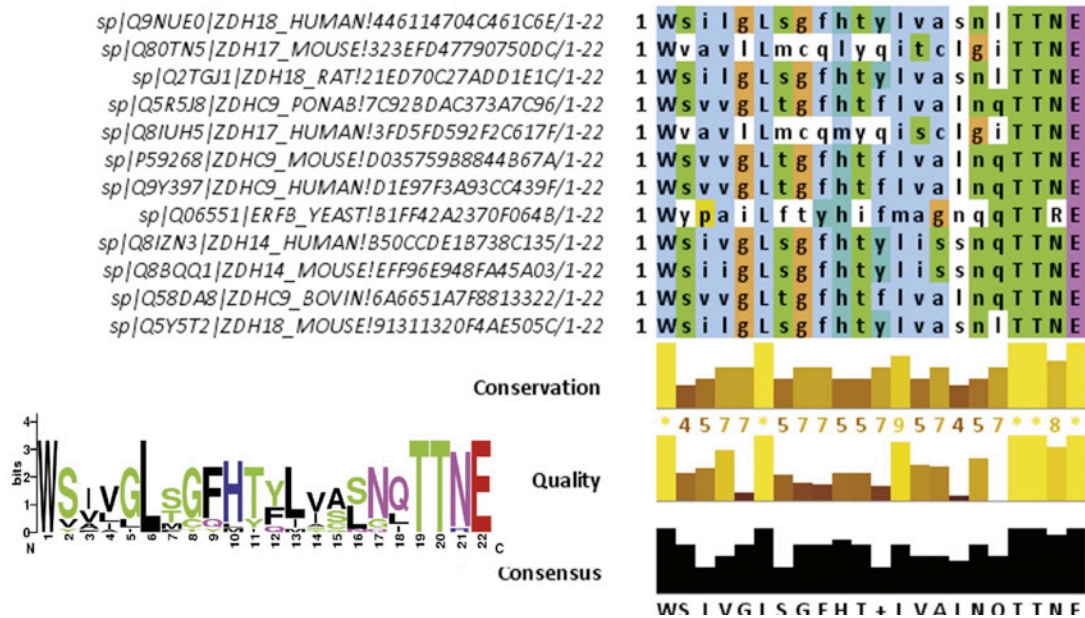


Figure 3.3 Consensus sequence alignment of mammalian and yeast genome Hits identified by the PROSITE scan of ‘W-X4-L-X12-TTNE’, showing high degree of conservation and fidelity. (Reproduced from Rocks et al., 2010).

3.3 Results

3.3.1 *Dictyostelium discoideans* as a model organism

Analysis of the completed *Dictyostelium* genome has revealed a total of 119 genes encoding small GTPases, encompassing all the five Ras subfamilies. The first *Dictyostelium* Ras protein to be characterized was RasD (Reymond et al., 1984). RasG, like RasD is highly homologous to the mammalian Hras, particularly in the effector loop. A third gene, rasB, is also closely related to the mammalian Hras, though with less similarity than rasD and rasG.

Dictyostelium Hras homologues differ from farnesylated human Hras in a way that all of them are geranylgeranylated and lack any palmitoylatable cysteine (Figure 3.4). The C-terminus of *Dictyostelium* Ras proteins bear poly-cationic residues instead. Despite this, *Dictyostelium* genome consists of 8 DHHC PATs, None of these are homologous to known human Ras PATs such as DHHC9, 17, 18. Absence of any reported human Ras specific PATs in *Dictyostelium* thus makes it an ideal candidate to study broad specificity of PATs by observing palmitoylation of human Hras in *Dictyostelium*.

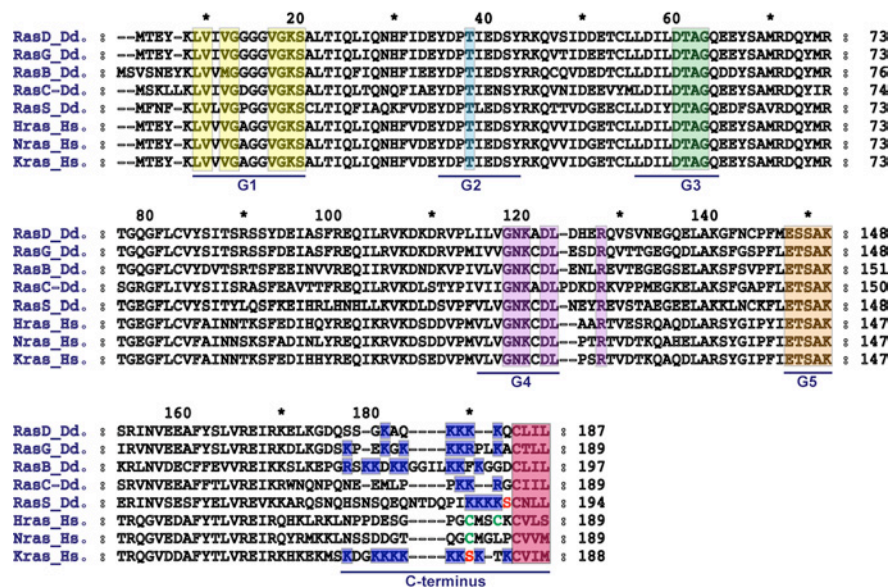


Figure 3.4 Sequence alignment of *Dictyostelium* Ras proteins

G box consensus sequences are shown in shaded yellow (G1 domain), light blue (G2 domain), green (G3 domain), purple (G4 domain), orange (G5 domain). C terminal CaaX box is shown in shaded pink, polybasic residues are highlighted in blue, palmitoylatable cysteines in green and phosphorylatable serine in red.

3.3.2 *Subcellular localization of human Hras in Dictyostelium discoideans*

In order to visualize the spatial distribution of Ras in *Dictyostelium discoideans*, cDNA encoding human Hras (Hras_Hs) was tagged into *Dictyostelium* expression vector bearing a genetically encoded green fluorescent protein – pDm317 GFP (Veltman et al., 2009). The plasmid DNA was then electroporated into vegetative *Dictyostelium* cells. Transformed cells were then observed on a confocal microscope for the plasmid expression. Upon excitation with 488nm laser, spatial distribution of exogenously expressed GFP tagged human Hras was visualized. *Dictyostelium* cells displayed an equal partitioning of Hras_Hs at the plasma membrane (PM) and Golgi apparatus similar to that observed in mammalian cells. Vegetative, nutrient starved as well as immobilized cells displayed similar localization (Figure 3.5A).

Additionally, in case of vegetative cells we also observed some labeling of the endosomal compartments as well as some brightly illuminated structures in the cytoplasm of the cells. The endosomes that originates from the PM are abundantly present in *Dictyostelium* cells (Gerisch et al., 2004). However, on serum starvation the endosomal localization was lost but these cells retained the unspecific brightly stained structures. Since *Dictyostelium* display cellular autofluorescence at a wavelength range from 500 to 650 with maxima at 510nm (Engel et al., 2006), we compared the untransfected *Dictyostelium* cells (Figure 3.5C) excited with the same wavelength in order to differentiate between GFP tagged Human-Hs labeling and cellular autofluorescence. As evident from Figure 3.5C, the untransfected cells displayed similar bright staining in the cytoplasm, indistinguishable from polarized cells.

The PM and Golgi enrichment of Hras_Hs indicated that human Hras was indeed palmitoylated in *Dictyostelium* cells since palmitoylation is an important requisite for the PM targeting of human Hras (Hancock et al., 1989; Cadwallader et al., 1994; Rocks et al., 2005). In contrast, expression of GFP tagged human Hras palmitoylation mutant (Hras C181S/C184S_Hs) did not show any specific preference to a specific membrane compartment and appeared on all endomembranes including Golgi (Figure 3.5B). Mutating both the palmitoylatable cysteines C181 and C184 in Hras to serines render the Hras molecules unrecognized by PATs thus leading to an unspecific low affinity binding to the endomembranes (Rocks et al., 2005). This unpalmitoylated fraction was represented by the bright fluorescence in the cytoplasm (Figure 3.5B).

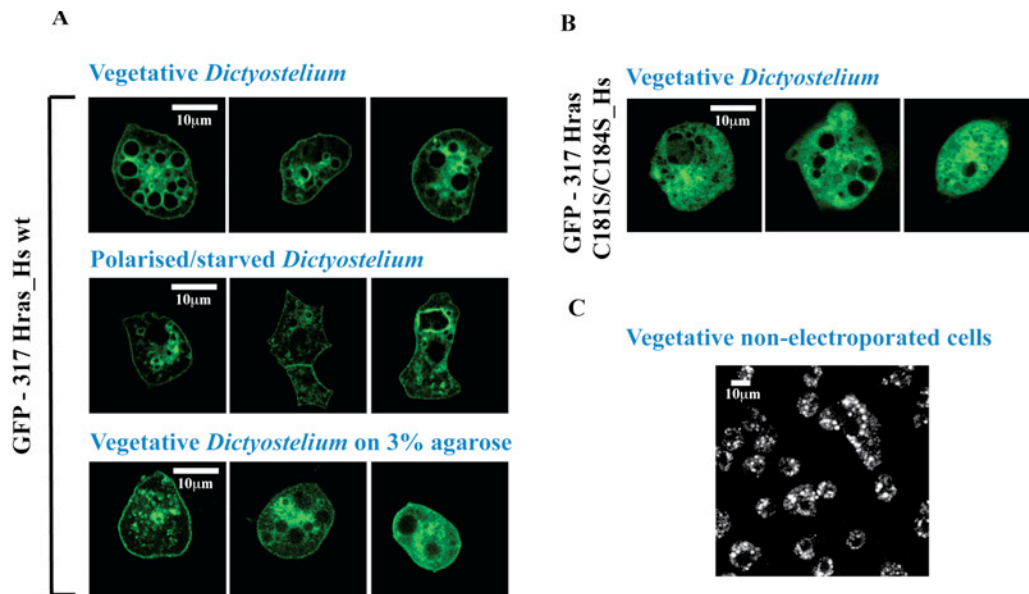


Figure 3.5 Human Hras spatial localization in *Dictyostelium discoideans*
 (A) GFP tagged human Hras expressed *Dictyostelium* AX2 strains in either vegetative (upper), polarized (middle) or immobilized stage showing enrichment at the PM and Golgi apparatus. (B) *Dictyostelium* AX2 strain expressing GFP-317 Hras C181S/C184S_Hs in vegetative stage. (C) Non-electroporated *Dictyostelium* AX2 strain excited at 488nm wavelength.

3.3.3 Effect of 2-Bromopalmitate on subcellular localization of human Ras in *Dictyostelium*

Palmitoylation promotes stable attachment of otherwise cytosolic proteins to intracellular membranes such as PM and Golgi apparatus (Hancock et al., 1990; Cadwallader K.A et al., 1994; Rocks et al., 2005). In order to ensure that PM and Golgi enrichment of human Ras in *Dictyostelium* was due to the effective palmitoylation via PATs, human Hras transformed *Dictyostelium* cells were treated with palmitoylation inhibitor 2-Bromopalmitate (2-BP). 2-BP has been demonstrated as an inhibitor of fatty acid acylation (Webb et al., 2000). Treatment for 30 min in cells expressing GFP-317 Hras_Hs wt indeed caused redistribution of palmitoylated proteins to endomembranes and a decrease in PM localization (Figure 3.6) similar to that observed in case of depalmitoylated Hras C181S/C184S_Hs.

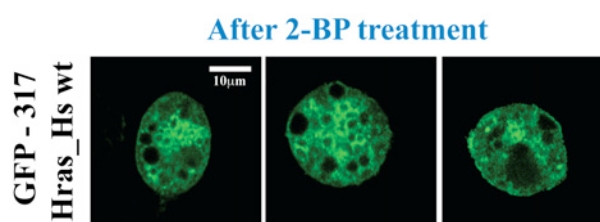


Figure 3.6 2-Bromopalmitate inhibits human Hras palmitoylation

3.3.4 Depalmitoylated Hras displays faster diffusion kinetics over wildtype

The rate of Ras trafficking is dictated by the stability of palmitate attachment (Rocks et al., 2005, Goodwin et al., 2005). Therefore, we examined the diffusion kinetics of Hras wt in comparison to depalmitoylated Ras mutant. Ras recovery rates were determined after photobleaching either a part of cell or half the size of the cell. Hras wt showed slow recovery kinetics ($t_{1/2}=183.3\pm 3.8s$). Hras wt diffusion mostly comprised of a slowly diffusing component mostly originating from PM and a faster diffusing component arising from the newly synthesized, solely farnesylated Hras as shown in Figure 3.7A. On the other hand, for depalmitoylated Hras mutant very fast uniform recovery was observed within few seconds ($t_{1/2}=5.6\pm 1.4s$) (Figure 3.7B). Palmitoylation deficient mutant (Hras C181S/C184S) show weak binding affinity towards membranes henceforth contributes to the faster diffusing population whereas addition of palmitate moiety to Hras wt enhances its binding stability toward PM that accounts for slowly diffusing population. These results were in accordance with the Hras diffusion kinetics observed in mammalian cells. This experiment clearly demonstrates that PM and Golgi enrichment of human Ras in *Dictyostelium* cells is tightly regulated by activity of palmitoyl acyltransferases albeit lack of reported Ras specific PATs. In conclusion, no specific PAT activity exists for Ras.

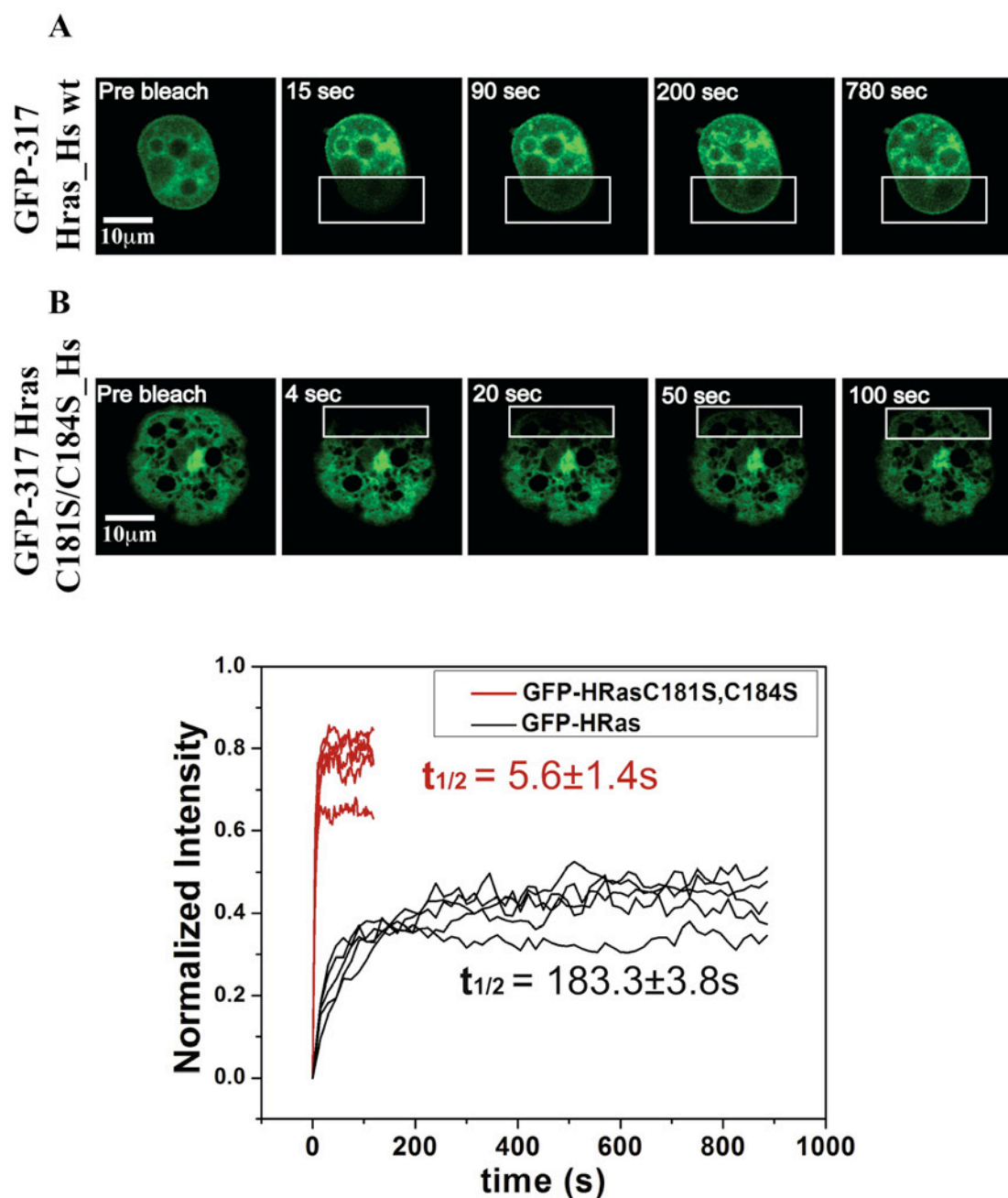


Figure 3.7 FRAP kinetics of human Hras in *Dictyostelium*
FRAP performed on *Dictyostelium discoideans* expressing GFP-317 Hras_Hs wt (A) and GFP-317 Hras C181S/C184S_Hs (B). Lower graph: FRAP curves (n=5 each) indicating diffusion kinetics of human Hras wt (black) and Hras C181S/C184S (red).

3.4 Discussion and future perspectives

Substrate tolerance of palmitoylation machinery

In this work using human Ras as a model the contribution of DHHC PATs to global palmitoylation has been evaluated. The ability of Dictyostelium PATs to palmitoylate human Ras in absence of Ras specific PATs was demonstrated. Ectopic expression of human Ras in Dictyostelium shows similar localization as observed in mammalian cells. The PM and golgi localization of human Ras in Dictyostelium was lost when the Hras C181S/C184S mutant was expressed indicating that the Dictyostelium DHHC PATs are indeed palmitoylating the human Ras protein. Pharmacological intervention using 2-Bromopalimate and FRAP experiments further corroborated the hypothesis that there are no specific PATs for Ras proteins. This was in agreement with the lack of a universal palmitoylation consensus motif that can be recognized by PATs (Bijlmakers and Marsh, 2003; Smotryst and Linder, 2004). The experiments performed with D amino acids and non-natural synthetic peptides demonstrate that the sequence flanking the target cysteine on the substrate does not contribute to PAT enzyme specificity (Rocks et al., 2010). A recent study in yeast further supports the assumption of overlapping specificities (Hou et al., 2009). In addition, deletion of the gene for Erf2 (yeast PAT) reduced the palmitoylation of broad spectrum of substrates (Bartels, D.J et al., 1999). These observations explain the compensation in palmitoylation upon loss of one or more DHHC proteins. Such a compensation mechanism can be beneficial for cellular systems in two ways:

Firstly, the notion of dedicated PATs for specific substrates creates the need for a large number of PATs, in order to meet the requirement of expanding family of palmitoylatable substrates. So far in humans, nearly 50 of substrates subjected to palmitoylation have been identified (Resh, 1999; Bijlmakers and Marsh, 2003; Smotryst and Linder, 2004). Additionally, more than 1100 confirmed eukaryotic myristoylated proteins bearing a palmitoylatable cysteine in the HVR adjacent to the myristoyl group have been reported (Maurer-Stroh et al., 2004). Moreover a large number of undefined C-terminal palmitoylatable substrates might be present. But an account of most of these palmitoylated substrates in human genome is difficult to acquire, due to the lack of palmitoylation specific consensus sequence. Therefore further amplifying the demand for substrate specific PATs. Although a eukaryotic cell

might have a large pool of putative palmitoylatable substrates, overlapping substrate specificity seems like a reasonable choice thus maintaining a constrained PAT repertoire in the genome.

Secondly, redundant substrate recognition can serve in regulating proteins that have high turn over at the membranes at the level of DHHC activity, for example Ras. Since the palmitoylation and depalmitoylation reactions are uncoupled from specific sequence recognition motifs thus suggesting that a universal acylation/de-acylation mechanism is involved in regulating distribution of various palmitoylated membrane proteins.

However, the presence of large number of DHHC PATs in yeast, Dictyostelium and mammals is still a mystery. One possibility could be that DHHC proteins might have other biological functions apart from PAT activity. Recently it has been shown that in yeast the DHHC protein Swf1p is involved in polarized secretion (Dighe and Kozminski, 2008).

Based on the current knowledge, palmitoylation requires two-tier regulation:

1) Thiolate formation on the substrate protein in close proximity to membrane. The presence of one or more lipid anchors further enhances the lipid-bilayer interaction. In certain Ras family proteins the prenyl group adjacent to the target cysteines ensures the transient interaction with lipid-bilayer and proximity of substrate protein with the membrane. The sulphhydryl group of a substrate cysteine has an ionization constant pK_A of 8.5. Since the cytosolic condition of the cell is maintained at neutral pH the formation of a thiolate group is unlikely. However, the presence of basic or charged residues in close proximity to the cysteine in the substrate protein might modulate the potential to form a thiolate (Mössner et al., 2000; Bizzozero et al., 2001). Similar to the modulation of cysteines by changes in redox environment, the presence of an additional protein in close proximity might also facilitate the thiolation. The deprotonation of cysteine can either achieved by enhancing the accessibility of the sulphhydryl group, or by changing the local pK_a of the target cysteine. The other noteworthy aspect of palmitoylation reaction is that palmitate (C16) is not the only substrate added to the cysteines. Studies have shown that apart from C-16 palmitate, other lipid moieties such as palmitoleate (C16:1), stearate (C18) and oleate (C18:1) have been found on the target cysteines (Hallak et al., 1994; Schroeder et al., 1996; Liang et al., 2002, 2004). These findings also indicate that the DHHC PAT enzymes must be less specific towards the substrate recognition *in vivo*.

2) Transfer of palmitate from palmitoyl Co-A to substrate's thiolate

The second important aspect of palmitoylation involves palmitate transfer from cellular palmitoyl Co-A to the substrate thiols by DHHC PATs. It has been demonstrated that the DHHC proteins can undergo spontaneous autoacylation (Lobo et al., 2002) in the presence of long-chain acyl Co-As. Therefore the PATs forms a thioester intermediate with palmitate group, thereby the DHHC PATs additionally is involved in storage, accumulation and presentation of palmitoyl Co-A. When these PAT thioester intermediates encounter a substrate with thiolated cysteine, they rapidly catalyze the transfer reaction. Thus the DHHC PATs maintain higher palmitoylation rates and ensuring more coordinated substrate encounter. The DHHC PAT thioester intermediates also transfers the palmitate group irrespective of recognizable specific structures on the palmitoylatable substrate other than the target cysteine. In general the DHHC PAT thioester intermediate merely reduces the activation energy of the palmitoylation reaction due to thiolate stabilization. Thus, individual PAT/substrate pairs will not make any difference to the palmitate transfer reaction and in return will attenuate palmitoylation efficiency.

A few mammalian DHHC PATs contain protein interaction domains such as ankyrin repeat in DHHC13, SH3 in DHHC6 and PDZ binding motifs in DHHC5/8/14 (Tsutsumi et al., 2008; Huang et al., 2009). This suggests that these additional domains might be involved in enhancing interactions with specific substrates or sub-cellular localization. But the influence of such interactions on global palmitoylation machinery still remains elusive and needs to be tested.

IV

The GDI-like solubilizing factor PDE δ sustains the spatial organization and signaling of Ras family proteins

4.1 Abstract

The distribution of Ras-family G-proteins in cellular membranes dictates their signaling capacity and potential to alter cell phenotype. The outcome of this study was that the GDI-like solubilizing factor (GSF), PDE δ determines Ras protein distribution by rapidly mobilizing depalmitoylated or plasma membrane (PM) desorbed polycationic forms of Ras. The GDI-like pocket of PDE δ binds and solubilizes farnesylated Ras proteins to allow more effective trapping of depalmitoylated Ras proteins at the Golgi and polycationic Ras proteins at the PM. Thereby, PDE δ plays a dual role in maintaining the equilibrium distribution of polybasic Kras at the PM and the non-equilibrium distribution of palmitoylated N/Hras at the Golgi and PM. Importantly, PDE δ activity augments K/Hras signaling by enriching Ras at the PM; conversely, PDE δ down-modulation not only suppresses regulated signaling and proliferation via wild-type Ras, but also constitutive oncogenic Ras signaling in cancer cells. Thus, the essential role of PDE δ in determining Ras topography has implications for cancer therapy.

4.2 Rationale and Hypothesis

Lipid modifications at the C-terminus of the Ras family of GTP-binding proteins are essential for their function in a wide range of signal transduction processes (Colicelli, 2004). Hras and Nras proteins undergo two types of modifications: an irreversible farnesylation at the cysteine (Cys) residue of the CAAX box followed by a reversible palmitoylation at specific Cys residue(s) in the C-terminal hyper variable region (HVR). For the palmitoylated Ras proteins, three factors cooperate to confer a higher stability of accumulation in specific membranes - first, repeated cycles of Ras de/repalmitoylation, second, Golgi trapping by palmitoylation and third, the directionality of the secretory pathway. Together, these factors counter entropy-driven equilibration of palmitoylated Ras over all membranes (Goodwin et al., 2005; Rocks et al., 2010; Rocks et al., 2005). Thus, cleavage of the palmitoyl anchor by thioesterases (Camp and Hofmann, 1993; Dekker et al., 2010) reduces membrane affinity (Sang and Silvius, 2005) and enhances effective diffusion in the cytoplasm and redirection to the PM by the secretory pathway (Peyker et al., 2005; Rocks et al., 2005, 2010). However, Ras family proteins such as Kras contain polybasic residues in their HVR, instead of reversibly palmitoylated Cysteine residues. For polybasic Ras proteins, the negatively charged PM serves as a thermodynamically favored trapping structure that causes their accumulation. The major conundrum in the field is how the slow diffusion of prenylated Ras on the membranes in the cytoplasm is affected to enhance the kinetics of Ras trapping at the PM and thereby counter the randomization of the Ras distribution on intracellular membranes by the inward flow of endocytic vesicles. The involvement of GDI-like protein has long been suggested and it has been even speculated that PDE δ might transport lipidated Ras proteins (Hanzal-Bayer et al., 2002a; Nancy et al., 2002; Zhang et al., 2004). But till date the mechanism of how or if not whether PDE δ mediates shuttling of Ras protein pools between PM, Golgi, ER and cytoplasm is not known. Therefore in this study, the hypothesis was put to test using cell biological, biochemical and imaging methods.

4.3 Results

4.3.1 *PDE δ affects spatial distribution of Ras family proteins*

Prenylated, peripheral Ras family proteins can be divided into two main subgroups based on the differences in their hypervariable (HVR) region. Ras proteins bearing palmitoylatable cysteines in their HVR region such as Hras, Nras etc. and the other subclass comprise of Ras proteins bearing polybasic residues in their HVR for example Kras, Rheb etc.

Prenylated, palmitoylated Ras family proteins

In order to determine whether binding of PDE δ regulates the spatial localization of palmitoylated Ras proteins, MDCK cells were transiently co-transfected with various Ras family proteins fused to the monomeric yellow fluorescent protein Citrine (Griesbeck et al., 2001) and PDE δ fused to the monomeric red fluorescent protein mCherry (Shaner et al., 2004). Palmitoylated Nras and Hras predominantly localize at the PM and Golgi as reported earlier (Choy et al., 1999; Rocks et al., 2005). PDE δ over-expression in these cells resulted in solubilization of membrane bound Nras while no clear effect was observed for Hras (Figure 4.1). This difference may arise because Hras is more stably associated with the PM than Nras, due to its stable palmitoylation on two cysteine residues in the C-terminus of the protein as compared to only one palmitoylatable cysteine in case of Nras (Figure 4.1). Supporting evidence for this hypothesis comes from the efficient solubilization of the more labile mono-palmitoylated HrasC181S and Hras C184S mutant or depalmitoylated HrasC181S/C184S mutant upon co-expression of mCherry-PDE δ (Figure 4.1). This result suggests that the stability of palmitate attachment influences the effect of PDE δ on the localization of Ras.

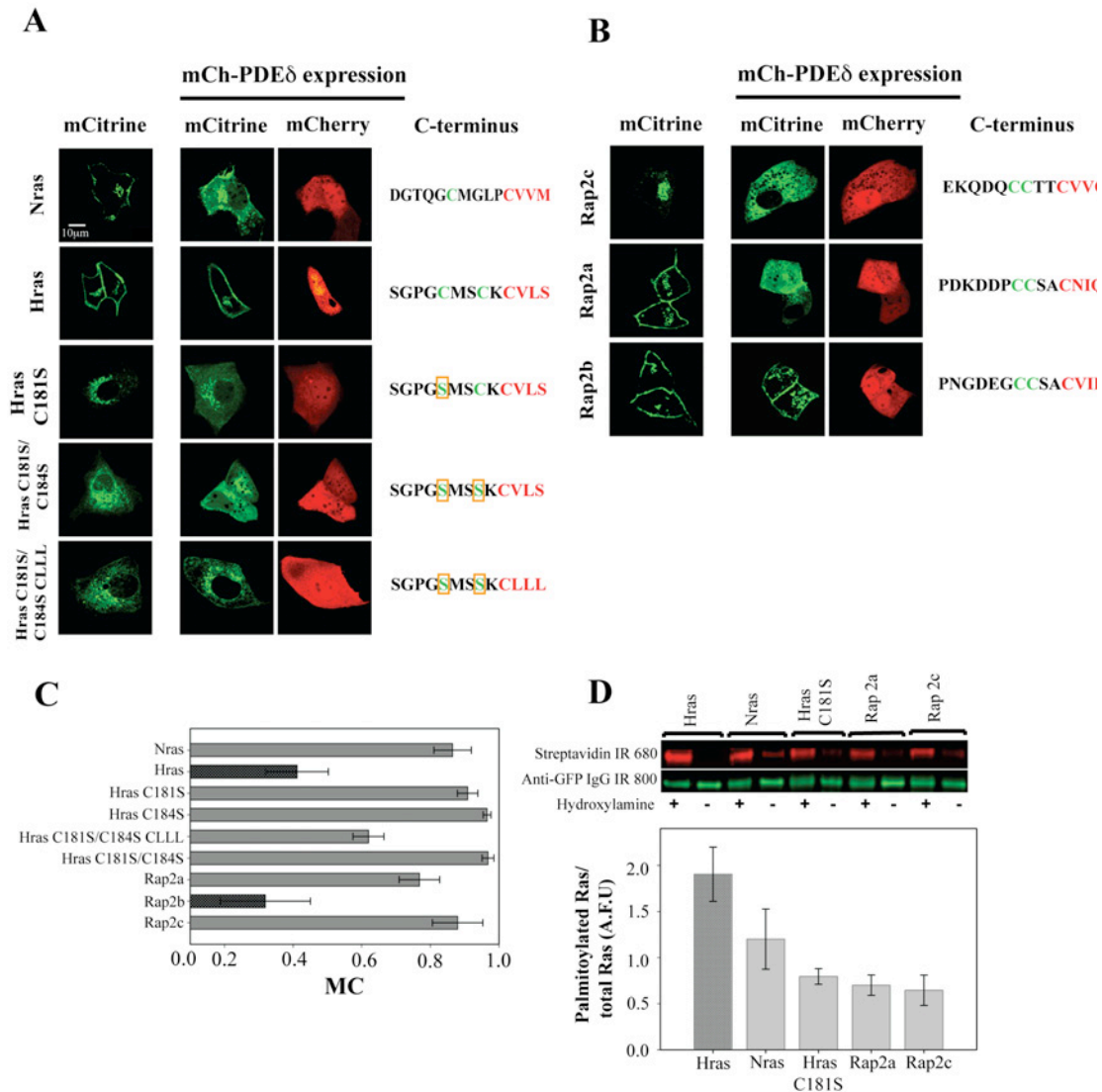


Figure 4.1 PDE δ affects the spatial distribution of palmitoylated Ras proteins

(A) Steady state localization of mCit fused Ras proteins (green) in MDCK cells alone (left panel) and co-transfected with mCh-PDE δ (red), right panel. On the right are the C-terminal sequences of the respective Ras proteins. The CaaX box is shown in red, C-terminal cysteines that are potential substrates for palmitoyl transfer are highlighted in green. Yellow boxes indicate replacement of these cysteines by serines. (B) Steady state localization of Rap proteins bearing two putative palmitoylation sites in the C-terminus in the presence (right panel) /absence (left panel) of mCh-PDE δ . (C) Bar graph: Mean Manders' coefficients (MC) for co-localization of different mCit-Ras proteins and mCh-PDE δ (n=10). High Manders' coefficients indicate better co-localization of mCit-Ras proteins with PDE δ . Values less than 0.5 indicate no co-localization, denoted in dark grey stripes. (D) Palmitoylation levels determined by biotin acyl exchange assay: Upper panel: Western blot of immunoprecipitated Ras proteins on protein G-sepharose 4B showing biotinylated protein labeled with streptavidin IR 680 and total protein with anti-GFP (mouse). Lower panel: Quantification of the normalized palmitoylated fraction for each Ras and Rap isoform (n=4 blots).

Palmitoylated Rap2a and Rap2b were localized to the PM and Golgi apparatus, whereas Rap2c exhibited a Golgi and ER specific localization which may be conferred by its higher palmitate lability similar to the HrasC181S mutant (Rocks et al., 2005). Co-expression of PDE δ resulted in a shift in the distribution of the Rap2 proteins to the cytoplasm indicating solubilization (Nancy et al., 2002) with the exception of Rap2b (Figure 4.1). These observations suggest that the loose association of Ras proteins with membranes is a key determinant for the interaction with PDE δ . Indeed, double lipid modified palmitoylated proteins seem to resist the solubilizing PDE δ effect (Figure 4.1), contrary to previous findings (Nancy et al., 2002). Unexpectedly, the farnesylated Rap2 proteins (Rap2a, -c) that also contain two potential palmitoylation sites in their HVR were also effectively solubilized by PDE δ . We therefore compared the steady state level of palmitoylation in these Ras family proteins by the biotin acyl exchange (BAE) assay (Drisdell and Green, 2004). Interestingly, the effective palmitoylation level of these proteins (Hras > Nras > HrasC181S) decreased in the order of their tendency to be solubilized by PDE δ with the Rap proteins showing the lowest levels of palmitoylation (Figure 4.1). These experiments confirm that PDE δ interacts preferentially with the farnesylated, depalmitoylated state of Ras proteins during the acylation cycle.

PDE δ directly binds palmitoylatable Ras family proteins

The influence of PDE δ on the steady-state localization of palmitoylatable Ras proteins can either result from indirect regulation by accessory proteins or through a direct interaction. To address this, Fluorescence Lifetime Imaging Microscopy (FLIM)-based quantitative FRET measurements (Wouters et al., 2001) were performed using mCitrine on the N-terminus of Ras proteins as donor, and dCherry (mCherry-tandem spaced by a linker) fused to the C-terminus of PDE δ as acceptor. FLIM allows the quantification of the interacting fraction (α) of molecules that exhibit FRET as apparent from the lower fluorescence lifetime of the donor mCitrine (Wouters et al., 2001). Co-expression of mCit-Nras and dCh-PDE δ showed a marked decrease in fluorescence lifetime in the cytoplasm of these cells indicating an interacting fraction (α) of mCit-Nras with PDE δ . In contrast, the higher lifetime of the PM-bound mCit-Nras indicated a non-interacting population (Figure 4.2). Unlike mCit-Nras, doubly palmitoylated mCit-Hras (Figure 4.2) and its G12V mutant (not shown) didn't show a clear interaction with dCh-PDE δ . However, the mono-palmitoylated Hras mutants

(C181S or C184S) and the non-palmitoylated (C181S, 184S) mutant exhibited a clear interaction with dCh-PDE δ as measured by FLIM (Figure 4.2). We attribute this to the increased lability of palmitoylation on the mono-palmitoylated Hras mutants as compared to wt Hras, which increases the steady-state concentration of the depalmitoylated state capable of interacting with PDE δ . Other palmitoylated Ras family members like mCit-Rap2a and Rap2c (Figure 4.2) also showed a large fraction of molecules that interacted with dCh-PDE δ .

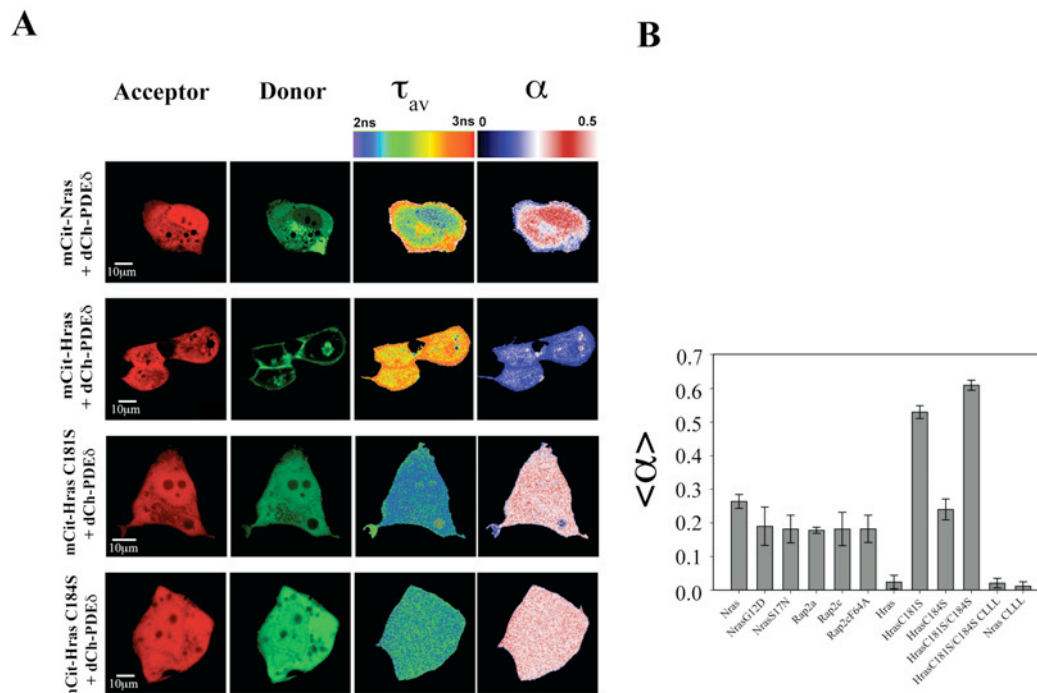


Figure 4.2 FRET-FLIM based PDE δ -Ras interaction studies
 (A) Upper panel: MDCK cells co-expressing either mCit fused to Nras (first row), Hras (second row) or Hras palmitoylation mutants (lower two rows) and dCh-PDE δ . For each sample, the fluorescence intensity of mCit-Ras (donor), the fluorescence intensity of dCh-PDE δ (acceptor), the spatial distribution of the mean fluorescence lifetime (τ_{av}) and the molar fraction of interacting molecules (α) are shown according to the false color lookup tables. (B) Bar graph: Quantified average α values for different Ras proteins with dCh-PDE δ as acceptor.

Prenylated, polycationic Ras family proteins

To investigate whether the important classes of prenylated peripheral Ras family proteins that have a polybasic (HVR) instead of palmitoylatable cysteines next to the CaaX box also require PDE δ to sustain their spatial organization. A prototypical member of that G-protein family is Kras with 8 basic residues in its HVR. Stable anchorage of these proteins to the PM seems to require two components: an electrostatic interaction with negatively charged phospholipids and the partitioning of

the hydrophobic prenyl group into the lipid bilayer. Co-expression of mCh-PDE δ with Ras proteins that have five or more basic residues in the HVR (Kras, Diras) did not lead to a significant change in their spatial localization (Figure 4.3). However, Ras proteins with fewer basic residues in the HVR were more effectively solubilized by PDE δ as is clearly evident from the cytoplasmic distribution of farnesylated Rheb and Rheb-L1 that contain either two or one basic residue (Figure 4.3). A correlation was thus apparent between the extent of solubilization of Ras proteins by PDE δ and the amount of basic residues that they contain in the HVR. We then investigated with FRET-FLIM whether the solubilization of Ras proteins containing polybasic stretches requires direct interaction with PDE δ . mCit-Kras/ mCit-KrasG12V that are mostly associated with the PM showed no change in fluorescence lifetime upon co-expression of mCh-PDE δ ; in contrast, a homogeneously distributed population of mCit-Rheb molecules exhibited an interaction with PDE δ (Figure 4.3). We then generated mutants of Kras that have a gradual replacement of the basic lysines by acidic glutamates in the HVR (Kras Δ 2E, Δ 4E, Δ 6E) and measured the extent of their solubilization by PDE δ . This replacement resulted in a gradual destabilization of Kras from the PM in increasing order of acidity. The redistribution to endomembranes was matched by an increased solubilization by PDE δ (Figure 4.3) and increased interaction with dCh-PDE δ (Figure 4.3). This implies that high affinity binding of polycationic Ras proteins to the negatively charged PM (Heo et al., 2006; Yeung et al., 2006, 2008, 2009) hinders their association with PDE δ . On the other hand, weaker PM association of less positively charged proteins leads to a higher dissociation rate that allows solubilization by PDE δ . This is indicative of the fact that PDE δ might sequester Kras mostly from endomembranes, thereby delineating its function in the spatial organization of polybasic stretch containing Ras molecules. Thus, membrane-bound Kras must be desorbed before it can interact with PDE δ .

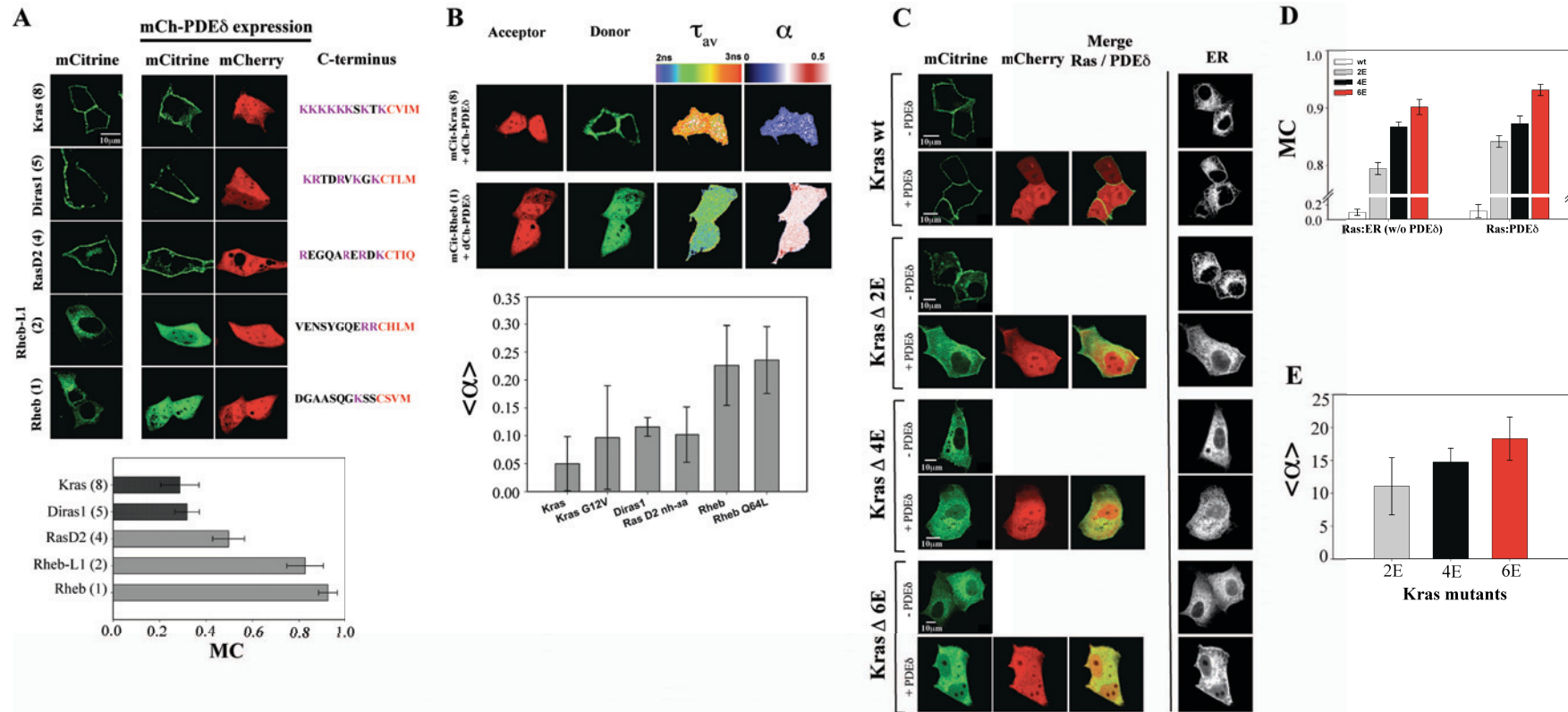


Figure 4.3 PDE δ solubilizes polybasic stretch containing Ras proteins

(A) Left panel: Steady state localization of mCit fused to polybasic stretch containing Ras proteins in MDCK cells. Right panel: MDCK cells co-transfected with plasmids encoding for mCit tagged polybasic Ras proteins (green) and mCh-PDE δ (red). Right: C-terminal sequences of the respective Ras proteins showing basic residues in pink and the CaaX-box in red. Lower bar graph: Manders' coefficients (MC, n=10 each) displaying co-localization of different Ras polycationic proteins with PDE δ . The number of basic residues at the C-terminus is given in brackets. Manders' coefficient less than 0.5 denote no co-localization (dark grey). (B) FLIM-FRET measurements in MDCK cells co-expressing either mCitrine fused to Kras (8 basic residues, upper row) or Rheb (one basic residue, lower row) with dCh-PDE δ . Lower bar graph: Quantified average α values (fraction of interacting molecules) for different Ras proteins with dCh-PDE δ . (C) The number of cationic residues in the HVR affects Kras distribution and solubilization by PDE δ . The four panels show the fluorescence distribution of mCit tagged Kras where 0, 2, 4 or 6 lysines in the polybasic stretch have been replaced by glutamic acid. The upper row in each panel shows the fluorescence distribution of mCit-Kras wild type and mutants (mCitrine) as well as the distribution of the ER-marker mTFP-Calreticulin. (D) Fluorescence distribution of mCit-Kras wild type and mutants in cells co-expressing mCh-PDE δ (mCherry) as well as the merge of both channels. Lower bar graph: Quantification of co-localization of mCit-Kras mutants with the ER marker (mTFP-Calreticulin) or mCh-PDE δ using Manders' coefficients (n=10 each). (E) Quantified average molar fraction of interacting Kras mutants with dCh-PDE δ (n=5 each).

4.3.2 Prenylation/farnesylation is essential for PDE δ -Ras interaction

Rap2b bears similar modifications at the C-terminus as Rap2a and Rap2c except for the CVIL CaaX box which is a substrate for geranylgeranyl transferase (Farrell et al., 1993; Winegar et al., 1991). This indicates a specificity of PDE δ for farnesylated Ras over geranylgeranylated Ras proteins. Indeed, when the C-terminus of the non-palmitoylated HrasC181S/C184S mutant was replaced with a CaaX box for geranylgeranylation (CLLL) its solubilization was abolished (Figure 4.4). FLIM experiments also showed that a geranylgeranylated Nras mutant (mCit-Nras CLLL) did not interact with PDE δ in stark contrast to farnesylated Nras wt (CVVM) (Figure 4.4).

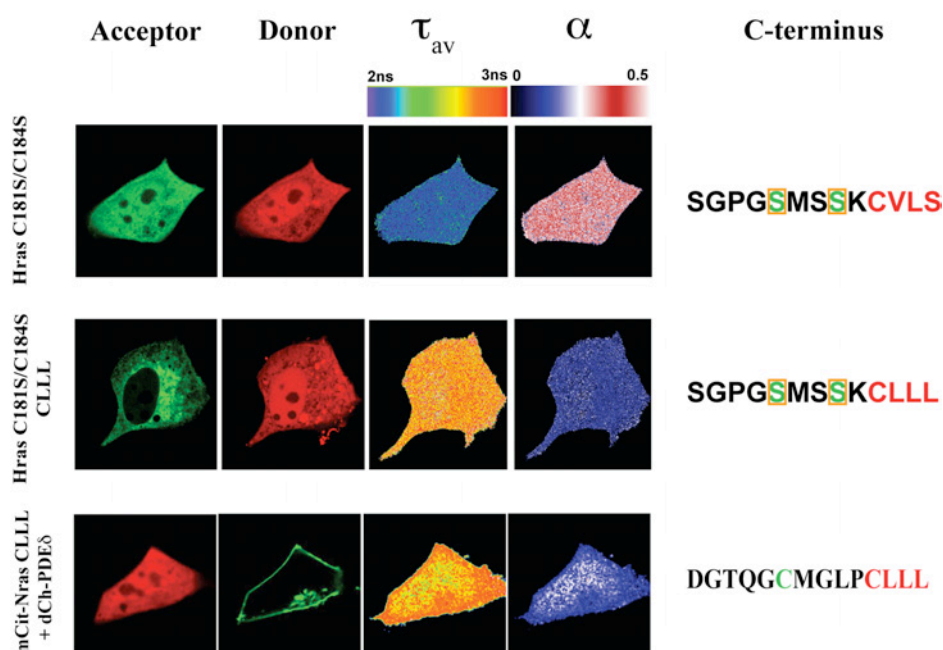


Figure 4.4 PDE δ does not interact with geranylgeranylated Ras proteins
 FLIM-FRET measurements in MDCK cells co-expressing either Hras mutant bearing a geranylgeranylated C-terminal (CLLL CaaX box) fused to mCitrine HrasC181S/C184S CLLL or Nras geranylgeranylated mutant (mCit-NrasCLLL) and dCh-PDE δ shows no interaction as well as no change in spatial localization. The upper row show example of farnesylated mCit-HrasC181S/C184S interacting fraction with dCh-PDE δ . For each sample, the fluorescence intensity of mCit-Ras (donor), the fluorescence intensity of dCh-PDE δ (acceptor), the spatial distribution of the mean fluorescence lifetime (τ_{av}) and the fraction of interacting molecules (α) are shown according to the false color lookup tables.

This was consistent with the fact that the localization of the Nras CLLL mutant was not affected by PDE δ and that farnesylated but not geranylgeranylated Nras protein

could be pulled down with recombinant human PDE δ (Figure 4.5). An increased affinity of PDE δ for farnesylated over geranylgeranylated moieties was also demonstrated in previous *in vitro* experiments by (Zhang et al., 2004).

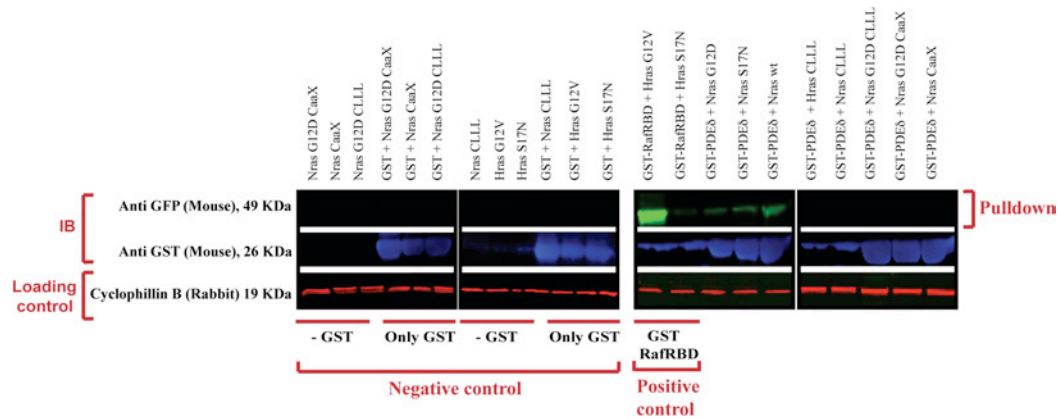


Figure 4.5 GST pull-down assay

MDCK whole cell lysates transiently transfected with Hras, Nras wt and various other mutants were subjected to GST pull-down assays by either recombinantly purified GST-RafRBD (positive control) or GST-PDE δ . Samples were treated with beads containing either no GST or only GST to serve as negative control (left side panel). Pulled down proteins were detected by immunoblotting against mouse anti-GFP (49KDa) and the total amount of loaded protein in each lane was verified by probing blots with rabbit anti cyclophilin-B.

4.3.3 PDE δ -Ras interaction is independent of Ras nucleotide bound state

From the similarity in the structures of PDE δ and Rho-GDI, it was suggested that PDE δ has a GDI-like function (Alexander et al., 2009; Hanzal-Bayer et al., 2002). However, structural alignment of PDE δ with Rho-GDI bound to Rho shows that PDE δ has a shorter N-terminus (Figure 4.6) that cannot block the switch regions of the bound G-protein to stabilize the inactive, GDP bound conformation as is the case for Rho-GDI (Gosser et al., 1997).

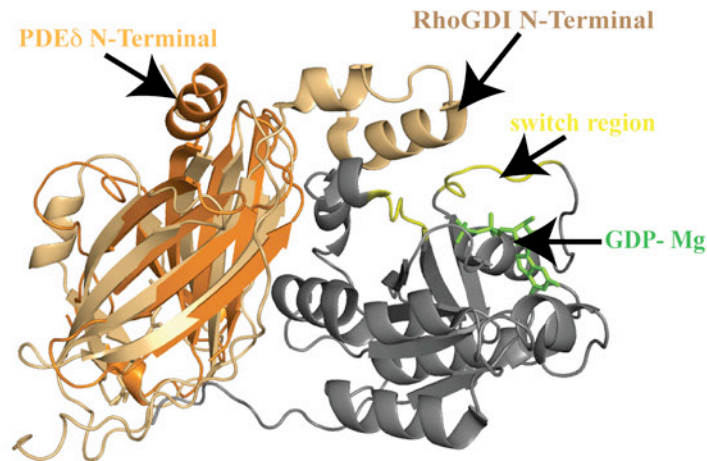


Figure 4.6 Structural overlay of PDE δ with Rho-RhoGDI complex
 Ribbon representations of PDE δ (in orange) and Rho (Gray)- RhoGDI (Brown). The switch region of Rho is indicated in yellow where blockage of effector binding occurs by the extended N-terminus of RhoGDI. In case of PDE δ the N terminus (as marked by black arrow) lacks a helical extension compared to RhoGDI and is unable to interact with the switch regions in the G-domain.

Indeed, as shown above, PDE δ showed equivalent binding affinity to wt Nras, dominant negative Nras (S17N) and constitutively active Nras (G12D) mutants. Also, no interactions of Nras Δ CaaX mutants with PDE δ could be detected even though these mutants retain intact effector binding switch regions (Figure 4.7). Thus, one can conclude from here that PDE δ -mediated solubilization of farnesylated Ras proteins occurred to the same extent regardless of whether they were bound to GDP or GTP and thus occurs independently of the nucleotide state of the protein (Nancy et al., 2002). This differs from the role of RhoGDI proteins in solubilizing prenylated G-proteins, which preferentially affects the GDP-bound forms (Gosser et al., 1997; Longenecker et al., 1999). Hence, the term GDI-like solubilizing factor (GSF) reflects the function of PDE δ as an efficient solubilizer of Ras proteins irrespective of the bound nucleotide state.

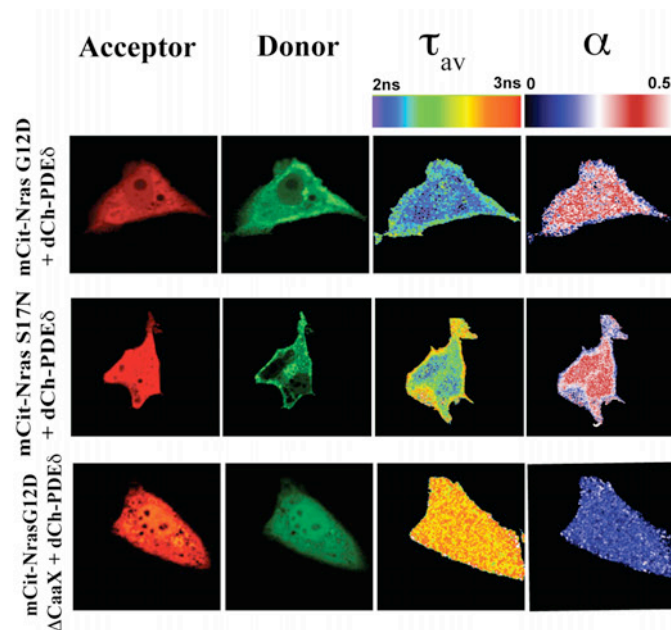


Figure 4.7 PDE δ shows no preference to GDP or GTP bound Ras
 FLIM-FRET measurements in MDCK cells co-expressing either constitutively active NrasG12D mutant (upper panel) or dominant negative NrasS17N mutant (middle panel), NrasG12D without C-terminal CaaX box mutant (NrasG12D Δ CaaX, lower panel) and dCh-PDE δ . For each sample, the fluorescence intensity of mCit-Ras (donor), the fluorescence intensity of dCh-PDE δ (acceptor), the spatial distribution of the mean fluorescence lifetime (τ_{av}) and the fraction of interacting molecules (α) are shown according to the false color lookup tables.

4.3.4 PDE δ downregulation alters Ras spatial localization

As evident from above results, spatial localization of polycationic Kras as well as doubly palmitoylated Hras was not affected on expression of PDE δ . A feasible explanation of this comes from the fact that the cells still have enough endogenous PDE δ that interact with stably associated Ras isoforms with higher affinity in order to maintain their spatial localization. A parallel *in vitro* study done with full-length semi-synthetic proteins revealed that affinity of PDE δ toward polycationic Kras was much higher as compared to other Ras isoforms (Chen et al., 2010). Although the *in vitro* studies were done in absence of any charged membranes, which points out that the strong electrostatic affinity of Kras towards PM might have a role in regulating interaction with PDE δ . In order to determine the relative stoichiometry of endogenous Ras isoforms compared to endogenous PDE δ , concentrations of recombinant H/N/Rheb and PDE δ proteins were determined by densitometric analysis of coomassie blue-stained gels using BSA as a standard. Various amounts of lysates

(10-80 μ g) were analyzed alongside titrated recombinant protein standards by SDS-PAGE and immunoblotted using antisera against N/K/H/Rheb and PDE δ . Immunodetected proteins were quantified densitometrically and cellular concentrations were calculated (**Figure 4.8**). The endogenous levels of PDE δ were approximately four times those of Ras in both the cell lines (Table 4.1) although molar sum of all the Ras proteins together was approximately equal to the molar amount of PDE δ . This correlates well with high endogenous levels, high affinity of PDE δ for polycationic Kras and presence of very low amounts of unphosphorylated and endomembrane bound Kras in the cytoplasm.

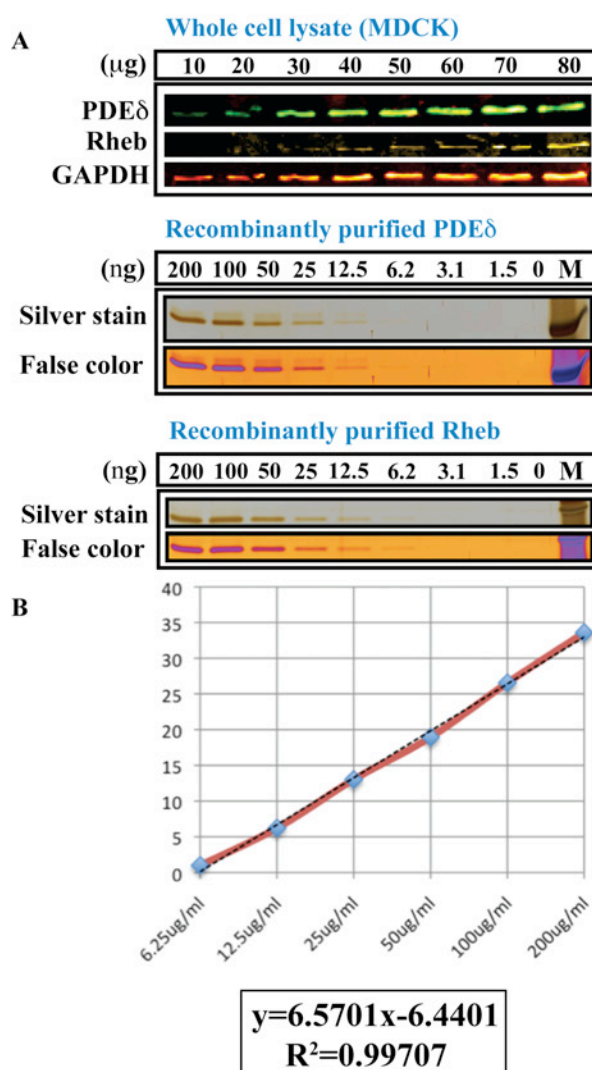


Figure 4.8 Endogenous PDE δ , Ras protein concentration determination
(A) **Upper panel:** Whole cell lysate of MDCK probed with Anti PDE δ , Anti-Rheb and GAPDH (loading control) analyzed alongside titrated protein standard. **Middle panel:** Recombinantly purified PDE δ protein standard and recombinantly purified Rheb (**Lower panel**) for concentration determination using silver staining. (B) Densitometric analysis of silver stained protein standards to calculate subcellular concentrations of proteins.

Table 4.1 Relative Content of Ras-GTPase and PDE δ in two cell lines

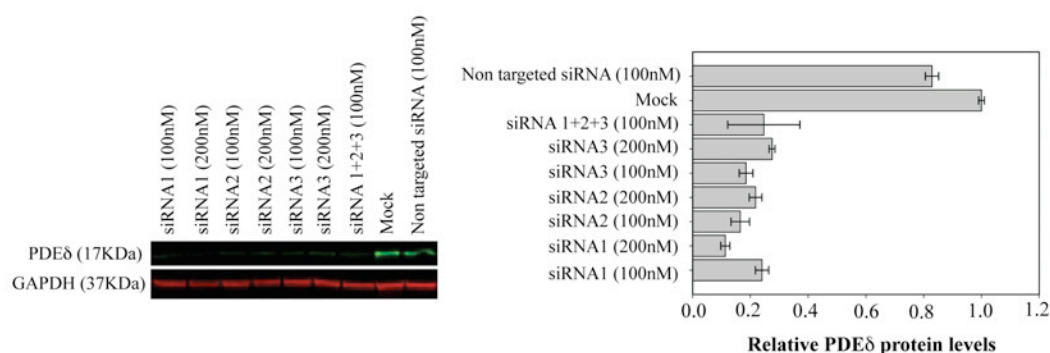
	MDCK	HEK293T
PDE δ	230ng/10 ⁶ cells	320ng/10 ⁶ cells
Rheb/Ras	56ng/10 ⁶ cells	88ng/10 ⁶ cells
Molar Ratio	1:4	1:4

To test if this hypothesis, PDE δ was downregulated in MDCK cells using dog specific PDE δ siRNA (Table 2.1, experimental procedures, 2.1.7). Cells were treated with four different dog-PDE δ siRNAs for 48-72h and were assessed for downregulation in these cells. Three out of four siRNA sequences showed effective PDE δ downregulation after 48h (Figure 4.9) on analysis via western blotting. Same siRNA sequences were also analyzed for PDE δ downregulation after incubation for 72h by quantifying mRNA levels using RT-PCR.

Further, to investigate the whether the role of PDE δ is to constitutively regulate Ras spatial localization the spatial partitioning of mCitrine fused palmitoylated Ras proteins (H/N/Kras) in MDCK cells either untreated or treated with PDE δ -specific siRNA (Table 2.1) was analyzed. The down-regulation of PDE δ protein expression (Figure 4.10) resulted in loss of PM and Golgi specific H/Nras localization, shifting the distribution to non-specific labeling of endomembranes (Figure 4.10). This was distinct from Ras distribution in cells over-expressing PDE δ that show a more homogeneous, cytoplasmic distribution. The randomized endomembrane distribution of mCit-Kras (Figure 4.10) in cells treated with PDE δ -specific siRNA indeed indicates that PDE δ plays a constitutive role in the maintenance of Ras at the PM. The affect of spatial distribution of Ras on PDE δ downregulation was quantified using Manders co-localization coefficient (MC). MC serves as an index of the fraction of Ras protein that co-localized with the ER marker (mTFP-Calreticulin) in untreated as well as PDE δ siRNA treated cells. As evident from the Figure 4.10 cells treated with PDE δ siRNA showed increased overlap with the ER marker indicated by higher overlap coefficient as compared to untreated cells. This indicates that on depleting PDE δ endogeneous pool, most of the Ras proteins fail to escape endomembrane after post-translational modifications at the ER and hence are not able to reach PM. This result in drastically altering PM bound Kras and Golgi/PM steady state localization in case of H/Nras. From this one can also decipher that PDE δ plays an important role on

transport of polycationic proteins from ER to PM presumably via solubilization.

A



B

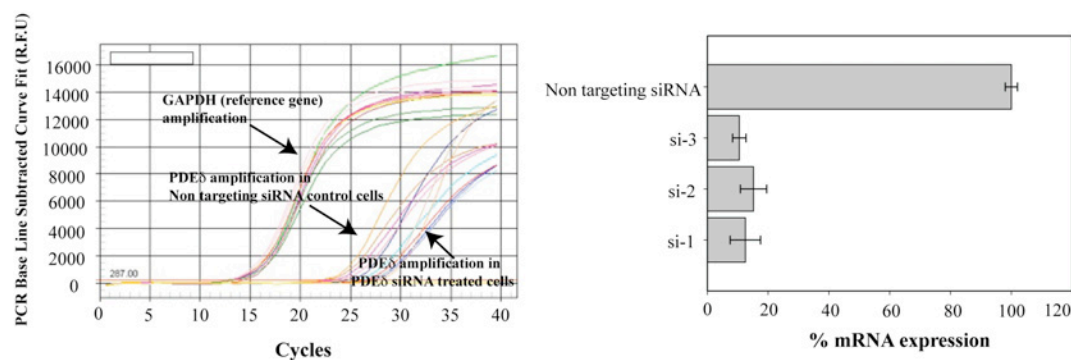


Figure 4.9 Validation of siRNA specificity towards canine PDEδ

(A) siRNA mediated PDEδ downregulation in MDCK cells analyzed by western blot (left) and relative PDEδ protein levels quantified (right) in knockdown cells using unspecific scrambled siRNA as negative, and GAPDH as loading controls. (B) Validation of PDEδ knockdown in MDCK cells by real-time PCR: Amplification curves were generated using a SYBR green detection kit. The real-time PCR curves show a ~2 fold delay in amplification in cells treated with PDEδ siRNA as compared to unspecific scrambled and GAPDH siRNA (left). Bar graph: mRNA levels in PDEδ-specific siRNA treated MDCK cells as quantified by real time PCR (right).

Another interesting aspect of this PDEδ mediated regulation of polycationic Ras proteins is their electrostatic interaction with the PM. The electrostatic interaction which targets signaling Ras molecules to the phosphatidylserine (PS)-enriched endomembranes can be modulated by varying surface charge of the membrane or by altering the net charge on the protein. Alteration in surface charge results in externalization of plasmalemma PS and PI(4,5)P2 hydrolysis. As a result, the plasmalemma surface charge decreases and becomes comparable to that of endomembranes, which can now compete effectively for binding with Kras. Kras,

which carries +8 charge at its C-terminus and localizes primarily at the PM in resting cell showed dramatic redistribution to the endomembranes on PDE δ downregulation (Figure 4.10). In order to ensure that this relocation is not an effect of redistribution of surface charges on the PM and endomembranes, the endogenous distribution of Phosphatidylserine (PS) was analyzed. Using a PS specific probe, Lact-C2 was probed (Yeung et al., 2008) on these charged membranes in untreated as well as PDE δ siRNA treated cells. To verify the specificity of Lact-C2 probe towards PS, the GFP-Lact-C2 probe was co-expressed in MDCK cells along with endomembrane marker (mTFP-Calreticulin) and its intracellular distribution was observed by fluorescence confocal microscopy. GFP-Lact-C2 localized prominently at the PM, confirming the presence of PS on its inner leaflet. Interestingly, in some of the cells intracellular vesicles were also labeled with GFP-Lact-C2 but mostly all the cells demonstrated PM specific labeling. Cells treated with PDE δ specific siRNA also exhibited similar distribution reflecting that PDE δ downregulation does not alter the surface charge distribution of the membranes (Figure 4.11).

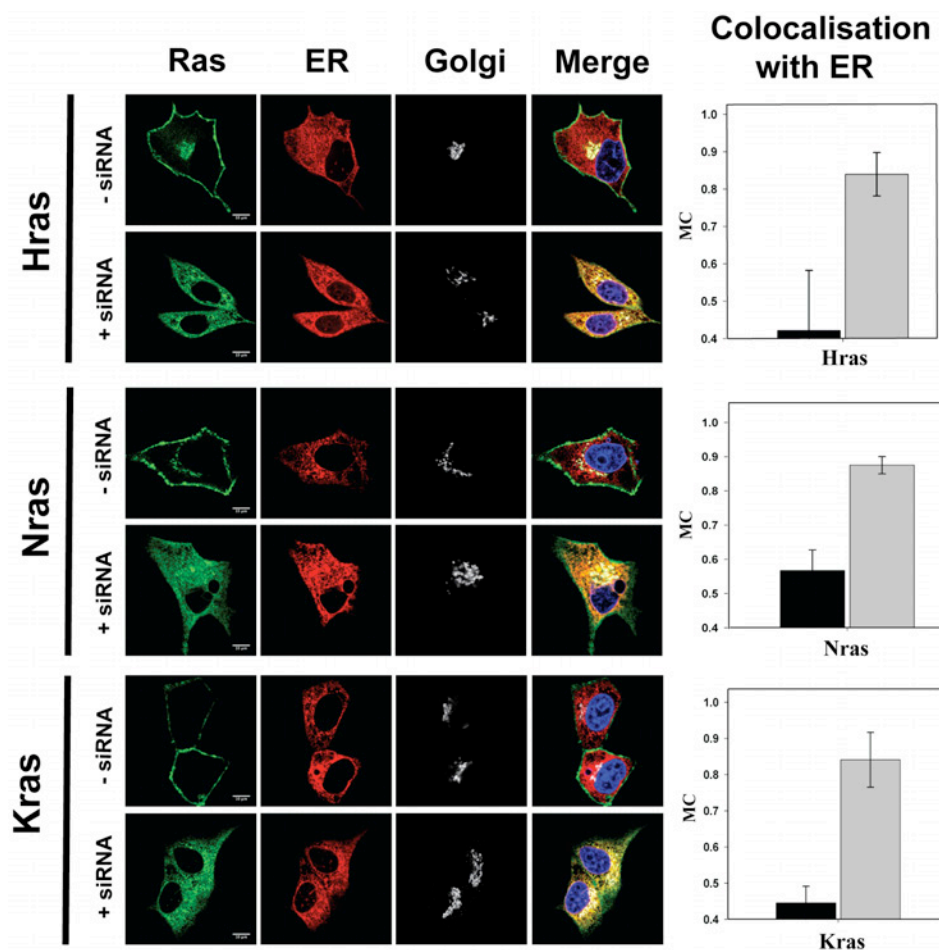


Figure 4.10 siRNA mediated downregulation of PDE δ causes redistribution of Ras

Hras (**upper two rows**), Nras (**middle two rows**) and Kras (**lower two rows**) redistributes to endomembranes/ endoplasmic reticulum (ER). The ER marker mTFP-Calreticulin (second column) and the Golgi marker TagRFP-T-GalT (third column) were co-expressed in all cells. The fourth column shows a merge of the three fluorescence channels with DAPI. Micrographs are representative of at least 10 individual measurements. Bar graph: Manders' coefficients (MC) for colocalization of Ras isoforms with the ER marker (mTFP-Calreticulin) in cells with (gray)/without (black) PDE δ downregulation (n=10).

In another experiment, subjecting cells expressing R-pre-mRFP (Figure 4.12) (a Kras analogue with a polyarginated/ unphosphorylatable {HVR} as described in (Yeung et al., 2008) to PDE δ siRNA exhibited a similar endomembrane distribution to that of Kras upon PDE δ downregulation (Figure 4.10). This delineates the role of the polycationic tail in the specific high affinity interaction with the PM and minimal requirement of the farnesyl moiety for the interaction with PDE δ , regardless of the HVR sequence.

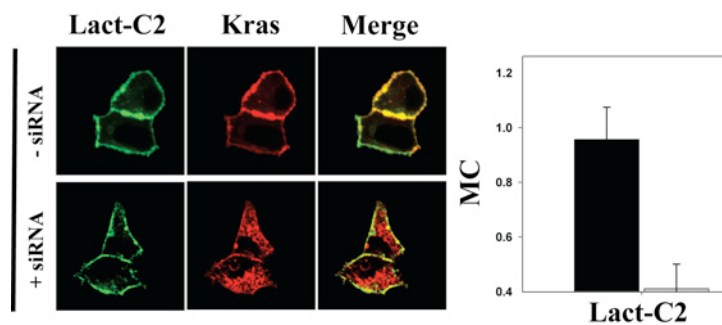


Figure 4.11 PDE δ downregulation does not alter surface charge distribution on the PM

MDCK cells co-transfected with Lact-C2-GFP (green) and mCh-Kras wt (red) in the absence (upper row) or presence (lower row) of PDE δ siRNA. Right bar graph: Mean Manders' coefficient (n=8 cells) indicating extent of overlap between Lact-C2 -GFP and mCh-Kras wt in cells with (gray) or without (black) siRNA downregulation.

R-pre: ---ARDGRRRRRRRARCVIM

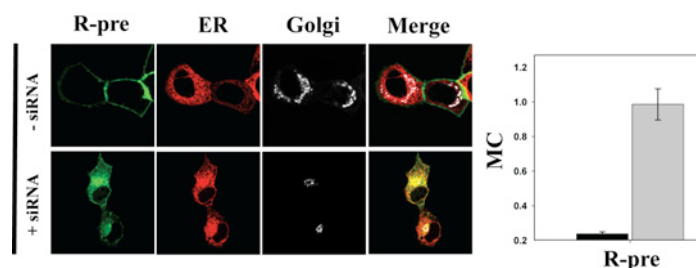


Figure 4.12 Farnesylation is the only pre-requisite for PDE δ -Ras interaction
Distribution of R-pre (a Kras analogue with a polyarginated/ unphosphorylatable HVR, green) in MDCK cells (upper row) and cells

treated with PDE δ specific siRNA (lower row). mTFP-Calreticulin is used as ER/endomembrane (red) and ECFP-GalT (white) as Golgi marker. Overlay of R-pre RFP and mTFP-Calreticulin is shown in fourth column. Right bar graph: Mean Manders' coefficient (n=10 cells) indicating extent of overlap between R-pre-RFP and mTFP-Calreticulin in cells with (gray) or without (black) siRNA downregulation.

4.3.5 *PM desorbed Kras interacts with PDE δ*

Phosphorylation of amino acids in a positively charged protein domain decreases its net charge thereby dissociating it from the PM (Kim et al., 1994). Such a phosphorylation event has been reported for polycationic Kras (Bivona et al., 2006) mediated by PKC activation and translocation. As demonstrated above that affinity of PDE δ towards Ras isoforms increases with decrease in PM interaction (Figure 4.2A, Figure 4.3A). In such a scenario, desorbing polycationic Kras by reducing net effective charge on the protein will help us visualize the dynamics of Kras-PDE δ interaction, which is otherwise not possible in presence of high affinity interaction between the two. To monitor the dynamics of Kras interaction with PDE δ , a PKC agonist Bryostatin-1 was used. Bryostatin-1, along with the phorbol esters and the endogenous ligand diacyl glycerol (DAG), modulate PKC activity by binding to the C1 domain of the protein and thus initiating PKC translocation from the cytosol to the cellular membranes (Szallasi et al., 1994; Bivona et al., 2006). This activated PKC then induces phosphorylation of Kras at S181 next to the polybasic stretch and thereby causes its redistribution to endomembranes (Bivona et al., 2006). MDCK cells co-expressing mCit-Kras and mCh-PDE δ were treated with Bryostatin-1. Over a period of 50 minutes a marked redistribution of Kras from the PM to the cytoplasm was observed (Figure 4.13). Concomitant with this cytoplasmic redistribution an increased fraction (α) of interacting mCit-Kras and mCh-PDE δ was observed. In this case, Bryostatin-1 treatment increases the pool of less cationic Kras that desorbs more readily from PM and thereby can be sequestered by PDE δ . This phosphorylated Kras likely has a more comparable affinity for the PM and endomembranes due to the partial alleviation of the electrostatic interaction at the PM. On the other hand, unphosphorylated Kras that is (mis)-localized on endomembranes gets more readily solubilized by PDE δ and can thereby quickly diffuse in the cytoplasm to be (re)-captured at the negatively charged PM. The interaction of Kras with endomembranes is independent of the polybasic stretch and therefore much weaker. This results in a higher endomembrane-off-rate and interaction with PDE δ in the cytoplasm. Instead,

Kras at the PM is tightly bound via electrostatic interactions and therefore has a low membrane off-rate that precludes its interaction with PDE δ in the cytoplasm. PDE δ thereby increases the kinetics of electrostatic trapping at the PM and in doing so maintains a non-homogeneous equilibrium distribution.

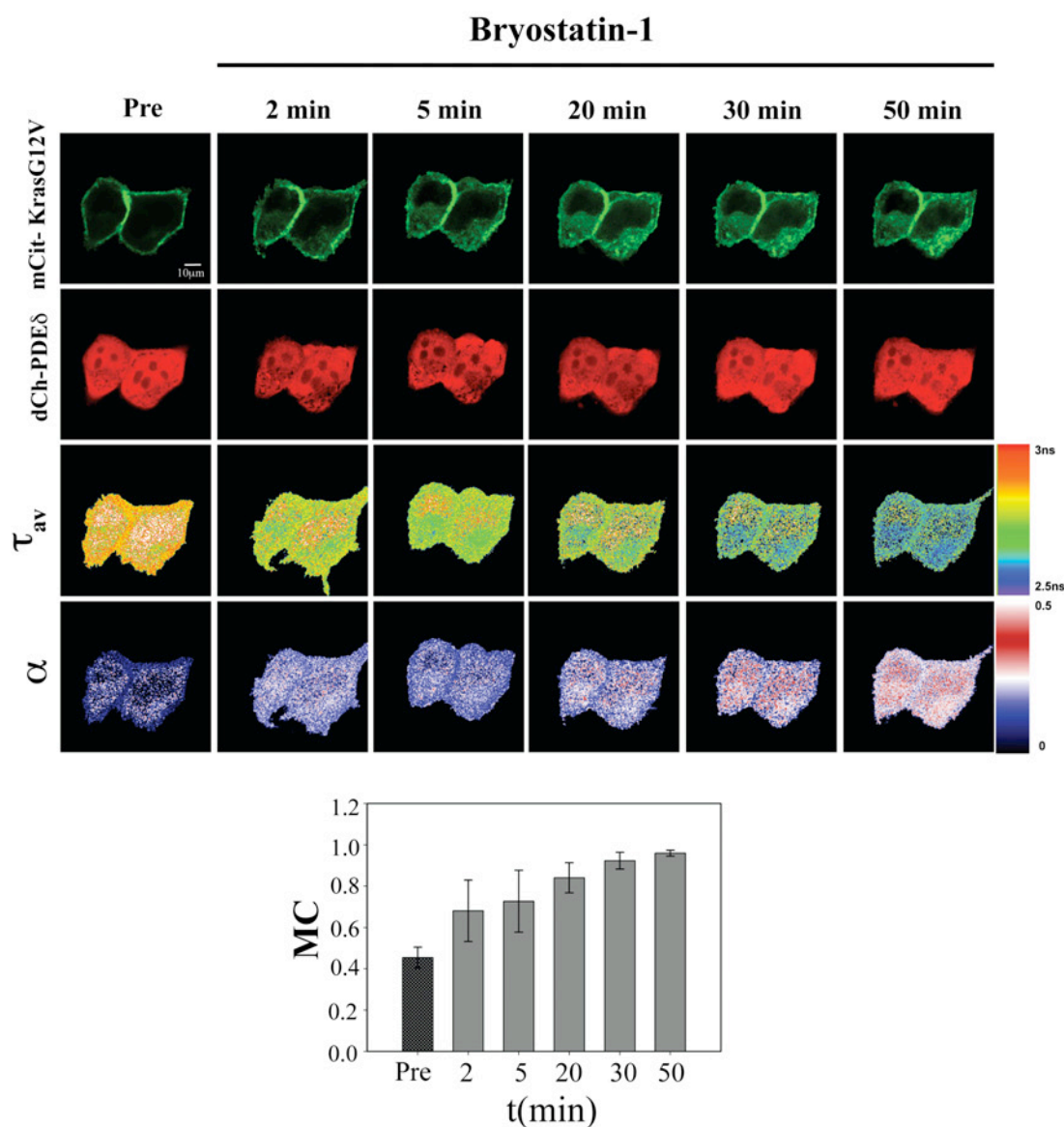


Figure 4.13 PDE δ solubilizes Kras mostly from endomembranes

FLIM time series on cells expressing mCit-KrasG12V and mCh-PDE δ indicate increasing interaction between KrasG12V and PDE δ in the cytoplasm after 100 nM of the protein kinase C agonist Bryostatin-1 treatment. Upper two rows: fluorescence intensity distribution of the indicated fluorescent fusion proteins. Lower two rows: average fluorescence lifetime τ_{av} and molar fraction (α) of interacting mCit-KrasG12V with mCh-PDE δ . Bar Graph: Quantification of co-localization of mCit-KrasG12V with mCh-PDE δ after 100 nM Bryostatin-1 treatment at different time-points using Manders' coefficients (n=6 each).

4.3.6 Pharmacological intervention of Ras acylation cycle

Unlike Nras, doubly palmitoylated Hras wt and its G12V mutant did not show a clear interaction with PDE δ (Figure 4.2 A,B). However, partially mutating palmitoylation sites as in case of HrasC181S, HrasC184S and non-palmitoylated mutant (C181S/C184S) resulted in a clear interaction with PDE δ as measured by FLIM (Figure 4.2 A,B and Figure 4.4). This indicates that only depalmitoylated, prenylated Hras is solubilized by interaction with PDE δ . In case of the mono-palmitoylated Hras mutants the increased lability of palmitoylation as compared to wt Hras causes an increase in the steady state concentration of depalmitoylated state that can interact with PDE δ (Figure 4.2 A,B). Therefore in order to corroborate the importance of reversible palmitoylation on Ras-PDE δ interaction we investigated if increased Ras palmitoylation/depalmitoylation by selective inhibition of Ras de-acylation/acylation cycle influence the interaction with PDE δ . Localized palmitoylation activity of the PATs at the Golgi apparatus and thioesterase activity all over the cells (Rocks et al., 2010) contributes to the partitioning of palmitoylatable Ras. Blocking either of the reactions will influence the distribution of palmitoylated over depalmitoylated Ras. If this is true, then pharmacological inhibition of Hras palmitoylation should increase PDE δ -Ras interaction, whilst the suppression of depalmitoylation should have the opposite effect. Indeed, treatment of mCit-HrasG12V transfected MDCK cells with 50 μ M of the palmitoylation inhibitor 2-Bromopalmitate (2-BP) (Webb et al., 2000) resulted in a significant increase in the interacting fraction (α) of mCit-HrasG12V (Figure 4.14). Blocking palmitoylation with inhibitor of palmitate synthesis increased the net unpalmitoylated form of Ras. This unpalmitoylated Ras form confers low membrane affinity and hence was easily solubilized by PDE δ as observed (Figure 4.14). Conversely, selective inhibition of Ras de-acylation by the thioesterase inhibitor Palmostatin-B gave rise to a fully palmitoylated but randomized endomembrane Ras distribution (Dekker et al., 2010) that did not interact with PDE δ (Figure 4.14). Equilibrium distribution of this palmitoylated endomembrane localized Ras was similar to depalmitoylated Ras form obtained on treatment with 2-BP.

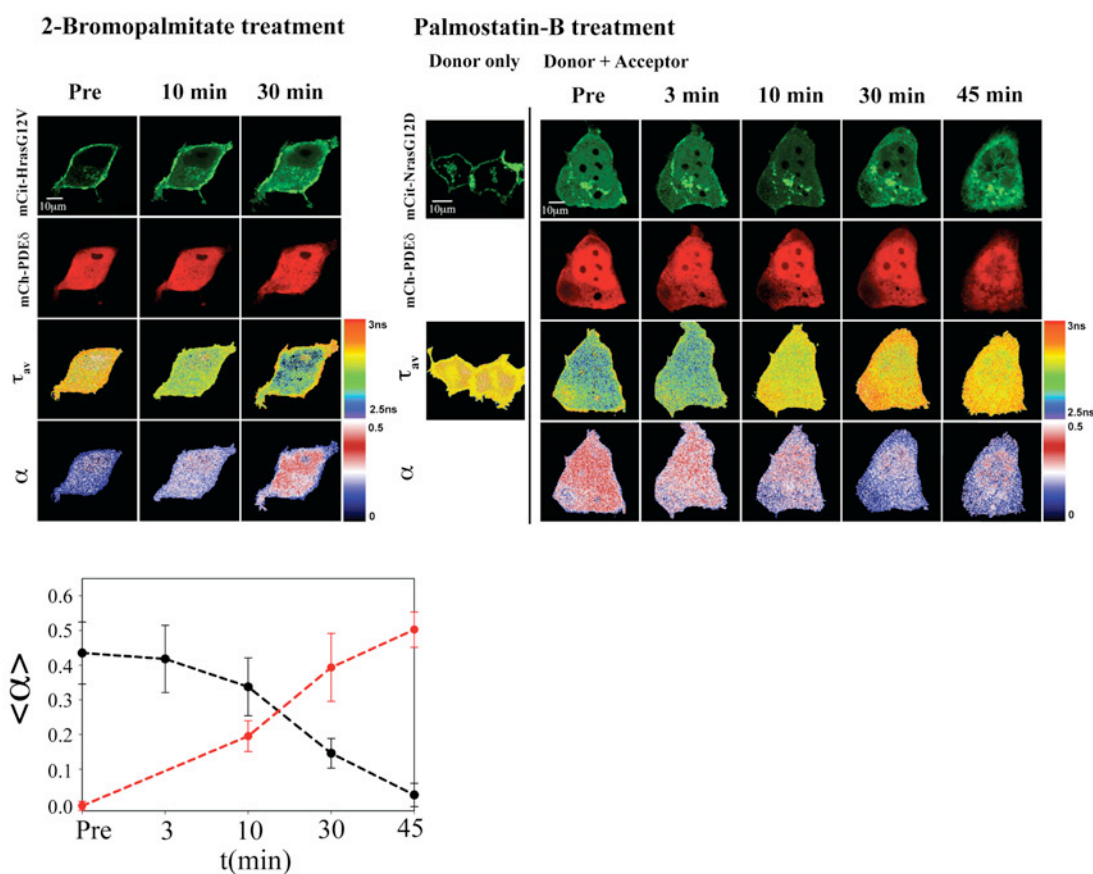


Figure 4.14 Pharmacological intervention with the Ras acylation cycle affects PDE δ activity

Left panel: Inhibition of palmitoyl transferase activity by 50 mM 2-Bromopalmitate. FLIM time series on cells expressing mCit-HrasG12V and mCh-PDE δ indicate increasing interaction between HrasG12V and PDE δ in the cytoplasm after 2-Bromopalmitate treatments. Upper two rows: fluorescence intensity distribution of the indicated fluorescent fusion proteins. Lower two rows: average fluorescence lifetime (τ_{av}) of mCit-HrasG12V and molar fraction (α) of interacting mCit-HrasG12V with mCh-PDE δ . **Right panel:** Time lapse FLIM of mCit-NrasG12D and mCh-PDE δ transfected MDCK cells show the loss of PDE δ -NrasG12D interaction after thioesterase inhibition by Palmostatin-B treatment. Quantified change in average HrasG12V/ NrasG12D populations interacting with PDE δ $\langle\alpha\rangle$, calculated from cells incubated with 2-Bromopalmitate (red) or Palmostatin-B (black) (n=4 per data point).

This shows that the depalmitoylated fraction and not simply the cellular localization of Ras proteins is the major factor that determines the interaction with PDE δ . This also explains why the more labile palmitoylation of Nras facilitates a much more efficient solubilization by PDE δ than for Hras at steady state in cells. Comparison of the palmitoylation level of Ras using the Biotin Acyl Exchange (BAE) assay in cells treated with and without Palmostatin-B indeed showed that about half of the Nras molecules are depalmitoylated versus a quarter of the Hras molecules at steady state (Figure 4.15). This also shows that at least 50% of Nras is already depalmitoylated

when it reaches the PM via the secretory pathway, accentuating the role of acylation cycle dynamics in the maintenance of palmitoylatable Ras protein localization.

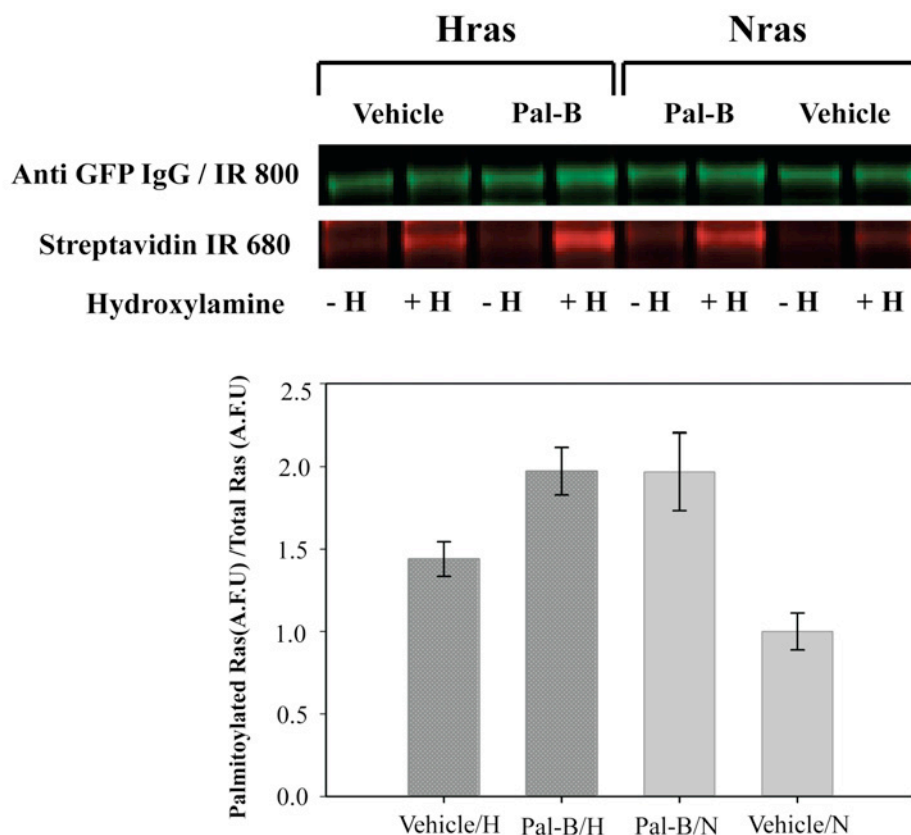


Figure 4.15 Palmitoylated Ras levels after thioesterase inhibition (BAE assay)
Comparative increase in the fraction of palmitoylated Hras versus Nras protein in live cells upon treatment with Palmostatin-B as measured by the BAE method (Dekker et al., 2010; Drisdell and Green, 2004). Arbitrary fluorescence units (A.F.U.) determined using IR dyes were quantified from western blots representing 3 independent experiments. Samples left to right: DMSO vehicle treated Hras expressing MDCK cells; Palmostatin-B treated Hras expressing MDCK cells; Palmostatin-B treated Nras expressing MDCK cells; DMSO vehicle treated Nras control cells. Palmostatin-B treatment caused a remarkable 2-fold difference in palmitoylated Nras levels relative to control cells, compared to only a 1.3-fold increase in palmitoylated Hras levels under the same experimental conditions.

4.3.7 PDE δ acts as a shuttling factor for palmitoylatable Ras

To clarify the role of PDE δ as a shuttling factor for depalmitoylated Ras proteins and to ascertain that the mobility of palmitoylated and non-palmitoylated Ras proteins is affected by PDE δ expression. The diffusional properties of the non-palmitoylated HrasC181S/C184S mutant fused to a photoactivatable variant of GFP (paGFP) were measured by FLAP (Fluorescence Loss After Photoactivation) (Figure 4.16). paGFP

displays little fluorescence initially on excitation with 488nm wavelength. However, exposure to short irradiation with near-UV light lead to hundred times increase in fluorescence that allows imaging of selected protein pools within a single cell (Patterson and Lippincott-Schwartz, 2002). A small circular region in the cytoplasm of the cell was shortly illuminated by 405 nm laser light. This selectively photoconverted fraction of cytoplasmic depalmitoylated Ras pool but not the protein on endomembranes. Diffusion of photoconverted molecules within this small region was then observed to deduce the diffusion rate of these molecules. Ectopic expression of PDE δ led to an increase in the effective diffusion of paGFP-HrasC181S/C184S as compared to cells lacking ectopic PDE δ expression, whereas downregulation of PDE δ by siRNA led to a much slower effective diffusion (Figure 4.16). In agreement with results that PDE δ cannot solubilize geranylgeranylated Ras, the effective diffusion of geranylgeranylated paGFP-HRasC181/C184S CLLL mutant was not affected by the expression of PDE δ (Figure 4.16) and was comparable to that of paGFP-HrasC181S/C184S in PDE δ -specific siRNA treated cells (Figure 4.16). Similarly, the effective diffusion of Δ CaaX box mutant of Nras was not affected by PDE δ expression (Figure 4.16, Table 4.2).

FRAP experiments were performed to ascertain role of PDE δ in affecting kinetics of Ras diffusion from Golgi to PM. MDCK cells transiently transfected with the Golgi marker GalT-CFP and mCit-Nras in the presence /absence of mCh-PDE δ were treated with cycloheximide for 2-3 h prior experiment and maintained at 37°C (Figure 4.17). mCitrine fluorescence was bleached at the Golgi and the time course of fluorescence recovery was obtained. mCh-PDE δ expression substantially increased the fluorescence recovery at the Golgi (Figure 4.17, lower panel), showing that PDE δ enhances the effective diffusion of the depalmitoylated Nras thereby increasing the probability of encounter with the Golgi and thus the rate at which Ras gets re-palmitoylated.

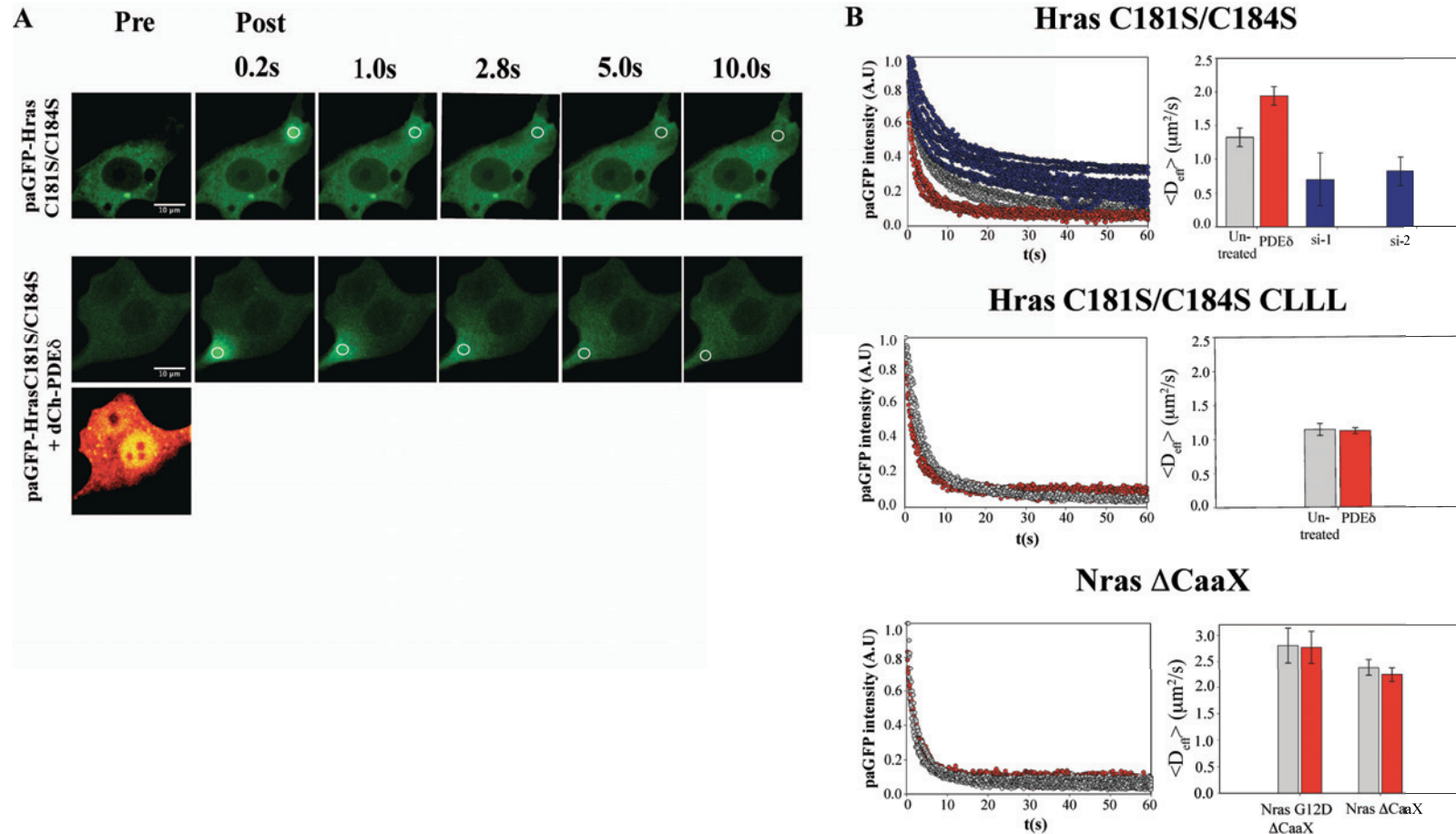


Figure 4.16 PDE δ enhances the effective diffusion of farnesylated Ras proteins

(A) Fluorescence loss after photoactivation (FLAP) in a defined region in the cytoplasm of solely farnesylated paGFP-HrasC181S/C184S fusion proteins in the presence (lower panel) or absence (upper panel) of dCh-PDE δ ectopic expression. A white circle in the image time series outlines the photoactivated region. (B) Left panels: Overlay of FLAP curves: paGFP-HrasC181S/C184S (upper, n=10), paGFP-HrasC181S/C184S CLLL (middle, n=7) and Nras ΔCaaX (lower, n=8). Red curves indicate fluorescence loss after photoactivation in cells co-expressing dCh-PDE δ , grey curves indicate cells without dCh-PDE δ expression and blue curves represents cells after siRNA mediated PDE δ knockdown (n=8). All curves are normalized to one. Right panels: Mean diffusion constant D_{eff} was determined from $D_{\text{eff}} = r^2/(4\tau_D)$ where τ_D was obtained from fitting the fluorescence loss in the ROI with $f(t) = 1 - (1 - \eta) \exp(-2\tau_D/t)[I_0(2\tau_D/t) + I_1(2\tau_D/t)] + \eta$ in different measurements. siRNA1/2 represent two different siRNA sequences used to downregulate PDE δ . Calculated mean D_{eff} and relation time (τ_D) are also shown in table 4.1.

Table 4.2 Calculated τ_D and D_{eff} from FLAP performed on different Ras mutants**a) Relaxation time (τ_D)**

	Untreated	PDEδ expression
Hras C181S/C184S	2.80 \pm 0.3 sec	1.82 \pm 0.14 sec
Hras C181S/C184S CLLL	3.53 \pm 0.18 sec	3.45 \pm 0.17 sec
NrasG12D ΔCaaX	1.19 \pm 0.15 sec	1.21 \pm 0.11 sec
Nras ΔCaaX	1.25 \pm 0.10 sec	1.23 \pm 0.21 sec
Hras C181S/C184S_siRNA-1	4.75 \pm 0.62 sec	n.a
Hras C181S/C184S_siRNA-2	4.20 \pm 0.78 sec	n.a

n.a = not applicable

b) Effective Diffusion (D_{eff})

	Untreated	PDEδ expression
Hras C181S/C184S	1.32 \pm 0.14 mm ² /sec	1.94 \pm 0.14 mm ² /sec
Hras C181S/C184S CLLL	1.14 \pm 0.03 mm ² /sec	1.12 \pm 0.04 mm ² /sec
NrasG12D ΔCaaX	2.80 \pm 0.33 mm ² /sec	2.77 \pm 0.3 mm ² /sec
Nras ΔCaaX	2.38 \pm 0.15 mm ² /sec	2.25 \pm 0.14 mm ² /sec
Hras C181S/C184S_siRNA-1	0.70 \pm 0.29 mm ² /sec	n.a
Hras C181S/C184S_siRNA-2	0.82 \pm 0.11 mm ² /sec	n.a

n.a = not applicable

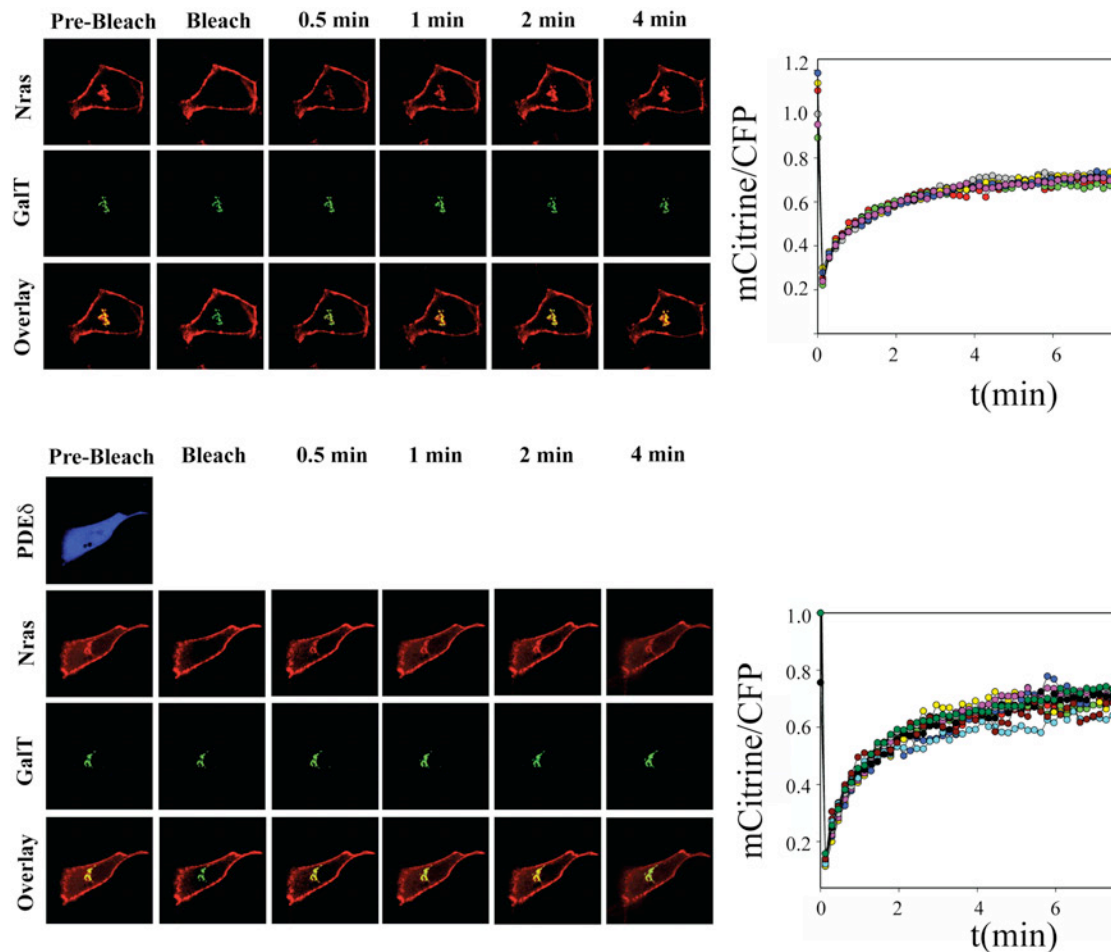


Figure 4.17 **PDE δ enhances the effective diffusion of Ras**

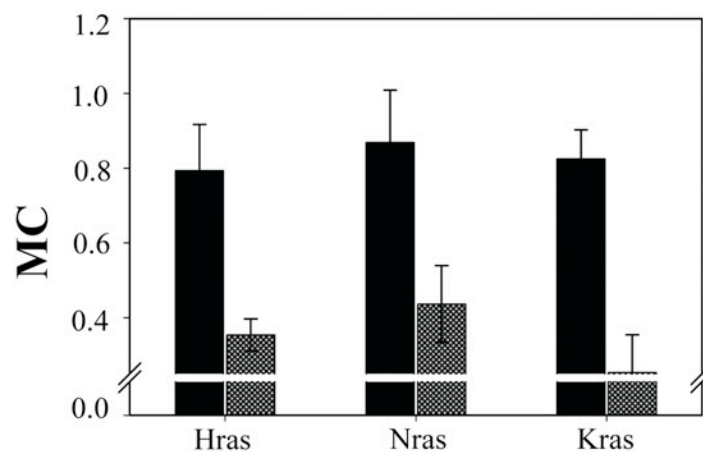
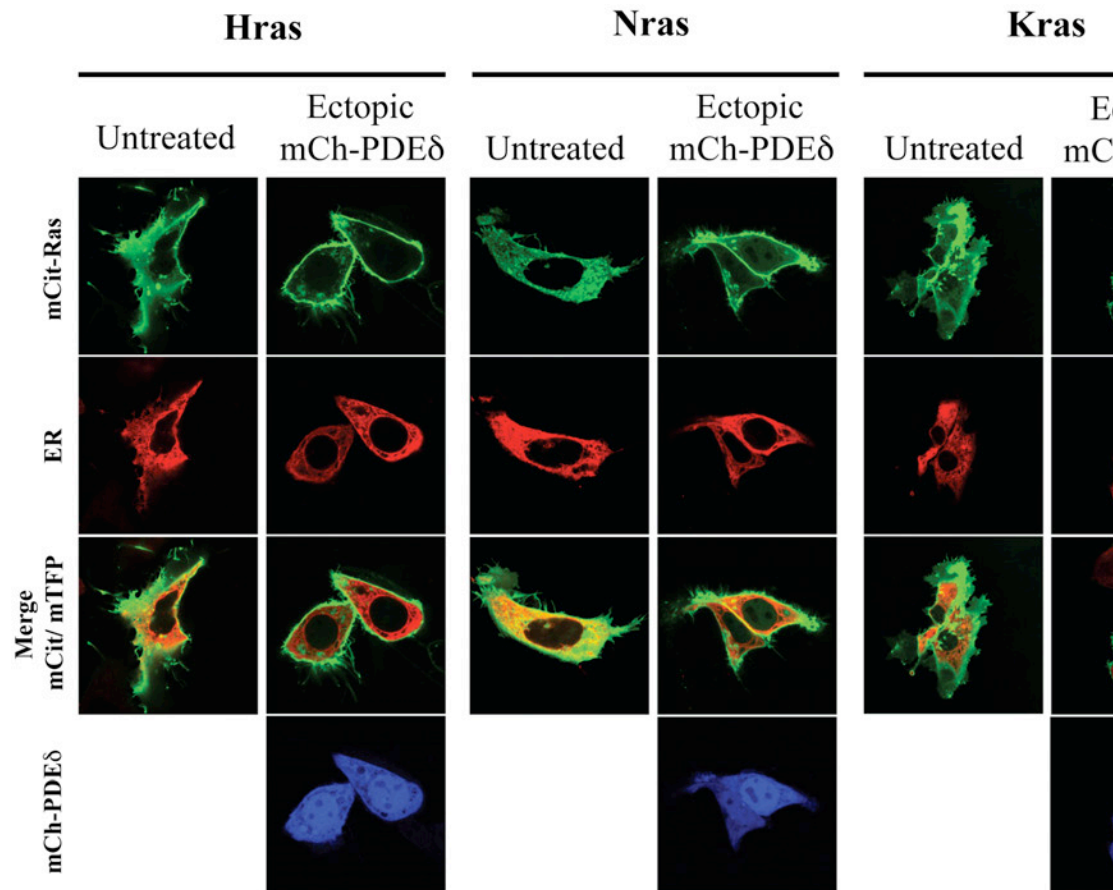
Fluorescence recovery after selective photobleaching at the Golgi of mCit-Nras in the absence (upper panel, $n=6$) or presence of ectopic mCh-PDE δ expression (lower panel, $n=10$) was ratiometrically quantified using local GalT-CFP fluorescence intensity as a reference (see methods). MDCK cells were treated with cycloheximide to block protein synthesis. An overlay of all the curves is shown on the right side of both panels.

4.3.8 PDE δ rescues Ras localization in HepG2 cells

To substantiate the role of PDE δ as a regulator of Ras localization, spatial distribution of Ras proteins in cells where endogenous PDE δ expression is low or absent was assessed. Human liver carcinoma cells (HepG2) lack PDE δ (Wilson and Smyth, 2006) and have been reported to undergo TPA-induced PKC α -mediated MEK activation, independent of Ras and Raf, to trigger sustained ERK (MAPK) signaling and cell cycle arrest (Wen-Sheng, 2006). Indeed, the steady state localization of H/N/K-Ras proteins in these cells was remarkably disorganized as compared to other cell lines that express PDE δ , such as MDCK cells (Figure 4.18, odd columns). Ras proteins mostly exhibited non-specific endomembrane distribution marked by overlap

with ER marker mTFP-Calreticulin. Strikingly, by expressing PDE δ in these HepG2 cells, the PM enrichment of the three Ras isoforms could be reinstated as shown in (Figure 4.18, even columns). This was apparent from the sharp ring of green fluorescence at the periphery of cells that over-express PDE δ . PDE δ expression induced dramatic redistribution of mCit-H/Nras to the PM and the Golgi apparatus while mCit-Kras was highly enriched at the PM. Similar effect was observed for constitutively active Ras isoforms (Figure 4.19).

In the case of Hras and Nras, the Golgi localized Ras fraction was not prominent presumably because of slower palmitate turnover kinetics in these cells. This was confirmed by inhibiting vesicular transport by temperature block (16°C). At temperatures below 17°C, endocytosis and other known forms of vesicular transport are blocked (Punnonen et al., 1998). As expected shift in the steady state distribution of wild type and constitutively active (G12V) mCit-H/Nras towards the Golgi apparatus was observed in HepG2 cells (Figure 4.19, lower panel).



Colocalization with ER marker

Figure 4.18 PDE δ expression reinstates PM Ras localization in HepG2 cells
 Confocal images of HepG2 cells expressing mCitrine labeled Hras (left 2 columns), Nras (middle two columns) and Kras (right two columns) in the presence (even columns) and absence (uneven columns) of mCh-PDE δ expression. The ER was marked by expression of mTFP-Calreticulin (second row). Bar graph: Mean Manders' coefficient (MC) calculated for each Ras isoform indicating extent of overlap with ER marker (mTFP-Calreticulin) in untreated and cells expressing ectopic mCh-PDE δ . In the latter case values of Manders' coefficient are less than 0.5 (dark grey) indicating no colocalization.

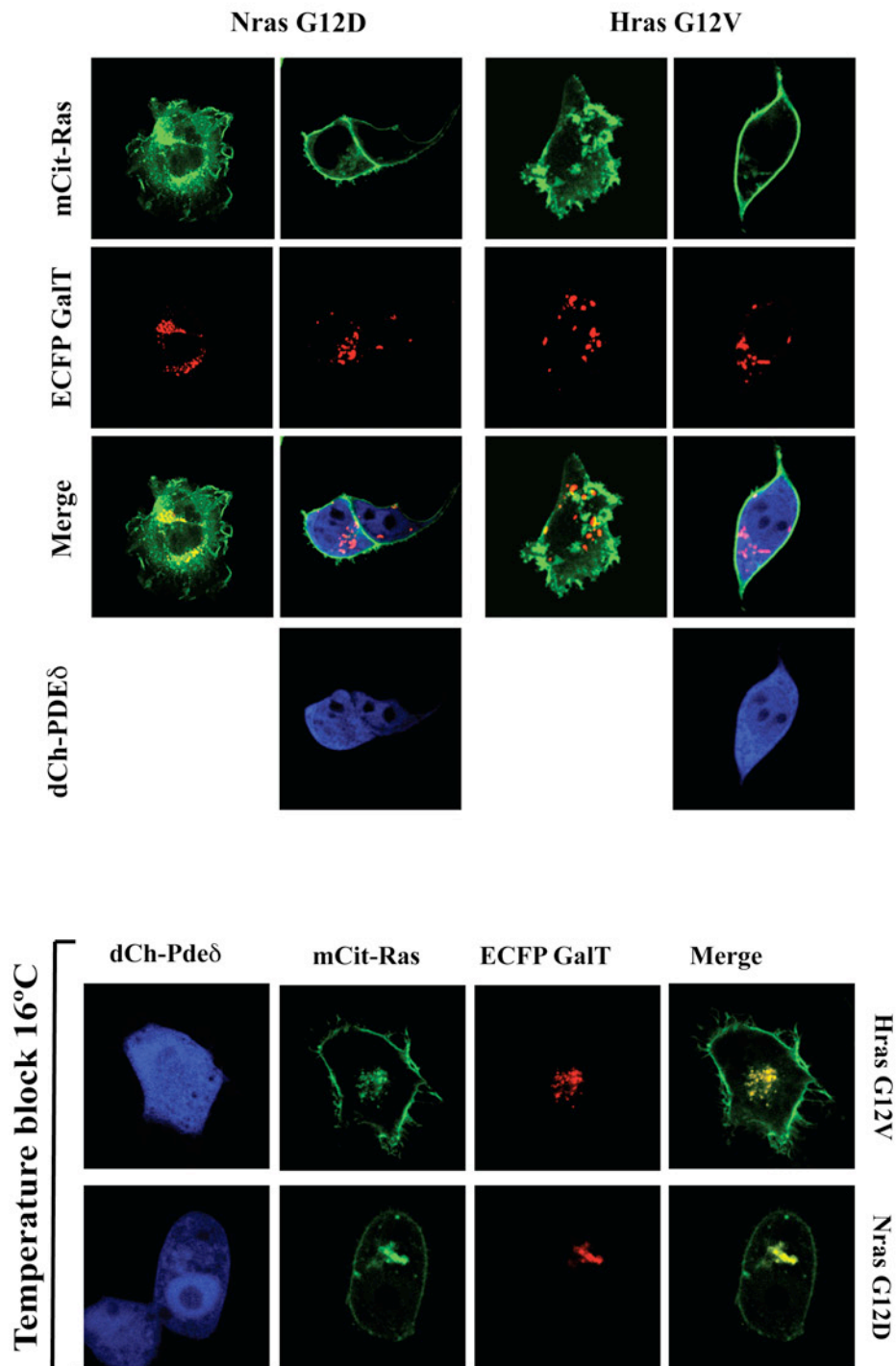


Figure 4.19 Confocal imaging of HepG2 cells

Upper panel: Confocal images of HepG2 cells expressing mCitrine tagged constitutively active Ras proteins alone or co-expressing dCh-PDE δ and the Golgi marker ECFP-GalT indicating unspecific membrane distribution and their dramatic PM redistribution after dCh-PDE δ expression. **Lower panel:** Temperature block of secretory pathway performed at 16°C for 4-8 hr on HepG2 cells co-expressing mCit-Ras, dCh-PDE δ and ECFP-GalT (Golgi marker).

4.3.9 *PDE δ modulates Ras signaling response in normal and transformed cells*

The dynamic regulation of Ras localization is tightly coupled to its signaling output (Dekker et al., 2010; Lorentzen et al., 2010). For example, long-term inhibition of thioesterase activity by Palmostatin-B down-modulates oncogenic HrasG12V signaling through loss of PM localization (Dekker et al., 2010). Since PDE δ restores PM localization of Ras in HepG2 cells, it might also be relevant in altering growth factor signaling output in these cells. HepG2 cells that ectopically expressed PDE δ , indeed showed a several fold increase in phosphorylated extracellular regulated kinase (pErk)1/2 levels upon EGF stimulation (Figure 4.20). MDCK cells that express endogenous PDE δ showed further enhancement of pErk1/2 levels after stimulation with EGF upon ectopic expression of mCh-PDE δ . Conversely, downregulation of PDE δ by RNA interference in these cells reduced phosphorylated Erk1/2 levels (Figure 4.20). These results show that Ras induced downstream Erk activity is tightly coupled to the PDE δ -mediated enrichment of Ras at the PM.

Signaling downstream of oncogenic Ras is a potent driver of cancerous growth in a variety of different tissues. It is considered pivotal for both the initiation and the maintenance of the malignant phenotype, while more recently it has further emerged as a predictor of response to targeted therapies. Somatic Hras, Nras and Kras-4B mutations encode mutant proteins with reduced intrinsic GTPase activity and resistance to GAP (GTPase activating protein) activity that therefore accumulate in the GTP-bound, active conformation. Therefore, tuning of PDE δ levels could also affect constitutive signaling via oncogenic Ras. To test this hypothesis that PDE δ down-regulation could suppress constitutive Ras signaling in cells expressing oncogenic Ras, BJ-hTERT/SV40 cells ectopically expressing Hras G12V were treated with PDE δ specific siRNA for 48-72 hrs. Downregulation of PDE δ in these cells indeed resulted in significantly reduced pErk1/2 levels (Figure 4.21).

However, mutant oncogenic Ras in human cancer is frequently expressed from its endogenous locus under normal regulatory control; indeed, several studies show that the native expression of a constitutively active Ras mutant has distinct phenotypic outcomes when compared to the exogenous over-expression of a Ras transgene (Sarkisian et al., 2007; Tuveson et al., 2004). Therefore similar studies were extended

to murine pancreatic ductal adenocarcinoma cells (mPDAC) from a genetically engineered mouse model that faithfully recapitulates the key clinical, histological and molecular features of the human disease (Tuveson et al., 2004; Hingorani et al., 2005). In this model, a tissue-specific conditional KrasG12D allele (Hingorani et al., 2005, 2003; Skoulidis et al., 2010) has been ‘knocked in’ to a single endogenous locus, and is expressed under native regulatory control just as in the corresponding human cancers. KrasG12D activation is triggered via tissue-specific expression of Cre recombinase, driven by the regulatory elements of the pancreatic and duodenal homeobox 1 (Pdx1) promoter, with or without concurrent expression of the Trp53R270H trans-dominant mutant. Thus, KrasG12D (and Trp53R270H, where present) are expressed in Pdx1-positive pancreatic progenitors, which are a cell of origin of pancreatic cancer (Gidekel Friedlander et al., 2009). Primary cultures of early passage mPDAC cells were subjected to PDE δ downregulation via siRNA treatment (Figure 4.21). Notably, variable knockdown of PDE δ resulted in significantly reduced levels of phosphorylated Erk1/2 without affecting total Ras levels and regardless of the Trp53 status of the primary tumor analyzed 48-72 hrs after PDE δ depletion (Figure 4.21). Here, a clear correlation between the residual expression of PDE δ and phosphorylated Erk1/2 levels became apparent from a 2D-histogram of PDE δ levels versus pErk1/2 levels as obtained from the western blot analysis of the three cell lines (Figure 4.21).

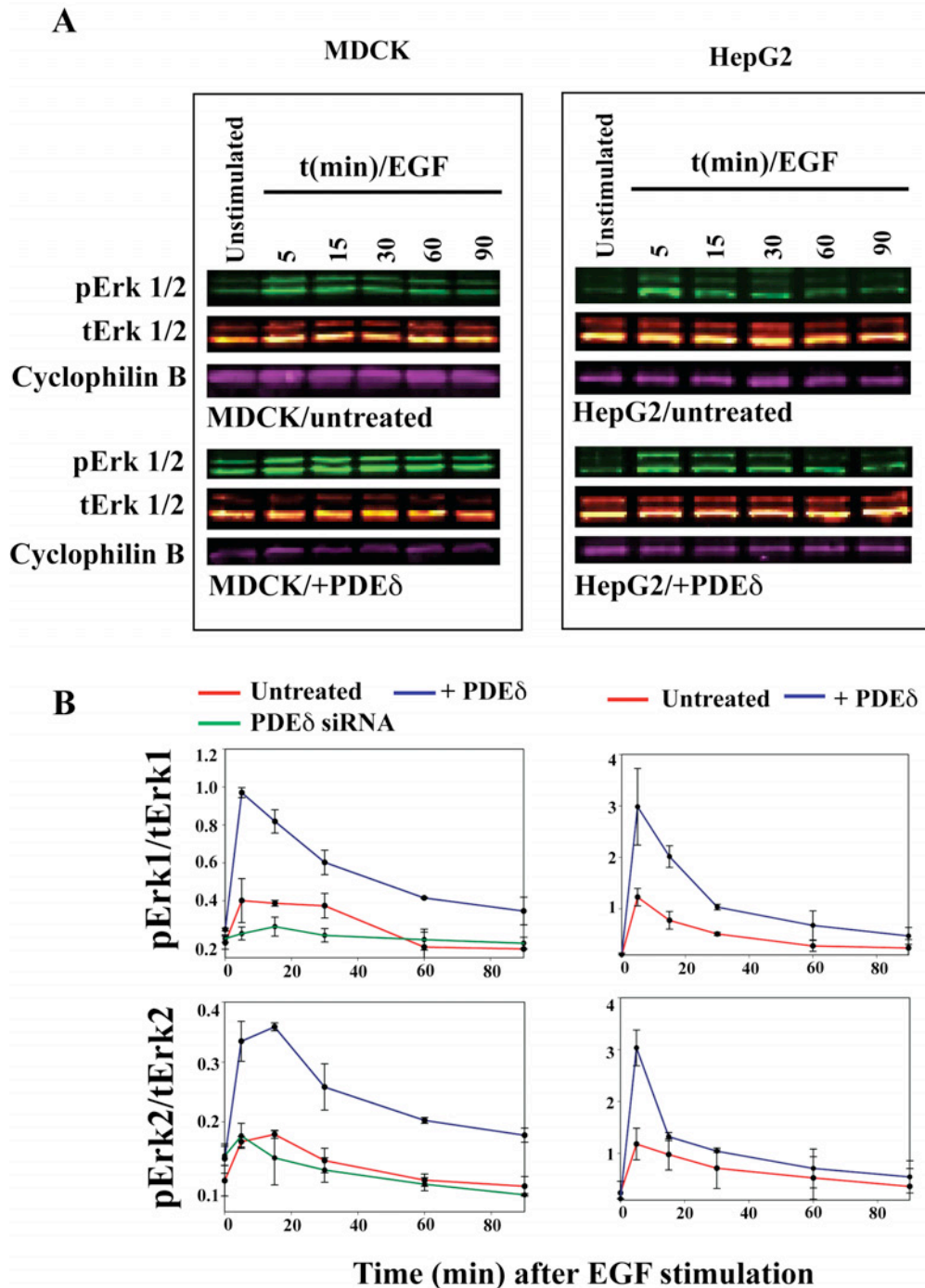


Figure 4.20 PDE δ modulates wild type Ras signaling

(A) Western blot analysis of Erk1/2 phosphorylation levels in response to EGF stimulation (100 ng/ml) in MDCK and HepG2 cells, in the absence and presence of PDE δ ectopic expression at indicated time points. (B) Densitometric quantification of Erk1/2 phosphorylation levels from western blots in response to EGF stimulation in MDCK (n=4) and HepG2 cells (n=4), in the absence (red lines) and presence (blue lines) of mCh-PDE δ ectopic expression. Green lines show the Erk1/2 phosphorylation response to EGF in MDCK cells with siRNA-mediated downregulation of PDE δ (n=4). The signal for pErk1/2 was normalized to total Erk levels.

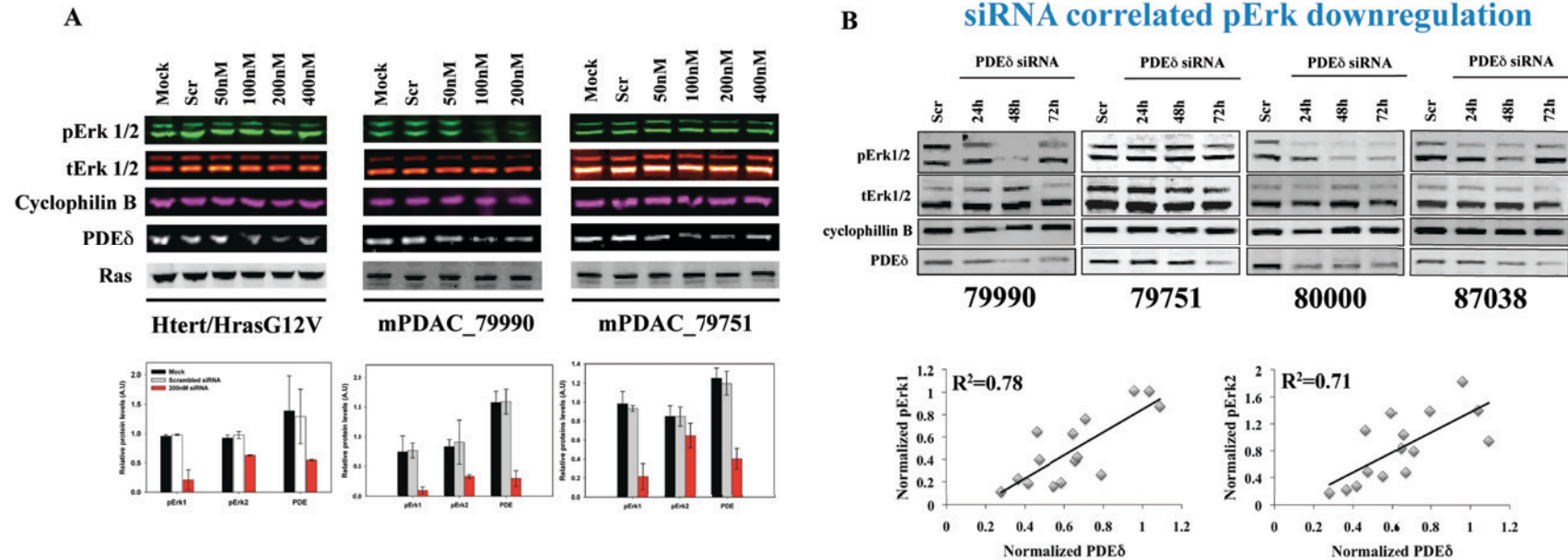


Figure 4.21 Effect of siRNA mediated PDE δ down-regulation on pErk1/phosphorylation levels in oncogenic Ras transformed cells
(A) Upper panel: Western blot analysis of siRNA mediated PDE δ downregulation in Human foreskin fibroblast BJ-hTERT/SV40/HrasG12V (left), mouse pancreatic ductal adenocarcinoma cells (mPDAC) engineered to stably express KrasG12D on one allele (clone 79990, middle) or, with additional knock-in of p53 (R270H) (clone 79751, right). Immunoblotting was performed with pErk1/2, tErk1/2, PDE δ , cyclophilin-B and H/Kras antibodies to determine endogenous protein levels following treatment with different concentrations of PDE δ specific siRNA. **Lower panel:** Relative Erk1/2 phosphorylation levels were measured by densitometric analysis of western blots ($n=3$) in mock (black), scrambled siRNA (gray) and PDE δ specific siRNA (200nM, red) transfected cells. **(B) Upper panel:** siRNA mediated PDE δ knockdown correlates with pErk downregulation at different time points (24h, 48h, 72h) in various mPDAC cell lines as indicated. **Lower scatter plots:** Western blot analysis shows the correlation between phosphorylated Erk1/2 and PDE δ levels for all siRNA treated cells. pErk and PDE δ levels are relative to those in cells treated with scrambled siRNA.

In order to verify that PDE δ knockdown also affects the distribution of endogenous Ras in these cancer cell lines, we compared the distribution of active, GTP-loaded Ras in fixed, permeabilized mPDAC cells with/without PDE δ knockdown by incubation with recombinantly purified, Cy3.5 labeled triple (3X)-RBD (Ras binding domain of Raf). mPDAC cells treated with PDE δ siRNA showed an endomembrane distribution of (3X)-RBD in contrast to the clear PM localization in untreated cells (Figure 4.22), confirming the role of PDE δ in maintaining Ras at the PM.

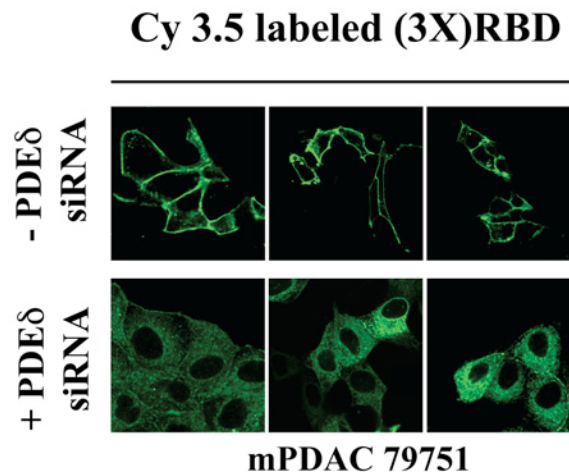


Figure 4.22 PDE δ downregulation disturbs oncogenic KrasG12D spatial partitioning

mPDAC cells (clone 79751) engineered to express oncogenic KrasG12D and Trp53R270H were stained with Cy3.5 labeled triple RBD ((3X)-RBD) to detect GTP-loaded endogenous Ras localization in cells treated with (right)/without (left) PDE δ specific siRNA.

4.3.10 PDE δ ablation inhibits cell proliferation and viability in oncogenic Ras transformed cells

To examine the inhibitory effect of PDE δ knockdown on cell proliferation and viability, clonogenic assays were performed. Both BJ hTERT-SV40/HrasG12V and mPDAC/KrasG12D cell lines in which stable, long-term PDE δ downregulation was achieved by shRNA. PDE δ down-regulation in these cancer lines resulted in reduced colony formation that correlated with PDE δ expression levels (Figure 4.23). By quantifying PDE δ and pErk1/2 levels by Western blot analysis under different shRNA-mediated downregulation conditions, there was a clear correlation between residual PDE δ and pErk1 or pErk2 levels at 72 hours after onset of PDE δ downregulation (Figure 4.23).

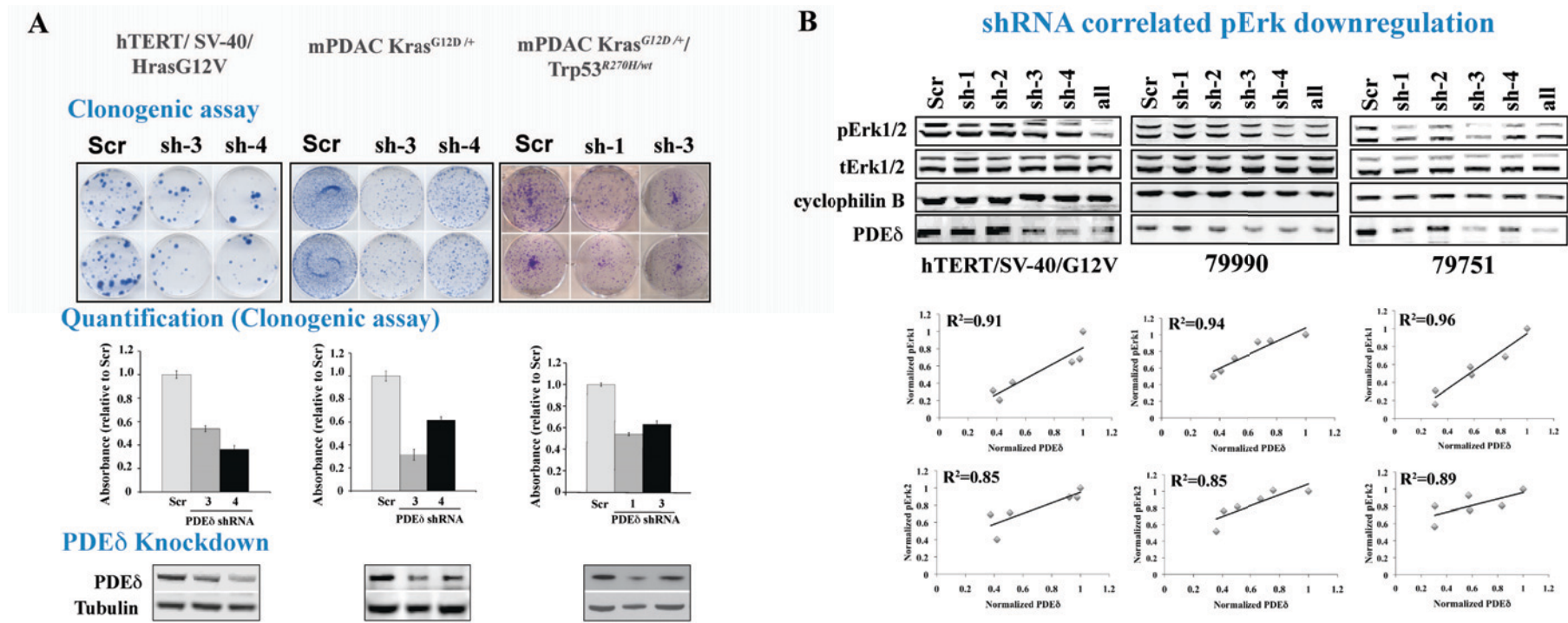


Figure 4.23 Effect of PDE δ ablation on Ras induced proliferative growth and viability

(A) **Upper panel:** Clonogenic assay performed on BJ-hTERT/SV40/HrasG12V (left), mPDAC Kras^{G12D/+} (clone 79990, middle) and mPDAC Kras^{G12D/+}/Trp53^{R270H/wt} (clone 79751, right) cells treated with scrambled or two different PDE δ specific shRNAs and stained with crystal violet 6 days post transfection. **Middle panel:** Quantified absorbance measured at 595nm after dye extraction with 10% acetic acid. Values were normalized to the absorbance of scrambled shRNA samples. **Lower panels:** western blot analysis of PDE δ levels in shRNA transfected cells by probing with anti-tubulin (loading control) and PDE δ antibody. (B) mPDAC cell lines treated with different shRNA specific to PDE δ for 72h showing correlation between residual PDE δ and pErk levels. Different mPDAC cell lines responded to different shRNA as shown. Lower scatter plots as obtained from western blot analysis showing the correlation between pErk1 (red) / pErk2 (blue) and PDE δ levels in shRNA treated BJ-hTERT/SV40/HrasG12V (left), mPDAC-79990 (middle) and mPDAC-79751 (right) cells after 72 h. pErk and PDE δ levels are relative to those in cells treated with scrambled shRNA.

Strikingly, the phosphorylated Erk1/2 levels in one of the tested mPDAC cell lines increased after 13 days of shRNA incubation and exhibited no correlation with residual PDE δ levels (Figure 4.24). This increase in pErk levels with time after PDE δ down-regulation may represent a selection process of cells that overcome the lack of PDE δ mediated Ras signaling from the PM by switching to a Ras-independent signaling pathway or alternatively strongly overexpress oncogenic Ras to survive. Thus collectively, these observations suggest that oncogenic Hras and Kras-induced Erk signaling in a number of different settings can be controlled by modulating PDE δ expression or by affecting the interaction between PDE δ and Ras.

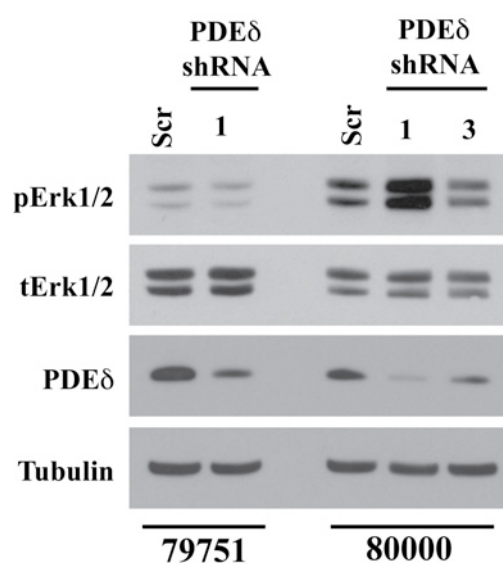


Figure 4.24 Long-term PDE δ shRNA treatment

Blots showing increased pErk1/2 levels in mPDAC clone 79751 and clone 80000 cells after 13 days of PDE δ downregulation by shRNA transfection.

4.4 Discussion and future perspectives

PDE δ is a GDI-like solubilizing factor (GSF) that is essential for the spatial organization of Ras family proteins. The GSF acts by facilitating diffusion and thereby enhancing the kinetics of trapping at a specific membrane compartment. In the case of palmitoylatable Ras proteins, PDE δ solubilizes Ras proteins that have been depalmitoylated by thioesterase activity such that they can rapidly diffuse and get trapped and concentrated at the Golgi by (re)-palmitoylation. In this case, PDE δ helps maintain a non-equilibrium distribution of Ras on the Golgi and the PM. This is facilitated by intermembrane diffusion of Ras and thereby enhancing the encounter probability with the Golgi. From there, the Ras proteins are redirected to PM by the secretory pathway. PDE δ thus effectively enhances the speed of redirection of Ras to the PM, to continuously counter the entropic tendency of lipidated Ras molecules to occupy all membranes in the cell (Silvius and l' Heureux, 1994; Shahinian and Silvius, 1995).

4.4.1 Polycationic Ras protein trafficking and membrane targeting

Contrary to the vesicular transport mechanism of H/Nras, no clear mechanism has been demonstrated for the transport and trapping of Kras at the PM. The polybasic stretch containing Ras proteins such as Kras, is solubilized by PDE δ is therefore play essential role in maintaining proper localization. Newly synthesized Kras will acquire a membrane affinity after being farnesylated, and will thus predominantly interact with the most abundant endomembrane system (endoplasmic reticulum). Binding to endomembranes is highly dynamic and does not require secondary targeting signals (Choy et al., 1999). Endomembrane-bound polybasic Ras undergoes slow spontaneous transmembrane transfer and is finally trapped at the PM because this association is favored by the overall higher negative electrostatic profile of the PM. As compared to other intracellular membranes the PM is mainly contributed by the monovalent phospholipids such as phosphatidylserine and phosphatidylinositol (Heo et al., 2006; van Meer et al., 2008; Yeung et al., 2006, 2008, 2009). This spontaneous transmembrane exchange of farnesylated Ras is consistent with the previous observation that Kras reaches the PM via a nonvesicular, diffusional mechanism (Apolloni et al., 2000; Choy et al., 1999). However, this intermembrane exchange of

farnesylated Ras enroute to the PM trap is a relatively slow process (Daleke, 2003; Williamson and Schlegel, 1994) that is actively countered by the inward membrane flow of endocytic vesicles, which tend to randomize the Ras distribution over all membranes. As evident from the earlier reports (Yokoe and Meyer, 1996) (Leventis and Silvius, 1998b), rate of exchange between PM and cytoplasm (K_{off}) for polycationic proteins particularly those bearing hydrophobic anchorage site is much faster, involves secretory pathway (active process) and highly dynamic. Solubilization by PDE δ thus increases the speed at which Kras can get (re)-trapped at the PM by electrostatic interactions, and thereby counters the entropic tendency of the dynamic PM to redistribute Ras over endomembranes. In contrast to the role of PDE δ in the acylation cycle where it helps maintain an asymmetric out of equilibrium Ras distribution, in case of polybasic stretch containing Ras proteins it helps re-instate an asymmetric equilibrium distribution. In both cases, the diffusional exploration of the system is increased by PDE δ to enhance trapping at the right membrane compartment.

4.4.2 Inter-compartmental exchange of palmitoylated and polycationic Ras

Supporting evidence suggests that inter-lipid-bilayer transfer and recruitment of Kras to other compartments like mitochondria (Bivona et al., 2006) and Golgi (Fivaz and Meyer, 2005) or rapamycin-induced recruitment to mitochondrial membranes (Silvius et al., 2006) also occur by diffusion through endomembranes rather than vesicular membrane trafficking. Interventricular membrane trafficking occur at much slower rate at lower temperatures as compared to rapamycin induced redistribution to various intracellular sites at the same temperature observed in case of FRB-Ras system (Silvius et al., 2006). Additionally simultaneous depletion from different membranous compartments occur at much faster rate at 22°C which might not true if vesicular membrane trafficking is involved (Silvius et al., 2006). This affirms the role of a generic solubilization based diffusion system for protein exchange between diverse cellular membranes, which is unaccountable by specific membrane trafficking pathway.

4.4.3 Prenylation specificity of PDE δ and its homologues

Characterizing the binding constants of PDE δ towards semi-synthetic Ras proteins showed its preference towards farnesylated, carboxymethylated Ras proteins (Chen et al., 2010). Confirming our findings, this *in vitro* study also revealed that PDE δ does

not binds geranylgeranylated Ras proteins with similar affinity. Although it is clear that PDE δ is not a GSF for geranylgeranylated Ras proteins, details regarding the involvement of any other GDI-like protein in their active transport are still elusive. One such candidate is the Human retinal gene 4 (HRG4) or UNC119, a photoreceptor synaptic protein homologous to PDE δ . HRG4 also interacts with Arl2 in a nucleotide dependent manner (Veltel et al., 2008). Since HRG4 has similar residues as in the binding pocket of PDE δ and interacts with Arl2, it is tempting to suggest that HRG4 might have a chaperone activity for the transport of lipidated proteins.

UNC119, a *C. elegans* ortholog of HRG4 is predominantly present in retinal cells and is involved in transducin trafficking. Although UNC119 main function has been described in photoreceptors, it is also expressed in leukocytes, T cells, fibroblasts etc. Also UNC119 has been found in flagellar prosites, indicating that UNC119 could function in transport of wide range of proteins apart from GPCRs. Recently a crystal structure of UNC119 in complex with transducin-alpha ($T\alpha$) was solved (Zhang et al., 2011). The structure shows UNC119 adopts an immunoglobulin like fold and has a hydrophobic pocket similar to PDE δ and RhoGDI. The complex structure also shows, how a lipid moiety, in this case a myristoyl group could bind to the UNC119 lipid binding pocket. Unlike the structures RhoGDI and PDE δ with a lipid moiety in the hydrophobic pocket (see chapter 5), the UNC119 complex structure reveals the entrance of beta-sandwich fold pried open. The opening of the UNC119 pocket is occupied by the first six amino acids of $T\alpha$ with the myristoyl chain deeply inserted into the cavity. Therefore from the structure and biochemical studies it was suggested that in UNC119 the amino acids adjacent to the lipidation site could play a role in specificity (Zhang H et al., 2011).

In another dimension, the structure also shed light in to the specificity of HRG4/UNC119 towards different lipid moieties. Since the UNC119- $T\alpha$ – myristoyl group shows that the myristoyl group is inserted deep in the pocket and the entrance is occupied by six amino acids from the $T\alpha$ (14 carbon + 6 amino acids). This suggests that the UNC119/HRG4 could potentially accommodate a geranylgeranyl group (20 carbon) in the pocket. Moreover, the first few amino acids adjacent to the acyl group are GAGASA, which has no or small side chains in a way similar to the carbon chain in long chain fatty acids further supporting the notion of a geranylgeranyl group and HRG4 interaction, which still needs to be tested.

In a recent complementary study in collaboration with Ismail et al., 2011 (unpublished) it was demonstrated that the delivery of farnesylated Ras to the right (trapping) membrane compartment is an active, regulated process, where unloading from PDE δ is facilitated by the interaction with the local active state of another G-protein (see chapter 5). Such a mechanism not only emphasizes a crucial role of PDE δ in spatially and temporally regulating farnesylated Ras proteins. But also projects its potential as an indispensable mediator of synergy between Arl and Ras signaling pathways. An interesting proposition regarding such a crosstalk is regulation of PDE δ by Arl2/3 in release and /or uptake of these prenylated Ras proteins, which has been tested and discussed in chapter 5 of this thesis. Interaction of Arl2 with PDE δ involves β -sheet/ β -sheet interface (Hanzal-Bayer et al., 2002) and not the hydrophobic pocket hence raising prospect for formation of a transient ternary complex. Hence, Ras:PDE δ complex can be regulated by local concentration of activated Arl2/3. Such an event will lead to displacement of Ras and subsequent termination of Ras signaling. Further investigation will decipher other important aspect of PDE δ synchronization with Arl family proteins and their effect on Ras signaling, most essentially implications of regulatory microtubular/cytoskeletal machinery by Arl-PDE δ complex (Zhou et al., 2006a). Such findings can emphasis on the role played by cytoskeletal machinery in impeding long-range lateral diffusion within PM of Kras like proteins.

Whether PDE δ is involved in active extraction of prenylated, lipidated Ras proteins from the PM?

Considering the fact that not all interaction partners of PDE δ process palmitoyl modifications that can be cleaved by depalmitoylating enzymes, it remains an open issue how an active solubilization event occurs that mediate extraction of different proteins and how is it triggered, if solely the C-termini of the proteins are the binding determinants. Although involvement of PDE δ in mediating active protein extraction from PM as described in case of RhoGDIs is still unknown. As in such a scenario the overexpression of PDE δ will result in rapid solubilization of polycationic Ras protein, which is indeed not the case (Figure 4.3A). PKC mediated phosphorylating events at S181 of Kras-4B (Bivona et al., 2006) triggers the dissociation of the Kras protein from the PM and its reassociation with low affinity endomembranes thus suggesting a model in which PDE δ is not actively involved in extracting Ras proteins. Instead

PDE δ functions as diffusion facilitator and aids in mixing by solubilization to rapidly relocate mistargeted, depalmitoylated dephosphorylated Ras in order to restore equilibrium.

4.4.4 Modulating Ras signaling at the PM

Dynamic regulation of compartmentalized and segregated Ras proteins is essential for maintaining their signaling specificity (Rotblat et al., 2004; Dekker et al., 2010; Rocks et al., 2005). Proteins attain various reversible and irreversible modifications in order to gain access to specific signaling compartments and thus sustain their signaling capacity. The steady state distribution of Ras proteins maintained by acylation cycle, as well as their inter compartmental exchange-rate maintained by specific GEFs and GAPs thereby regulating their signaling potential. Affecting the spatial organization of Ras thus provides a new means of modulating Ras signaling. PDE δ levels in cells serve as an important determinant of the signaling outcome of Ras activity by growth factor receptor stimulation or due to oncogenic mutation. In human hepatocarcinomas (HepG2) cells, the Erk (MAPK) signaling is triggered by PKC α mediated MEK activation, independent of Ras and Raf (Wen-Sheng W, 2006). By re-introducing PDE δ in HepG2 cells, Ras localization (Figure 4.18, Figure 4.19) and thereby EGF-induced Ras-mediated signaling (Figure 4.20) could be re-instated. This indicates that the restoration of Ras spatial localization by PDE δ gears up Ras-Raf mediated Erk stimulation from the PM. This partnership determines the strength, duration, and selectivity of the Ras signal. Ability of PDE δ to redeem Ras-Raf dependent Erk signaling might also rescue HepG2 cells from growth inhibition observed due to TPA induced PKC α hyperactivity (Wen-Sheng W., 2006).

Similarly, down-regulation of PDE δ levels in both human transformed cell lines engineered to stably express oncogenic HrasG12V and mPDAC lines expressing endogenous oncogenic KrasG12D caused decreased phosphorylated Erk levels (Figure 4.21) as well as reduced cell proliferation (Figure 4.23), indicated that PDE δ also modulates the signaling from oncogenic Ras by affecting its localization. Selection processes in the clonogenic assay, that became apparent after several days, can lead to the restoration of phosphorylated Erk levels without increase in downregulated PDE δ levels. This suggests that these tumorigenic cells either switch to a Ras-independent Erk signaling pathway or, alternatively, strongly overexpress oncogenic Ras. In the latter case, the high level of spatially randomized oncogenic

Ras generates a sufficiently high residual population at the PM, which efficiently couples to the Raf/Mek/Erk pathway.

4.4.5 PDE δ gene targeting studies

PDE δ specific gene targeting studies performed on mice showed anomalous photoreceptor physiology attributed to defective transport of membrane associated proteins and progressive rod/cone dystrophy (Zhang et al., 2004). Although, PDE δ knockout mice exhibit a notable reduction in body weight (20-30%) as compared to wild-type controls, lack of embryonic lethality argues against its functional relevance. These findings are logical with regard to reduced cell proliferation observed in case of oncogenic Kras transformed mPDAC cell-lines as demonstrated in this work (Figure 4.23). The biological significance of PDE δ mediated Ras signaling has also been challenged by the broad spectrum of PDE δ interacting farnesylated proteins. In argument to this, while Hras/Nras double knockout mice are viable (Esteban et al., 2001; Umanoff et al., 1995), Kras gene disruption results in embryonic lethality (Koera et al., 1997; Plowman et al., 2003) exhibiting its' indispensable nature. Hence even though PDE δ has a broad range of effects on different Ras family protein, there remains a good possibility that the weight reduction phenotype observed in PDE δ knockout mice indeed stems from Kras mislocalization and reduced Kras signaling during development.

By knocking down PDE δ in "normal" cells, Ras is diluted over all membranes in the cell, yet the remaining Ras at the PM can still signal – although with lower strength and thereby can maintain a basal functionality as in the developmental processes in mice. However, in oncogenic Ras transformed cells, down-regulation of PDE δ lowers the dose of (strong) oncogenic Ras signaling from the PM. In this case, the residual wild type Ras (encoded by the other of the two alleles) can signal in a low-dose regime from the PM that now allows cells to respond to extracellular cues again and thereby reinstate their normal function. Therefore interrupting the PDE δ -Ras interaction can be therapeutically very valuable since it would still allow "normal" cells" to exhibit sufficient external-cue-guided Ras signaling to function, whereas persistent oncogenic signaling would be strongly decreased. Thus the regulation of Ras localization and signaling by the solubilizing factor PDE δ (GSF) implicates this mechanism as an attractive target for cancer therapeutics. The spatial and temporal regulation of the PDE δ -Ras complex is crucial for Ras enrichment at the PM and thus

has a profound effect on oncogenic Ras signaling by coupling to downstream effectors. Pharmacological targeting of this interaction might also provide a means to lower the oncogenic Ras dose at the PM below a threshold that fully activates the wild-type Ras expressed from the non-mutated allele. Here, the allosteric RasGTP binding site on SOS (Margarit et al., 2003) might provide the feedback that activates wild-type Ras by binding oncogenic Ras in a dose dependent manner. By lowering the dose of Ras at the PM this local feedback is weakened to a point that again allows growth factor induced switching of the wild type Ras, and thereby cellular decisions to be taken. However, if the dose of oncogenic RAS at the plasma membrane is high enough to overcome a threshold, all Ras in the cell is activated and can no longer switch in response to extracellular stimulation as observed mostly in case of transformed, tumor cells. This situation is analogous to PDE δ downregulation obtained on treatment with siRNA/shRNA, which can reduce effective dose of oncogenic Ras in proximity to the plasma membrane below a threshold needed to activate SOS feedback.

V

Regulation of a GDI-like transport system for farnesylated cargo by Arl2/3-GTP

5.1 Abstract

GDI like solubilizing factor (GSF)- PDE δ binds, solubilizes prenylated Ras proteins and aids in delivering Ras proteins to their specific, cognate membrane compartments. Here a novel, GDI displacement factor (GDF) that can release GSF PDE δ from prenylated Ras proteins has been described. Crystal structure of fully modified farnesylated Rheb in complex with PDE δ [Ismail S.A et al., 2011, Nature Chem. Biol., 2011(In press)] deciphered in collaboration with this study contributes to our knowledge of how farnesylated group interacts with residues in the hydrophobic pocket. Live cells experiments performed concomitantly along with structural, biochemical evidence provides a mechanistic overview of how G-proteins Arl2/Arl3 act in a GTP-dependent manner as allosteric release factors for farnesylated cargo. Thus a novel transport mechanism specific for PDE δ binding farnesylated G-proteins and regulation by its decisive GDF has been described in this work.

5.2 Rationale and hypothesis

GDI like solubilizing factor (GSF)- PDE δ binds, solubilizes prenylated Ras proteins (GNBPs) and aids in delivering Ras proteins to their specific membrane compartments {Chandra et al (unpublished)}. However, the mechanism involving the release of prenylated Ras from PDE δ is still elusive. Various factors (GDI dissociation factors- GDFs) has been described previously that mediate release of prenylated GNBPs from their corresponding GDIs (Dirac-Svejstrup et al., 1997; Takahashi et al., 1997). GNBPs complexed to their GDI in the GDP-bound form are not substrates for their cognate GEFs (Takai et al., 1995). Rather, GDFs are needed to dissociate the GNBPs from their GDI before activation can take place.

Arl2 forms complex with PDE δ in a nucleotide dependent manner (Hanzal-Bayer et al., 2002) and based on similarity to Arf family proteins and their important contribution in intracellular vesicular transport, it has been hypothesized that Arl proteins might mediate transport of prenylated proteins in conjugation with PDE δ in photoreceptor cells (Figure 5.1) (Zhang & Baehr., 2006).

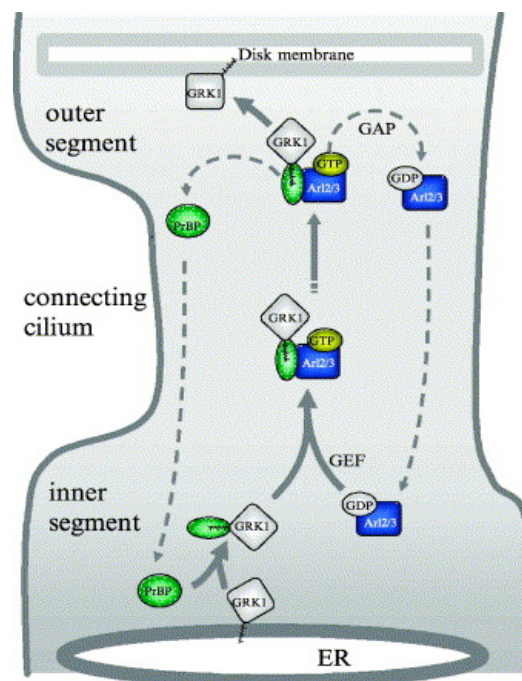


Figure 5.1 Proposed role of Arl in photoreceptor physiology
(From Zhang & Baehr et al., 2005).

According to the proposition, in the photoreceptor cells prenyl-binding protein (PDE δ) solubilizes C-terminal prenylated GRK1 from the endoplasmic reticulum

(ER) for post-translational modifications. The resulting soluble protein complex interacts with a trafficking protein such as Arl2/3-GDP. An unidentified guanine nucleotide exchange factor (GEF) exchanges GDP with GTP to activate Arl2/3, and the complex is then transported through the connecting cilium. When a GTPase activating protein (GAP) accelerates GTP hydrolysis on Arl2/3, the complex falls apart and GRK1 associates with the disk membrane in the outer segment. Concurrently, Arl2/3-GDP and PDE δ return to the inner segment to participate in another round of protein transport.

The hypothetical model raises several concerns including proposed role of Arl. Contrary to previous belief, it has been reported that intraflagellar transport (IFT) that is required for the assembly and maintenance of cilia (ciliogenesis), is negatively regulated by Arl3 (Li et al., 2010). Which contradicts the proposed function of Arl in facilitating diffusion of prenylated proteins and rather presents Arl2/3 as a potential candidate for GDI displacement factor (GDF) for PDE δ . This further adds an additional level of complexity to the spatial activity of Ras family proteins. Moreover, as proposed in the aforementioned model where PDE δ prematurely binds Arl2-GDP and later is activated by a specific GEF. This seems highly implausible as interaction with PDE δ is dependent on GTP and the binding substantially stabilizes GTP binding, increasing affinity and decreasing dissociation rates by a similar factor (Hanzal-Bayer et al., 2005; Hanzal-Bayer et al., 2002). Thirdly, unlike most other Ras proteins, Arl2 has micromolar affinity for nucleotides that allows rapid exchange and precludes the requirement of a GEF (Hanzal-Bayer et al., 2005).

Considering the cellular environment where three times lower affinity for nucleotides and the estimated 50-fold higher concentration of GTP would result in most of the Arl2 in GTP bound form. Hence Arl2 would be able to interact with effectors where reduced GTP dissociation will assist in increased stability and lifetime of the complex. In such a scenario Arl2-specific GAP would not be able to form complex with Arl2. Since PDE δ seems to be involved in binding farnesylated CaaX box GNBPs, the regulation of the Arl2-GTP binding cycle might thus not be due to the action of GEF and GAP, but rather due to the transport and release of prenylated proteins.

Thus in order to delineate role of Arl2/3 in regulating PDE δ binding to prenylated GNBPs, in this work the following aspects has been investigated:

Whether PDE δ *Arl & PDE δ *Ras complex are mutually exclusive or involves either a stable or transient tertiary complex formation?

Whether Arl2/3 contributes to diffusion/transport of PDE δ bound prenylated Ras or it mediates release of Ras from PDE δ complex?

What is the mechanism that accounts for release of Ras from PDE δ in presence of Arl2/3?

Visualizing spatial activity of PDE δ -Arl2/3 complex and its role in regulating PDE δ -Ras activity in mammalian cells.

Characterizing PDE δ mutants, defective for Arl2/3 binding and their effect in vivo.

5.3 Results

5.3.1 Conformational differences between *far-Rheb*•PDE δ and *Arl2*•GTP•PDE δ complexes

In a collaborative study with Shehab Ismail [Ismail S.A et al., 2011 (unpublished)], structure of PDE δ in complex with C-terminally modified (S-farnesylated, carboxymethylated) full length Rheb (Chen et al., 2010) was determined (Figure 5.2). The structure clearly revealed the binding pocket of PDE δ with Rheb farnesyl group embedded into the hydrophobic pocket. Additional electron density for C-terminal 177-181 residues, contacting the PDE δ with main chain atoms that involves a PDE δ flexible loop (residues 111 to 117) was observed.

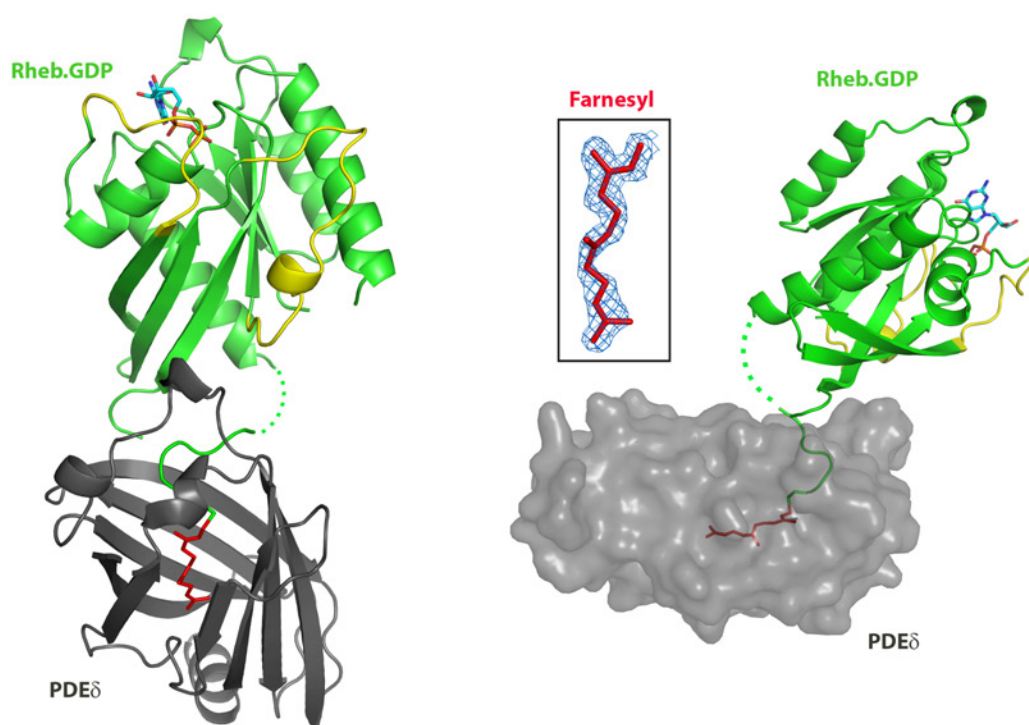


Figure 5.2 Structural analysis of farnesylated Rheb*PDE δ complex

(A) Ribbon representation of F-Rheb in green, with the farnesyl group in red and switches in yellow, in complex with PDE δ in grey and the flexible loop in light brown. GDP bound to Rheb is shown as ball-and-stick (B) Surface presentation of PDE δ , with transparency set at 40%, showing the farnesyl deeply penetrating PDE δ . Farnesylated Rheb*PDE δ complex was solved by Shehab Ismail (Post-doctoral fellow in laboratory of Prof. Alfred Wittinghofer). Figure reproduced from Ismail S.A et al., 2011 (unpublished).

Analogous to Rac**RhoGDI* complex (PDB: 1HH4) (Figure 5.3), the structure, also displayed negative charge on the surface close to C-terminus of Rheb [Ismail S.A et al., 2011(unpublished)] (Figure 5.3). This would explain the binding of polycationic C-terminus containing Ras proteins for instance Kras-4B as reported in chapter 4. In contrast to *RhoGDI*, the *PDE δ* binds prenylated Ras only at the C-terminus, not involving the switch regions as indicated in Figure 4.6 (Chapter 4). In addition to this, the binding does not involve contributions from prenylated Ras unlike CDC42-*RhoGDI* binding.

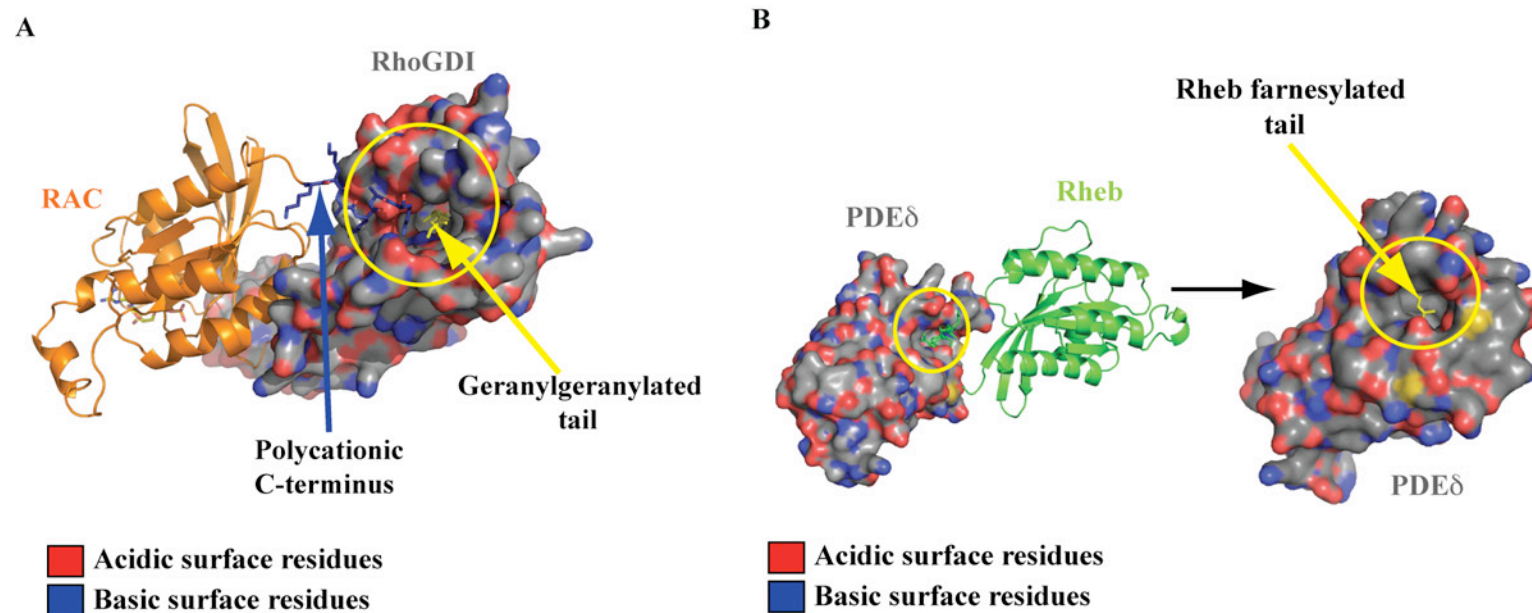


Figure 5.3 Electrostatic surface charge distribution

(A) *RhoGDI* (gray) bound to Rac (orange) (B) *PDE δ* (gray) in complex with Rheb (green) showing the negative charges surrounding the opening of the farnesyl binding pocket (marked by yellow circle). The polycationic C-terminus of Rac and Rheb is indicated in blue and the C-terminus geranylgeranylated lipid moiety (A) and farnesylated peptide (B) is shown in yellow.

5.3.2 Rationale design of PDE δ mutants: Structural insights

(A) Mutants influencing prenylated Ras*PDE δ interaction:

Mutations were designed to interrupt the binding of farnesylated group into the PDE δ binding pocket. Based on the structural similarity to RhoGDI, the lipid-binding pocket in the PDE δ structure could be deduced. From the Arl-PDE δ complex structure, two residues were chosen which are present at the entrance of PDE δ pocket (Figure 5.4). V80 and V127 were mutated to tyrosine (Y). Tyrosine has a bulky side chain and the presence of a bulky residue might sterically hinder the prenyl group from entering in to the PDE δ pocket. Although V127 is not visible in the structure, based on sequence similarity and UV cross-linking studies (Alexander et al., 2009) V127 residue was also mutated (Figure 5.4).

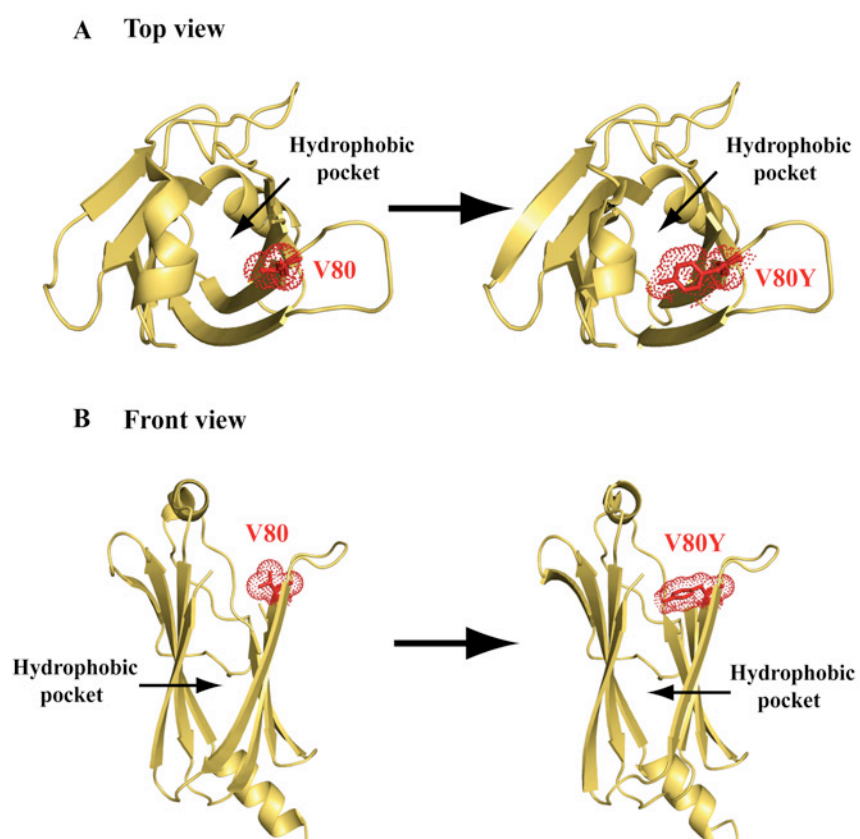


Figure 5.4 Diagrammatic representation of hydrophobic pocket of PDE δ (yellow) in complex with Arl2 (not shown)

(A) Top view (B) Front view indicating mutation at residue V80 (red) (left side pane) present at the entry of the prenyl-binding pocket. Right side panel: The V80 position when mutated to tyrosine (Y) The V80Y mutation was modelled in 1KSG pdb coordinates.

*(B) Mutants influencing Arl2*PDE δ interaction:**Arl2*PDE δ interface:*

The complex structure of Arl2*PDE δ (Figure 5.5) was used to introduce mutations in PDE δ to disrupt Arl2 binding (Hanzal-Bayer et al., 2002). Out of 8 main chain - main chain interactions, two residues in PDE δ , Q106 and T104 were mutated to lysine in the interface of Arl2- β 2*PDE δ - β 7 complex. Since the Arl2- β 2*PDE δ - β 7 sandwich is dominated by main chain interaction Q106K and T104K did not affect the interface (data not shown).

PDE δ F94A/I98A mutation:

On the other hand a large number of hydrophobic residues from PDE δ are involved in the interface with Arl2 (Figure 5.5). Therefore, Phe 94 and Ile 98 were mutated to Ala (A) to disrupt Arl2 binding. In the meantime the farnesylated Rheb*PDE δ complex structure was solved and showed that the Phe94 undergoes a conformational change between open and closed states [Ismail S.A et al., 2011(unpublished)]. Therefore, these two residues might be good candidates for testing the effect on the allosteric regulation by Arl2.

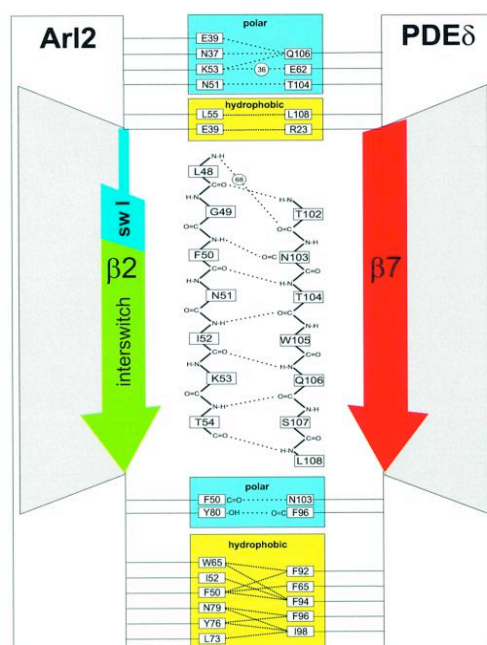


Figure 5.5 The interface of Arl2 and PDE δ -Schematic representation
Interactions as dotted lines. Residues are boxed; circles represent water molecules. Figure reproduced from Hanzal-Bayer et al., 2002.

PDE δ G28V mutation:

Due to cloning artifact, PDE δ featured an additional mutation at Gly 28 to Val (G28V). As shown in (Figure 5.5), substitution of Val in place of Gly at position 28 could affect the Arl2-PDE δ interface. Although the G28V on itself did not show any observable effect *in vitro* and *in vivo* (see section 5.3.5). The V80Y mutation in the G28V background showed dramatic effects. This could be due to the presence a bulky residue at the entrance of PDE δ lipid binding pocket. This bulky residue could lead to a distortion in the binding pocket, which is transmitted to the Arl2 interface. Therefore, the G28V mutation was further analyzed using cell biological and biochemical methods (see section 5.3.5).

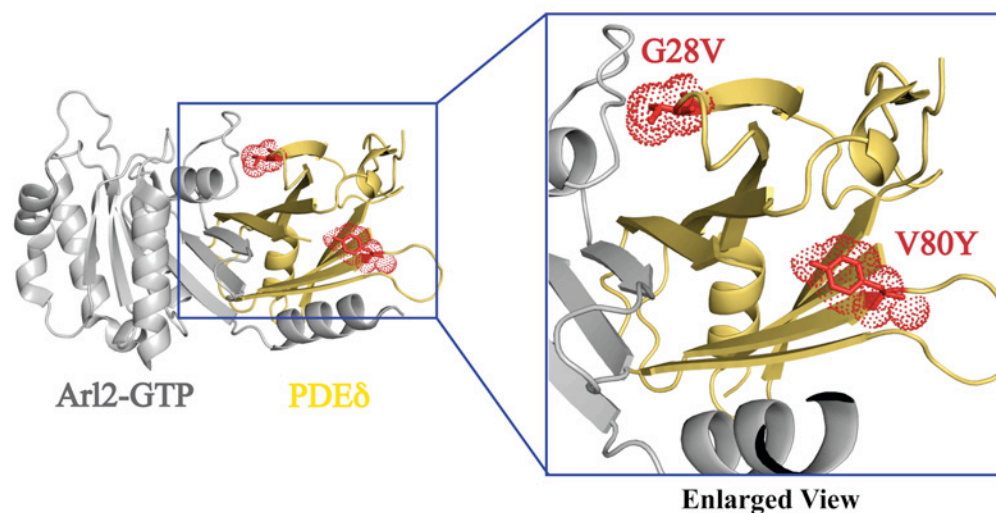


Figure 5.6 Mutations influencing Arl2*PDE δ interaction

PDE δ (yellow) in complex with Arl2-GTP (gray). Mutations are shown in red were modeled in to the 1KSG pdb coordinates. Enlarged pictogram is depicted on right side.

5.3.2.1 Spatial distribution of Ras*PDE δ in presence of constitutive active Arl2

Based on these structural predictions, the regulation of PDE δ *Ras complex by Arl2 in living cells was investigated. The effect of PDE δ on the spatial localization of Rheb was observed in presence or absence of Arl2. Since the binding of Arl2 to PDE δ is dependent on nucleotide state (Hanzal-Bayer et al., 2002), a constitutively active Arl2 mutant (Arl2Q70L) was thus expressed to visualize the effect. MDCK cells were transiently transfected with either wild-type Rheb labeled with monomeric Cherry fluorescent protein (mCherry-Rheb) or co-expressed with monomeric citrine (mCitrine) fused to PDE δ . As expected the cells expressing mCherry-Rheb showed a

clear endomembrane localization mostly labeling Golgi apparatus and ER (Figure 5.7; first row). Co-expression of mCherry-Rheb and mCitrine-PDE δ resulted in an apparent homogenous cytoplasmic distribution of Rheb supporting the idea that PDE δ is a solubilizing factor for farnesylated Rheb (Figure 5.7; second row) (chapter 4 of this thesis). Interestingly, in cells co-expressing mCherry-Rheb, mCitrine-PDE δ and mTFP-Arl2Q70L no Rheb solubilization was observed. Instead, mCherry-Rheb localized at the endomembranes analogous to the steady state distribution of mCherry-Rheb observed when Rheb was expressed alone (Figure 5.7; third row). Similarly, the partially solubilized mCherry-Nras coexpressed with PDE δ (Figure 5.7; third row), relocated to its specific plasma membrane (PM) and Golgi compartment in the presence of mTFP-Arl2Q70L. This suggests that Arl2 and farnesyl-Rheb/Nras binding to PDE δ is mutually exclusive. In the presence of Arl2, PDE δ and Rheb/Nras binding is abrogated thus resulting in restoration of Rheb/Ras spatial distribution.

To test this, PDE δ mutants defective in responding to Arl2 were designed as explained in section 5.3.2. Expression of mCitrine-PDE δ F94A/I98A mutant in MDCK cells resulted in complete solubilization of Rheb/Nras (Figure 5.7; fourth row) similar to that observed for PDE δ wild-type (Figure 5.7; second row). However, MDCK cells expressing all the three plasmids DNA encoding mCitrine-PDE δ F94A/I98A, mCherry-Rheb/Nras wt and mTFP-Arl2Q70L displayed partial solubilization with reduced soluble fraction in the nucleus (Figure 5.7; fifth row). This was indicative of impaired function of PDE δ mutant in presence of Arl2Q70L, probably due to its weakened binding to Arl2.

In order to quantify the effective solubilization of mCherry-Rheb/Nras in MDCK cells co-expressing either mCitrine-PDE δ wt or F94A/I98A mutant in presence and absence of mTFP-Arl2Q70L, spectral overlap coefficients (Manders coefficients) were determined. Manders coefficient were generated by applying Intensity Correlation Analysis (ICA) (Li.Q et al., 1004) representing co-localization of mCherry-Rheb/mCherry-NRas with either mCitrine-PDE δ wt or PDE δ F94A/I98A (Figure 5.7; lower right bar graphs). Even though marked change in solubilization of Rheb/Nras in case of PDE δ wt and PDE δ F94A/I98A mutant was observed, on quantification using Manders coefficient, no significant difference was determined. Thus, fluorescence intensity in the nucleus of these cells was determined and

compared in each case. The integrated nuclear intensity obtained after background subtraction was normalized to total cell intensity and a comparison was made for each situation. As expected very less nuclear intensity values were obtained in case of triple expression with PDE δ wt comparable to expression of Rheb/Nras alone indicating so solubilization. In contrast, values obtained in case of triple expression with PDE δ F94A/I98A mutant were more as compared to the previous case but were significantly low as compared to situation that represented complete solubilization. These observations were consistent with the biochemical experiments performed using C-terminally modified lipidated farnesylated-Rheb peptide in collaboration with A.Wittinghofer group [Ismail A. S et al., 2011 (unpublished)]. While visual examination of individual cells indicated a difference between co-expressing Rheb/NRas and PDE δ and coexpressing Rheb/NRas, PDE δ (F94A/I98A) and Arl2Q70L in localizing Rheb/NRas, in particular the nucleus, the Manders coefficient, which summarizes the fluorescence intensity difference between the two channels pixel by pixel over a number of cells, clearly showed that the PDE δ mutant does not release Rheb or NRas

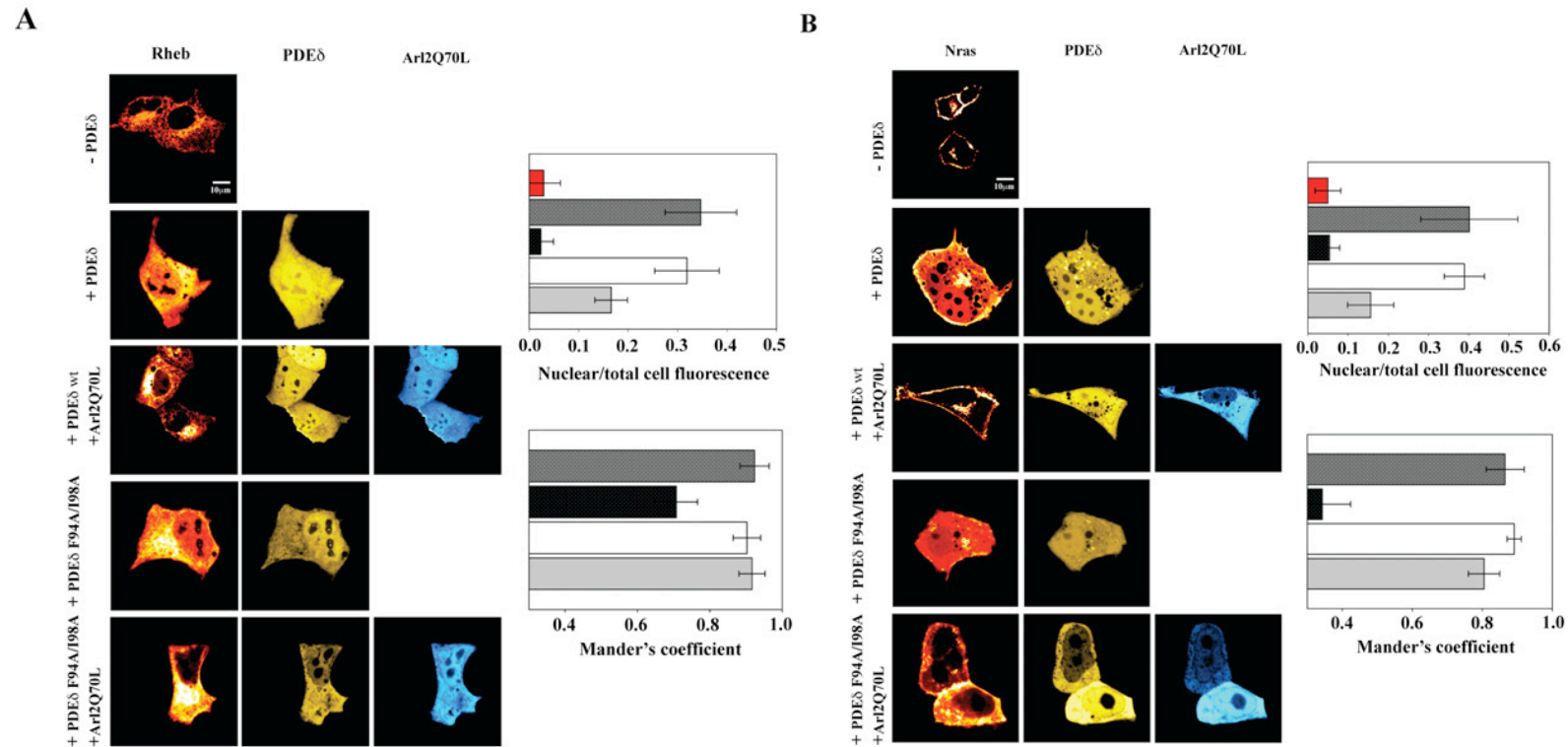


Figure 5.7 Restoration of Rheb and NRas cellular steady state localization upon Arl2Q70L expression

(A) The first panel, MDCK cells expressing Rheb labeled with monomeric Cherry fluorescent protein (mCherry-Rheb) (green) the second panel, MDCK cells expressing mCherry-Rheb (green) and PDEδ labeled with monomeric Citrine fluorescent protein (mCitrine-PDEδ) (red) the third panel, cells expressing mCherry-Rheb (green), mCitrine-PDEδ (red) and Arl2Q70L labeled with monomeric teal fluorescent protein (mTFP-Arl2Q70L) (gray), the fourth panel is the same as third panel with the double mutant (94/98) PDEδ instead of the wild type (B) Same experiment as in (A), with mCherry-NRas instead of mCherry-Rheb. Bar graph on extreme right of each panel: Manders' coefficient (n= 8-10 cells each) representing co-localization of mCherry-Rheb/mCherry-NRas with mCitrine-PDEδ wt (bar 1) or with mCitrine-PDEδ wt in the presence of Arl2Q70L (bar 2) or with mCitrine-PDEδ F94A/I98A in the presence of Arl2Q70L (bar3).

5.3.3 Disruption of Rheb*PDE δ complex by Arl2Q70L

The above data and findings from biochemical, FCCS experiments done in collaboration (Yong Xiang Chen and Alexandra Rusinova) suggested that Arl2 and farnesyl-peptide binding is mutually exclusive. Since for both Arl2 and Rheb/Ras PDE δ binding sites are non-overlapping (farnesylated moiety of Rheb binds in the hydrophobic pocket whereas Arl2 share a β sheet- β sheet interaction), one would deduce an allosteric mode of regulation. *In vitro* fluorescence polarization experiments also indicated a reduced polarization signal on addition of Arl2GppNHP to the F-Rheb*PDE δ complex formed initially (indicated by high polarization signal) in a nucleotide and concentration dependent manner [Ismail S. A et al., 2011(unpublished)]. In a different experiment with labeled F-Rheb peptide indicated that the release of Rheb from PDE δ by Arl2 is also concentration dependent [Ismail S. A et al., 2011(unpublished)]. Hence, in order to validate the mechanism for release of farnesylated Rheb/Ras from PDE δ by Arl2 in cellular environment, we performed FRET based FLIM (Fluorescence Lifetime Imaging Microscopy) in MDCK cells. Fluorescence lifetimes of FRET pair donor mTFP fused to Arl2 Q70L were measured in presence and absence of PDE δ and Rheb/Nras. Fluorescence lifetime of mTFP-Arl2Q70L alone was detected around 2.7ns similar to the reported lifetime of mTFP fluorophore at 37°C (Walther et al., 2011) ensuring that the mutation does not influence the lifetime decay of mTFP. Next, cells co-expressing mTFP-Arl2Q70L and mCitrine-PDE δ wt were measured. A significant reduction in donor fluorescence lifetime was recorded (τ_{AV} = 2.4 \pm 0.1ns) indicating efficient FRET between donor mTFP-Arl2Q70L and acceptor mCitrine-PDE δ (Figure 5.8, left bar graph). FRET efficiency was also determined indicated by alpha (α) values (Figure 5.8, right bar graph). Then, the lifetime decay curves of donor mTFP-Arl2Q70L were obtained in cells co-expressing either mCitrine-PDE δ wt (Figure 5.8, second row in each panel) or mCitrine-PDE δ F94A/I98A (Figure 5.8, third row in each panel) along with mCherry-Rheb (Figure 5.8A)/mCherry-Nras (Figure 5.8) to determine if the binary complex of Arl2 and PDE δ sustains in presence of Rheb/Ras. As indicated in Figure 5.8, reduction in fluorescence lifetime of mTFP fused to ArlQ70L in this case (binary complex) was comparable to that of cells in absence of Rheb/Nras (τ_{AV} = 2.3 \pm 0.10ns). The Rheb/Nras localization in these cells was similar to their steady state distribution. The PDE δ F94A/I98A mutant also demonstrated similar binding affinity with

comparable α with exception to solubilization effect on Rheb/Nras as described previously (Figure 5.7). This affirms the previous findings from biochemical data that the interaction of Rheb/Nras*PDE δ and Arl2*PDE δ is mutually exclusive and Arl2 acts as a displacement factor for farnesylated proteins bound to PDE δ .

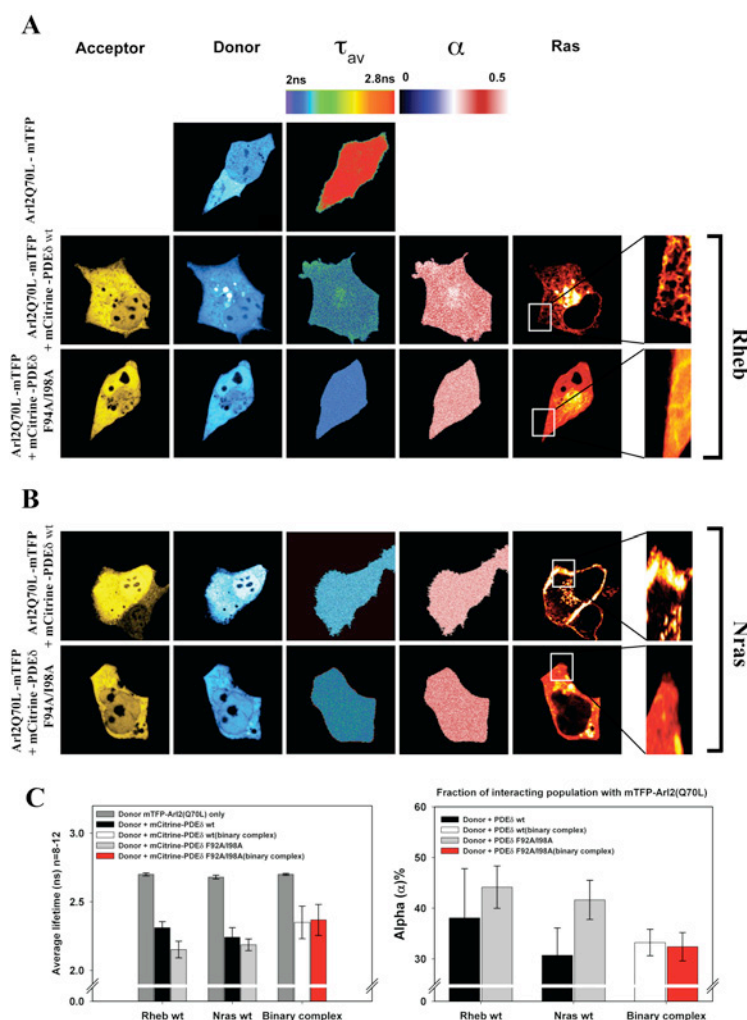


Figure 5.8 PDE δ double mutant and wild type interaction with Arl2 Q70L

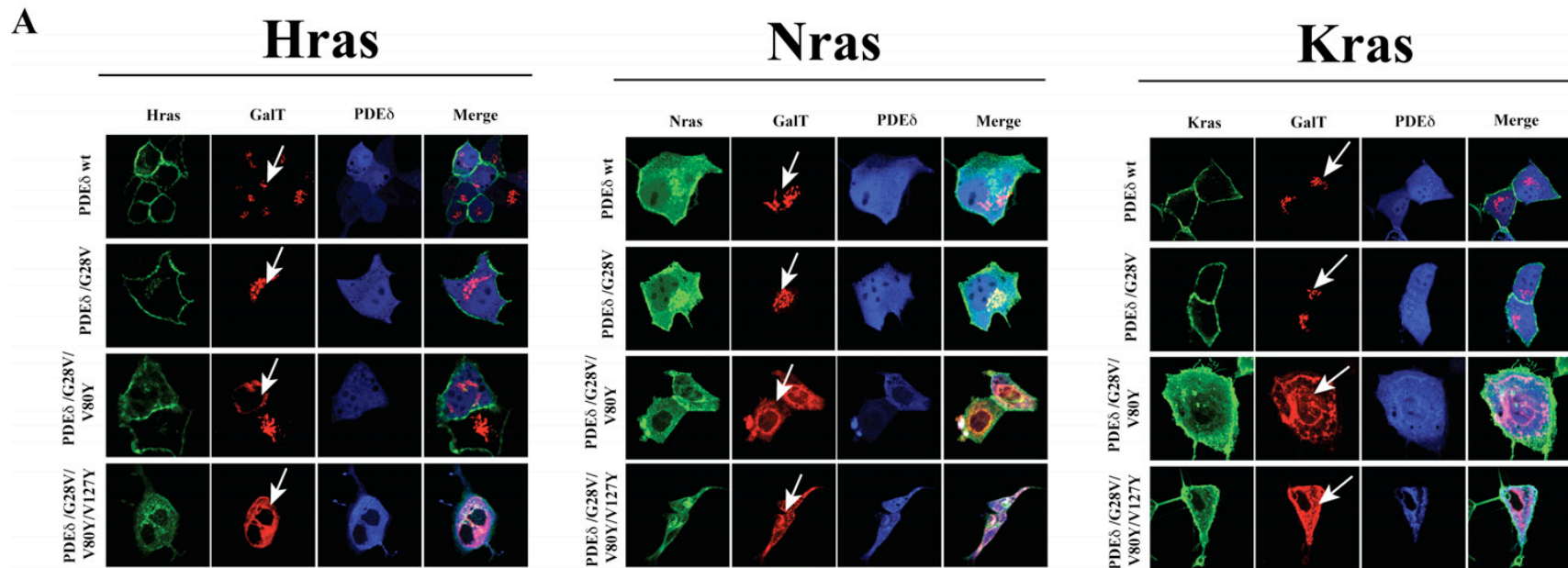
FLIM-FRET measurements in MDCK cell co-expressing mTFP-Arl2Q70L and mCitrine-PDE δ in the presence of mCherry-Rheb (A) or mCherry-Nras (B). For each sample, the fluorescence intensity of mTFP-Arl2Q70L (donor), the fluorescence intensity of mCitrine-PDE δ (acceptor), the spatial distribution of the mean fluorescence lifetime (τ_{av}) and the fraction of interacting molecules (α) are shown according to the false color lookup tables. τ_{av} values are distributed between 2 - 2.8ns where the higher lifetimes are indicated by red and the lower lifetimes are indicated by blue color. Fluorescent lifetime of the donor mTFP-Arl2Q70L is close to 2.7ns. On the extreme right hand side, enlarged micrograph exhibiting distribution of Ras proteins such as Rheb (A) and Nras (B) is shown. Lower row in each panel (A & B) represents FLIM measurements performed with mCitrine-PDE F94A/I98A double mutant. Enlarged micrograph of mCherry-Rheb distribution (extreme right) in these cells shows partial solubilization. Presented micrographs are representative of at least 8-12 independent measurements. (C) Quantified average lifetimes (left graph) and mean α

(right graph) for donor mTFP-ArlQ70L with mCitrine-PDE δ wt (black) or mCitrine-PDE δ F94A/I98A (gray) as acceptor in cells coexpressing mCherry-Rheb/Nras. Values for average lifetime and α in cells expressing donor mTFP-Arl2Q70L with mCitrine-PDE δ wt or mCitrine-PDE δ F94A/I98A as acceptor in absence of mCherry-Rheb/Nras are represented in white and red bars respectively (n=8-12).

5.3.4 Influence of PDE δ mutants on Golgi apparatus

To characterize the PDE δ mutants designed to block interaction with Ras (described in section 5.3.2), MDCK cells were transfected with mCitrine-Ras and mCherry fused PDE δ mutants co-expressed with either GalT (Golgi specific marker) or Calreticulin (ER specific marker). Cells were then visualized on a confocal microscope to specify the spatial distribution of Ras in presence of these mutants. All of the PDE δ mutants also featured an additional mutation Gly 28 to Valine (G28V) (Section 5.3.2). As shown in Figure 5.9 cells expressing PDE δ constructs with only G28V mutation displayed similar Ras distribution, as in case of PDE δ wt expression. In contrast, the ectopic expression of PDE δ G28V/V80Y in MDCK cells affected Hras spatial distribution to some extent and exhibited dispersed Golgi apparatus with considerable size (Figure 5.9, left side panels). Golgi resident enzymes marked by GalT fluorescence (Golgi resident human galactosyltransferase enzyme) showed a remarkable distributed appearance (white arrows) and labeled the neighboring membranes. Introduction of an additional V127Y mutation (Section 5.3.2) further aggravated the leakage of Golgi resident enzymes across all membranes in the cell. Ras seemed to be trapped in membrane compartments. These PDE δ mutants showed no effect on ER indicated by Calreticulin staining (Figure 5.9). Similar observations were made for other Ras isoforms for instance Nras (Figure 5.9, middle panel) and Kras (Figure 5.9, right panel). To reevaluate the contribution of G28V mutation towards observed Golgi and Ras distribution, mutated Val was substituted back to Gly. Cells expressing PDE δ V80Y/V127Y without G28V mutation showed no redistribution of either Ras or Golgi resident enzymes (marked by GalT) (Figure 5.10).

Also expression of only PDE δ G28V mutant with GalT resulted in a similar dispersed Golgi organization indicating that this effect is independent of Ras* PDE δ interaction and probably interferes with Arl2/3*PDE δ interaction. This also confirmed that G28V mutation alone has no impact on Golgi structure and organization but together with other mutations of residues lining the entrance of the PDE δ hydrophobic pocket may have a regulatory role in maintaining Golgi structure and function.



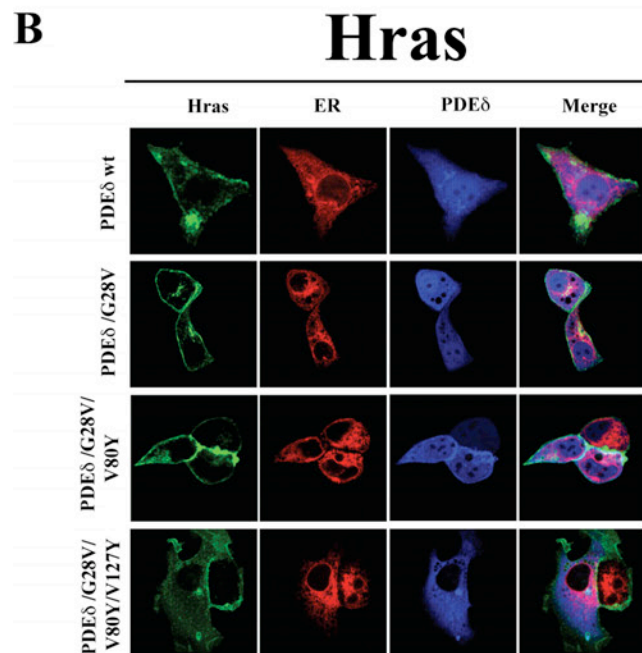


Figure 5.9 **Effect of PDE δ mutants on Golgi apparatus**
 (A) MDCK cells expressing ECFP-GalT (Golgi specific marker) and mCitrine-Hras (left panel), mCitrine-Nras (middle panel), mCitrine-Kras (right panel) in presence of either PDE δ wt (First row of each panel), PDE δ G28V (second row of each panel), PDE δ G28V/V80Y (third row of each panel) or PDE δ G28V/V80Y/V127Y (fourth row of each panel). (B) Same as (A) with exception of second column indicating mTFP-Calreticulin (ER marker) co-expression in MDCK cells. Representative micrograph of 10-15 cells each. Dispersed Golgi apparatus is indicated with white arrows in each panel.

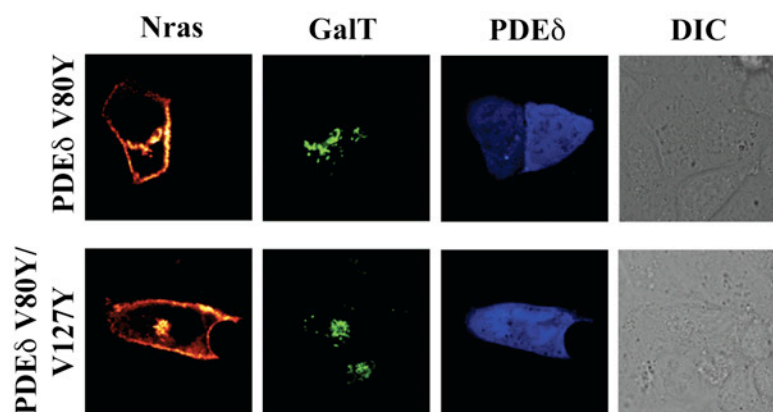


Figure 5.10 **Substitution of mutated valine to glycine**
 Ras steady state localization on remutating Val at position 28 back to Gly in PDE δ . Ras is indicated in red, GalT (Golgi specific marker) in green and PDE δ mutant expression in blue. DIC image is also shown (fourth column).

In order to further investigate the dramatic impact of PDE δ G28V/V80Y and G28V/V80Y/V127Y mutants on Golgi structure and organization, PDE δ sequences obtained from various species were aligned. The alignment showed that the Gly28 residue is highly conserved across kingdoms (Figure 5.11). This observation raises a possibility for structural and functional conservation of Gly28 across the various species, thus implicating a pivotal role of Gly28 in maintaining Golgi structure by regulating Arl.

```

Q6IB24|Q6IB24_HUMAN      MSAKDERAREILRGFKLNWMNLRDAETKILWQGTEDLSVPGVEHEARVP
O43924|PDE6D_HUMAN      MSAKDERAREILRGFKLNWMNLRDAETKILWQGTEDLSVPGVEHEARVP
Q3TDQ8|Q3TDQ8_MOUSE     MSAKDERARDILRGFKLNWMNLRDAETKILWQGTEDLSVPGVEHEARVP
Q3URU9|Q3URU9_MOUSE     MSAKDERARDILRGFKLNWMNLRDAETKILWQGTEDLSVPGVEHEARVP
O55057|PDE6D_MOUSE      MSAKDERARDILRGFKLNWMNLRDAETKILWQGTEDLSVPGVEHEARVP
Q95142|PDE6D_BOVIN      MSAKDERAREILRGFKLNWMNLRDAETKILWQGTEDLSVPGVEHEARVP
Q9XT54|PDE6D_CANFA      MSAKDERAREILRGFKLNWMNLRDAETKILWQGTEDLSVPGVEHEARVP
A8MWU0|A8MWU0_HUMAN      -----FKKNWMNLRDAETKILWQGTEDLSVPGVEHEARVP
Q6DH83|Q6DH83_DANRE     MSSDEDRAKEILRGFKLNWMNLRDAETKVLWQGTEDLSLPGVEHEARVP
A7SFK7|A7SFK7_NEMVE     MGSK-ERSEKILGGFKLNWMNLRDADTKVLWQGSSEDLSPGVEHEARVP
** *****:***:****:****:*****

```

Figure 5.11 PDE δ sequence alignment in different species

Sequence alignment of PDE δ shows conserved Gly28 in different species. Gly28 is highlighted in yellow.

5.4 Discussion and future perspectives

5.4.1 Arl2 acts as a displacement factor for PDE δ in cells

Understanding the mechanisms by which signaling events are localized and the physiological consequences of spatial restriction is an important subject of investigation. This study was performed in collaboration with Ismail et al., 2011(unpublished) where, a novel regulator [GDI displacement factor (GDF)] of GSF-PDE δ in complex with Rheb/Ras has been described. Insights from structural information derived from PDE δ *Rheb complex [Ismail et al., 2011(unpublished)] together with previously determined PDE δ *Arl2 complex (Hanzal-Bayer et al., 2002) provides a mechanistic overview of Arl2 function in teasing apart GSF/GTPase interaction. GDF Arl2 promote displacement and help recruit GTPase Rheb/Ras onto the membranes thus modulating G-proteins activation spatially and temporally. Since PDE δ is a pleiotropic factor capable of interacting with many different members of the same family, this suggests a generic role of Arl2 in modulating several of Ras family GTPases.

G-protein bound RabGDI and RhoGDI structures revealed a fully open hydrophobic pocket. In analogy to the system described here, a GDF Arl2/3 would thus be expected to allosterically stabilize a closed conformation of the GDI. The different conformation of PDE δ in the two complexes together with mutual exclusion of the two interactions make the possibility of forming a ternary complex highly unlikely, although a short-lived transient complex is formed. Inability of allosterically defective Arl2 mutant F94A/I98A to displace Rheb from lipid-binding site of PDE δ in living cells further substantiated this claim. Such a mechanism would also seem logical for cells to temporally and developmentally regulate the process of membrane attachment via GDFs.

In chapter 4 of this thesis, it has been demonstrated how signaling via wild-type as well as oncogenic Ras is affected by its subcellular distribution which in turn is modulated by Ras*PDE δ interaction [Chandra et al., 2011(unpublished)]. The establishment of Arl2/3 in allosterically regulating PDE δ -Ras/Rheb interaction opens up new prospects for targeting mutated Ras in tumorigenic models.

5.4.2 Functional significance of regulated Ras release mechanism

Much is known about the spatial regulation of Ras proteins, which are dominated by the lipid modifications (Rocks et al., 2005; Goodwin et al., 2005; Hancock et al., 1989, 1990) and/or regulation by GEFs and GAPs. Although this modulates the biological activity of the protein, very little information about dynamic interaction of Ras with membrane microenvironments is available. Lipid microenvironments on the cell surface known as lipid rafts or caveolae also take part in the signal transduction process (Simons and Toomre, 2000); (Foster et al., 2003). In response to intra- or extracellular stimuli, signaling proteins enriched in these lipid rafts and caveolae undergo changes in either size or composition in order to activate signaling cascades. This has been demonstrated in a variety of membrane-anchored proteins such as Hras (Roy et al., 1999)(Prior et al., 2001). Hras association with lipid rafts allows it to exist in a dynamic equilibrium between the liquid-ordered and disordered plasma membrane. It has been demonstrated that GTP-loading redistributes Hras from rafts into bulk plasma membrane by a mechanism involving adjacent hypervariable region of Hras. GTP bound Hras moves in and out of these liquid-ordered and disordered membranes in a regulated manner thereby efficiently activating the Raf kinase. For such a regulated event, the proposed function of Arl in mediating Ras release as described in the work will help us understand the mechanics behind this event.

PDE δ have been implicated in trafficking of agonist-induced internalization and recycling of IP receptors (Wilson and Smyth, 2006). IP receptors are mostly expressed partly in the lipid rafts (Liu et al., 2008) (Ostrom and Insel, 2004). Stimulation of the cell with a hormone or growth factor would lead to the transient fusion of lipid rafts. Alternatively, rafts could contain a nearly complete signaling pathway that would be activated when a receptor or other required molecule that is normally localized in the non-raft portion of the membrane is recruited into the raft. Thus, regulation either on account of Arl2/3 cycle or similar molecules could in principle be a way of enhancing the signaling specificity by receptor localization to a particular class of rafts that contain a specific subset of signaling components. Such a restriction would limit access of the receptor to the components of other signaling pathways and prevent crosstalk thus altering the spatial and temporal pattern of agonist-induced internalization and trafficking of these receptors.

Furthermore, the spatial localization of various Ras family proteins in the lipid rafts would suggest a similar regulatory mechanism where Arl2/3 mediated regulation could support focal activation of various pathways, introducing additional specificity into the response.

Another interesting candidate - Rho6 [Rnd1; (Nobes et al., 1998)] is a binding partner of PDE δ (Hanzal-Bayer et al., 2002a). At the subcellular level, Rnd1 controls rearrangements of the actin cytoskeleton and changes in cell adhesion considering its high concentration at adherens junctions both in confluent fibroblasts and in epithelial cells. This Rho homologue has no GTPase activity as a result of low affinity for GDP and spontaneously exchanges nucleotide rapidly in physiological buffer. Furthermore, Rnd1 lacks intrinsic GTPase activity suggesting that *in vivo*, it might be constitutively in a GTP-bound form. Expression of Rnd1 or Rnd3/RhoE in fibroblasts inhibits the formation of actin stress fibers, membrane ruffles, and integrin-based focal adhesions and induces loss of cell-substrate adhesion leading to cell rounding. The transient interaction with PDE δ , regulated by the Arl2/3 cycle, could thus in a way regulate its spatial localization and biological activity at the focal adhesions, axon guidance and cell migration.

5.4.3 GDI (-like) regulation via GGBP cross-talk

Signal transduction pathways involving GNBPs are often regulated by other sub-family GNBPs. For example, several Ras effectors in turn regulate the GEF and GAP activities of Rho and Arf family proteins. Although this type of regulation across GGBP sub families is a common theme in cell signaling, regulation via transport factors is often overlooked. In the case of Rho-GDI, so far few regulatory protein has been identified which aids or enhance the release of geranylgeranylated Rho family proteins. However, the Rho-GDIs have a role in stabilizing nucleotide and interacts with the switch regions of Rho proteins. It is widely accepted that the Rho-GDI binding interferes with GEF and GAP activity and also vice versa. Thereby facilitating the release of geranylgeranylated Rho family proteins at the right place and time (Gregory R. Hoffman, 2000).

Unlike the Rho-GDIs, the recently identified transport factor for Ras proteins, PDE δ is a GSF for Ras and an effector of Arl2/3 proteins [Chandra et al., 2011 (unpublished); (Hanzal-Bayer et al., 2002)]. From the crystal structure of Far-Rheb-

PDE δ , cell biological and biochemical experiments it is clear that the PDE δ does not bind to the Ras proteins except for the C-terminus. Therefore, it is thermodynamically unfavorable to release the farnesylated Ras protein, once the farnesyl group binds in to the PDE δ pocket. This creates a need for an external factor (GDF) such as Arl2/3, where the PDE interacts with ARL2/3-GTP, thereby inducing the conformational changes to release the farnesylated Ras. The allosteric regulation of PDE δ (a transport factor for Ras family) by Arf family (Arl2/3) represents a novel example of GNBPs cross talking involving an additional tier of spatial and temporal regulation.

5.4.4 Arl2*PDE δ mediated Golgi structure and function maintenance

The Arl proteins exhibit a great diversity of functions as they have been implicated as regulators of microtubule-dependent processes [Arl2 and Arl3 (Bhamidipati et al., 2000; Zhou et al., 2006b; Sharer et al., 2002; Hoyt et al., 1990)], lysosome mobility, and microtubule binding [Arl8 (Hofmann and Munro, 2006; Okai et al., 2004)], ciliogenesis [Arl3 and Arl6 (Avidor-Reiss et al., 2004; Chiang et al., 2004; Fan et al., 2004; Li et al., 2004; Pazour et al., 2005)], and tumorigenesis [Arl11 (Calin et al., 2005; Petrocca et al., 2006)]. Evidence for a role for Arl2 in microtubule growth in cells and more recently in maintenance of energy (ATP) levels by newly identified Arl2 GAPs/effectors in the ELMO (Engulfment and cell motility) family indicates its involvement in regulation of mitochondria and golgi morphology. As described in this study, the effect of PDE δ mutants on Golgi morphology hence adds another key player in understanding Arl2 mediated complex signaling pathways. However, additional experiments need to be done in order to gain insight regarding involvement of PDE δ in regulating Arl2/3 and to determine the extent of overlap in their actions and protein partners thus affecting its biological functions. Several interesting propositions in this regard can be made for instance it can be postulated that ELMOD1 act in cells as an ArfGAP (Bowzard et al., 2007) in order to attenuate Arf signaling at the Golgi and impact membrane traffic also at the TGN, where it has effector properties.

Apart from this the idea of Golgi-derived microtubules and their importance in organizing the Golgi itself also seems very tempting (Miller et al., 2009). Previous studies emphasizing on the role of microtubules in the organization and localization of Golgi apparatus (Miller et al., 2009; Sandoval et al., 1984; Wehland et al., 1983)

also provide scope for further investigation of these PDE δ mutants and to decipher the mode of regulation of Arl2/3 proteins via PDE δ .

5.4.4 Significance of Arl mediated regulation in ciliary dysfunction

The association of renal and retinal diseases with ciliary dysfunction is becoming increasingly appreciated. The functions of primary cilia in some organs are now being elucidated but in many other organs it has not been studied at all, and much remains to be done. Retinal photoreceptor physiology has been extensively studied in light of the visual transduction cascade--a prototypical G-protein coupled receptor transduction pathway.

The human Arf subfamily of Ras superfamily contains 16 Arl proteins (Gillingham and Munro, 2007), most of which are uncharacterized with unidentified regulatory factors such as GEFs and GAPs. Both Arl2/3 and PDE δ has been implicated in photoreceptor physiology where PDE δ has been shown to be involved in trafficking of prenylated proteins such as catalytic subunit of PDE6 and GRK1 to the outer segment of photoreceptors via connecting cilium (Norton et al., 2005). Knocking out PDE δ resulted in reduced in 20-30% reduction in mice body weight thus implicating its role in mice development, mistargeting of prenylated proteins in the photoreceptor outer and inner segments as well as retinal degeneration (Zhang et al., 2007). On the other hand, Arl3 has been implicated in ciliary disease affecting the kidney, ciliary tract, pancreas, and retina. Mice with Arl3 (-/-) knockout exhibited abnormal development of renal, hepatic and pancreatic tubule structures indicative of autosomal recessive polycystic kidney disease. Excessive photoreceptor degeneration and abnormal epithelial cell proliferation and cyst formation were also characteristic of these Arl3 mutant mice. Inability of these mutants to thrive after 3 weeks suggests that it is an important regulator of intracellular signaling, vesicular trafficking pathways, and/or movement of cellular components within or along cilia.

The mechanistic control of PDE δ activity by Arl as described in this work thus explains role of Arl3 to polarize the ciliated epithelial cells and prevent mislocalization of critical proteins via IFT. This is firmly supported by mislocalization of rhodopsin in Arl3 (-/-) rod cell bodies. With expression of PDE δ in renal tissues, one can speculate that dysfunctioning of renal primary cilia that modulate renal tubular epithelial cell proliferation and differentiation as reported in

Arl2(-/+) mice might involve spatial control of PDE δ mediated trafficking of ciliary proteins by Arl3 similar to what is described in this work.

Several point mutations in Arl3 specific GAP – ‘RP2’ have been reported in case of retinal degenerative diseases such as X-linked retinitis pigmentosa. Additionally, PDE δ is also reported to interact and regulate another X-linked RP gene (RPGR) hence highlighting the specific functional role of different Arl proteins (Arl2/Arl3) in mediating ciliary transport. Based on the therapeutic significance of these mutations in regulating retinal signal transduction pathways, an intensive study involving ciliary protein transport will prove to be very promising in finding drug targets to treat retinitis pigmentosa.

VI

References

Ahumada, A., Slusarski, D. C., Liu, X., Moon, R. T., Malbon, C. C., and Wang, H.-yu (2002). Signaling of Rat Frizzled-2 Through Phosphodiesterase and Cyclic GMP. *Science* 298, 2006 -2010.

Alexander, M., Gerauer, M., Pechlivanis, M., Popkirova, B., Dvorsky, R., Brunsveld, L., Waldmann, H., and Kuhlmann, J. (2009). Mapping the isoprenoid binding pocket of PDEdelta by a semisynthetic, photoactivatable N-Ras lipoprotein. *Chembiochem* 10, 98-108.

Allen, L. H., and Aderem, A. (1995). A role for MARCKS, the alpha isozyme of protein kinase C and myosin I in zymosan phagocytosis by macrophages. *The Journal of Experimental Medicine* 182, 829 -840.

Anant, J. S., Ong, O. C., Xie, H. Y., Clarke, S., O'Brien, P. J., and Fung, B. K. (1992). In vivo differential prenylation of retinal cyclic GMP phosphodiesterase catalytic subunits. *Journal of Biological Chemistry* 267, 687 -690.

Aoki, Y., Niihori, T., Kawame, H., Kurosawa, K., Ohashi, H., Tanaka, Y., Filocamo, M., Kato, K., Suzuki, Y., Kure, S., et al. (2005). Germline mutations in HRAS proto-oncogene cause Costello syndrome. *Nat Genet* 37, 1038-1040.

Apolloni, A., Prior, I. A., Lindsay, M., Parton, R. G., and Hancock, J. F. (2000). H-ras but not K-ras traffics to the plasma membrane through the exocytic pathway. *Mol. Cell. Biol* 20, 2475-2487.

Artemyev, N. O., Natochin, M., Busman, M., Schey, K. L., and Hamm, H. E. (1996). Mechanism of photoreceptor cGMP phosphodiesterase inhibition by its gamma-subunits. *Proc Natl Acad Sci U S A* 93, 5407-5412.

Avidor-Reiss, T., Maer, A. M., Koundakjian, E., Polyanovsky, A., Keil, T., Subramaniam, S., and Zuker, C. S. (2004). Decoding Cilia Function: Defining Specialized Genes Required for Compartmentalized Cilia Biogenesis. *Cell* 117, 527-539.

Axelrod, D., Koppel, D. E., Schlessinger, J., Elson, E., and Webb, W. W. (1976). Mobility measurement by analysis of fluorescence photobleaching recovery kinetics. *Biophys J* 16, 1055-69.

Baehr, W., Devlin, M. J., and Applebury, M. L. (1979). Isolation and characterization of cGMP phosphodiesterase from bovine rod outer segments. *Journal of Biological Chemistry* 254, 11669 -11677.

Bartels, D. J., Mitchell, D. A., Dong, X., and Deschenes, R. J. (1999). Erf2, a Novel Gene Product That Affects the Localization and Palmitoylation of Ras2 in *Saccharomyces cerevisiae*. *Mol Cell Biol* 19, 6775-6787.

- Bhagatji, P., Leventis, R., Rich, R., Lin, C. J., and Silviu, J. R. (2010). Multiple Cellular Proteins Modulate the Dynamics of K-ras Association with the Plasma Membrane. *Biophys J* 99, 3327-35.
- Bhamidipati, A., Lewis, S. A., and Cowan, N. J. (2000). Adp Ribosylation Factor-like Protein 2 (Arl2) Regulates the Interaction of Tubulin-Folding Cofactor D with Native Tubulin. *The Journal of Cell Biology* 149, 1087 -1096.
- Bhatnagar, R. S., and Gordon, J. I. (1997). Understanding covalent modifications of proteins by lipids: where cell biology and biophysics mingle. *Trends in Cell Biology* 7, 14-20.
- Bijlmakers, M.-J., and Marsh, M. (2003). The on-off story of protein palmitoylation. *Trends in Cell Biology* 13, 32-42.
- Bivona, T. G., Quatela, S. E., Bodemann, B. O., Ahearn, I. M., Soskis, M. J., Mor, A., Miura, J., Wiener, H. H., Wright, L., Saba, S. G., et al. (2006). PKC regulates a farnesyl-electrostatic switch on K-Ras that promotes its association with Bcl-XL on mitochondria and induces apoptosis. *Mol Cell* 21, 481-93.
- Bizzozero, O. A., Bixler, H. A., and Pastuszyn, A. (2001). Structural determinants influencing the reaction of cysteine-containing peptides with palmitoyl-coenzyme A and other thioesters. *Biochimica et Biophysica Acta (BBA) - Protein Structure and Molecular Enzymology* 1545, 278-288.
- Bourne, H. R., Sanders, D. A., and McCormick, F. (1991). The GTPase superfamily: conserved structure and molecular mechanism. *Nature* 349, 117-127.
- Bowzard, J. B., Cheng, D., Peng, J., and Kahn, R. A. (2007). ELMOD2 Is an Arl2 GTPase-activating Protein That Also Acts on Arfs. *Journal of Biological Chemistry* 282, 17568 -17580.
- Cadwallader, K. A., Paterson, H., Macdonald, S. G., and Hancock, J. F. (1994). N-terminally myristoylated Ras proteins require palmitoylation or a polybasic domain for plasma membrane localization. *Mol. Cell. Biol.* 14, 4722-4730.
- Calin, G. A., Trapasso, F., Shimizu, M., Dumitru, C. D., Yendamuri, S., Godwin, A. K., Ferracin, M., Bernardi, G., Chatterjee, D., Baldassarre, G., et al. (2005). Familial cancer associated with a polymorphism in ARLTS1. *N. Engl. J. Med* 352, 1667-1676.
- Camp, L. A., and Hofmann, S. L. (1993). Purification and properties of a palmitoyl-protein thioesterase that cleaves palmitate from H-Ras. *J Biol Chem* 268, 22566-74.
- Casey, P. J., and Seabra, M. C. (1996). Protein Prenyltransferases. *Journal of Biological Chemistry* 271, 5289 -5292.
- Chandra A., Grecco H.E, Pisupati. V, Perera.D, Cassidy.L, Skoulidis. F, Hedberg. C, Hanzal-Bayer. M, Venkitaraman. A.A, Wittinghofer. A, Bastiaens P.I.H (2011). The GDI-like solubilizing factor PDE δ sustains the spatial organization and signaling of Ras family proteins. *Cell* (Unpublished).

- Chardin, P., Camonis, J., Gale, N., van Aelst, L., Schlessinger, J., Wigler, M., and Bar-Sagi, D. (1993). Human Sos1: a guanine nucleotide exchange factor for Ras that binds to GRB2. *Science* 260, 1338 -1343.
- Chen, Y. X., Koch, S., Uhlenbrock, K., Weise, K., Das, D., Gremer, L., Brunsveld, L., Wittinghofer, A., Winter, R., Triola, G., et al. (2010). Synthesis of the Rheb and K-Ras4B GTPases. *Angew Chem Int Ed Engl* 49, 6090-5.
- Chiang, A. P., Nishimura, D., Searby, C., Elbedour, K., Carmi, R., Ferguson, A. L., Secrist, J., Braun, T., Casavant, T., Stone, E. M., et al. (2004). Comparative Genomic Analysis Identifies an ADP-Ribosylation Factor–like Gene as the Cause of Bardet-Biedl Syndrome (BBS3). *Am J Hum Genet* 75, 475-484.
- Choy, E., Chiu, V. K., Silletti, J., Feoktistov, M., Morimoto, T., Michaelson, D., Ivanov, I. E., and Philips, M. R. (1999). Endomembrane trafficking of ras: the CAAX motif targets proteins to the ER and Golgi. *Cell* 98, 69-80.
- Colicelli, J. (2004). Human RAS superfamily proteins and related GTPases. *Sci STKE* 2004, RE13.
- Conibear, E., and Davis, N. G. (2010). Palmitoylation and depalmitoylation dynamics at a glance. *Journal of Cell Science* 123, 4007 -4010.
- Conti, M., and Jin, S. L. (1999). The molecular biology of cyclic nucleotide phosphodiesterases. *Prog. Nucleic Acid Res. Mol. Biol* 63, 1-38.
- Cook, T. A., Ghomashchi, F., Gelb, M. H., Florio, S. K., and Beavo, J. A. (2000). Binding of the Delta Subunit to Rod Phosphodiesterase Catalytic Subunits Requires Methylated, Prenylated C-Termini of the Catalytic Subunits†. *Biochemistry* 39, 13516-13523.
- Daleke, D. L. (2003). Regulation of transbilayer plasma membrane phospholipid asymmetry. *J Lipid Res* 44, 233-42.
- Dekker, F. J., Rocks, O., Vartak, N., Menninger, S., Hedberg, C., Balamurugan, R., Wetzel, S., Renner, S., Gerauer, M., Scholermann, B., et al. (2010). Small-molecule inhibition of APT1 affects Ras localization and signaling. *Nat Chem Biol* 6, 449-56.
- Denayer, E., de Ravel, T., and Legius, E. (2008). Clinical and molecular aspects of RAS related disorders. *Journal of Medical Genetics* 45, 695 -703.
- Deterre, P., Bigay, J., Forquet, F., Robert, M., and Chabre, M. (1988). cGMP phosphodiesterase of retinal rods is regulated by two inhibitory subunits. *Proceedings of the National Academy of Sciences of the United States of America* 85, 2424-2428.
- Dever, T. E., Glynias, M. J., and Merrick, W. C. (1987). GTP-binding domain: three consensus sequence elements with distinct spacing. *Proceedings of the National Academy of Sciences* 84, 1814 -1818.
- Dighe, S. A., and Kozminski, K. G. (2008). Swf1p, a Member of the DHHC-CRD Family of Palmitoyltransferases, Regulates the Actin Cytoskeleton and Polarized Secretion Independently of Its DHHC Motif. *Mol Biol Cell* 19, 4454-4468.

- Digilio, M. C., Conti, E., Sarkozy, A., Mingarelli, R., Dottorini, T., Marino, B., Pizzuti, A., and Dallapiccola, B. (2002). Grouping of Multiple-Lentiginos/LEOPARD and Noonan Syndromes on the PTPN11 Gene. *The American Journal of Human Genetics* *71*, 389-394.
- Dirac-Svejstrup, A. B., Sumizawa, T., and Pfeffer, S. R. (1997). Identification of a GDI displacement factor that releases endosomal Rab GTPases from Rab-GDI. *EMBO J* *16*, 465-472.
- Drisdell, R. C., and Green, W. N. (2004). Labeling and quantifying sites of protein palmitoylation. *Biotechniques* *36*, 276-85.
- Dunphy, J. T., and Linder, M. E. (1998). Signalling functions of protein palmitoylation. *Biochimica et Biophysica Acta (BBA) - Molecular and Cell Biology of Lipids* *1436*, 245-261.
- Van Dyke, K., Robinson, R., Urquilla, P., Smith, D., Taylor, M., Trush, M., and Wilson, M. (1977). An analysis of nucleotides and catecholamines in bovine medullary granules by anion exchange high pressure liquid chromatography and fluorescence. Evidence that most of the catecholamines in chromaffin granules are stored without associated ATP. *Pharmacology* *15*, 377-391.
- El-Husseini, A. E.-D., Schnell, E., Dakoji, S., Sweeney, N., Zhou, Q., Prange, O., Gauthier-Campbell, C., Aguilera-Moreno, A., Nicoll, R. A., and Brecht, D. S. (2002). Synaptic Strength Regulated by Palmitate Cycling on PSD-95. *Cell* *108*, 849-863.
- Elson, E. L., and Magde, D. (1974). Fluorescence correlation spectroscopy. I. Conceptual basis and theory. *Biopolymers* *13*, 1-27.
- Engel, R., Van Haastert, P. J. M., and Visser, A. J. W. G. (2006). Spectral characterization of Dictyostelium autofluorescence. *Microsc. Res. Tech* *69*, 168-174.
- Ershova, G., Derré, J., Chételain, S., Nancy, V., Berger, R., Kaplan, J., Munnich, A., and de Gunzburg, J. (1997). cDNA sequence, genomic organization and mapping of PDE6D, the human gene encoding the delta subunit of the cGMP phosphodiesterase of retinal rod cells to chromosome 2q36. *Cytogenet. Cell Genet* *79*, 139-141.
- Esteban, L. M., Vicario-Abejón, C., Fernández-Salguero, P., Fernández-Medarde, A., Swaminathan, N., Yienger, K., Lopez, E., Malumbres, M., McKay, R., Ward, J. M., et al. (2001). Targeted genomic disruption of H-ras and N-ras, individually or in combination, reveals the dispensability of both loci for mouse growth and development. *Mol. Cell. Biol* *21*, 1444-1452.
- Fan, Y., Esmail, M. A., Ansley, S. J., Blacque, O. E., Boroevich, K., Ross, A. J., Moore, S. J., Badano, J. L., May-Simera, H., Compton, D. S., et al. (2004). Mutations in a member of the Ras superfamily of small GTP-binding proteins causes Bardet-Biedl syndrome. *Nat Genet* *36*, 989-993.
- Fanning, A. S., and Anderson, J. M. (1998). PDZ domains and the formation of protein networks at the plasma membrane. *Curr. Top. Microbiol. Immunol* *228*, 209-233.

- Farrell, F. X., Yamamoto, K., and Lapetina, E. G. (1993). Prenyl group identification of rap2 proteins: a ras superfamily member other than ras that is farnesylated. *Biochem J* 289 (Pt 2), 349-55.
- Fivaz, M., and Meyer, T. (2005). Reversible intracellular translocation of KRas but not HRas in hippocampal neurons regulated by Ca²⁺/calmodulin. *J Cell Biol* 170, 429-41.
- Florio, S. K., Prusti, R. K., and Beavo, J. A. (1996). Solubilization of membrane-bound rod phosphodiesterase by the rod phosphodiesterase recombinant delta subunit. *J Biol Chem* 271, 24036-47.
- Foster, L. J., De Hoog, C. L., and Mann, M. (2003). Unbiased quantitative proteomics of lipid rafts reveals high specificity for signaling factors. *Proc. Natl. Acad. Sci. U.S.A* 100, 5813-5818.
- Francis, S. H., Turko, I. V., and Corbin, J. D. (2001). Cyclic nucleotide phosphodiesterases: relating structure and function. *Prog. Nucleic Acid Res. Mol. Biol* 65, 1-52.
- Fukata, M., Fukata, Y., Adesnik, H., Nicoll, R. A., and Brecht, D. S. (2004). Identification of PSD-95 Palmitoylating Enzymes. *Neuron* 44, 987-996.
- Gerisch, G., Benjak, A., Köhler, J., Weber, I., and Schneider, N. (2004). GFP-golgesin constructs to study Golgi tubulation and post-Golgi vesicle dynamics in phagocytosis. *Eur. J. Cell Biol* 83, 297-303.
- Gidekel Friedlander, S. Y., Chu, G. C., Snyder, E. L., Girnius, N., Dibelius, G., Crowley, D., Vasile, E., DePinho, R. A., and Jacks, T. (2009). Context-dependent transformation of adult pancreatic cells by oncogenic K-Ras. *Cancer Cell* 16, 379-89.
- Gillespie, P. G., and Beavo, J. A. (1988). Characterization of a bovine cone photoreceptor phosphodiesterase purified by cyclic GMP-sepharose chromatography. *Journal of Biological Chemistry* 263, 8133 -8141.
- Gillingham, A. K., and Munro, S. (2007). The small G proteins of the Arf family and their regulators. *Annu. Rev. Cell Dev. Biol* 23, 579-611.
- Goldenberg, N. M., and Steinberg, B. E. (2010). Surface Charge: A Key Determinant of Protein Localization and Function. *Cancer Research* 70, 1277 -1280.
- Golebiewska, U., Gambhir, A., Hangyás-Mihályiné, G., Zaitseva, I., Rädler, J., and McLaughlin, S. (2006). Membrane-Bound Basic Peptides Sequester Multivalent (PIP₂), but Not Monovalent (PS), Acidic Lipids. *Biophysical Journal* 91, 588-599.
- González Montoro, A., Quiroga, R., Maccioni, H. J. F., and Valdez Taubas, J. (2009). A novel motif at the C-terminus of palmitoyltransferases is essential for Swf1 and Pfa3 function in vivo. *Biochem. J* 419, 301.
- Goodwin, J. S., Drake, K. R., Rogers, C., Wright, L., Lippincott-Schwartz, J., Philips, M. R., and Kenworthy, A. K. (2005). Depalmitoylated Ras traffics to and from the Golgi complex via a nonvesicular pathway. *J Cell Biol* 170, 261-72.

- Gosser, Y. Q., Nomanbhoy, T. K., Aghazadeh, B., Manor, D., Combs, C., Cerione, R. A., and Rosen, M. K. (1997). C-terminal binding domain of Rho GDP-dissociation inhibitor directs N-terminal inhibitory peptide to GTPases. *Nature* *387*, 814-9.
- Grecco, H. E., Roda-Navarro, P., and Verveer, P. J. (2009). Global analysis of time correlated single photon counting FRET-FLIM data. *Opt Express* *17*, 6493-508.
- Gregory R. Hoffman, R. A. C. (2000). Regulation of the RhoGTPases by RhoGDI. Available at: <http://www.ncbi.nlm.nih.gov/books/NBK6041/> [Accessed July 8, 2011].
- Griesbeck, O., Baird, G. S., Campbell, R. E., Zacharias, D. A., and Tsien, R. Y. (2001). Reducing the environmental sensitivity of yellow fluorescent protein. Mechanism and applications. *J Biol Chem* *276*, 29188-94.
- Hallak, H., Muszbek, L., Laposata, M., Belmonte, E., Brass, L. F., and Manning, D. R. (1994). Covalent binding of arachidonate to G protein alpha subunits of human platelets. *Journal of Biological Chemistry* *269*, 4713 -4716.
- Hancock, J. F., Magee, A. I., Childs, J. E., and Marshall, C. J. (1989). All ras proteins are polyisoprenylated but only some are palmitoylated. *Cell* *57*, 1167-1177.
- Hancock, J. F., Paterson, H., and Marshall, C. J. (1990). A polybasic domain or palmitoylation is required in addition to the CAAX motif to localize p21ras to the plasma membrane. *Cell* *63*, 133-139.
- Hanzal-Bayer, M., Renault, L., Roversi, P., Wittinghofer, A., and Hillig, R. C. (2002a). The complex of Arl2-GTP and PDE delta: from structure to function. *EMBO J* *21*, 2095-106.
- Hanzal-Bayer, M., Linari, M., and Wittinghofer, A. (2005). Properties of the Interaction of Arf-like Protein 2 with PDE[delta]. *Journal of Molecular Biology* *350*, 1074-1082.
- Hanzal-Bayer, M., Renault, L., Roversi, P., Wittinghofer, A., and Hillig, R. C. (2002b). The complex of Arl2-GTP and PDE delta: from structure to function. *EMBO J* *21*, 2095-2106.
- Hart, T. C., Zhang, Y., Gorry, M. C., Hart, P. S., Cooper, M., Marazita, M. L., Marks, J. M., Cortelli, J. R., and Pallos, D. (2002). A Mutation in the SOS1 Gene Causes Hereditary Gingival Fibromatosis Type 1. *Am J Hum Genet* *70*, 943-954.
- Hayashi, T., Rumbaugh, G., and Huganir, R. L. (2005). Differential Regulation of AMPA Receptor Subunit Trafficking by Palmitoylation of Two Distinct Sites. *Neuron* *47*, 709-723.
- Heo, W. D., Inoue, T., Park, W. S., Kim, M. L., Park, B. O., Wandless, T. J., and Meyer, T. (2006). PI(3,4,5)P3 and PI(4,5)P2 lipids target proteins with polybasic clusters to the plasma membrane. *Science* *314*, 1458-61.
- Herrmann, C., Horn, G., Spaargaren, M., and Wittinghofer, A. (1996). Differential Interaction of the Ras Family GTP-binding Proteins H-Ras, Rap1A, and R-Ras with the Putative Effector Molecules Raf Kinase and Ral-Guanine Nucleotide Exchange Factor. *Journal of Biological Chemistry* *271*, 6794 -6800.

- Herrmann, C., Martin, G. A., and Wittinghofer, A. (1995). Quantitative Analysis of the Complex between p21 and the Ras-binding Domain of the Human Raf-1 Protein Kinase. *Journal of Biological Chemistry* *270*, 2901 -2905.
- Hingorani, S. R., Petricoin, E. F., Maitra, A., Rajapakse, V., King, C., Jacobetz, M. A., Ross, S., Conrads, T. P., Veenstra, T. D., Hitt, B. A., et al. (2003). Preinvasive and invasive ductal pancreatic cancer and its early detection in the mouse. *Cancer Cell* *4*, 437-50.
- Hingorani, S. R., Wang, L., Multani, A. S., Combs, C., Deramaudt, T. B., Hruban, R. H., Rustgi, A. K., Chang, S., and Tuveson, D. A. (2005). Trp53R172H and KrasG12D cooperate to promote chromosomal instability and widely metastatic pancreatic ductal adenocarcinoma in mice. *Cancer Cell* *7*, 469-83.
- Hofmann, I., and Munro, S. (2006). An N-terminally acetylated Arf-like GTPase is localised to lysosomes and affects their motility. *Journal of Cell Science* *119*, 1494 -1503.
- Hou, H., John Peter, A. T., Meiringer, C., Subramanian, K., and Ungermann, C. (2009). Analysis of DHHC Acyltransferases Implies Overlapping Substrate Specificity and a Two-Step Reaction Mechanism. *Traffic* *10*, 1061-1073.
- Hoyt, M. A., Stearns, T., and Botstein, D. (1990). Chromosome instability mutants of *Saccharomyces cerevisiae* that are defective in microtubule-mediated processes. *Mol. Cell. Biol.* *10*, 223-234.
- Huang, K., Sanders, S., Singaraja, R., Orban, P., Cijssouw, T., Arstikaitis, P., Yanai, A., Hayden, M. R., and El-Husseini, A. (2009). Neuronal palmitoyl acyl transferases exhibit distinct substrate specificity. *FASEB J* *23*, 2605-2615.
- Huang, K., Yanai, A., Kang, R., Arstikaitis, P., Singaraja, R. R., Metzler, M., Mullard, A., Haigh, B., Gauthier-Campbell, C., Gutekunst, C.-A., et al. (2004). Huntingtin-Interacting Protein HIP14 Is a Palmitoyl Transferase Involved in Palmitoylation and Trafficking of Multiple Neuronal Proteins. *Neuron* *44*, 977-986.
- Huang, L., Hofer, F., Martin, G. S., and Kim, S.-H. (1998). Structural basis for the interaction of Ras with RaIGDS. *Nat Struct Mol Biol* *5*, 422-426.
- Hurwitz, R. L., Bunt-Milam, A. H., Chang, M. L., and Beavo, J. A. (1985). cGMP phosphodiesterase in rod and cone outer segments of the retina. *Journal of Biological Chemistry* *260*, 568-573.
- Kang, R., Wan, J., Arstikaitis, P., Takahashi, H., Huang, K., Bailey, A. O., Thompson, J. X., Roth, A. F., Drisdell, R. C., Mastro, R., et al. (2008). Neural palmitoyl-proteomics reveals dynamic synaptic palmitoylation. *Nature* *456*, 904-909.
- Keller, C. A., Yuan, X., Panzanelli, P., Martin, M. L., Alldred, M., Sassoè-Pognetto, M., and Lüscher, B. (2004). The γ 2 Subunit of GABAA Receptors Is a Substrate for Palmitoylation by GODZ. *The Journal of Neuroscience* *24*, 5881 -5891.

- Kim, J., Shishido, T., Jiang, X., Aderem, A., and McLaughlin, S. (1994). Phosphorylation, high ionic strength, and calmodulin reverse the binding of MARCKS to phospholipid vesicles. *J Biol Chem* 269, 28214-9.
- Koera, K., Nakamura, K., Nakao, K., Miyoshi, J., Toyoshima, K., Hatta, T., Otani, H., Aiba, A., and Katsuki, M. (1997). K-ras is essential for the development of the mouse embryo. *Oncogene* 15, 1151-1159.
- Kornau, H., Schenker, L., Kennedy, M., and Seeburg, P. (1995). Domain interaction between NMDA receptor subunits and the postsynaptic density protein PSD-95. *Science* 269, 1737 -1740.
- Lam, K. K. Y., Davey, M., Sun, B., Roth, A. F., Davis, N. G., and Conibear, E. (2006). Palmitoylation by the DHHC protein Pfa4 regulates the ER exit of Chs3. *J Cell Biol* 174, 19-25.
- Laude, A. J., and Prior, I. A. (2008). Palmitoylation and localisation of RAS isoforms are modulated by the hypervariable linker domain. *Journal of Cell Science* 121, 421 - 427.
- Lemmon, M. A. (2003). Phosphoinositide Recognition Domains. *Traffic* 4, 201-213.
- Leong, W. F., Zhou, T., Lim, G. L., and Li, B. (2009). Protein Palmitoylation Regulates Osteoblast Differentiation through BMP-Induced Osterix Expression. *PLoS ONE* 4, e4135.
- Leventis, R., and Silviu, J. R. (1998a). Lipid-Binding Characteristics of the Polybasic Carboxy-Terminal Sequence of K-ras4B†. *Biochemistry* 37, 7640-7648.
- Leventis, R., and Silviu, J. R. (1998b). Lipid-Binding Characteristics of the Polybasic Carboxy-Terminal Sequence of K-ras4B†. *Biochemistry* 37, 7640-7648.
- Li, J. B., Gerdes, J. M., Haycraft, C. J., Fan, Y., Teslovich, T. M., May-Simera, H., Li, H., Blacque, O. E., Li, L., Leitch, C. C., et al. (2004). Comparative Genomics Identifies a Flagellar and Basal Body Proteome that Includes the BBS5 Human Disease Gene. *Cell* 117, 541-552.
- Li, N., Florio, S. K., Pettenati, M. J., Rao, P. N., Beavo, J. A., and Baehr, W. (1998). Characterization of human and mouse rod cGMP phosphodiesterase delta subunit (PDE6D) and chromosomal localization of the human gene. *Genomics* 49, 76-82.
- Li, Y., Wei, Q., Zhang, Y., Ling, K., and Hu, J. (2010). The small GTPases ARL-13 and ARL-3 coordinate intraflagellar transport and ciliogenesis. *The Journal of Cell Biology*.
- Liang, X., Lu, Y., Neubert, T. A., and Resh, M. D. (2002). Mass Spectrometric Analysis of GAP-43/Neuromodulin Reveals the Presence of a Variety of Fatty Acylated Species. *Journal of Biological Chemistry* 277, 33032 -33040.
- Liang, X., Lu, Y., Wilkes, M., Neubert, T. A., and Resh, M. D. (2004a). The N-terminal SH4 Region of the Src Family Kinase Fyn Is Modified by Methylation and Heterogeneous Fatty Acylation. *Journal of Biological Chemistry* 279, 8133 -8139.

- Liang, X., Lu, Y., Wilkes, M., Neubert, T. A., and Resh, M. D. (2004b). The N-terminal SH4 Region of the Src Family Kinase Fyn Is Modified by Methylation and Heterogeneous Fatty Acylation. *Journal of Biological Chemistry* 279, 8133 -8139.
- Liang, X., Nazarian, A., Erdjument-Bromage, H., Bornmann, W., Tempst, P., and Resh, M. D. (2001). Heterogeneous Fatty Acylation of Src Family Kinases with Polyunsaturated Fatty Acids Regulates Raft Localization and Signal Transduction. *Journal of Biological Chemistry* 276, 30987 -30994.
- Linari, M., Ueffing, M., Manson, F., Wright, A., Meitinger, T., and Becker, J. (1999). The retinitis pigmentosa GTPase regulator, RPGR, interacts with the delta subunit of rod cyclic GMP phosphodiesterase. *Proc Natl Acad Sci U S A* 96, 1315-1320.
- Linder, M. E., and Deschenes, R. J. (2007). Palmitoylation: policing protein stability and traffic. *Nat Rev Mol Cell Biol* 8, 74-84.
- Liu, X., Thangavel, M., Sun, S. Q., Kaminsky, J., Mahautmr, P., Stitham, J., Hwa, J., and Ostrom, R. S. (2008). Adenylyl cyclase type 6 overexpression selectively enhances beta-adrenergic and prostacyclin receptor-mediated inhibition of cardiac fibroblast function because of colocalization in lipid rafts. *Naunyn Schmiedebergs Arch. Pharmacol* 377, 359-369.
- Livak, K. J., and Schmittgen, T. D. (2001). Analysis of relative gene expression data using real-time quantitative PCR and the 2(-Delta Delta C(T)) Method. *Methods* 25, 402-8.
- Lobo, S., Greentree, W. K., Linder, M. E., and Deschenes, R. J. (2002). Identification of a Ras Palmitoyltransferase in *Saccharomyces cerevisiae*. *Journal of Biological Chemistry* 277, 41268 -41273.
- Longenecker, K., Read, P., Derewenda, U., Dauter, Z., Liu, X., Garrard, S., Walker, L., Somlyo, A. V., Nakamoto, R. K., Somlyo, A. P., et al. (1999). How RhoGDI binds Rho. *Acta Crystallogr D Biol Crystallogr* 55, 1503-15.
- Lopez, A., Dupou, L., Altibelli, A., Trotard, J., and Tocanne, J. F. (1988). Fluorescence recovery after photobleaching (FRAP) experiments under conditions of uniform disk illumination. Critical comparison of analytical solutions, and a new mathematical method for calculation of diffusion coefficient D. *Biophys J* 53, 963-70.
- Lorentzen, A., Kinkhabwala, A., Rocks, O., Vartak, N., and Bastiaens, P. I. (2010). Regulation of Ras localization by acylation enables a mode of intracellular signal propagation. *Sci Signal* 3, ra68.
- Lorenz, B., Migliaccio, C., Lichtner, P., Meyer, C., Strom, T. M., D'Urso, M., Becker, J., Ciccodicola, A., and Meitinger, T. (1998). Cloning and gene structure of the rod cGMP phosphodiesterase delta subunit gene (PDED) in man and mouse. *Eur. J. Hum. Genet* 6, 283-290.
- Ma, L., and Wang, H.-yu (2007). Mitogen-activated Protein Kinase p38 Regulates the Wnt/Cyclic GMP/Ca²⁺ Non-canonical Pathway. *Journal of Biological Chemistry* 282, 28980 -28990.

- Margarit, S. M., Sondermann, H., Hall, B. E., Nagar, B., Hoelz, A., Pirruccello, M., Bar-Sagi, D., and Kuriyan, J. (2003). Structural Evidence for Feedback Activation by Ras·GTP of the Ras-Specific Nucleotide Exchange Factor SOS. *Cell* *112*, 685-695.
- Marzesco, A. M., Galli, T., Louvard, D., and Zahraoui, A. (1998). The rod cGMP phosphodiesterase delta subunit dissociates the small GTPase Rab13 from membranes. *J Biol Chem* *273*, 22340-5.
- Maurer-Stroh, S., Gouda, M., Novatchkova, M., Schleiffer, A., Schneider, G., Sirota, F. L., Wildpaner, M., Hayashi, N., and Eisenhaber, F. (2004). MYRbase: analysis of genome-wide glycine myristoylation enlarges the functional spectrum of eukaryotic myristoylated proteins. *Genome Biol* *5*, R21-R21.
- McLaughlin, S. (1989). The Electrostatic Properties of Membranes. *Annu. Rev. Biophys. Biophys. Chem.* *18*, 113-136.
- McLaughlin, S., Wang, J., Gambhir, A., and Murray, D. (2002). PIP(2) and proteins: interactions, organization, and information flow. *Annu Rev Biophys Biomol Struct* *31*, 151-175.
- McLaughlin, S., and Aderem, A. (1995). The myristoyl-electrostatic switch: a modulator of reversible protein-membrane interactions. *Trends in Biochemical Sciences* *20*, 272-276.
- McLaughlin, S., and Murray, D. (2005). Plasma membrane phosphoinositide organization by protein electrostatics. *Nature* *438*, 605-611.
- van Meer, G., Voelker, D. R., and Feigenson, G. W. (2008). Membrane lipids: where they are and how they behave. *Nat Rev Mol Cell Biol* *9*, 112-24.
- Mesilaty-Gross, S., Reich, A., Motro, B., and Wides, R. (1999). The *Drosophila* STAM gene homolog is in a tight gene cluster, and its expression correlates to that of the adjacent gene *ial*. *Gene* *231*, 173-186.
- Michaelson, D., Silletti, J., Murphy, G., D'Eustachio, P., Rush, M., and Philips, M. R. (2001). Differential Localization of Rho Gtpases in Live Cells. *J Cell Biol* *152*, 111-126.
- Milburn, M., Tong, L., deVos, A., Brunger, A., Yamaizumi, Z., Nishimura, S., and Kim, S. (1990). Molecular switch for signal transduction: structural differences between active and inactive forms of protooncogenic ras proteins. *Science* *247*, 939 - 945.
- Miller, P. M., Folkmann, A. W., Maia, A. R. R., Efimova, N., Efimov, A., and Kaverina, I. (2009). Golgi-derived CLASP-dependent microtubules control Golgi organization and polarized trafficking in motile cells. *Nat Cell Biol* *11*, 1069-1080.
- Mitchell, D. A., Vasudevan, A., Linder, M. E., and Deschenes, R. J. (2006). Thematic review series: Lipid Posttranslational Modifications. Protein palmitoylation by a family of DHHC protein S-acyltransferases. *Journal of Lipid Research* *47*, 1118 - 1127.

- Murray, D., Hermida-Matsumoto, L., Buser, C. A., Tsang, J., Sigal, C. T., Ben-Tal, N., Honig, B., Resh, M. D., and McLaughlin, S. (1998). Electrostatics and the membrane association of Src: Theory and experiment. *Biochemistry* 37, 2145-2159.
- Mössner, E., Iwai, H., and Glockshuber, R. (2000). Influence of the pKa value of the buried, active-site cysteine on the redox properties of thioredoxin-like oxidoreductases. *FEBS Letters* 477, 21-26.
- Nadolski, M. J., and Linder, M. E. (2009). Molecular Recognition of the Palmitoylation Substrate Vac8 by Its Palmitoyltransferase Pfa3. *Journal of Biological Chemistry* 284, 17720 -17730.
- Nancy, V., Callebaut, I., El Marjou, A., and de Gunzburg, J. (2002). The delta subunit of retinal rod cGMP phosphodiesterase regulates the membrane association of Ras and Rap GTPases. *J Biol Chem* 277, 15076-84.
- Nassar, N., Horn, G., Herrmann, C. A., Scherer, A., McCormick, F., and Wittinghofer, A. (1995). The 2.2 Å crystal structure of the Ras-binding domain of the serine/threonine kinase c-Raf1 in complex with Rap1A and a GTP analogue. *Nature* 375, 554-560.
- Neal, S. E., Eccleston, J. F., Hall, A., and Webb, M. R. (1988). Kinetic analysis of the hydrolysis of GTP by p21N-ras. The basal GTPase mechanism. *Journal of Biological Chemistry* 263, 19718 -19722.
- Niihori, T., Aoki, Y., Narumi, Y., Neri, G., Cave, H., Verloes, A., Okamoto, N., Hennekam, R. C. M., Gillessen-Kaesbach, G., Wiczorek, D., et al. (2006). Germline KRAS and BRAF mutations in cardio-facio-cutaneous syndrome. *Nat Genet* 38, 294-296.
- Nobes, C. D., Lauritzen, I., Mattei, M.-G., Paris, S., Hall, A., and Chardin, P. (1998). A New Member of the Rho Family, Rnd1, Promotes Disassembly of Actin Filament Structures and Loss of Cell Adhesion. *J Cell Biol* 141, 187-197.
- Norton, A. W. (2004). Evaluation of the 17-kDa Prenyl-binding Protein as a Regulatory Protein for Phototransduction in Retinal Photoreceptors. *Journal of Biological Chemistry* 280, 1248-1256.
- Norton, A. W., D'Amours, M. R., Grazio, H. J., Hebert, T. L., and Cote, R. H. (2000). Mechanism of Transducin Activation of Frog Rod Photoreceptor Phosphodiesterase. *Journal of Biological Chemistry* 275, 38611 -38619.
- Norton, A. W., Hosier, S., Terew, J. M., Li, N., Dhingra, A., Vardi, N., Baehr, W., and Cote, R. H. (2005). Evaluation of the 17-kDa Prenyl-binding Protein as a Regulatory Protein for Phototransduction in Retinal Photoreceptors. *Journal of Biological Chemistry* 280, 1248 -1256.
- Ohno, Y., Kihara, A., Sano, T., and Igarashi, Y. (2006). Intracellular localization and tissue-specific distribution of human and yeast DHHC cysteine-rich domain-containing proteins. *Biochimica et Biophysica Acta (BBA) - Molecular and Cell Biology of Lipids* 1761, 474-483.

- Okai, T., Araki, Y., Tada, M., Tateno, T., Kontani, K., and Katada, T. (2004). Novel small GTPase subfamily capable of associating with tubulin is required for chromosome segregation. *Journal of Cell Science* *117*, 4705 -4715.
- Okeley, N. M., and Gelb, M. H. (2004). A Designed Probe for Acidic Phospholipids Reveals the Unique Enriched Anionic Character of the Cytosolic Face of the Mammalian Plasma Membrane. *Journal of Biological Chemistry* *279*, 21833 -21840.
- Olive, K. P., Jacobetz, M. A., Davidson, C. J., Gopinathan, A., McIntyre, D., Honess, D., Madhu, B., Goldgraben, M. A., Caldwell, M. E., Allard, D., et al. (2009). Inhibition of Hedgehog signaling enhances delivery of chemotherapy in a mouse model of pancreatic cancer. *Science* *324*, 1457-1461.
- Olivotto, M., Arcangeli, A., Carlà, M., and Wanke, E. (1996). Electric fields at the plasma membrane level: a neglected element in the mechanisms of cell signalling. *Bioessays* *18*, 495-504.
- Ostrom, R. S., and Insel, P. A. (2004). The evolving role of lipid rafts and caveolae in G protein-coupled receptor signaling: implications for molecular pharmacology. *Br J Pharmacol* *143*, 235-245.
- Pacold, M. E., Suire, S., Perisic, O., Lara-Gonzalez, S., Davis, C. T., Walker, E. H., Hawkins, P. T., Stephens, L., Eccleston, J. F., and Williams, R. L. (2000). Crystal Structure and Functional Analysis of Ras Binding to Its Effector Phosphoinositide 3-Kinase [γ]. *Cell* *103*, 931-944.
- Pandit, B., Sarkozy, A., Pennacchio, L. A., Carta, C., Oishi, K., Martinelli, S., Pogna, E. A., Schackwitz, W., Ustaszewska, A., Landstrom, A., et al. (2007). Gain-of-function RAF1 mutations cause Noonan and LEOPARD syndromes with hypertrophic cardiomyopathy. *Nat Genet* *39*, 1007-1012.
- Di Paolo, G., and De Camilli, P. (2006). Phosphoinositides in cell regulation and membrane dynamics. *Nature* *443*, 651-657.
- Patterson, G. H., and Lippincott-Schwartz, J. (2002). A photoactivatable GFP for selective photolabeling of proteins and cells. *Science* *297*, 1873-7.
- Pazour, G. J., Agrin, N., Leszyk, J., and Witman, G. B. (2005). Proteomic analysis of a eukaryotic cilium. *The Journal of Cell Biology* *170*, 103 -113.
- Pepinsky, R. B., Zeng, C., Wen, D., Rayhorn, P., Baker, D. P., Williams, K. P., Bixler, S. A., Ambrose, C. M., Garber, E. A., Miatkowski, K., et al. (1998). Identification of a Palmitic Acid-modified Form of Human Sonic hedgehog. *Journal of Biological Chemistry* *273*, 14037 -14045.
- Petrocca, F., Iliopoulos, D., Qin, H. R., Nicoloso, M. S., Yendamuri, S., Wojcik, S. E., Shimizu, M., Di Leva, G., Vecchione, A., Trapasso, F., et al. (2006). Alterations of the Tumor Suppressor Gene ARLTS1 in Ovarian Cancer. *Cancer Research* *66*, 10287 -10291.
- Peyker, A., Rocks, O., and Bastiaens, P. I. (2005). Imaging activation of two Ras isoforms simultaneously in a single cell. *ChemBiochem* *6*, 78-85.

- Plowman, S. J., and Hancock, J. F. (2005). Ras signaling from plasma membrane and endomembrane microdomains. *Biochimica et Biophysica Acta (BBA) - Molecular Cell Research* 1746, 274-283.
- Plowman, S. J., Williamson, D. J., O'Sullivan, M. J., Doig, J., Ritchie, A.-M., Harrison, D. J., Melton, D. W., Arends, M. J., Hooper, M. L., and Patek, C. E. (2003). While K-ras is essential for mouse development, expression of the K-ras 4A splice variant is dispensable. *Mol. Cell. Biol* 23, 9245-9250.
- Politis, E. G., Roth, A. F., and Davis, N. G. (2005). Transmembrane topology of the protein palmitoyl transferase Akr1. *J Biol Chem* 280, 10156-63.
- Prior, I. A., Harding, A., Yan, J., Sluimer, J., Parton, R. G., and Hancock, J. F. (2001). GTP-dependent segregation of H-ras from lipid rafts is required for biological activity. *Nat Cell Biol* 3, 368-375.
- Punnonen, E. L., Ryhänen, K., and Marjomäki, V. S. (1998). At reduced temperature, endocytic membrane traffic is blocked in multivesicular carrier endosomes in rat cardiac myocytes. *Eur. J. Cell Biol* 75, 344-352.
- Putilina, T., Wong, P., and Gentleman, S. (1999). The DHHC domain: a new highly conserved cysteine-rich motif. *Mol. Cell. Biochem* 195, 219-226.
- Qin, N., Pittler, S. J., and Baehr, W. (1992). In vitro isoprenylation and membrane association of mouse rod photoreceptor cGMP phosphodiesterase alpha and beta subunits expressed in bacteria. *Journal of Biological Chemistry* 267, 8458 -8463.
- Quinn, P. J. (2002). Plasma membrane phospholipid asymmetry. *Subcell. Biochem* 36, 39-60.
- Raju, R. V., and Sharma, R. K. (1999). Preparation and assay of myristoyl-CoA:protein N-myristoyltransferase. *Methods Mol. Biol* 116, 193-211.
- Razzaque, M. A., Nishizawa, T., Komoike, Y., Yagi, H., Furutani, M., Amo, R., Kamisago, M., Momma, K., Katayama, H., Nakagawa, M., et al. (2007). Germline gain-of-function mutations in RAF1 cause Noonan syndrome. *Nat Genet* 39, 1013-1017.
- Resh, M. D. (1999). Fatty acylation of proteins: new insights into membrane targeting of myristoylated and palmitoylated proteins. *Biochim Biophys Acta* 1451, 1-16.
- Resh, M. D. (2006). Trafficking and signaling by fatty-acylated and prenylated proteins. *Nat Chem Biol* 2, 584-590.
- Resh, M. D. (2004). A myristoyl switch regulates membrane binding of HIV-1 Gag. *Proc Natl Acad Sci U S A* 101, 417-418.
- Reymond, C. D., Gomer, R. H., Mehdy, M. C., and Firtel, R. A. (1984). Developmental regulation of a dictyostelium gene encoding a protein homologous to mammalian ras protein. *Cell* 39, 141-148.
- Ridge, K. D., Abdulaev, N. G., Sousa, M., and Palczewski, K. (2003). Phototransduction: crystal clear. *Trends in Biochemical Sciences* 28, 479-487.

- Roberts, A. E., Araki, T., Swanson, K. D., Montgomery, K. T., Schiripo, T. A., Joshi, V. A., Li, L., Yassin, Y., Tamburino, A. M., Neel, B. G., et al. (2007). Germline gain-of-function mutations in *SOS1* cause Noonan syndrome. *Nat Genet* *39*, 70-74.
- Rocks, O., Gerauer, M., Vartak, N., Koch, S., Huang, Z. P., Pechlivanis, M., Kuhlmann, J., Brunsveld, L., Chandra, A., Ellinger, B., et al. (2010). The palmitoylation machinery is a spatially organizing system for peripheral membrane proteins. *Cell* *141*, 458-71.
- Rocks, O., Peyker, A., Kahms, M., Verveer, P. J., Koerner, C., Lumbierres, M., Kuhlmann, J., Waldmann, H., Wittinghofer, A., and Bastiaens, P. I. (2005). An acylation cycle regulates localization and activity of palmitoylated Ras isoforms. *Science* *307*, 1746-52.
- Rotblat, B., Prior, I. A., Muncke, C., Parton, R. G., Kloog, Y., Henis, Y. I., and Hancock, J. F. (2004). Three separable domains regulate GTP-dependent association of H-ras with the plasma membrane. *Mol. Cell. Biol* *24*, 6799-6810.
- Roth, A. F., Wan, J., Bailey, A. O., Sun, B., Kuchar, J. A., Green, W. N., Phinney, B. S., Yates, J. R., 3rd, and Davis, N. G. (2006). Global analysis of protein palmitoylation in yeast. *Cell* *125*, 1003-1013.
- Roth, A. F., Feng, Y., Chen, L., and Davis, N. G. (2002). The yeast DHHC cysteine-rich domain protein Akr1p is a palmitoyl transferase. *J Cell Biol* *159*, 23-28.
- Roy, M.-O., Leventis, R., and Silviu, J. R. (2000). Mutational and Biochemical Analysis of Plasma Membrane Targeting Mediated by the Farnesylated, Polybasic Carboxy Terminus of K-ras4B†. *Biochemistry* *39*, 8298-8307.
- Roy, S., Luetterforst, R., Harding, A., Apolloni, A., Etheridge, M., Stang, E., Rolls, B., Hancock, J. F., and Parton, R. G. (1999). Dominant-negative caveolin inhibits H-Ras function by disrupting cholesterol-rich plasma membrane domains. *Nat Cell Biol* *1*, 98-105.
- Sandoval, I. V., Bonifacino, J. S., Klausner, R. D., Henkart, M., and Wehland, J. (1984). Role of microtubules in the organization and localization of the Golgi apparatus. *J. Cell Biol* *99*, 113s-118s.
- Sang, S. L., and Silviu, J. R. (2005). Novel thioester reagents afford efficient and specific S-acylation of unprotected peptides under mild conditions in aqueous solution. *J Pept Res* *66*, 169-80.
- Saraste, M., Sibbald, P. R., and Wittinghofer, A. (1990). The P-loop -- a common motif in ATP- and GTP-binding proteins. *Trends in Biochemical Sciences* *15*, 430-434.
- Sarkisian, C. J., Keister, B. A., Stairs, D. B., Boxer, R. B., Moody, S. E., and Chodosh, L. A. (2007). Dose-dependent oncogene-induced senescence in vivo and its evasion during mammary tumorigenesis. *Nat Cell Biol* *9*, 493-505.
- Schreiber, F. S., Deramautd, T. B., Brunner, T. B., Boretti, M. I., Gooch, K. J., Stoffers, D. A., Bernhard, E. J., and Rustgi, A. K. (2004). Successful growth and

characterization of mouse pancreatic ductal cells: functional properties of the Ki-RASG12V oncogene. *Gastroenterology* 127, 250-260.

Schroeder, H., Leventis, R., Shahinian, S., Walton, P. A., and Silvius, J. R. (1996). Lipid-modified, cysteinyl-containing peptides of diverse structures are efficiently S-acylated at the plasma membrane of mammalian cells. *J. Cell Biol* 134, 647-660.

Schubbert, S., Zenker, M., Rowe, S. L., Boll, S., Klein, C., Bollag, G., van der Burgt, I., Musante, L., Kalscheuer, V., Wehner, L.-E., et al. (2006). Germline KRAS mutations cause Noonan syndrome. *Nat Genet* 38, 331-336.

Shahinian, S., and Silvius, J. R. (1995). Doubly-lipid-modified protein sequence motifs exhibit long-lived anchorage to lipid bilayer membranes. *Biochemistry* 34, 3813-22.

Shaner, N. C., Campbell, R. E., Steinbach, P. A., Giepmans, B. N., Palmer, A. E., and Tsien, R. Y. (2004). Improved monomeric red, orange and yellow fluorescent proteins derived from *Discosoma* sp. red fluorescent protein. *Nat Biotechnol* 22, 1567-72.

Sharer, J. D., Shern, J. F., Van Valkenburgh, H., Wallace, D. C., and Kahn, R. A. (2002). ARL2 and BART Enter Mitochondria and Bind the Adenine Nucleotide Transporter. *Mol. Biol. Cell* 13, 71-83.

Shaw, A. C., Kalidas, K., Crosby, A. H., Jeffery, S., and Patton, M. A. (2007). The natural history of Noonan syndrome: a long-term follow-up study. *Arch Dis Child* 92, 128-132.

Shehab I.A, Chen. Y.X, Kravchenko. A, Chandra. A, Bierbaum. M, Gremer. L, Triola.G, Waldmann.H, Bastiaens P.I.H and Wittinghofer.A (2011). Regulation of a GDI-like transport system for farnesylated cargo by Arl2/3-GTP. *Nature Chemical Biology* (Unpublished)

Silvius, J. R., Bhagatji, P., Leventis, R., and Terrone, D. (2006a). K-ras4B and prenylated proteins lacking “second signals” associate dynamically with cellular membranes. *Mol Biol Cell* 17, 192-202.

Silvius, J. R., and l' Heures, F. (1994). Fluorimetric evaluation of the affinities of isoprenylated peptides for lipid bilayers. *Biochemistry* 33, 3014-22.

Silvius, J. R., Bhagatji, P., Leventis, R., and Terrone, D. (2006b). K-ras4B and Prenylated Proteins Lacking “Second Signals” Associate Dynamically with Cellular Membranes. *Mol. Biol. Cell* 17, 192-202.

Simons, K., and Toomre, D. (2000). Lipid rafts and signal transduction. *Nat Rev Mol Cell Biol* 1, 31-39.

Skoulidis, F., Cassidy, L. D., Pisupati, V., Jonasson, J. G., Bjarnason, H., Eyfjord, J. E., Karreth, F. A., Lim, M., Barber, L. M., Clatworthy, S. A., et al. (2010). Germline Brca2 Heterozygosity Promotes Kras(G12D) -Driven Carcinogenesis in a Murine Model of Familial Pancreatic Cancer. *Cancer Cell* 18, 499-509.

- Smotrys, J. E., and Linder, M. E. (2004). Palmitoylation of intracellular signaling proteins: regulation and function. *Annu Rev Biochem* *73*, 559-87.
- Smotrys, J. E., Schoenfish, M. J., Stutz, M. A., and Linder, M. E. (2005). The vacuolar DHHC-CRD protein Pfa3p is a protein acyltransferase for Vac8p. *The Journal of Cell Biology* *170*, 1091 -1099.
- Smyth, P. (1997). Belief networks, hidden Markov models, and Markov random fields: A unifying view. *Pattern Recognition Letters* *18*, 1261-1268.
- Soderling, S. H., and Beavo, J. A. (2000). Regulation of cAMP and cGMP signaling: new phosphodiesterases and new functions. *Current Opinion in Cell Biology* *12*, 174-179.
- Squire, A., and Bastiaens, P. I. (1999). Three dimensional image restoration in fluorescence lifetime imaging microscopy. *J Microsc* *193*, 36-49.
- Strickfaden, S. C., Winters, M. J., Ben-Ari, G., Lamson, R. E., Tyers, M., and Pryciak, P. (2007). A Mechanism for Cell-Cycle Regulation of MAP Kinase Signaling in a Yeast Differentiation Pathway. *Cell* *128*, 519-531.
- Suber, M. L., Pittler, S. J., Qin, N., Wright, G. C., Holcombe, V., Lee, R. H., Craft, C. M., Lolley, R. N., Baehr, W., and Hurwitz, R. L. (1993). Irish setter dogs affected with rod/cone dysplasia contain a nonsense mutation in the rod cGMP phosphodiesterase beta-subunit gene. *Proceedings of the National Academy of Sciences* *90*, 3968 -3972.
- Subramanian, K., Dietrich, L. E. P., Hou, H., LaGrassa, T. J., Meiringer, C. T. A., and Ungermann, C. (2006). Palmitoylation determines the function of Vac8 at the yeast vacuole. *Journal of Cell Science* *119*, 2477 -2485.
- Swarthout, J. T., Lobo, S., Farh, L., Croke, M. R., Greentree, W. K., Deschenes, R. J., and Linder, M. E. (2005). DHHC9 and GCP16 Constitute a Human Protein Fatty Acyltransferase with Specificity for H- and N-Ras. *Journal of Biological Chemistry* *280*, 31141 -31148.
- Sytsma, Vroom, De Grauw, and Gerritsen (1998). Time-gated fluorescence lifetime imaging and microvolume spectroscopy using two-photon excitation. *Journal of Microscopy* *191*, 39-51.
- Szallasi, Z., Denning, M. F., Smith, C. B., Dlugosz, A. A., Yuspa, S. H., Pettit, G. R., and Blumberg, P. M. (1994). Bryostatin 1 protects protein kinase C-delta from down-regulation in mouse keratinocytes in parallel with its inhibition of phorbol ester-induced differentiation. *Mol. Pharmacol* *46*, 840-850.
- Takahashi, K., Sasaki, T., Mammoto, A., Takaishi, K., Kameyama, T., Tsukita, S., Tsukita, S., and Takai, Y. (1997). Direct Interaction of the Rho GDP Dissociation Inhibitor with Ezrin/Radixin/Moesin Initiates the Activation of the Rho Small G Protein. *Journal of Biological Chemistry* *272*, 23371 -23375.
- Takai, Y., Sasaki, T., Tanaka, K., and Nakanishi, H. (1995). Rho as a regulator of the cytoskeleton. *Trends in Biochemical Sciences* *20*, 227-231.

- Tartaglia, M., Pennacchio, L. A., Zhao, C., Yadav, K. K., Fodale, V., Sarkozy, A., Pandit, B., Oishi, K., Martinelli, S., Schackwitz, W., et al. (2007). Gain-of-function SOS1 mutations cause a distinctive form of Noonan syndrome. *Nat Genet* 39, 75-79.
- Tsutsumi, R., Fukata, Y., and Fukata, M. (2008). Discovery of protein-palmitoylating enzymes. *Pflugers Arch - Eur J Physiol* 456, 1199-1206.
- Turnbull, A. P., Kümmel, D., Prinz, B., Holz, C., Schultchen, J., Lang, C., Niesen, F. H., Hofmann, K.-P., Delbrück, H., Behlke, J., et al. (2005). Structure of palmitoylated BET3: insights into TRAPP complex assembly and membrane localization. *EMBO J* 24, 875-884.
- Tuveson, D. A., Shaw, A. T., Willis, N. A., Silver, D. P., Jackson, E. L., Chang, S., Mercer, K. L., Grochow, R., Hock, H., Crowley, D., et al. (2004). Endogenous oncogenic K-ras(G12D) stimulates proliferation and widespread neoplastic and developmental defects. *Cancer Cell* 5, 375-87.
- Umanoff, H., Edelmann, W., Pellicer, A., and Kucherlapati, R. (1995). The murine N-ras gene is not essential for growth and development. *Proc. Natl. Acad. Sci. U.S.A* 92, 1709-1713.
- Valdez-Taubas, J., and Pelham, H. (2005). Swf1-dependent palmitoylation of the SNARE Tlg1 prevents its ubiquitination and degradation. *EMBO J* 24, 2524-2532.
- Veltel, S., Kravchenko, A., Ismail, S., and Wittinghofer, A. (2008). Specificity of Arl2/Arl3 signaling is mediated by a ternary Arl3-effector-GAP complex. *FEBS Letters* 582, 2501-2507.
- Veltman, D. M., Akar, G., Bosgraaf, L., and Van Haastert, P. J. M. (2009). A new set of small, extrachromosomal expression vectors for *Dictyostelium discoideum*. *Plasmid* 61, 110-118.
- Vetter, I. R., Linnemann, T., Wohlgemuth, S., Geyer, M., Kalbitzer, H. R., Herrmann, C., and Wittinghofer, A. (1999). Structural and biochemical analysis of Ras-effector signaling via RalGDS. *FEBS Letters* 451, 175-180.
- Vetter, I. R., and Wittinghofer, A. (2001). The Guanine Nucleotide-Binding Switch in Three Dimensions. *Science* 294, 1299 -1304.
- Wallace, M. R., Marchuk, D. A., Andersen, L. B., Letcher, R., Odeh, H. M., Saulino, A. M., Fountain, J. W., Brereton, A., Nicholson, J., and Mitchell, A. L. (1990). Type 1 neurofibromatosis gene: identification of a large transcript disrupted in three NF1 patients. *Science* 249, 181-186.
- Walther, K. A., Papke, B., Sinn, M. B., Michel, K., and Kinkhabwala, A. (2011). Precise measurement of protein interacting fractions with fluorescence lifetime imaging microscopy. *Mol Biosyst* 7, 322-336.
- Wan, J., Roth, A. F., Bailey, A. O., and Davis, N. G. (2007). Palmitoylated proteins: purification and identification. *Nat. Protocols* 2, 1573-1584.

- Wang, Z., Wen, X.-H., Ablonczy, Z., Crouch, R. K., Makino, C. L., and Lem, J. (2005). Enhanced Shutoff of Phototransduction in Transgenic Mice Expressing Palmitoylation-deficient Rhodopsin. *J. Biol. Chem.* *280*, 24293-24300.
- Webb, Y., Hermida-Matsumoto, L., and Resh, M. D. (2000). Inhibition of protein palmitoylation, raft localization, and T cell signaling by 2-bromopalmitate and polyunsaturated fatty acids. *J Biol Chem* *275*, 261-70.
- Wehland, J., Henkart, M., Klausner, R., and Sandoval, I. V. (1983). Role of microtubules in the distribution of the Golgi apparatus: effect of taxol and microinjected anti-alpha-tubulin antibodies. *Proc. Natl. Acad. Sci. U.S.A* *80*, 4286-4290.
- Wen-Sheng, W. (2006). Protein kinase C alpha trigger Ras and Raf-independent MEK/ERK activation for TPA-induced growth inhibition of human hepatoma cell HepG2. *Cancer Lett* *239*, 27-35.
- Williamson, P., and Schlegel, R. A. (1994). Back and forth: the regulation and function of transbilayer phospholipid movement in eukaryotic cells. *Mol Membr Biol* *11*, 199-216.
- Wilson, S. J., and Smyth, E. M. (2006). Internalization and recycling of the human prostacyclin receptor is modulated through its isoprenylation-dependent interaction with the delta subunit of cGMP phosphodiesterase 6. *J Biol Chem* *281*, 11780-6.
- Winegar, D. A., Molina y Vedia, L., and Lapetina, E. G. (1991). Isoprenylation of rap2 proteins in platelets and human erythroleukemia cells. *J Biol Chem* *266*, 4381-6.
- Wouters, F. S., Verveer, P. J., and Bastiaens, P. I. (2001). Imaging biochemistry inside cells. *Trends Cell Biol* *11*, 203-211.
- Wright, L. P., and Philips, M. R. (2006). Thematic review series: Lipid Posttranslational Modifications CAAX modification and membrane targeting of Ras. *Journal of Lipid Research* *47*, 883 -891.
- Xue, L., Gollapalli, D. R., Maiti, P., Jahng, W. J., and Rando, R. R. (2004). A Palmitoylation Switch Mechanism in the Regulation of the Visual Cycle. *Cell* *117*, 761-771.
- Yanai, A., Huang, K., Kang, R., Singaraja, R. R., Arstikaitis, P., Gan, L., Orban, P. C., Mullard, A., Cowan, C. M., Raymond, L. A., et al. (2006). Palmitoylation of huntingtin by HIP14 is essential for its trafficking and function. *Nat Neurosci* *9*, 824-831.
- Yeung, T., Gilbert, G. E., Shi, J., Silvius, J., Kapus, A., and Grinstein, S. (2008). Membrane phosphatidylserine regulates surface charge and protein localization. *Science* *319*, 210-3.
- Yeung, T., Heit, B., Dubuisson, J. F., Fairn, G. D., Chiu, B., Inman, R., Kapus, A., Swanson, M., and Grinstein, S. (2009). Contribution of phosphatidylserine to membrane surface charge and protein targeting during phagosome maturation. *J Cell Biol* *185*, 917-28.

- Yeung, T., Terebiznik, M., Yu, L., Silvius, J., Abidi, W. M., Philips, M., Levine, T., Kapus, A., and Grinstein, S. (2006). Receptor activation alters inner surface potential during phagocytosis. *Science* *313*, 347-51.
- Yokoe, H., and Meyer, T. (1996). Spatial dynamics of GFP-tagged proteins investigated by local fluorescence enhancement. *Nat Biotech* *14*, 1252-1256.
- Zhang, H., Li, S., Doan, T., Rieke, F., Detwiler, P. B., Frederick, J. M., and Baehr, W. (2007). Deletion of PrBP/delta impedes transport of GRK1 and PDE6 catalytic subunits to photoreceptor outer segments. *Proc Natl Acad Sci U S A* *104*, 8857-62.
- Zhang, H., Liu, X. H., Zhang, K., Chen, C. K., Frederick, J. M., Prestwich, G. D., and Baehr, W. (2004). Photoreceptor cGMP phosphodiesterase delta subunit (PDEdelta) functions as a prenyl-binding protein. *J Biol Chem* *279*, 407-13.
- Zhang, H., Constantine, R., Vorobiev, S., Chen, Y., Seetharaman, J., Huang, Y. J., Xiao, R., Montelione, G. T., Gerstner, C. D., Davis, M. W., et al. (2011). UNC119 is required for G protein trafficking in sensory neurons. *Nat Neurosci* *14*, 874-880.
- Zhou, C., Cunningham, L., Marcus, A. I., Li, Y., and Kahn, R. A. (2006a). Arl2 and Arl3 Regulate Different Microtubule-dependent Processes. *Mol Biol Cell* *17*, 2476-2487.

VII

Acknowledgements

I would first like to thank Prof. Philippe Bastiaens for being a great mentor for the last four years. His profound insight and passion for science is a tremendous source of encouragement. It has truly been a wonderful experience working with him and being able to learn about all the different aspects of cell biology as well as about scientific research in general. I have benefited tremendously from his expertise and experience in biology and I could not have done this thesis work without his supervision and encouragement. I especially valued his efforts in setting me up with exciting and yet realistic projects and for constantly helping me troubleshoot through technical and experimental difficulties. I also appreciate the flexibility and intellectual freedom that was given to me. The countless redrafts, brainstorming sessions and formulation of papers and conference posters have culminated in this piece of work and will no doubt formulate my attitude and character for the rest of my career.

I would also like to thank Prof. Alfred Wittinghofer for co-supervising me over the years and for being the second examiner for this thesis. I am grateful for the time and advice that he has so generously provided.

I also cherished the warm and hospitable environment that has been fostered in the department, in which I had the fortune to meet and work with so many very talented and dedicated people. Specially, I would like to thank previous and present members of the Bastiaens's and Wittinghofer's lab - Dr. Oliver Rocks, Dr. Mark Hink, Dr. Anna Peyker, Dr. Silvia Santos, Dr. Hernan Grecco, Dr. Pedro Roda-Navarro, Dr. Malte Schmick, Dr. Ali Kinkhabwala, Dr. Kirtsen Walther, Dr. Christina-Maria Hecker, Dr. Markus Grabenbauer, Dr. Shehab Ismail, Dr. Yong Xiang Chen, Jian Hou, Ola Sabet, Björn Papke, Eulashini Chuntharpursat, Sven Fengler, Nachiket Vartak, Sven Muller, Márton Gelléri, Justine Mondry, Jenny Ibach, Franziska Thorwirth and Michael Sulc.

Additionally, I would like to thank the technical staff for their support and help from time to time with special mention for Kirsten Michel, Jutta Luig, Hendrike Schütz, Anette Langerak and Petra Glitz. I would also like to thank Doro Vogt, Patricia Stege and Carolin Körner for teaching me and also providing great deal of technical support during the course of my graduate studies.

I convey a special thanks to Dr. Astrid Kramer, Tanja Forck and Rita Schebaum for being always there (even in the absence of Boss) and for keeping everything well organized. I also highly acknowledge the financial support received from International Max Planck Research School in order to pursue my research.

Last but not the least I would like to thank Minhaj for being my strength and emotional support through all the turbulent times in my PhD, especially for being patient and understanding. I would also like to acknowledge his contribution with respect to thesis correction and his knowledge regarding structural aspects related to my work.

It has truly been a pleasure working in the Philippe Bastiaens's lab. I will sorely miss all of you as I move on to the next phase of my academic training. But, I know that I will always have these fond memories to reflect on and to cherish.

VIII

Publications and presentations

Results of this work are presented in the following publications:

- Anchal Chandra^{*}, Hernán E Grecco, Venkat Pisupati, David Perera, Liam Cassidy, Ferdinandos Skoulidis, Christian Hedberg, Michael Hanzal-Bayer, Ashok R. Venkitaraman, Alfred Wittinghofer, Philippe I.H.Bastiaens (2011). The GDI-like solubilizing factor PDE δ sustains the spatial organization and signaling of Ras family proteins. *Nature Cell Biology* (Accepted, In press)
- Shehab A. Ismail^{*}, Yong-Xiang Chen^{*}, Aleksandra Kravchenko^{*}, Anchal Chandra^{*}, Martin Bierbaum, Lothar Gremer, Gemma Triola, Herbert Waldmann, Philippe I.H.Bastiaens and Alfred Wittinghofer (2011). Regulation of a GDI-like transport system for farnesylated cargo by Arl2/3-GTP. *Nature Chemical Biology* (Accepted, In press)
- Rocks, O^{*}, Gerauer, M^{*}, Vartak, N., Koch, S., Huang, Z., Pechlivanis, M., Kuhlmann, J., Brunsveld, L., Anchal Chandra, and Ellinger, B., Waldmann H, Philippe I.H.Bastiaens (2010). The Palmitoylation Machinery Is a Spatially Organizing System for Peripheral Membrane Proteins. *Cell* 141, 458-471.

^{*} (First authors)

Conference Proceedings and Talk:

- EMBO conference - Spatial 2011, Engelberg, Switzerland. May 2011. **Poster** (Poster prize).
- EMBO/EMBL conference – Seeing is Believing- Imaging the Processes of Life. March 2011. **Poster**.
- The Collaborative Research Centre (SFB) 642 "GTP and ATP-dependent Membrane Processes" at the Ruhr-University Bochum – Feb 2011. **Talk**.

IX

Curriculum Vitae

Personal details

Name: Anchal Chandra

Address: 27a, Tannenstrasse
Dortmund-44225
Germany

Email: *anchal.chandra@gmail.com*

Phone: +4917663152403

Nationality: Indian

Date of birth: 06.08.1982

University matriculation number: 113910 (Technical university, Dortmund)

Education and scientific experience

- ***Bachelor's degree in Genetics***
Institution: M.S Ramaiah Institute of technology, Bangalore University, India
Duration: 2001–2004
Grade: First class with distinction (83%)
- ***Master's degree in Biomedical genetics***
Institution: School of Biosciences and technology, VIT, India
Duration: 2004 – 2006
Grade/GPA: 9.6/10
Achievements: Gold medalist for academic achievements in both successive years
- ***Research Fellow***
Institution: National Center for Biological Sciences, Bangalore, India
Duration: Dec. 2005 – June 2006
Supervisor: Prof. M. K. Mathew
Thesis: Characterization of Voltage dependent anion channels in rice and mammalian system.
- ***Pre-doctoral research trainee***
Institution: European Molecular Biology Laboratory (EMBL),
Max Planck Institute for Molecular Physiology
Duration: Sept. 2006 – Dec. 2006
Supervisor: Prof. Philippe Bastiaens, Prof. Alfred Wittinghofer
- ***Doctoral fellow***
Institution: Max Planck Institute for Molecular Physiology
Duration: Jan 2007 – present
Supervisor: Prof. Philippe Bastiaens & Prof. Alfred Wittinghofer
Thesis: The space-time continuum of Ras signal transduction pathway